Universidad de Valladolid

Escuela de Doctorado Universidad de Valladolid

PROGRAMA DE DOCTORADO EN INGENIERÍA QUÍMICA Y AMBIENTAL

TESIS DOCTORAL:

BIOGAS CONVERSION INTO BIOPOLYMERS: Strategies to boost process performance

Presentada por **Yadira Rodríguez Muñoz** para optar al grado de
Doctora por la Universidad de Valladolid

Dirigida por:
Raúl Muñoz Torre
Raquel Lebrero Fernández

Universidad de Valladolid

Escuela de Doctorado Universidad de Valladolid

PROGRAMA DE DOCTORADO EN INGENIERÍA QUÍMICA Y AMBIENTAL

TESIS DOCTORAL:

CONVERSIÓN DE BIOGÁS EN BIOPOLÍMEROS: Estrategias para mejorar el rendimiento del proceso

Presentada por **Yadira Rodríguez Muñoz** para optar al grado de
Doctora por la Universidad de Valladolid

Dirigida por:
Raúl Muñoz Torre
Raquel Lebrero Fernández

A mi familia

Table of contents

Resumen

La humanidad se enfrenta en la actualidad a dos grandes desafíos que están estrechamente relacionados y que deben abordarse conjuntamente: la contaminación por plásticos y el cambio climático. Por un lado, reemplazar los plásticos convencionales y recalcitrantes por soluciones alternativas innovadoras y respetuosas con el medio ambiente es de suma importancia para paliar el devastador impacto medioambiental derivado del uso masivo del plástico, así como para mitigar las emisiones de gases de efecto invernadero (GEI) generadas en su producción. Por otro lado, promover la gestión de residuos a través de biotecnologías consolidadas como la digestión anaerobia puede contribuir a la reducción de las emisiones de GEI al tiempo que se genera biogás como subproducto, una fuente de energía renovable por su alto contenido en metano y que, como otras renovables, contribuye a reducir la fuerte dependencia de la economía del planeta de los combustibles fósiles.

La bioconversión de biogás en biopolímeros se presenta como una solución que aborda simultáneamente ambos retos ambientales. Además, la evolución de plantas de biogás hacia un modelo de biorrefinería abre una nueva ventana en términos de sostenibilidad económica en el sector del biogás. Asimismo, la utilización del biogás como materia prima (no alimentaria, económica y renovable) constituye una alternativa muy atractiva a las fuentes de carbono convencionales (azúcares) empleadas en la producción de polihidroxialcanoatos (PHA). Por su gran versatilidad metabólica, las bacterias metanótrofas representan una plataforma biológica prometedora para la bioconversión del metano presente en el biogás en una diversa gama de productos de valor añadido entre los que se encuentran los PHA.

La viabilidad del biogás como sustrato para el crecimiento y la síntesis de PHA ha sido recientemente demostrada en cultivos en lote empleando la especie *Methylocystis hirsuta*. No obstante, la síntesis continua de biopolímeros empleando biogás en biorreactores gas-líquido presenta múltiples limitaciones: i) bajo potencial de transferencia

por la escasa solubilidad acuosa del CH_4 y O_2, y gradientes de concentración pequeños por la dilución del biogás en aire, ii) bajas productividades de biomasa bajo las condiciones limitantes de nutrientes necesarias para inducir la síntesis de PHA, iii) conocimiento limitado de los mecanismos que gobiernan la asimilación de CH_4 y de nutrientes durante el crecimiento y la síntesis de PHA en metanótrofos de tipo II, y iv) escaso conocimiento sobre estrategias operacionales en biorreactores de alta transferencia de masa para favorecer la producción de PHA mediante la bioconversión de CH_4.

Esta tesis doctoral se centra en abordar dichas dificultades a través de la optimización de las condiciones de cultivo y de la evaluación de diferentes estrategias operacionales con el fin de maximizar el transporte de CH_4 y O_2, etapa limitante del proceso, y la bioconversión de biogás en polihidroxibutirato (PHB) utilizando metanótrofos de tipo II del género *Methylocystis.*

En este contexto, en el Capítulo 3 se evaluó la influencia de parámetros ambientales como la relación O_2:CH_4, la temperatura y la fuente de nitrógeno sobre el crecimiento y la síntesis de PHB en condiciones limitantes de nitrógeno de la bacteria metanótrofa de tipo II *Methylocystis hirsuta* CSC1 utilizando biogás como fuente de carbono y energía. Los diferentes ratios de O_2:CH_4 evaluados (1:1, 1.5:1 y 2:1) no afectaron significativamente los rendimientos de biomasa de *M. hirsuta* CSC1 (≈5 g biomasa mol^{-1} CH_4), aunque se alcanzaron tasas de eliminación de CH_4 más bajas bajo condiciones de O_2 limitantes (relación 1:1). El contenido más alto de PHB (45% w/w) se logró para un ratio de 2:1, siendo éste tres veces mayor que los obtenidos con ratios inferiores (≈15% w/w). El aumento de temperatura de 15 a 25ºC resultó en un aumento del rendimiento de biomasa (de 5 a 6 g biomasa mol^{-1} CH_4), y del contenido de PHB (de 32 a 40% w/w). A 37ºC, temperatura a la que no se logró crecimiento de biomasa bajo condiciones no limitantes de N, se obtuvo un contenido de PHB de 30% w/w. La fuente de nitrógeno también jugó un papel clave tanto en el crecimiento de *M. hirsuta* CSC1 como en la síntesis de PHB. Así, el empleo de NH_4^+ resultó en mayores rendimientos de biomasa (7 g biomasa mol^{-1} CH_4), aunque los mayores contenidos de PHB se alcanzaron cuando la biomasa se cultivó

previamente en NO_3^- como fuente de nitrógeno (41% w/w). Por último, el NO_2^- causó inhibición del crecimiento de *M. hirsuta* CSC1.

En el Capítulo 4, se construyó y validó un modelo matemático mecanicista capaz de describir los procesos metabólicos relevantes de *Methylocystis hirsuta* CSC1, sentando una base sólida para futuros trabajos y para la optimización de esta biotecnología con el fin de sintetizar PHA utilizando biogás. Con este fin, se diseñaron y realizaron ensayos en lote adicionales para la determinación de los parámetros experimentales empleados por el modelo. Los datos experimentales de los ensayos en lote y un protocolo de calibración/validación del modelo proporcionaron la estequiometría y la cinética de *Methylocystis hirsuta* por primera vez. En concreto, se obtuvieron los rendimientos de biomasa y síntesis de PHB sobre CH_4 (0.14 ± 0.01 g DQO g^{-1} DQO y 0.25 ± 0.02 g DQO g^{-1} DQO, respectivamente), las constantes de afinidad de CH_4 y O_2 (5.1 ± 2.1 g DQO m^{-3} y 4.1 ± 1.7 g O_2 m^{-3}, respectivamente), la tasa máxima de consumo de PHB (0.019 ± 0.001 g DQO g^{-1} DQO d^{-1}) y la tasa máxima de síntesis de PHB con CH_4 (0.39 ± 0.05 g DQO g^{-1} d^{-1}). El modelo desarrollado estimó una relación molar óptima O_2:CH_4 de 1.6 mol O_2 mol^{-1} CH_4 para maximizar la síntesis de PHB en *Methylocystis hirsuta*. El modelo y los parámetros obtenidos no sólo mejorarán el diseño y la operación de biorreactores destinados a síntesis de PHB a partir de biogás, sino que además facilitarán la selección de metanótrofos de tipo II de diversas muestras ambientales.

En el Capítulo 5 se investigó el potencial de un biorreactor de columna de burbujeo (BCB) equipado con recirculación interna de gas utilizando *M. hirsuta* como cepa productora de PHB y biogás como fuente de carbono y energía. El BCB se operó inicialmente con tiempos de residencia del gas (EBRT) entre 30 y 120 min, y tasas de recirculación de gas (Q_R Q_0^{-1}) de 0 a 30, para optimizar la transferencia de masa gas-líquido y la bioconversión de CH_4. Posteriormente, la columna se operó de forma continua bajo condiciones óptimas (R = 30 y EBRT = 60 min) en una primera etapa de estabilización, seguida de una segunda etapa de ciclos de alimentación-hambruna de N de 24h:24h para promover la síntesis de PHB. La recirculación del gas resultó determinante

en la transferencia gas-líquido de CH_4, proporcionando capacidades de eliminación de CH_4 casi cuatro veces más altas (≈41 g CH_4 m^{-3} h^{-1}, R = 30, EBRT = 60 min) que sin recirculación. Por otro lado, la operación en el periodo de estabilización del sistema bajo condiciones de exceso de N condujo a una acumulación de nitrito (inducida por condiciones limitantes de O_2), lo que resultó en una inhibición de la actividad metanotrófica por encima de ≈60 mg de N-NO_2^- L^{-1}. El ajuste de la carga de N-NO_3^- de acuerdo a la demanda biológica de N previno dicha acumulación. Posteriormente, con la implementación de ciclos alimentación-hambruna (24h:24h) se logró una conversión estable de CH_4 con eficacias de eliminación del 70% y con una producción continua de PHB, que resultó en acumulaciones de 14.5 ± 2.9% w/w y productividades de ≈50 g PHB m^{-3} d^{-1}. Estos resultados representan el primer paso hacia la integración de biorrefinerías de biogás en plantas de digestión anaerobia convencionales.

En el Capítulo 6 se evaluó el potencial de un sistema de crecimiento-acumulación de dos etapas para la producción continua de PHB a partir del CH_4 del biogás utilizando *Methylocystis hirsuta* CSC1. El sistema estaba constituido por dos biorreactores turbulentos, con alta capacidad de transferencia gas-líquido de metano y oxígeno, dispuestos en serie: un reactor continuo de tanque agitado (CSTR) y un biorreactor de columna de burbujeo con recirculación interna de gas. La primera etapa se diseñó para el crecimiento metanotrófico y la segunda etapa para la producción de PHB en condiciones limitantes de nitrógeno. Con este fin, se evaluaron dos estrategias operacionales con diferentes cargas de nitrógeno (N en exceso y balanceado) y velocidades de dilución. Así, una carga balanceada de N y velocidad de dilución de 0.3 d^{-1} resultó en las condiciones de operación más estables, obteniéndose productividades de PHB comparables a las del Capítulo 5 (≈53 g PHB m^{-3} d^{-1}). En general, las altas acumulaciones de PHB (hasta 48% w/w) obtenidas en el CSTR en condiciones de crecimiento junto con falta de estabilidad cuestionan la hipótesis de desacoplar crecimiento metanotrófico y acumulación de PHB, y las ventajas de la operación en sistemas multi-etapas frente a sistemas de una etapa para la producción de PHB a largo plazo.

Finalmente, el Capítulo 7 tuvo como objetivo diseñar estrategias de cultivo eficientes en sistemas de una sola etapa utilizando *Methylocystis parvus* OBBP como cepa productora de PHA, para maximizar la producción de biopolímero a partir de biogás. Concretamente, se investigó la producción de PHB y la eficacia de biodegradación de CH_4 bajo cargas de nitrógeno decrecientes en operación en continuo y regímenes de alimentación:hambruna de nitrógeno en ciclos de 24 horas (75, 54, 41 y 27 mg d^{-1}, correspondientes al 110%, 80%, 60% y 40% del requerimiento estequiométrico de nitrógeno, respectivamente), y regímenes de alimentación:hambruna de nitrógeno de 24h:24h y 24h:48h en un reactor de tanque agitado. La alimentación continua de N no promovió una producción efectiva de PHB a pesar de la existencia de condiciones limitantes de nitrógeno. Los ciclos alimentación-hambruna de nitrógeno de 24h:24h (50% de N estequiométrico) resultaron en producciones máximas de PHB (20 g PHB m^{-3} d^{-1}) sin comprometer la capacidad de eliminación de CH_4 (25 g m^{-3} h^{-1}). Ratios en la duración de los ciclos de alimentación:hambruna inferiores a 1:2 llevaron asociados el deterioro del proceso siempre que los aportes estequiométricos de nitrógeno fueron inferiores a 60%.

Los resultados obtenidos en esta tesis demostraron la viabilidad de las biotecnologías transformadoras de biogás a PHA como una plataforma innovadora para la generación de biopolímeros, abriendo el camino hacia un concepto de biorrefinería de biogás acoplado a la digestión anaerobia.

Abstract

Nowadays, mankind faces two major environmental challenges that are closely interconnected and should be tackled simultaneously: plastic pollution and climate change. On the one hand, innovation efforts devoted to the replacement of conventional recalcitrant plastics by environmentally friendly solutions are of utmost importance to mitigate the devastating environmental scenario caused by plastic pollution and to reduce greenhouse gas (GHG) emissions derived from their production. On the other hand, waste management via mature technologies such as anaerobic digestion can contribute to the reduction of GHG emissions while providing a renewable energy source (i.e. biogas) that will partially reduce the world dependence on fossil fuels.

In this context, biogas bioconversion into biopolymers can be of key relevance to address both challenges. Indeed, the development of an integrated anaerobic digestion biorefinery increasing the value of biogas opens up a new window in terms of economic sustainability and promotion of biogas industry growth. In addition, the utilization of biogas as a feedstock in industrial biotechnology constitutes a cost-effective, renewable and non-food competing alternative to sugar-based C sources for the generation of polyhydroxyalkanoates (PHA). Due to their metabolic plasticity, methanotrophs represent a promising biological platform for the bioconversion of CH_4-rich biogas into a diverse range of value-added chemicals such as PHA.

The feasibility of biogas to support methanotrophic growth and PHA synthesis has been recently demonstrated batchwise in a preliminary study using *Methylocystis hirsuta*. However, the continuous biopolymer synthesis along with continuous biogas utilization in gas-phase bioreactors entails multiple limitations: i) poor CH_4 and O_2 gas-liquid mass transfer rates, and reduced concentration gradients resulting from biogas dilution in air, ii) low biomass productivities under the nutrient deprivation conditions required to induce PHA synthesis, iii) limited understanding of the mechanisms governing CH_4 uptake and nutrient assimilation during growth and PHA synthesis in type-II methanotrophs, and iv)

limited knowledge about the optimal operating strategies in high mass transfer bioreactors devoted to PHA production via CH_4 bioconversion under continuous operation.

This PhD thesis focused on addressing the aforementioned limitations through the optimization of the environmental conditions and operating strategies with the aim of maximizing CH_4 and O_2 mass transfer (rate-limiting step) and biogas bioconversion into polyhydroxybutyrate (PHB) using type II methanotrophs from the genus *Methylocystis.*

In this context, **Chapter 3** investigated the influence of key environmental parameters (O_2:CH_4 ratio, temperature and nitrogen source) on the growth and PHB synthesis under nitrogen limiting conditions of the type II methanotroph *Methylocystis hirsuta* CSC1 using biogas as a feedstock. The O_2:CH_4 ratios tested (1:1, 1.5:1 and 2:1) did not affect significantly *M. hirsuta* CSC1 growth yields (≈5 g biomass mol^{-1} CH_4), although lower CH_4 removal rates were reached under O_2-limiting conditions (ratio 1:1). The highest PHB content (45% w/w) was achieved at a ratio 2:1 and was threefold higher than those obtained at lower ratios (≈15% w/w). The increase in temperature from 15 to 25ºC resulted in increases in the growth yield (from 5 to 6 g biomass mol^{-1} CH_4) and PHB content (from 32 to 40% w/w). Conversely, the lowest PHB content (30% w/w) was supported at 37ºC, together with a negligible growth under nutrient sufficient conditions. The nitrogen source also played a key role on both *M. hirsuta* growth and PHB synthesis. Thus, ammonium supported the highest growth yield (7 g biomass mol^{-1} CH_4), although the maximum PHB content was achieved when biomass was previously grown in nitrate as the nitrogen source (41% w/w). Nitrite exerted an inhibitory effect on *M. hirsuta* growth.

In **Chapter 4**, a mechanistic model capable of describing the relevant processes of *Methylocystis hirsuta* was developed and validated, laying a solid foundation for future practical demonstration and optimization of the PHA synthesis technology using biogas. To this end, additional dedicated batch tests were designed and conducted to obtain experimental data for key metabolic processes of *Methylocystis hirsuta*. The experimental data from well-designed batch tests and a step-wise model calibration/validation protocol

provided the stoichiometrics and kinetics of *Methylocystis hirsuta* for the first time, including the yields of biomass growth and PHA synthesis on CH_4 (0.14±0.01 g COD g^{-1} COD and 0.25±0.02 g COD g^{-1} COD, respectively), the CH_4 and O_2 affinity constants (5.1±2.1 g COD m^{-3} and 4.1±1.7 g O_2 m^{-3}, respectively), the maximum PHA consumption rate (0.019±0.001 g COD g^{-1} COD d^{-1}) and the maximum PHA synthesis rate on CH_4 (0.39±0.05 g COD g^{-1} d^{-1}). An optimal O_2:CH_4 molar ratio of 1.6 mol O_2 mol^{-1} CH_4 was estimated by the developed model to maximize PHA synthesis by *Methylocystis hirsuta*. The model and parameters obtained would not only benefit the design and operation of gas-phase bioreactors performing PHA synthesis from biogas, but also enable specific research on selection for type II methanotrophs in diverse environments.

Chapter 5 assessed the operational feasibility of a bubble column bioreactor (BCB) constructed with internal gas recirculation using *M. hirsuta* as polyhydroxybutyrate (PHB)-producing strain and biogas as carbon and energy source. The BCB was initially operated at empty bioreactor residence times (EBRTs) ranging from 30 to 120 min and gas recirculation ratios (Q_R Q_0^{-1}) from 0 to 30 to assess the gas-to-liquid mass transfer and bioconversion of CH_4. Subsequently, the BCB was continuously operated under optimal conditions (R = 30 and EBRT = 60 min) in a preliminary stabilization stage followed by nitrogen feast-famine cycles of 24h:24h to trigger PHB synthesis. Gas recirculation played a major role in CH_4 gas-liquid mass transfer, providing almost fourfold higher CH_4 elimination capacities (≈41 g CH_4 m^{-3} h^{-1}) at the highest R and an EBRT of 60 min. The long-term operation under N excess conditions entailed nitrite accumulation (induced by O_2 limiting conditions), which resulted in inhibition of the methanotrophic activity above ≈60 mg N-NO_2^- L^{-1}. Adjusting the N-NO_3^- supply to match microbial N demand successfully prevented nitrite accumulation. Finally, the N feast-famine 24h:24h strategy supported a stable CH_4 conversion with a removal efficiency of 70% along with a continuous PHB production, which yielded PHB accumulations of 14.5 ± 2.9% w/w and productivities of ≈50 g PHB m^{-3} d^{-1}. These outcomes represent the first step towards the integration of biogas biorefineries into conventional anaerobic digestion plants.

Chapter 6 investigated the potential of a two-stage growth-accumulation system for the continuous production of biogas-based PHB and simultaneous CH_4 utilization using *Methylocystis hirsuta* CSC1 as cell factory. The system consisted of two turbulent bioreactors in series to enhance methane and oxygen mass transfer: a continuous stirred tank reactor (CSTR) and a bubble column bioreactor with internal gas recirculation. The first stage was devoted to methanotrophic growth under balanced nutrient conditions and the second stage to PHB production under nitrogen limiting conditions. For this purpose, two operational approaches under different nitrogen loading rates (excess and balanced N) and dilution rates were assessed. A balanced nitrogen loading rate at a dilution rate of 0.3 d^{-1} resulted in the most stable operating conditions, obtaining comparable PHB productivities to those reported in Chapter 5 (≈53 g PHB m^{-3} d^{-1}). Overall, the high PHB contents (up to 48% w/w) obtained in the CSTR under theoretically nutrient balanced conditions and the lack of sustained stability challenged the hypothesis of decoupling methanotrophic growth and PHB accumulation and the advantages conferred by multi-stage *vs* single-stage for long-term PHB production processes.

Finally, **Chapter 7** aimed at designing efficient cultivation strategies in a single-stage process using *Methylocystis parvus* OBBP to boost biopolymer production from biogas. In this work, biogas-based polyhydroxybutyrate production and CH_4 biodegradation performance were investigated under decreasing nitrogen loading rates in continuous mode and alternating feast:famine regimes within 24h-cycles (75, 54, 41 and 27 mg d^{-1}, corresponding to 110%, 80%, 60% and 40% of the stoichiometric nitrogen requirements, respectively), and alternating feast:famine regimes of 24h:24h and 24h:48h in a stirred tank reactor. Continuous N feeding did not support an effective PHB production despite the occurrence of nitrogen limiting conditions. Feast-famine cycles of 24h:24h (with 50% stoichiometric nitrogen supply) supported the maximum PHB production (20 g PHB m^{-3} d^{-1}) without compromising the CH_4 elimination capacity (25 g m^{-3} h^{-1}) of the system. Feast:famine ratios ≤ 1:2 entailed the deterioration of process performance at stoichiometric nitrogen inputs ≤ 60%.

The results herein obtained demonstrated the feasibility of biogas-to-PHA biotechnologies as an innovative platform for the generation of biopolymers, paving the way towards a biogas biorefinery concept coupled to anaerobic digestion.

List of publications

The following publications are presented within the scope of this thesis. Three of them (Manuscripts I to III) have been published in international journals indexed in Clarivate Analytics' Web of Science (WoS). Manuscript IV is to date in preparation and Manuscript V has been submitted for publication.

Rodríguez, Y., Firmino, P.I.M., Arnáiz, E., Lebrero, R., Muñoz, R. 2020. Elucidating the influence of environmental factors on biogas-based polyhydroxybutyrate production by *Methylocystis hirsuta* CSC1. *Science of The Total Environment*, 706, 135136. https://doi.org/10.1016/j.scitotenv.2019.135136

Chen, X., Rodríguez, Y., López, J.C., Muñoz, R., Ni, B.J., Sin, G. 2020. Modeling of Polyhydroxyalkanoate Synthesis from Biogas by *Methylocystis hirsuta*. *ACS Sustainable Chemistry & Engineering*, 8(9), 3906-3912. https://doi.org/10.1021/acssuschemeng.9b07414

Rodríguez, Y., Firmino, P.I.M., Pérez, V., Lebrero, R., Muñoz, R. 2020. Biogas valorization via continuous polyhydroxybutyrate production by *Methylocystis hirsuta* in a bubble column bioreactor. *Waste Management*, 113, 395-403. https://doi.org/0.1016/j.wasman.2020.06.009

Rodríguez, Y., García, S., Lebrero, R., Muñoz, R. Continuous polyhydroxybutyrate production from biogas in an innovative two-stage bioreactor configuration (In preparation).

Rodríguez, Y., García, S., Pérez, R., Lebrero, R., Muñoz, R. Optimization of nitrogen feeding strategies for improving polyhydroxybutyrate production from biogas by *Methylocystis parvus* OBBP in a stirred tank reactor. Submitted for publication in *Chemosphere.*

Contribution to the articles included in the thesis

Manuscript I. In this work, I was responsible for the design, start-up and operation of the experimental set-up under the supervision of Dr. Raúl Muñoz and Dr. Raquel Lebrero. I also performed the biopolymer extraction and analysis assisted by Dr. Esther Arnaiz. I was responsible for the formal analysis of the results and writing of the original manuscript with the collaboration of Dr. Paulo Igor Milen Firmino in the discussion section. The review and edition of the original manuscript was conducted by Dr. Raúl Muñoz and Dr. Raquel Lebrero.

Manuscript II. During this research, I was in charge of the start-up, operation and monitoring of batch assays under the supervision of Dr. Raúl Muñoz. Previous tests were carried out by Juan Carlos López. Dr. Xueming Chen was the main responsible of the model development and manuscript preparation, in which I partially contributed. Dr. Gürkan Sin and Dr. Bing-Jie Ni reviewed the manuscript.

Manuscript III. In this research, I was responsible for the design, start-up and operation of the bioreactor, formal analysis of results and manuscript writing under the supervision of Dr. Raúl Muñoz and Dr. Raquel Lebrero. Víctor Pérez and Dr. Paulo Igor Milen Firmino contributed to the bioreactor monitoring during the mass transfer tests and the cyclic operation, respectively. The review of the original manuscript was conducted by Dr. Raúl Muñoz and Dr. Raquel Lebrero.

Manuscript IV. In this work, I was in charge of the design, start-up and operation of the bioreactor. Silvia García assisted in the bioreactor monitoring as part of her BSc thesis. I conducted results evaluation and prepared the original manuscript, which was reviewed and edited by Dr. Raúl Muñoz and Dr. Raquel Lebrero.

Manuscript V. In this research, I was in charge of the design, start-up and operation of the bioreactor under the supervision of Dr. Raúl Muñoz and Dr. Raquel Lebrero. Part of the bioreactor monitoring was carried out by Silvia García and Dr. Rebeca Pérez. I performed

results evaluation and prepared the original manuscript, which was reviewed and edited by Dr. Raúl Muñoz and Dr. Raquel Lebrero.

1.

Introduction

Part of the content of this chapter was adapted from:

Rodríguez, Y., Pérez, V., López, J.C., Bordel, S., Firmino, P.I., Lebrero, R., Muñoz, R. (2020) Coupling Biogas with PHA Biosynthesis, in: The Handbook of Polyhydroxyalkanoates. Microbial Synthesis and Feedstocks (1st ed.). Edited by: M. Koller. CRC Press, pp. 357-376. doi: 10.1201/9780429296611

López, J.C., **Rodríguez, Y.**, Pérez, V., Lebrero, R., Muñoz, R. (2019) CH_4-Based Polyhydroxyalkanoate Production: A Step Further Towards a Sustainable Bioeconomy. In: Biotechnological Applications of Polyhydroxyalkanoates. Edited by: V.C. Kalia, Springer Singapore, pp. 283-321. doi: 10.1007/978-981-13-3759-8_11

1.1 Tackling the global plastic problem

1.1.1 The need for biopolymer production. Global market drivers and trends

Since the mid-20th century, thermoplastics have become one of the most versatile and universally-used materials, bringing many technological advances and contributing to the overall welfare of citizens. Thermoplastics are characterized for having unrivalled properties, such as high strength-to-weight ratio, corrosion-resistance, durability, good electrical insulating properties and low cost, which have supported a vast range of applications in many sectors (packaging, construction, automotive, electrical and electronic, etc.). The global plastic production has increased from less than 2 million metric tonnes (Mt) in 1950 up to 368 Mt in 2019 (PlasticsEurope 2013, 2020), and it is expected to continue their massive growth, with a threefold increase estimated by 2050 reaching a cumulative production volume over 25 billion tonnes (Geyer et al., 2017;WEF, 2016). In Europe, plastic converters demand amounted 50.7 Mton in 2019, packaging being the major end-use market with nearly 40% of the total demand (PlasticsEurope, 2020).

Packaging materials are mainly designed for a short first-use cycle, and therefore the environmental implications of their disposal should be taken into due consideration. It is estimated that only 14% of the plastic packaging waste (<10% of plastic waste in general) is collected for recycling, whereas other 14% is incinerated for energy recovery. This means that an overwhelming 72% of plastic packaging is either dumped into landfills or mismanaged (Porta, 2019;WEF, 2016). Interestingly, some European countries such as Austria or The Netherlands are leading restrictions in this regard with zero landfilling of plastic post-consumer (PPC) waste since 2018.

The leading resins in packaging applications (polypropylene (PP), polyethylene (PE), polyethylene terephthalate (PET) and polystyrene (PS)) are the most frequently encountered not only in the municipal waste but also in the marine debris (Lebreton and

Andrady, 2019). On the other hand, fragmented plastics derived from textile, cars or intentionally included 'microbeads' in healthcare products, i.e. microplastics (<5 mm of diameter), represent as well an emerging threat to natural habitats (Garcia-Depraect et al., 2021; UNEP, 2014). The flux of land-based plastic waste entering the oceans averages 9 Mt every year, while its accumulation is expected to grow up to 250 Mt by 2025 (Jambeck et al., 2015; WEF, 2016). The environmental damages of such after-use 'mismanagement' include entanglement in fishing gear of mammals, damage to ecosystems (e.g. coral reefs), chemical contamination, and mortality or injury of marine organisms and seabirds through plastic ingestion (UNEP, 2014). Other negative consequences associated to the use of these recalcitrant plastics are the greenhouse gases emitted in their production, which heavily relies on finite virgin fossil stocks (>90% of the plastic production), and their incineration; together with the health/environmental impacts derived from compounds used as additives (plasticisers, flame retardants, stabilisers or pigments) (WEF, 2016).

Hence, in the current context of awareness about the environment and biodiversity, the European Union has built a legal framework to counteract plastic pollution and set the bases of a new plastic economy. For instance, the Directive (EU) 2019/904 includes some ambitious measures in order to meet the United Nations Sustainable Development Goal 12, which is meant to ensure sustainable consumption and production patterns. Among these measures, it envisages the prohibition since July 2021 of placing on the market selected single-use plastic products (SUPs) and products made from oxo-degradable plastics; and a minimum separate collection target of 90% for plastic bottles by 2029 (OJ L 155, 12.6.2019, p. 1-19).

However, the only adoption of plastic reuse and recycling policies might not be sufficient to tackle this devastating scenario of plastic pollution, which needs to be complemented with approaches based on new technologies to turn plastic into 'bio-benign'. The main routes towards plastic pollution mitigation are based on strategies aiming at either reducing the degradation timeframe of chemically synthesized polymers of recalcitrant nature, i.e., by creating engineered polymers based on reversible covalent chemistry such

as polyglyoxylates or by using living organisms or enzymes able to decompose polymers (e.g., PET degradation by the larvae *Galleria mellonella*); or replacing conventional oil-based plastics with biodegradable plastics (Porta, 2019; Zhang et al., 2018).

In particular, the present PhD thesis focused on the sustainable production of biodegradable bioplastics using biotechnological processes. The term '*bioplastics*', which is commonly misused, refers to a broad family of materials that comprises bio-based and/or biodegradable/compostable materials. Thus, bioplastics can be classified into: 1) bio-based: non-biodegradable plastics synthetized from renewable sources, such as bio-based PE or PET; 2) bio-based and biodegradable: naturally (i.e., '*biopolymers'*) or synthetic plastics from renewable sources capable of undergoing biodegradation such as polyhydroxyalkanoates (PHA) or polylactic acid (PLA); and 3) biodegradable fossil-based plastics such as polybutylene adipate terephthalate (PBAT) (EUBP, 2018).

Bioplastics are key players in the transition towards a circular economy as they allow i) decoupling plastic production from the utilization of fossil-based feedstock, thus reducing carbon footprint, and ii) improving resource efficiency by reducing value losses intrinsically linked to conventional reuse and recycling loops (WEF, 2016). Moreover, besides possessing comparable properties to those of their conventional counterparts (see Section 1.1.2), bioplastics offer alternative end-of-life (EOL) options such as organic recycling (i.e. composting or anaerobic digestion) (EUBP, 2020a; Garcia-Depraect et al., 2021). Regulations issued in this respect, such as the EU Waste Framework Directive 2008/98/EC (amended in 2018), encourage "*the use of materials produced from bio-waste*" and state that "*bio-based recyclable products and compostable bio-degradable products could represent therefore an opportunity to stimulate further research and innovation and to substitute fossil fuel-based feedstock with renewable resources*" (OJ L 150, 14.6.2018, p. 109–140).

Currently, the global production of bioplastics contributes to less than 1% of the total plastics production share. In 2020, it accounted for 2.11 Mton and it was forecasted to grow up to 2.87 Mton by 2025 (see **Fig. 1.1**) (EUBP, 2020b). Interestingly, this growth is being

driven by biopolymers such as PHAs, whose production capacity (36000 ton year^{-1}) is expected to increase by ten times within the next five years as a result of its large-scale entry. Nowadays, Asia is the major bioplastics production hub (46%) followed by Europe with one-quarter of the global production capacity. The global production capacity by type of bioplastic is shown in **Fig. 1.2**. Bio-based and biodegradable plastic manufacture primarily relies on the use of agricultural feedstock (sugarcane, vegetable oils, corn, etc.). The land devoted to cultivate these crops amounted for 0.7 million ha in 2020, which corresponds to 0.05% of the total arable land (1.4 billion ha). Thus, although land requirements so far are not significant, the impact of land use change on ecosystems must be taken into consideration. As bioplastics industry is predicted to rapidly grow in the coming decades, it is crucial to ensure that bio-based plastics are sourced responsibly, minimizing food competition and not displacing food crops (BFA, 2015).

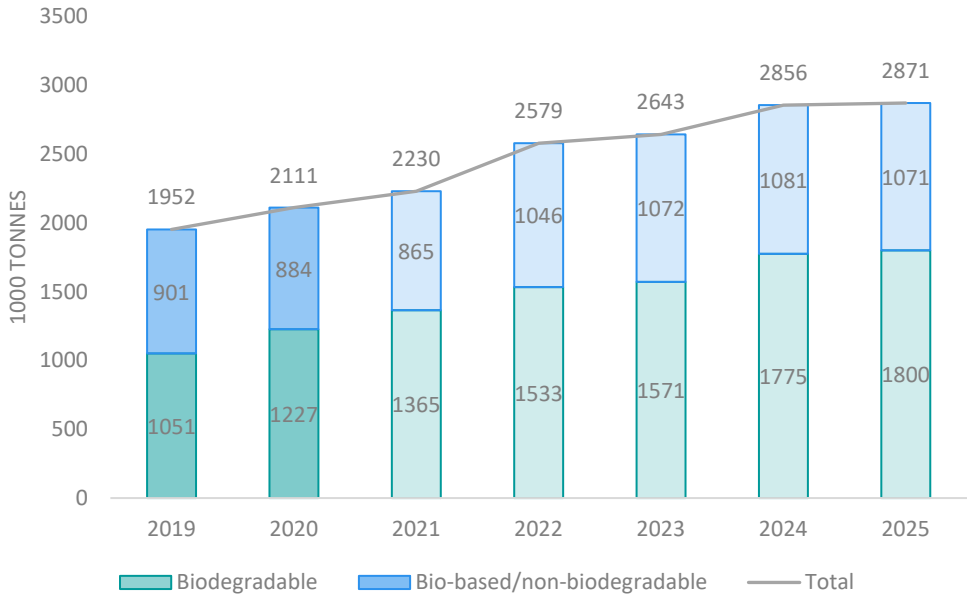

Fig. 1.1. *Global production capacity of bioplastics. Bars in lighter colour indicate production forecast (Adapted from European Bioplastics)*

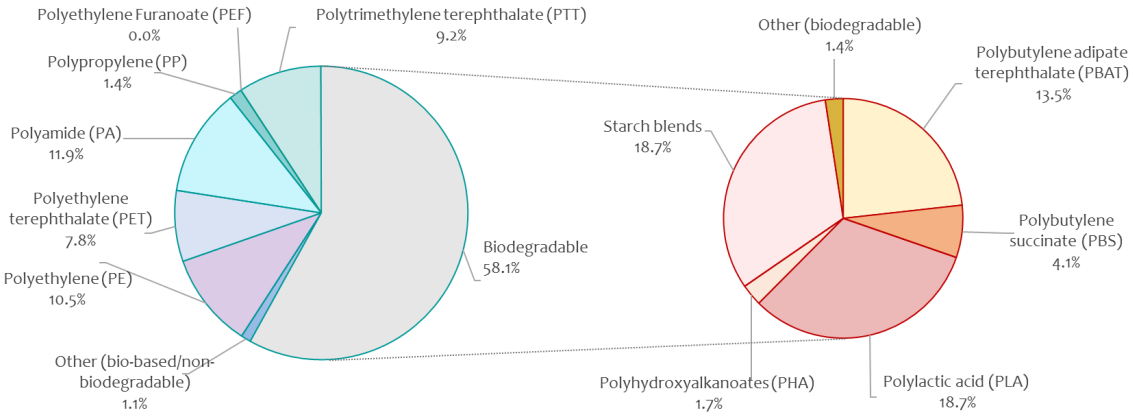

Fig. 1.2. *Global production capacity by type of bioplastic (Adapted from European Bioplastics)*

1.1.2 Polyhydroxyalkanoates. Properties and applications

Polyhydroxyalkanoates (PHAs) are naturally occurring biopolyesters synthetized intracellularly by numerous prokaryotic microorganisms (Castilho et al., 2009; Choi et al., 2020). These biopolymers, in the form of cytoplasmic inclusions, are classically accumulated under carbon sufficient and nutrient-limiting conditions, serving as carbon and energy storage compounds (Strong et al. 2016). PHAs represent a promising alternative for replacing petroleum-based plastics as they are renewably sourced, non-toxic, biocompatible and readily biodegradable thermoplastics (Meereboer et al., 2020).

Based on the number of carbon in their monomeric units, PHAs can be mainly grouped into short-chain-length (*scl*-PHA: ≤5 carbon atoms) and medium-chain-length (*mcl*-PHA: 6-14 carbon atoms) polymers, while PHA backbone containing >14 carbon atoms are very rare (Singh and Mallick, 2008) **(Fig. 1.3)**. PHA type and monomeric composition is determined by the strain, the substrate(s) availability and culture conditions (Mozejko-Ciesielska and Kiewisz, 2016). Among the limitless possibilities for PHA combination (≈150 monomers identified), the most well-known PHA is the homopolymer *scl*-PHA poly(3-hydroxybutyrate) [P(3HB) or PHB]. PHB exhibits comparable mechanical and thermal properties to those of propylene (PP) but a high degree of crystallinity (60-70%) and a narrow processing window for melt extrusion (similar melting and decomposition temperature) (Koller et al., 2010; Li et al., 2016). However, PHA properties can be customized targeting a wide range of applications by incorporating distinct precursors such as 3-hydroxyvalerate (3HV) or 3-hydroxyhexanoate (3-HHx) to form the *scl*-PHA copolymer poly(3-hydroxybutyrate-*co*-3-hydroxyvalerate) [P(3HB-*co*-3HV) or PHBV] or the *scl*-*mcl*-PHA copolymer poly(3-hydroxybutyrate-*co*-3-hydroxyhexanoate) [P(3HB-*co*-3HHx) or PHBHHx]. The main thermal and mechanical properties of representative PHA homo- and co-polymers are summarized in **Table 1.1**. On the other hand, PHA properties can be also fine-tuned expanding their applicability either via blending with other polymers and natural raw materials such as lignin, starch, cellulose or PLA; or via chemical modification to form new copolymers (Li et al., 2016).

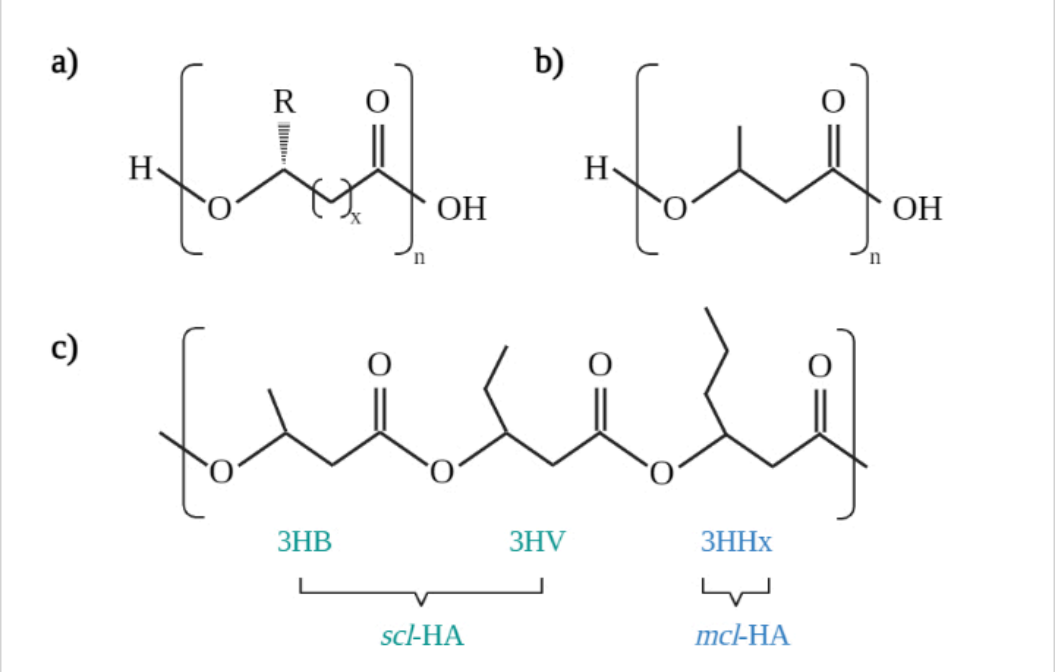

Fig. 1.3. *a) Polyhydroxyalkanoates general structural formula (x = 1-4), n varies from 100 to 1000; b) P(3HB) homopolymer and c) Some examples of* scl- *and* mcl-*PHA monomers: 3-hydroxybutyrate (3HB), 3-hydroxyvalerate (3HV), 3-hydroxyhexanoate (3HHx), 3-hydroxyoctanoate (3HO)* (Created in BioRender.com)

Therefore, these biopolymers hold an untapped potential for several applications. For instance, in the medical-related field, PHAs have been utilized for tissue engineering, bone and cartilage repair, development of medical devices (e.g. valves, stents, staples, surgical sutures and meshes) and even for organ reconstruction, among others (Chen, 2010). In pharmacology, their use as drug delivery carriers (e.g. anticancer therapy) has been also tested. PHAs have been widely used as packaging materials in cosmetic and food industries (e.g. bottles, containers, films), since they offer superior barrier properties toward oxygen and moisture permeation, allowing a prolonged product lifetime (Boey et al., 2021). It is also well-known their potential in the manufacturing of disposable items (e.g. utensils, hygiene products, compostable bags, etc.) and in the agriculture field for controlled release of fertilizers or pesticides (Bugnicourt et al., 2014; Costa et al., 2019; Poltronieri and Kumar, 2019). Very promising applications are also found in the fuel industry as biofuels (e.g. hydroxyalkanoate methyl ester (HAME) or hydroxybutyrate methyl ester (HBME)) through methyl esterification, as a high degree of PHA purity is not required (Riaz et al., 2021). Finally, (R)-3-hydroxycarboxylic acids (3HA monomers) derived from PHAs via

either accumulation followed by depolymerization or direct microbial production, can be used as chiral precursors/building blocks in the synthesis of fine chemicals such as antibiotics (Yanez et al., 2020).

Table 1.1 *Thermal and mechanical properties of some representative PHAs and their oil-based counterparts (Doi et al., 1995; Koller et al., 2010; Mozejko-Ciesielska and Kiewisz, 2016).*

	Melting temp. (ºC)	**Glass transition temp. (ºC)**	**Young's modulus (GPa)**	**Tensile strength (MPa)**	**Elongation to break (%)**
P(3HB)	177	4	3.5	43	5
P(3HB-*co*-20% 3HV)	145	-1	1.2	32	50
P(3HB-co-10% 3HHx)	127	-1	-	21	400
P(3HB-co-6% 3HD)	130	-8	-	17	680
P(4HB)	60	-50	149	104	1000
PP	176	-10	1.7	38	400

P(3HB): poly(3-hydroxybutyrate; P(3HB-co-20%3HV): poly(3-hydroxybutyrate-*co*-20% 3-hydroxyvalerate); P(3HB-co-10%3HHx): poly(3-hydroxybutyrate-*co*-10% 3-hydroxyhexanoate); P(3HB-co-6%3HD): poly(3-hydroxybutyrate-*co*-6% 3-hydroxydecanoate); P(4HB): poly(4-hydroxybutyrate): PP: polypropylene

1.1.3 Current status of polyhydroxyalkanoate production. Conventional and alternative feedstock.

PHAs were marketed for the first time by Imperial Chemical Industries in the 1980s. PHBV, commercialized by the proprietary Biopol® trade name, was synthetized by using the PHA-producing *Cupriavidus necator* (formerly named as *Ralstonia eutropha*) in the presence of propionic acid and glucose (Jiang et al., 2016). *C. necator* together with *Pseudomonas putida*, *Burkholderia sacchari* or *Azohydromonas lata* (see **Table 1.2**) are the most widely used bacterial species within the PHA-producers platform. In addition, the application of genetic engineering tools to obtain a superior PHA production through recombinant species (e.g. using *Escherichia coli* as host strain) has increasingly attracted research interest in the past few decades.

Over 30 companies located in the US, Europe and Asia are currently involved in PHA manufacturing, Danimer Scientific being the largest PHA supplier with a current PHA capacity of 10 kton year^{-1}. Danimer, which merged with Meredian in 2014, forecasts to achieve a PHA finished products volume of 85 kton year^{-1} by 2027, once completed the expansion of their facility based in Kentucky and the ongoing Greenfield facility's construction (Axial, 2021). On the other hand, the Japanese manufacturer Kaneka, inaugurated in the late 2019 a 5 kton year^{-1} PHBH plant, increasing its capacity five times (Kaneka, 2019). In Europe, Bio-On was at the forefront of PHA production on a commercial basis until 2019, when declared bankruptcy. At that time, the Italian venture, founded in 2007, had completed the construction of a 1 kton year^{-1} plant devoted to the development of products for high-added value niche markets such as cosmetics (microbeads) and announced an agreement with the Russian TAIF JSC group for licensing Bio-On technology to produce 10 kton year^{-1} of PHA in the Republic of Tatarstan. In China, companies such as TianAn Biopolymers, Shenzhen Ecomann Biotechnology and Tianjin GreenBio have reported a combined capacity of 17 kton year $^{-1}$. Overall, although PHAs are gaining traction in numerous end-use sectors with a handful of suppliers at commercial development stage, the PHA-platform is still regarded as an emerging technology placed

at the beginning of the S-curve. Indeed, PHA demand exceeded considerably its production in 2020 (Ravenstijn, 2021). **Table 1.2** displays a selection of the main PHA producers worldwide, including the carbon sources, PHA-producing microorganisms, targeted products and their trade name, and current (or announced for 2021) capacity in tons $year^{-1}$.

Simple sugars (glucose, fructose, sucrose) present in sugarcane or beet molasses and triglycerides sourced from vegetable oils (e.g. palm and soybean oil) stand as the most common feedstock for commercial scale PHA production (Bugnicourt et al., 2014). However, the high monetary cost of these raw materials, which accounts for up to 40-50% of the total production costs, limits PHA industrialization due to their uncompetitive market price (Khatami et al., 2021; Sun et al., 2007; Tan et al., 2021). For instance, PHB with a selling price of 5-6 € kg^{-1} cannot outcompete on price their oil-based counterparts (1.0 and 1.5 € kg^{-1} for PP and PE, respectively) (van den Oever et al., 2017; Vandi et al., 2018).

In this context, significant efforts are being made on pursuing the so-called 2nd generation substrates, i.e. low-cost and non-food competing substrates such as lipid-rich wastes, wastewater, flue gases or other by-product/residual streams (whey, glycerol or molasses) (Riedel and Brigham, 2020). Biogas has recently attracted much attention as a low-cost carbon source for the manufacture of PHA and other value-added products based on its high content of CH_4 (50-70%) and wide availability (Cantera et al. 2019; (Mühlemeier et al., 2018). Its use as a feedstock would significantly decrease PHA production costs while generating value-added goods and reducing the carbon flow into the environment (Levett et al., 2016; Sundstrom and Criddle, 2015). Recent studies revealed that integrating PHB production with heat and power cogeneration from biogas would support a cost-competitive production of PHA with selling prices ranging from 1.5 to 6.9 € kg^{-1}, depending on the geographical location. On the contrary, when employing biogas entirely for PHA manufacture, production costs would be viable (4.1 € kg^{-1}) only in those countries with more affordable energy prices (Pérez et al., 2020).

Companies such as *Newlight Technologies* and *Mango Materials* have been created (in 2003 and 2010, respectively) with the aim of developing biotechnological processes

potentially capable of turning methane into biodegradable materials. Methane-to-PHAs production relies on the biopolymer accumulation ability of a class of methane oxidizing bacteria, namely type II methanotrophs (see section 1.3.1). *Newlight Technologies* isolated PHB-producing bacteria from seawater, whereas *Mango Materials* operates with a bacterial consortium naturally selected. After 10 years of research, *Newlight Techonologies* embarked on its core mission to scale up the technology by opening their first commercial-scale plant. In 2019, the company has expanded its capacity with the construction of a 23 kton $year^{-1}$ plant (Bioplastics Magazine, 2020). *Mango Materials* currently operates a pilot scale unit co-located with a biogas production facility in San Francisco Bay Area (Mango Materials, n.d.). However, the company has recently built a demonstration unit to achieve a material production of 100 kg-PHA per week branded as YOPP+ pellets (Tullo, 2019).

As a result of this increasing interest, the market has included methane fermentation as a new production method, being segmented now into three main categories (sugar, vegetable oil and methane fermentation).

Table 1.2 *Current PHA production: selected manufacturers, carbon source, commercialized products, biocatalysts and capacity*

Manufacturer	Location	Feedstock	Product	Trade name	Microorganism	Capacity (tons year^{-1})	References
Bio-on (TAIF Group)	Italy (Russia)	Sugar beet and sugar cane industry by-products	P3HB and PHBVV spheres	Minerv-PHA™	*C. necator*	1000 (10000) [(1)]	Bio-on.it
Biomer	Germany	Corn sugar	P3HB pellets	Biomer ™	*Azohydromonas lata*	1000	Biomer.de
CJ CheilJedang [(2)]	South Korea	Corn sugar	P(3HB-*co*-4HB)	CJ PHA	*E. coli*	5000	CJbio.net
Danimer Scientific (Meredian)	US	Canola oil	PHA and PLA blends	Nodax® PHA	n.r.	10000	Danimerscientific.com
Shenzhen Ecomann Biotech.	China	Sugar cane (glucose)	PHA, PHBV, P(3HB-*co*-4HB)	Ecomann® PHA	*E. coli*	5000	Ecomann.sx-gear.com
Kaneka Corp.	Japan	Vegetable oil	P3HB3HHx	Aonilex®	*C. necator*	5000	Kaneka.co.jp
Mango Materials	US	Waste biogas	P3HB	YOPP+ PHA pellets	Methanotrophic consortium	Pilot	Mangomaterials.com
Nafigate	Czech Republic	Waste cooking oil	P3HB	Hydal PHA	*C. necator*	Pilot	Nafigate.com
Newlight Technologies	US	Air and methane	P3HB	AirCarbon™	Isolated from the sea (Newlight's 9X biocatalyst)	n.r.	Newlight.com
PHB Industrial	Brazil	Sugar cane	P3HB	Biocycle ™	*Burkholderia sacchari and C. necator*	100	Biocycle.com.br
PolyFerm Canada	Canada	Vegetable oils, sugars	mcl-PHAs	VersaMer™	*Ralstonia eutropha, Aeromonas hydrophila, Pseudomonas putida*	<10 (Research)	Polyfermcanada.com
TianAn Biopolymer	China	Corn or cassava sugar and propionic acid	P3HBV	Enmat™	*C. necator*	2000	Tianan-enmat.com
Tianjin GreenBio	China	Sucrose	P(3HB-*co*-4HB)	SoGreen-00X	*C. necator and recombinant E. coli*	10000	Tjgreenbio.com
Yield10 Bioscience[(3)]	US	Camelina seed	P3HB	-	n.a.	Research	Yield10bio.com

n.r.: not reported (data not provided by the PHA supplier); n.a.: not applicable
[(1)] Licensed plant: entered the implementation phase in 2019
[(2)] CJ CheilJedang Corporation acquired biopolymer Metabolix assets in 2016 after ADM and Metabolix terminated their Telles joint venture
[(3)] Previously Metabolix

1.2 Biogas as a platform for generating value-added chemicals

1.2.1 Biogas. Current situation of biogas production

The climate emergency demands a steep transition into a cleaner way of energy production, as the energy sector represents more than 75% of the greenhouse gases (GHG) emissions (EC, 2020). The contribution of renewables amounted 11% (from which 5.1% corresponded to bioenergy) of the global energy demand (378 EJ/yr) in 2018, though it represented less than one-third of the total increase in energy demand (by 7%) that took place from 2013 to 2018 (REN21, 2020). In this context, biogas can play an important role in the much-needed decarbonization of the economy, not only by diminishing GHG emissions derived from waste disposal but also for being a versatile renewable fuel with an immense valorization potential (Kapoor et al., 2020). In the transition towards carbon neutrality, it has been estimated that biogas can account nearly 30% of the total waste-derived energy (250 million tons of oil equivalent) in the European Union by 2050 (Iglesias et al., 2021).

Biogas is obtained from the microbial conversion of biodegradable organic waste under anaerobic conditions. Its composition depends upon the feedstock (Red-ox state of the organic matter) and type of anaerobic digester (open or closed). Today, anaerobic digestion (AD) is a reliable and mature technology that is used to stabilize and treat organic wastes such as municipal solid waste, food and beverage industry residues, crop and livestock residues, or sewage sludge (EBA, 2020). Landfills provided with gas collection systems can be also a significant source of biogas. The gas mixture from the aforementioned digested feedstock in closed bioreactor is composed typically of CH_4 (50-70%) and CO_2 (30-45%) with minor levels of H_2S (0.005-2%), O_2 (<2%), N_2 (<5%), NH_3 (<1%), moisture (1-5%), and other trace pollutants (e.g. siloxanes or volatile organic compounds) (Kapoor et al., 2020; Muñoz et al., 2015).

Its high content in methane confers biogas an outstanding calorific value (up to 28 MJ m^{-3}) and a broad scope of applications, heat and power generation being its major end-use (with similar number of co-generation and electricity-only facilities), followed by heating in the residential sector and upgrading to biomethane (Liebetrau et al., 2020). Particularly in developing countries, biogas provides a local source of energy, being directly utilized for domestic cooking or lighting applications. Biogas quality standards vary based on its final application. For instance, upgraded biogas for injection into natural gas networks and use as a transportation fuel needs to comply with the specifications regulated by the Standard EN-16723 in Europe (Wellinger, 2017). To this end, there are physical-chemical technologies commercially available for CO_2 removal such as water/chemical/organic scrubbing, pressure swing adsorption, cryogenic or membrane separation. Recent biotechnologies based either on photosynthetic carbon fixation coupled to H_2S oxidation by algal-bacterial consortia or hydrogenotrophic CO_2 reduction to methane constitutes more sustainable approaches than the aforementioned technologies, but are still in an embryonic stage (Ángeles Torres et al., 2020).

Anaerobic digestion is not only regarded as a platform for renewable energy production but also for the recycling of nutrients present in the digestate, which can be used as a biofertilizer or soil improvement agent. Indeed, Europe has just announced the adoption of new regulations on soil that will allow the use of high-quality digestate to aid ecological restoration of soils (Giacomazzi, 2021).

Over the past decade, the number of operational biogas plants in Europe has increased from ≈10500 to almost 19000 **(Fig. 1.4)**. Germany stands as the clear-cut leader with almost 11300 biogas plants (140 plants per million of inhabitants) followed by Italy and United Kingdom. Relative to their population, Switzerland and the Czech Republic are right behind Germany in number of plants per capita, with 77 and 54 plants per million of inhabitants, respectively (EBA, 2020). This growth took place mainly within the first half of the decade (+ 66%), whereas from 2016 to 2019 the sector has experienced a significant deceleration and stabilization in the biogas production capacity and number of plants (EBA,

2018, 2020) **(Fig. 1.4).** This can be attributed to the new regulations limiting the use of energy crops for biogas production (the main anaerobic digestion feedstock in Germany) or to the reduction in tax incentives/compensation rates devoted to electricity production from biogas (Scarlat et al., 2018). In terms of electricity generation, there was a similar trend, with stagnation over the past four years. In 2019, 64 TWh (out of the 167 TWh generated from biogas worldwide) were produced in Europe, from which 66% were delivered in agricultural-based facilities, 14% in landfills and 8% in sewage sludge-based plants (EBA, 2020).

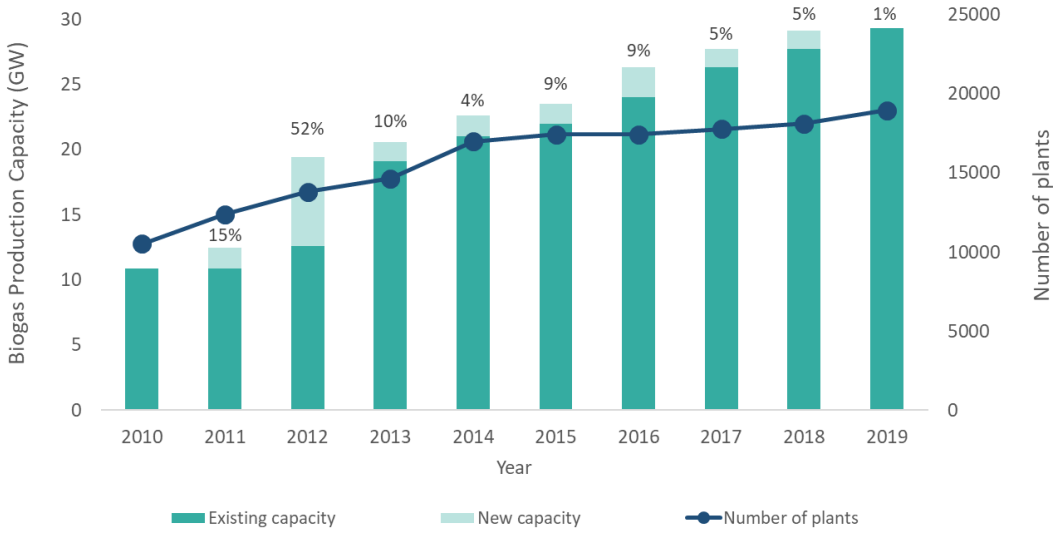

Fig. 1.4 *Biogas production capacity and number of plants in Europe (Adapted from EBA 2018, 2020)*

Conversely, the capacity of the sector relative to installed electricity capacity experienced a steady increase worldwide over the past decade according to the International Renewable Energy Agency, reaching 20150 MW by the end of 2020 **(Fig. 1.5)**. With an installed power capacity of 13826 MW in 2020, Europe is clearly the region leading the global biogas market, followed by the United States (2637 MW) and Asia (1957 MW) (IRENA, 2021). Energy crops were the main feedstock in Europe although more restricted policies are shifting primary choice towards agricultural residues and livestock waste. On

the other hand, biogas production in China and the United States comes mostly from animal manure and municipal solid waste, respectively (Iglesias et al., 2021).

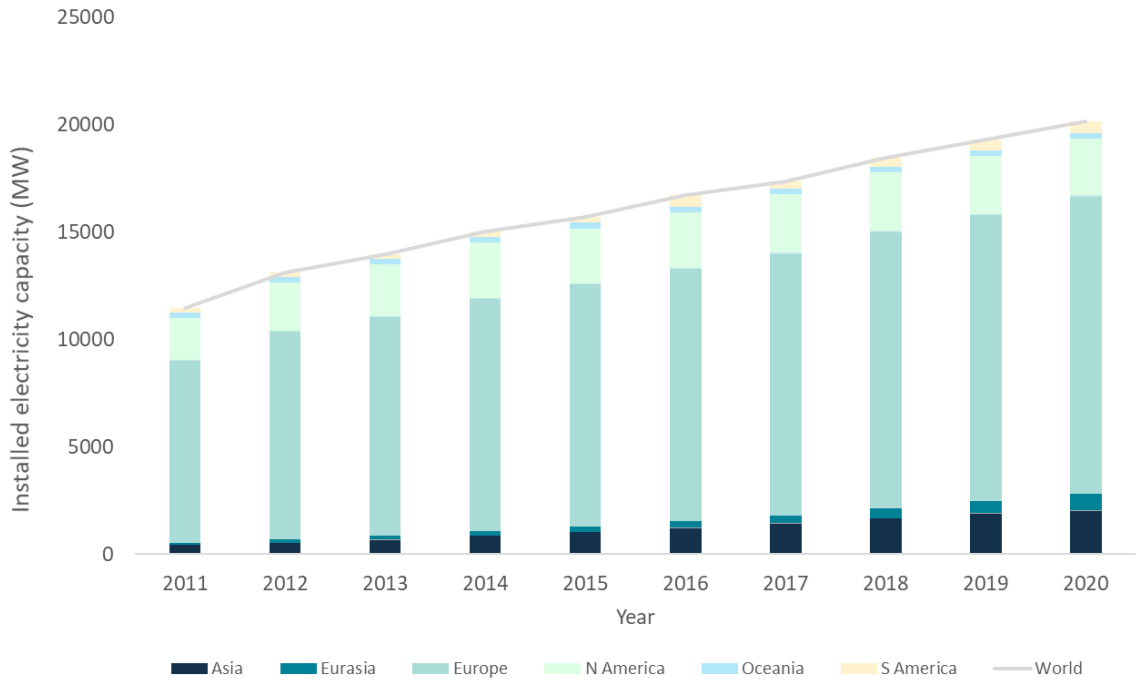

Fig. 1.5 *Worldwide power capacity by regions according to IRENA statistical report (IRENA, 2021)*

1.2.2 Future prospects of biogas. The biogas biorefinery concept

In the context of its long-term strategy towards developing a sustainable economy and meeting the Paris Agreement (global warming target below 1.5ºC), the European Commission has set an ambitious GHG emissions reduction target of at least 55% and 80% by 2030 and 2050, respectively, compared with 1990 levels (CE, 2020). As there is extraordinary room for growth, the biogas industry can play a key role in climate change mitigation by avoiding uncontrolled carbon emissions through the management of wastes combined with the generation of bioenergy and value-added chemicals. More specifically, the World Biogas Association recently reported that the global untapped potential for energy production from all feedstock combined is of ≈1040 Mtoe, which would correspond to a reduction of 3800 Mt CO_2 eq. per year (≈12% of global emissions). This energy could

satisfy up to a 9% of the primary energy consumption and replace up to 37% of the natural gas consumption if used as biomethane (WBA, 2019). Likewise, the International Energy Agency set the untapped potential value in 570 and 730 Mtoe for biogas and biomethane, respectively (IEA, 2020) **(Fig. 1.6)**.

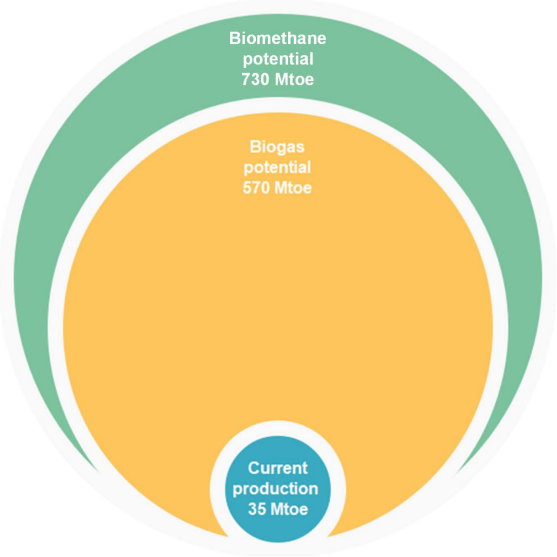

Fig. 1.6 *Biogas and biomethane potential. Adapted from IEA (2020)*

Beyond conventional uses, the utilization scope of biogas can be expanded by either its upgrading into biomethane (as aforementioned) or by turning biogas (chemically or biologically) into other compounds of interest. Therefore, a biogas biorefinery approach integrating innovative valorization strategies opens an opportunity window for biogas market to boost its growth.

Unlike the biogas industry, the biomethane market has experienced a continuous growth over the past decade. Over 95 new plants started operation during 2019, corresponding to the greatest increase (15%) to date and making up a total of 725 plants in operation across Europe (EBA, 2020). In terms of biomethane production, there was a steep increase from 0.8 TWh in 2011 to 25.7 TWh in 2019. Both sectors combined, biogas and biomethane, are expected to double by 2030, achieving a production of 467 TWh, and to quadruple by 2050 (BioenergyInternational, 2021). Upgrading followed by liquefaction or compression for the production of liquefied (bio-LNG) or compressed (bio-CNG)

biomethane is becoming one of the most innovative applications in the sector for large scale plants, and of special interest when there is no access to the gas network (WBA, 2021). Biomethane plants are also implementing technology to capture and/or store bio-CO_2 to be used in industrial processes, greenhouses or algae production (Kapoor et al., 2020).

Other emerging utilizable form of biogas is as feedstock of microbial cell factories for its bioconversion into value-added products. Methanotrophs, which will be further described in the following section (Section 1.3), can be exploited as biocatalysts for the generation of a varied portfolio of products including biopolymers such as polyhydroxyalkanoates (see Section 1.1.2), single cell protein (SCP), ectoine/hydroxyectoine, exopolysaccharides (EPS), lipids and methanol via methane bioconversion (Cantera et al., 2019; Sahoo et al., 2021). A scheme of the biogas biorefinery concept encompassing physical, chemical and bioconversion processes is pictured in **Fig. 1.7**.

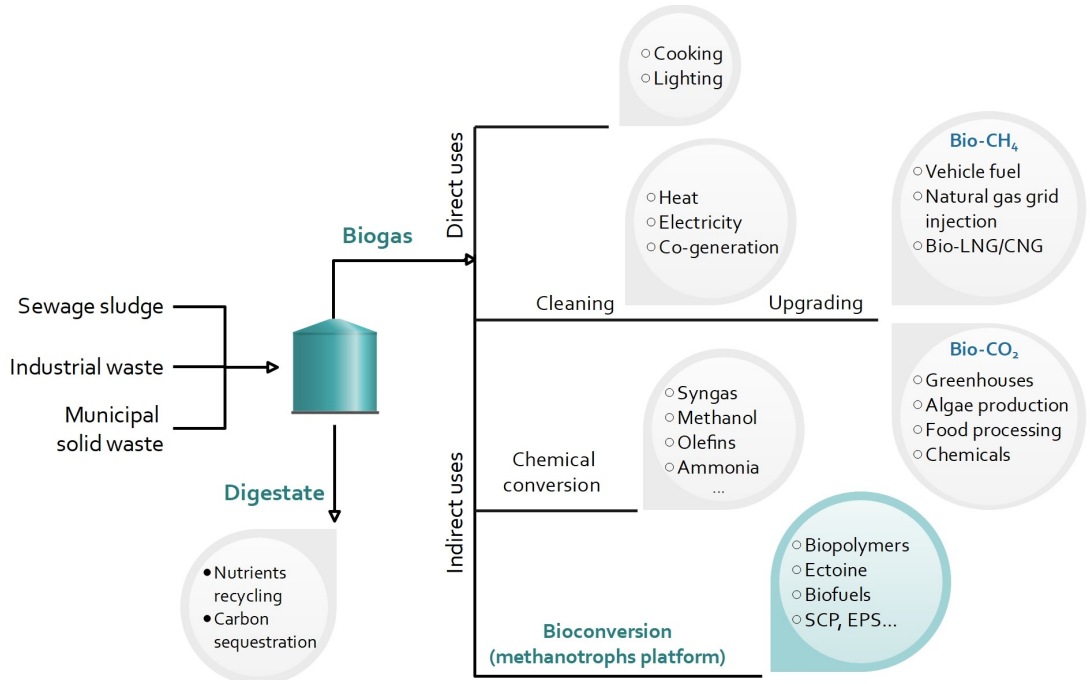

Fig. 1.7 *Schematic diagram of an integrated biogas biorefinery approach.*

1.3 Aerobic methanotrophy

1.3.1 Methane oxidizing bacteria

Aerobic methane oxidizers are methylotrophic microorganisms with the ability to oxidize CH_4 in the presence of O_2 and use it as their main carbon and energy source. Despite most aerobic methanotrophs are bacteria, other microorganisms such as yeasts, fungi and green microalgae have been also tentatively proposed as methane oxidizers (Lopez et al., 2013). Additionally, anaerobic oxidation of methane (AOM) can be conducted by anaerobic archaea and bacteria in marine sediments, where the process occurs coupled to sulfate, nitrate, nitrite, manganese and iron reduction (Cui et al., 2015). Aerobic methane oxidizers, herein after named methanotrophs, are widely distributed in environments such as wetlands, peat bogs, forests, rice paddies, groundwater, landfill cover soils, sewage sludge or marine sediments, and represent the major terrestrial sink for CH_4 (Rostkowski et al., 2013). Their growth preferentially occurs in the interphase between aerobic and anaerobic zones, where significant CH_4 fluxes are present (Semrau et al., 2010).

Methanotrophs are usually classified into three groups according to their physiological and morphological characteristics: type I, type II and type X methanotrophs (Karthikeyan et al., 2015). Type I includes methanotrophs that i) present intracytoplasmatic membranes as bundles of vesicular discs, ii) use the ribulose monophosphate (RuMP) pathway for carbon assimilation and iii) contain phospholipid fatty acids of 14/16 carbons length. Type II methanotrophs are characterized by i) an intracytoplasmic membrane aligned along the peripheral part of the cell, ii) the use of the serine pathway for carbon assimilation and iii) phospholipid fatty acids of 18 carbons length. On the other hand, type X (considered as a subset of type I) share characteristics of both type I and II methanotrophs, thus including the RuMP pathway to assimilate formaldehyde and using the enzyme ribulose biphosphate carboxylase from the serine pathway to fix CO_2 (Knief, 2015; Lopez et al., 2013). The current classification of known aerobic methanotrophs based on 16S rRNA encloses a wide phylogenetic distribution within two different phyla, Proteobacteria (subdivisions α- and γ-

Proteobacteria) and Verrucomicrobia. The most representative genera within the α-Proteobacteria phylum are *Methylocystis*, *Methylosinus*, *Methylocella* and *Methylocapsa*, which are type II methanotrophs and cluster within *Methylocystaceae* and *Beijerinckiaceae* families. On the other hand, those methanotrophs within γ-Proteobacteria (e.g. *Methylomonas*, *Methylobacter*, *Methylosarcina* or *Methylococcus* genera, among others) belong to the *Methylococcaceae* family and are known as type I methanotrophs. Finally, methanotrophs from Verrucomicrobia phylum are essentially affiliated within the *Methylacidiphilacecae* family, and more specifically to the *Methylacidiphilum* and *Methylacidimicrobium* genera (Pawlowska, 2014; Semrau et al., 2010). Based on their different ecophysiology and taxonomical affiliation, *Verrucromicrobia* methane oxidizers have been recently referred as type III methanotrophs (Sazinsky and Lippard, 2015). Furthermore, the phylogenetic relationships between methanotrophs are usually examined as a function of the enzyme MMO, which catalyses the conversion of methane to methanol. Thus, the particulate methane monooxygenase (pMMO) is found in most methanotrophs and is located in the cytoplasmatic membrane, while the soluble methane monooxygenase (sMMO) is present in the cytoplasm and can be expressed either as the sole form of MMO or together with pMMO. The enzyme sMMO has been traditionally associated with type II methanotrophs, though few genera of type I methanotrophs with the capability to synthesize sMMO have been recently identified (Knief, 2015).

Methane biodegradation comprises a multistage process, where the monooxygenase-mediated CH_4 oxidation to methanol represents the first step-reaction. Formaldehyde and formic acid are the successive metabolic intermediates formed, thus eventually ending up with the production of CO_2 (Lopez et al., 2013). It must be stressed that formaldehyde may be either converted to formic acid or used as building blocks for the synthesis of new cell material through the RuMP pathway in type I/X methanotrophs, or through the serine pathway in type II methanotrophs (Pawlowska, 2014). Notwithstanding, methanotrophs cannot achieve a complete conversion of methane into microbial biomass since assimilatory pathways result in a net production of at least 12 % CO_2 according to previous studies (Bédard and Knowles, 1989).

Methanotrophic growth stoichiometry may be expressed:

1. Based on the oxygen and nitrogen demand (Eq. 1.1 and 1.2, for the RuMP and the serine pathways, respectively) (Karthikeyan et al., 2015):

$$CH_4 + 1.5O_2 + 0.12NH_4^+ \rightarrow 0.12(C_4H_8O_2N) + 0.53CO_2 + 1.71H_2O + 0.12H^+ \quad (1.1)$$

$$CH_4 + 1.57O_2 + 0.10\ NH_4^+ \rightarrow 0.10(C_4H_8O_2N) + 0.59CO_2 + 1.75H_2O + 0.10H^+ \quad (1.2)$$

2. As a function of the fraction of electrons required by the electron donor for growth. According to Rostkowski et al. (2013), methanotrophic cell synthesis implies the use of a fraction of electrons (f_e) from CH_4 to reduce O_2 to H_2O (thus producing energy), while the remaining fraction (f_s) is devoted to cell synthesis. Thus, it can be assumed that CH_4 metabolism requires the use of O_2 as terminal electron acceptor to produce energy (Eq. 1.3), and as reactant in the initial attack on CH_4 within the electron donor reaction (Eq. 1.4):

$$f_e\,(1/4\ [O_2 + 4H^+ + 4e^- \rightarrow 2H_2O]) \quad (1.3)$$

$$1/4[CH_4 + O_2 \rightarrow CO_2 + 4H^+ + 4e^-] \quad (1.4)$$

The nature of the micro- and macronutrients greatly influences the stoichiometry of the cell synthesis half reaction, which can be given as in Eq. (1.5) when nitrate is the sole nitrogen source and the empirical formula $C_5H_7O_2N$ for biomass is assumed:

$$f_s\,(1/28\ [5CO_2 + NO_3^- + 29H^+ + 28e^- \rightarrow C_5H_7O_2N + 11H_2O]) \quad (1.5)$$

Thus, the overall stoichiometric reaction for the microbial CH_4 biodegradation (Eq. 1.6) can be obtained by summing up Eq. (1.3), (1.4) and (1.5):

$$1/4\ CH_4 + (1/4 + f_e/4)O_2 + (f_s/28)\ NO_3^- + (29/28f_s + f_e\ -1)H^+ \rightarrow$$
$$(1/4 - 5f_s/28)CO_2 + (f_e/2 + 11f_s/28)H_2O + (f_s/28)C_5H_7O_2N \quad (1.6)$$

It can be then concluded that the number of moles of O_2 consumed per mole of CH_4 oxidized is $1 + f_e$, where $f_e + f_s = 1$. In addition, the biomass yield (Y_X, expressed as gTSS per gCH_4) depends on the nitrogen source and can be calculated as $113f_s/28{:}4$ when nitrate is employed.

Both Monod and Michaelis-Menten models are commonly used to describe microbial CH_4 oxidation kinetics. However, the different experimental setups and models used for the estimation of the kinetic parameters usually hamper direct comparison of the data available in literature. Among the kinetic parameters, the Monod constant (K_S) characterizes the affinity of microorganisms for the substrates, and typically ranges from 1.0×10^{-6} to 4.7×10^{-4} M in the particular case of CH_4. pMMO-bearing bacteria, usually type I methanotrophs, have been reported to exhibit a higher affinity for CH_4 (lower K_S values) than those expressing sMMO (Amaral and Knowles, 1995; López et al., 2014). Moreover, the maximum specific biodegradation rates (q_{max}) for CH_4 typically range from 4.16×10^{-5} to 1.3×10^{-4} $gCH_4\ gX^{-1}\ h^{-1}$ and are greatly influenced by culture conditions (AlSayed et al., 2018a; Cantera et al., 2016b). In this context, microorganisms with a high q_{max} and a high affinity for CH_4 (low K_S) are desirable to guarantee an efficient biocatalytic activity and to reduce the start-up period of bioreactors devoted to CH_4 mitigation. However, it must be noted that most CH_4 biodegradation kinetic studies reported to date were carried out at high biomass concentrations, which did not ensure the absence of mass transport limitations and, therefore, the validity of the kinetic parameters obtained (Lopez et al., 2013). Regarding the CH_4 biodegradation efficiency provided through the two aforementioned metabolic pathways, the RuMP pathway (from type I methanotrophs) provides a higher CH_4 conversion efficiency since only 1 ATP molecule is required to assimilate 3 formaldehyde molecules during CH_4 oxidation. Conversely, despite type II methanotrophs are superior in terms of CH_4 storage as phospholipid fatty acids and

polyhydroxyalkanoates (PHAs), they require 3 ATP and 2 NADH molecules to fix 2 formaldehyde and 1 CO_2 molecules through the serine pathway (Karthikeyan et al., 2015). Hence, type I methanotrophs tend to prevail over type II strains, unless cultivation conditions ensure a competitive situation for the latter (AlSayed et al., 2018b).

Main driving forces enabling the selection of either type I or type II methanotrophs from mixed cultures are O_2 and CH_4 concentrations, temperature, pH, nitrogen source and concentration, and the concentration of micronutrients such as copper. In this context, it must be highlighted that an appropriate selection strategy to enrich type II over type I methanotrophs in mixed methanotrophic cultures is crucial prior PHA accumulation stages. Hence, according to the CH_4 biodegradation stoichiometry aforementioned, molar O_2:CH_4 ratios should be maintained ≥ 1.5:1 to enable CH_4 oxidation (Bédard and Knowles, 1989). However, previous studies demonstrated that low O_2:CH_4 ratios may favour the growth of type II methanotrophs, while high O_2:CH_4 ratios can promote the growth of type I methanotrophs (Henckel et al., 2000). These findings support the hypothesis that the enzymes sMMO (predominantly found in type II methanotrophs) and pMMO are respectively expressed at high and low CH_4 concentrations (van Teeseling Muriel et al., 2014). In addition, microbial kinetics of the type II methanotrophs *Methylosinus trichosporium* OB3b and *Methylocystis parvus* OBBP were recently studied under different oxygen partial pressures and nutrient sources (0.10 – 0.40 atm) (Rostkowski et al., 2013). These authors found that both strains clearly showed sensitivity to oxygen when molecular nitrogen was used as nitrogen source, which was attributed to the inactivation of the nitrogenase enzyme of these strains.

To date, studies assessing the influence of temperature as a selective pressure for either type I or type II methanotrophs have not been reported. In this regard, methanotrophs usually exhibit maximum biodegradation rates under mesophilic conditions (25-30 ºC), though thermotolerant and thermophilic type I methanotrophs such as *Methylotermus*, *Methylocaldum*, *Methylococcus* genera or several *Verrucomicrobia* strains have been isolated from active silts, hot springs and aquifers and volcanic soils, with optimal growths

in the range of 42-65 ºC (Knief, 2015; Pol et al., 2007). Similarly, psychrophilic strains of *Methylobacter*, *Methylosphaera* and *Methylomonas* have been isolated from tundra soils, Antarctic meromictic lakes and deep igneous groundwater, exhibiting an optimal growth range of 3.5-15 °C (Kalyuzhnaya et al., 2013; Pol et al., 2007).

Regarding the pH, most methanotrophs preferentially grow at neutral values (6.8-7.5), although recent studies have demonstrated that acidic environments promote the selection of type II methanotrophs over type I methanotrophs in mixed cultures (**Table 1.3**). (Pieja et al., 2011). Not only species belonging to the *Mehylocapsa* genera (obligate acidophilic), but also species from the *Methylocella* and *Methylocystis* genera tolerate low pH and have been found optimally growing under pH values of 5-6 and 3.6-4.5, respectively (Lopez et al., 2013; Pieja et al., 2011). The higher tolerance of type II methanotrophs to low pH has been attributed to their CO_2 requirements as an input of the serine cycle (Karthikeyan et al., 2015). In contrast, the CH_4 biodegradation ability of the halophilic type I *Methylomicrobium alcaliphilum* strain 20Z is enhanced at pH values as high as 9.0 (Kalyuzhnaya et al., 2013).

Solely type II methanotrophs (and some type I genera belonging to *Methylosoma, Methylosphaera* and *Methylococcus* genera) have demonstrated the capability to fix N_2, since they possess the *nifH* genes for the synthesis of the nitrogenase enzyme (Rostkowski et al., 2013). Moreover, nitrate and ammonium are the preferred nitrogen sources over nitrite for both type I and II methanotrophs (Dunfield and Knowles, 1995). Interestingly, a shift in a methanotrophic consortium towards a type II-dominated culture was feasibly achieved in a fluidized bed reactor (FBR) by using N_2 (instead of nitrate or ammonium) as a nitrogen source and decreasing the dissolved oxygen levels (Pfluger et al., 2011). However, several studies have successfully addressed the enrichment of type II methanotrophs (i.e. *Methylocystis* species, >60 % abundance) from fresh activated sludge even in less than one month using ammonium as nitrogen source (Fergala et al., 2018; Myung et al., 2015). In this regard, it is noteworthy that the maximum specific biodegradations rates reported in these studies were obtained when concentrations of

ammonium as low as 10 mM were employed for cultivation. These results are consistent with those findings reported by our group, since methanotrophic enrichments from landfill samples under different ammonium concentrations (0-200 mM) exhibited the highest specific biodegradation rates and the highest type II abundances at the lowest ammonium concentrations (q_{max} of $7.8 \times 10^{-4} \pm 10^{-5}$ gCH_4 gX^{-1} h^{-1} and >80 % *Methylocystis* at 4 mM) (**Table 1.3**) (López et al., 2018). Ammonium inhibition in methanotrophs has been reported to occur as a result of toxicity due to either nitrite or hydroxylamine accumulation from ammonium oxidation, which explains the significance of tuning the concentration of this nitrogen source (Nyerges et al., 2010). Despite nitrate supports the maximum specific growth rates reported in literature for methanotrophs, the absence of specificity towards type II methanotrophs makes this nitrogen source not suitable for enrichment processes. Overall, it can be stated that type I methanotrophs are dominant in environments under low CH_4/N conditions, whereas type II prevail under high CH_4/N conditions and outcompete type I methanotrophs under nutrient-limiting conditions (e.g. N-limitation) (Amaral and Knowles, 1995; Pieja et al., 2011).

Micronutrients are also a key parameter for methanotrophic metabolisms. In this context, copper seems to control the expression of the genes encoding for the MMO enzyme and positively regulate the activity of the enzymes pMMO and sMMO (Semrau et al., 2010). However, copper concentration in the cultivation broth must be adjusted in order to maintain copper homeostasis and prevent metal toxicity. Most methanotrophs grow optimally at copper concentrations lower than 4.3 mM, though enzymatic assays have demonstrated that sMMO in type II methanotrophs is properly synthesized at low Cu^{2+} concentrations (below 0.8 mM) (Bender and Conrad, 1995; Graham et al., 1993; Semrau et al., 2010). In this regard, the expression of the *pmoA* gene (encoding a subunit of pMMO) has been observed at significant levels regardless of the Cu^{2+} concentration, though the transcript numbers increased concomitantly with the concentration of copper (Murrell et al., 2000). However, the absence of copper as selection criterion for type II methanotrophs seems not to be sufficient. In their study, Pieja et al. (2011) demonstrated that a combined lack of copper and use of a diluted mineral salts medium (10 %) promoted the selection of

type II methanotrophs from mixed inocula, as well as the combined use of low pH values and carbonate (**Table 1.3**).

Table 1.3 *Reported enrichment culture conditions for the selection of type II methanotrophs.*

Reference	System	Inoculum	O_2:CH_4	N source (mM)	Other conditions[a]	q_{max} ($gCH_4\ gTSS^{-1}\ h^{-1}$)	Microbial selection (abundance)
Graham et al. (1993)	CSTR[b]	*M. trichosporium* OB3b/*M. albus* BG8 co-culture	i) 4:1 ii) 1:10	i) NO_3^- (1) ii) NO_3^- (0.5)	i) No Cu ii) -	-	i) *M. trichosporium* OB3b (>85 %) ii) *M. trichosporium* OB3b (≈100 %)
Nyerges et al. (2010)	Batch	*Methylocystis* sp./*Methylomicrobium album* co-culture	1:5	NH_4^+ (50)	-	-	*Methylocystis* sp.
Pfluger et al. (2011)	FBR[c]	Hot spring sediments	1:4	N_2	-	-	*Methylocystis*/*Methylosinus*
Pieja et al. (2011)	Batch	Activated sludge	1:1	NO_3^- (10)	i) No Cu, diluted medium (10 %) ii) pH 5, carbonate at 10 mM	-	*Methylocystis*/*Methylosinus*
Myung et al. (2015)	Fed-batch	Activated sludge	1.5:1	NH_4^+ (nd)	30 ºC	2.1×10^{-2}	*Methylocystis* (>70 %)
López et al. (2019a)	Fed-batch	Mixed landfill sample	1:5	NH_4^+ (4)	-	7.8×10^{-4}	*Methylocystis* (>80 %)

[a]Unless otherwise specified, temperature and pH were set at standard values of 25 ºC and 6.8-7.5, respectively;
[b]CSTR: Continuous stirred tank reactor;
[c]FBR: Fluidized bed reactor

1.3.2 Polyhydroxyalkanoate biosynthesis by type II methane oxidizing bacteria

The ability of accumulating PHAs from methane under nutrient limiting conditions correspond to bacteria belonging to the α-Proteobacteria class (also known as type-II methanotrophs), which assimilate C1 compounds via the serine pathway (Pieja et al., 2011), unlike the RuMP cycle, typically found in γ-Proteobacterial methanotrophs. Methane conversion (**Fig. 1.8**) is initiated by the enzyme MMO that mediates the production of methanol, which is further oxidized into formaldehyde by the enzyme methanol dehydrogenase (MDH) (containing the pyrroloquinoline quinone (PQQ) as catalytic center) (Khmelenina et al., 2018). In type II methanotrophs, formaldehyde can be metabolized into formate via two pathways, involving the participation of tetrahydromethanopterin (H_4MPT) or tetrahydrofolate (H_4F)-dependent enzymes, and whereby the substrate of the serine cycle, methylene–H_4F, is generated (Semrau et al., 2018; Vorholt, 2002). Methylene–H_4F reacts with glycine to form serine. The serine route ultimately yields malyl-CoA, which in turn produces glyoxylate and acetyl-CoA. The latter either enters the tricarboxylic acid (TCA) cycle under nutrient sufficient conditions, or the PHA biosynthetic pathway under nutrient limiting conditions (Strong et al. 2016). More precisely, the presence of the coenzyme A, which is released from the TCA cycle under nutrient sufficient conditions and acts as inhibitor of one of the key enzymes (β-ketothiolase) of the PHA cycle, determines the active metabolic route (López et al., 2019b). In the PHA pathway, the β-ketothiolase enzyme (*phaA* gene) converts acetyl-CoA into acetoacetyl-CoA, followed by the production of hydroxyacyl (HA)-CoA thioester by the acetoacetyl-CoA reductase enzyme (*phaB* gene). Subsequently, the enzyme PHA synthase (*phaC* gene) enables PHA formation via ester linkages. It must be underlined that type II methane oxidizing bacteria produce solely one type of PHA, poly-3-hydroxybutyrate (PHB or P3HB), when grown in CH_4 as the sole energy and carbon source (Pfluger et al., 2011;Pieja et al., 2017). The role of the internally accumulated PHB and the mechanism of

its consumption by the methanotrophic bacteria is explained elsewhere (Rodríguez et al., 2020). The theoretical yield for PHB accumulation reported in literature varies from 0.54 to 0.67 gPHB gCH_4^{-1} (Asenjo and Suk, 1986; Yamane, 1993). Higher yields result from not taking into account the regeneration of $NADP^+$ into NADPH needed for acetoacetyl-CoA production during PHB synthesis, which is likely mediated by isocitrate dehydrogenase in the TCA cycle (Yamane, 1993).

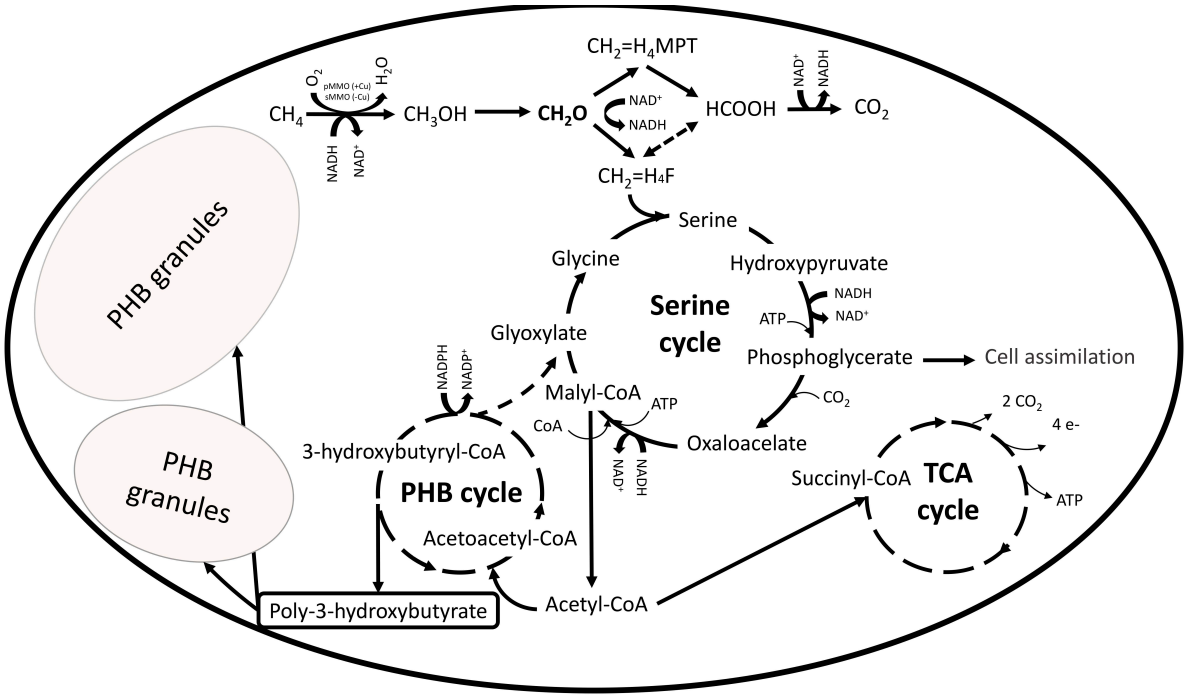

***Fig. 1.8**. Schematic representation of methane oxidation and PHB synthesis in type-II methanotrophs.*

Experimental yields and PHB contents strongly depend on the culture enrichment conditions and the feast-famine strategy selected, which typically consists of two-steps: (1) a period of cell growth under nutrient sufficient conditions and (2) a period of nutrient deprivation triggering PHA synthesis. The genus *Methylocystis*, which predominates in most of the enriched mixed cultures, and to a lesser extent the genus *Methylosinus,* are the genera most intensively studied for PHA synthesis due to their potential to produce bioplastics (Cantera et al., 2019; López et al., 2019b). In this regard, PHB contents up to 60 (Rostkowski et al., 2013), 54 (López et al., 2018) and 51% (on a dry weight basis)

(Zhang et al., 2017) have been reported for the species *Methylocystis parvus* OBBP, *Methylocystis hirsuta* CSC1 or *Methylosinus trichosporium* OB3b, respectively. Although the use of methane-utilizing mixed cultures seems to be preferred due to the potential benefits of a stable microbial community, under non-aseptic conditions the use of pure strains is foreseen to be viable for continuous PHA production.

The influence of environmental factors (e.g. nutrient requirements and limitation, pH, temperature or O_2:CH_4 ratio) on PHB cell synthesis from CH_4 has received significant attention over the past decade. Accordingly, nitrogen and phosphorous are the nutrients inducing higher PHA accumulations under deficiency, although the effect of magnesium, sulfur, potassium or iron limitation has been also investigated with distinct results depending on the type of limitation and strain (**Table 1.4**). Interestingly, it has been observed that a simultaneous limitation of N and P results in a reduced PHB synthesis, likely due to the lack of reducing equivalents, which are required for biopolymer synthesis (Zhang et al., 2017). Acidic environments provide a competitive scenario for the selection of type II methanotrophs among *Proteobacteria*. In this context, higher PHB accumulations were observed in methanotrophic communities enriched from activated sludge at low pH values (8 wt% at pH 4 and 14 wt% at pH 5) whereas no PHB was detected at higher pH values (Pieja et al., 2011). Similarly, PHB contents of 38 and 42% were recorded at pH 7 and 5.5, respectively, in mixed cultures enriched from *Sphagnum* with an abundance of 85 – 90% in the genus *Methylocystis* (Pérez et al., 2019).

A promising feature of these microorganisms is their ability to perform co-polymerization of 3-hydroxybutyrate (3HB) with alternative hydroxyalkanoate (HA) monomers, thus allowing the biosynthesis of co-polymers such as poly-3-hydroxybutyrate-*co*-hydroxyvalerate (PHBV) with superior mechanical properties (lower melting and glass transition temperatures, and higher elongation-to-break ratios) (Pieja et al., 2017; Strong et al., 2016). In this regard, process supplementation with valerate under nutrient-limiting conditions supported a HV fraction in the co-polymer of 60 mol% in *M. parvus* OBBP and *Methylocystis* sp. WRRC1 (Cal et al., 2016; Myung et al., 2016), and 25 mol% in *M. hirsuta*

(López et al., 2018). Recent approaches focused on the molecular design of the co-polymer through the addition of ω-hydroxyalkanoates monomers as co-substrates. Myung et al. (2017) successfully tailored PHAs consisting of monomer units other than 3HB and 3HV (poly(3-hydroxybutyrate-*co*-4-hydroxybutyrate), poly(3-hydroxybutyrate-*co*-5-hydroxyvalerate-*co*-3-hydroxyvalerate) or poly(3-hydroxybutyrate-*co*-6-hydroxyhexanoate-*co*-4-hydroxybutyrate)) using the strain *M. parvus* OBBP under nitrogen limiting conditions. Apart from the direct co-polymer synthesis in methanotrophic cultures, other potential strategies for the production of versatile PHAs using CH_4 as primary feedstock include the use of a co-culture that promotes PHBV synthesis by accumulating species such as *Ralstonia eutropha* or downstream PHA modification, which would ultimately result in intensive and costly processes (Strong et al., 2016)

Table 1.4 *Reported PHA accumulation under different limiting conditions*

Reference	CH_4 source	Type-II MOB	Reactor / O_2:CH_4 atmosphere % (v/v)	Limiting nutrient	PHAs content (% w/w)	PHA yield ($g_{PHB}\ g_{CH4}^{-1}$)
Wendlandt et al. (2001)	Methane	*Methylocystis* sp. GB25	Stirred tank reactor 4:1	N / P / Mg	51 / 47 / 28	0.52 / 0.55 / 0.37
Helm et al. (2006)	Methane	*Methylocystis* sp. GB25 (> 86%)	Stirred tank reactor 3:1	P	46.2	-
Helm et al. (2008)	Methane	*Methylocystis* sp. GB25 (> 86%)	Stirred tank reactor 3:1	K / S / Fe	34 / 33 / 10	0.45 / 0.40 / 0.22
Zhang et al. (2008)	Methane (+ citric acid, 0.3 g L^{-1})	*Methylosinus trichosporium* IMV 3011	Serum vials 1:1 (air:CH_4)	N	38.1	
Rostkowski et al. (2013)	Methane	*Methylosinus trichosporium* OB3b/ *Methylocystis parvus* OBBP	Serum vials 1:1	N	45 / 60 (grown in N_2 and NH_4^+, respectively)	1.1 / 0.9
Sundstrom and Criddle (2015)	Methane	*Methylocystis parvus* OBBP	Microbioreactors 1:1	N (control) / N + Cu / N + Ca / N + K / N + P / N + Cu + Ca	18 / 35 / 39 / 28 / 31 / 49	-
Myung et al. (2016)	Methane (+ none, 3-HB, propionate, valerate)	*Methylocystis parvus* OBBP	Serum vials 1.5:1	N	50 / 60 / 32 / 54	-
Zhang et al. (2017)	Methane	*Methylocystis trichosporium* OB3b	Serum vials 1:1	N	51 / 45 / 32 (grown in NO_3^-/NH_4^+/N_2, respectively)	-
García-Pérez et al. (2018)	Methane	*Methylocystis hirsuta* CSC1	Serum vials 2:1	Mn / K / N / (N + Fe excess)	8 / 13 / 28 / 19	-
López et al. (2018)	Synthetic biogas (70% CH_4, 30% CO_2, 0.5 H_2S)	*Methylocystis hirsuta* CSC1	Serum vials ≈2:1	N (NO_3^-)	43.1	0.44

1.4 Bioreactors for biogas bioconversion

1.4.1 Biological technologies for improved CH_4 mass transfer

Conventional gas-phase packed bed bioreactors such as biotrickling filters or biofilters have been traditionally used for waste gas treatment. However, they are not suitable for bioproduct recovery since biomass growth as biofilm hinders any subsequent biomass downstream processing. Likewise, bioscrubbers exhibit a poor mass transfer for scarcely water soluble pollutants such as CH_4 (Henry's law constant (H) = C_g C_{aq}^{-1} = 29 at 25ºC) (López et al., 2013). In this regard, suspended-growth bioreactors are the most suitable configuration for the bioconversion of CH_4-laden gas streams into added-value byproducts and their subsequent recovery.

An improved mass transfer in these bioreactors can be achieved via an increase in the gas-liquid concentration gradient or in the volumetric mass transfer coefficient ($K_la_{G/A}$). To date, the classical approach to enhance gas pollutant mass transport in the so-called turbulent bioreactors was based on increasing the energy input to the bioreactor (in order to increase the turbulence in the liquid side) by intensive mixing and pumping. The most common turbulent bioreactors applied in industrial fermentative processes are mechanically stirred tanks and bubble column bioreactors with controlled nutrient feeding (Kraakman et al., 2011; Stone et al., 2017).

Stirred tank reactors (STRs) are vessels where the liquid broth is mechanically agitated by an impeller and the polluted gas is supplied via a sparger located at the bottom of the reactor (**Fig. 1.9a**). CH_4 removal efficiencies of 50-60% have been achieved at relatively low gas residence times of 4-10 min (Cantera et al., 2016a; Rocha-Rios et al., 2009). However, the high power to volume ratios, the difficulties of ensuring proper mixing and heat removal in large scale bioreactors, and the excessive shear stress are key drawbacks of this configuration (Stone et al., 2017).

In the particular case of *bubble column bioreactors (BCBs),* no mechanical agitation is provided, and the increase in gas pollutant mass transfer is achieved either using micropore diffusers or installing a concentric draft-tube (riser) in airlift bioreactors (ALR) (CalRecycle, 2013) (**Fig. 1.9b and c**). In spite of the lower power requirements compared to STRs, and therefore the higher cost-effectiveness of this configuration, non-homogeneous nutrients distribution due to poor liquid circulation, partial CH_4 utilization or bubble coalescence are common shortcomings of BCBs (López, 2019b; Stone et al., 2017).

The conventional approach of enhancing mass transport based on increasing the energy input to the bioreactor entails sometimes prohibitive operating costs during CH_4 bioconversion due to the intensive power consumption. In this context, operating strategies such as internal gas recycling or the addition of a non-aqueous phase, and novel reactor designs such as Taylor flow, forced loop and membrane diffusion bioreactors, have been recently tested as suspended-growth platforms capable of supporting high CH_4 mass transfer rates compared to conventional biotechnologies at low-moderate energy demands (Cantera et al., 2018; Stone et al., 2017) **Table 1.5** provides an overview of the elimination capacities achieved in conventional and novel types of bioreactors.

Operating strategies to promote mass transfer

Two-phase partitioning bioreactors (TPPBs) are characterized by the addition of an immiscible, non-volatile, biocompatible and non-biodegradable non-aqueous phase (NAP) with a high affinity for the target gas pollutant (Pittman et al., 2015). The NAP mediates an additional and more efficient pathway for the transport of CH_4 from the gas phase to the methanotrophic community (as a result of the increased concentration gradient) and an increase in the interfacial areas gas-water and gas-NAP. For instance, the addition of 10% v/v of silicone oil as NAP resulted in improved CH_4 removals of 30 and 47% in a STR and a BCB, respectively (Rocha-Rios et al., 2010; Rocha-Rios et al., 2011).

The implementation of an *internal gas recirculation* allows decoupling the actual gas residence time and turbulence in the microbial broth from the overall empty bed residence

time. Studies evaluating this strategy for CH_4 bioconversion into PHB have achieved CH_4 removal efficiencies over 70% at an empty bed residence time of 30 min and 0.50 $m^3_{gas}\ m^{-3}_{reactor}\ min^{-1}$ of internal gas-recycling rate, with a PHB content of up to 35% (García-Pérez et al., 2018).

Novel bioreactor configurations

Taylor flow bioreactors are capillary multi-channel units where the gas-liquid hydrodynamics consists of an alternating sequence of gas bubbles and liquid slugs. This segmented flow regime entails a high gas-liquid interfacial area along with a reduced liquid thickness and high turbulence at the liquid side (**Fig. 1.9d**), which translates into mass transfer coefficients equivalent to those of turbulent reactors at the expenses of one order of magnitude lower power consumptions. Nevertheless, their implementation for CH_4 abatement is limited to the study of Rocha-Rios et al. (2013) using only 1 capillary, where a 50% improvement in CH_4 removal was obtained compared to two-phase STRs at significantly lower reactor size and pressure drop.

Forced circulation loop bioreactors (FCLB) are a modification of ALRs that include internal and external recirculation pipes equipped with extra fittings to enhance gas-liquid mass transfer (López, 2019b) (**Fig. 1.9e**). For instance, one of the most innovative industrial bioreactors designed to improve CH_4 abatement and the production of single cell proteins is the U-Loop fermenter patented by UniBio A/S, which is capable of handling a large biomass concentration while providing a high gas-liquid mass transfer (Cantera et al., 2018).

Membrane diffusion bioreactors are based on the use of a new generation of low gas-resistance ultrafiltration membranes (pore size 0.1-0.01 μm) capable of supporting an efficient gas diffusion at low pressure drops, thus allowing unprecedentedly high gas-liquid interfacial areas (Matsuura et al., 2011). These gas diffusion membranes can be implemented into column and airlift bioreactors (under single phase or TPPB configurations) (**Fig. 1.9f**).

Table 1.5 *Representative studies reported to date on continuous CH_4 abatement in conventional and novel reactor configurations.*

Reference	Reactor configuration	System features/ Operating conditions	EC ($g\ m^{-3}\ h^{-1}$)	EBRT (min)	CH_4 inlet load ($g\ m^{-3}\ h^{-1}$)	Biocatalyst
Rocha-Rios et al. (2010)	Two-phase partitioning stirred tank reactor	500 – 800 rpm Silicon oil fraction: 0-10% (v/v)	20 ± 3 (500 rpm, 0%) 33 ± 1 (800 rpm, 0%) 41 ± 3 (500 rpm, 5%) 48 ± 4 (800 rpm, 10%)	4.8	65	Methanotrophic consortium
Rocha-Rios et al. (2011)	Two-phase partitioning airlift bioreactor	Internal gas recirculation (1 vessel volumes per min) Silicon oil fraction: 10% (v/v)	21.2 ± 0.8 (0 % v/v) 18.9 ± 0.8 (10 % v/v)	7.3	171	Enriched methanotrophic culture from activated sludge
Rocha-Rios et al. (2013)	Two-phase partitioning capillary bioreactor	Silicon oil fraction: 0-10% (v/v)	1.6 (0 % v/v) - 2.8 (10 % v/v)	N.A.	N.A.	*Methylobacterium organophilum* dominant in an enriched culture from activated sludge
Estrada et al. (2014)	Biotrickling filter	Internal gas recirculation (Q_R = 18 L min^{-1}) D = 0.27 d^{-1}	≈22.5	4	230	Enriched methanotrophic culture from activated sludge
Lebrero et al. (2015)	Two-phase partitioning biotrickling filters (R1 and R2)	Polyurethane foam as packing material	48.5 ± 7.2 (**R1**) 44.4 ± 4.7 (**R2**)	4	410 (**R1**) 440 (**R2**)	*Methylosinus sporium* culture in **R1** / Hydrophobic consortium in **R2**
Lebrero et al. (2016)	Fungal-bacterial biofilter	Compost as packing material	36.6 ± 0.7	18	40	*Graphium* fungus
Cantera et al. (2016a)	Single (R1) and two (R2)-phase stirred tank reactors	**R1**: 500 rpm, D = 0.35 d^{-1} **R2**: 250 rpm, D = 0.30 d^{-1} Silicon oil fraction: 60%	91.1 ± 1.9 (**R1**) 46.0 ± 3.6 (**R2**)	10	150	Enriched culture from activated sludge and fresh cow manure
López et al. (2018)	Biofilters	**R1:** Continuous **R2 and R2:** feast-famine	8.3 (**R1**) 11.3 (**R2**), 11.0 (**R3**)	17.1	109	Enriched culture from activated sludge
García-Pérez et al. (2018)	Bubble column bioreactor	Internal gas recirculation (R=15), D = 0.5 d^{-1}	35.2 ± 0.4	30	48	*Methylocystis hirsuta*

N.A. Not available

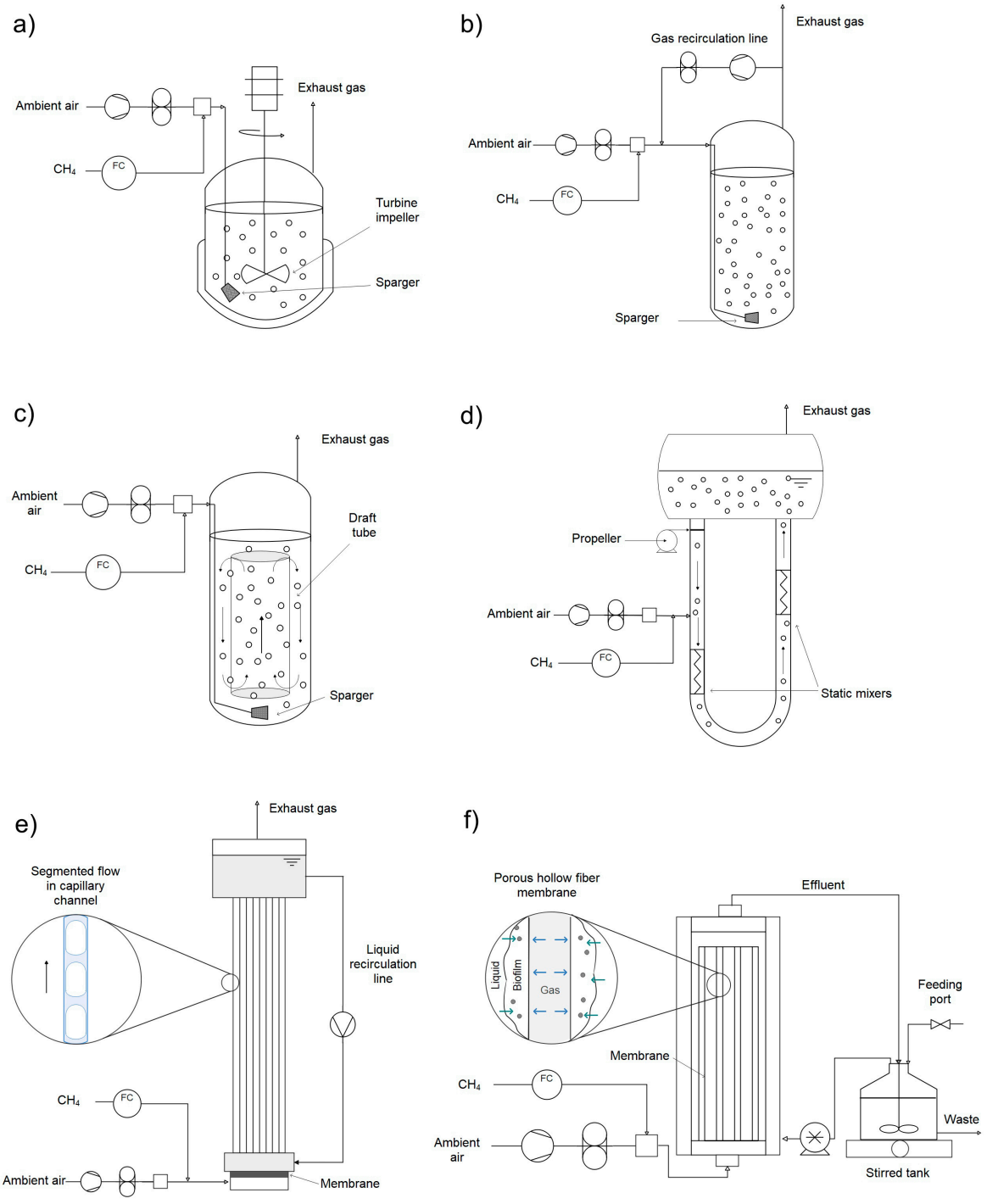

Fig. 1.9. *Schematic representation of the main bioreactor configurations suitable for biogas bioconversion: a) Stirred tank reactor (STR), b) Bubble column bioreactor (BCB) c) Airlift bioreactor (ALR), d) Taylor flow bioreactor, e) U-Loop fermenter and f) Membrane biofilm bioreactor*

1.4.2 Operating strategies for PHA production from biogas

As aforementioned, PHA production comprises usually a first stage of methanotrophic growth under balanced nutrient conditions and a second stage of biopolymer synthesis under nutrient limiting conditions. Thus, the optimal adjustment of process conditions to the physiological requirements of the microbial system is of major importance to enhance both methanotrophic growth and product synthesis (Kaur and Roy, 2015; Koller, 2018).

To date, PHA production coupled to methane utilization in high-mass transfer systems (section 1.4.1) has been attempted solely under **batch** or **cyclic/repeated batch processes**. To this purpose, pure strains or mixed consortia belonging to the genus *Methylocystis* have been cultivated. For instance, a two-stage batch process was conducted using *M. hirsuta* in a 200-mL BCB and a FCLB leading to accumulations of 40 and 50% w/w, respectively (Rahnama et al., 2012). This operation mode involves harvesting of the biomass after the growth period and re-suspension into a mineral media under nutrient deficiency for the subsequent PHB synthesis. Overall, batch processes result in low cell densities and PHB productivities as initial reactant concentrations are restricted to sub-inhibitory levels (Koller, 2018). Conversely, cyclic/repeated batch operation allows enhanced productivities by reducing downtime between batches. This strategy usually is approached by withdrawing a portion of the reactor and replacing that volume with fresh medium at intervals. Thus, the remaining broth serves as a seed for the subsequent cycle (Singhaboot and Kaewkannetra, 2015). Transient conditions between growth and synthesis phases occur within a single bioreactor (Blunt et al., 2018). Due to their similarity, some authors also refer to these systems as sequencing batch bioreactors (SBR). Pieja et al. (2012) evaluated for the first time the influence of sequential limitations of N, N + O_2, and N_2 + CH_4 on PHB production in a 4-L SBR under 24-h cycles. After 11 cycles, final PHA contents ranged from 11 to 17% w/w. Under a different feast-famine regime (24h:24h), García-Pérez et al. (2018) reported PHA accumulations up to 35% in a bubble column bioreactor with internal gas recirculation. These high contents may be attributed to a greater carbon source availability caused by an intense turbulence and to a prolonged deprivation period of

nitrogen. In this context, it is important to highlight that some works in literature do not clearly describe the biomass return carried out, which prevents a fair comparison among studies.

Two-stage processes comprising continuous and batch operation for growth and PHB accumulation phases, respectively, have been conducted in a 70-L pressurized STRs using *Methylocystis* sp. GB25 by Wendlandt et al. (2001) and (Helm et al. (2006, 2008) achieving PHB contents of up to 51%. Similarly, a two-stage process consisting of a long-term cycling and wasting regime (repeated-batch operation) for culture growth in a 2-L semi-continuous reactor followed by a 72-h period of N limiting conditions in 250-mL serum vials was implemented to evaluate the addition of odd-chain fatty acids. Maximum PHA contents of 14% were obtained when CH_4 and valeric acid were added. In contrast to the aforementioned works, the gas mixture in the latter study was provided into the headspace batchwise (Luangthongkam et al., 2019).

Unfortunately, process performance under continuous operation in relation to the gas phase has been scarcely addressed. Only García-Pérez et al. (2018) have reported the CH_4 abatement performance of the bioreactor, and no study in literature has employed other methane source than pure CH_4 or natural gas.

Single- or multi-stage continuous mode stands as the most attractive approach for PHA production, although it remains unaddressed for CH_4 bioconversion into PHA. Indeed, it is also regarded as a daunting challenge even for conventional carbon sources, where fed-batch is by far the most applied strategy (Blunt et al., 2018). Continuous processes, also imprecisely referred to as "chemostat" processes, can support high volumetric productivities and on-demand quality product on the monomeric level (Koller et al., 2018). In addition, as methane-driven PHA production is non-growth associated, a multi-stage approach confers the possibility of optimizing separately both growth and PHA synthesis stages. The dilution rate (D) is considered as one of the most critical parameters during process design, since exceeding the specific growth rate can lead to cell wash-out in the

bioreactor. Another critical factor that hinders CH_4-based PHA production is the high risk of microbial contamination (Kaur and Roy, 2015).

1.5 References

AlSayed, A., Fergala, A., Khattab, S. and Eldyasti, A. (2018a) Kinetics of type I methanotrophs mixed culture enriched from waste activated sludge. *Biochem Eng J* **132**, 60-67. doi:10.1016/j.bej.2018.01.003.

AlSayed, A., Fergala, A., Khattab, S., ElSharkawy, A. and Eldyasti, A. (2018b) Optimization of methane bio-hydroxylation using waste activated sludge mixed culture of type I methanotrophs as biocatalyst. *Appl Energy* **211**, 755-763. doi:10.1016/j.apenergy.2017.11.090.

Amaral, J.A. and Knowles, R. (1995) Growth of methanotrophs in methane and oxygen counter gradients. *FEMS Microbiol Lett* **126**(3), 215-220. doi:10.1111/j.1574-6968.1995.tb07421.x.

Ángeles Torres, R., Marín, D., Rodero, M.d.R., Pascual, C., González-Sanchez, A., de Godos Crespo, I., Lebrero, R. and Torre, R.M. (2020) Chapter 8 - Biogas treatment for H_2S, CO_2, and other contaminants removal. In: Soreanu, G. and Dumont, É. (eds) From Biofiltration to Promising Options in Gaseous Fluxes Biotreatment. Elsevier, 153-176. doi: 10.1016/B978-0-12-819064-7.00008-X.

Asenjo, J.A. and Suk, J.S. (1986) Microbial Conversion of methane into poly-β-hydroxybutyrate (PHB): Growth and intracellular product accumulation in a type II methanotroph. *J Ferment Technol* **64**(4), 271-278. doi: 10.1016/0385-6380(86)90118-4.

Axial. 2021. Deck Review with Danimer Scientific. *Axial* https://medium.com/@axialxyz/deck-review-with-danimer-scientific-ad515541e2d4 (Accessed: 19.10.2021).

Bédard, C. and Knowles, R. (1989) Physiology, biochemistry, and specific inhibitors of CH_4, NH_4^+, and CO oxidation by methanotrophs and nitrifiers. *Microbiol rev* **53**(1), 68-84. doi:10.1128/mr.53.1.68-84.1989.

Bender, M. and Conrad, R. (1995) Effect of CH_4 concentrations and soil conditions on the induction of CH_4 oxidation activity. *Soil Biol Biochem* **27**(12), 1517-1527. doi: 10.1016/0038-0717(95)00104-M.

BFA (2015) BFA White Paper. Responsible Bioplastics. Sustainable Sourcing and the Circular Economy, Bioplastic Feedstock Alliance.https://bioplasticfeedstockalliance.org/resources/ (Accessed: 12.09.2021).

BioenergyInternational (2021). New EBA report shows significant growth and potential for biomethane. https://bioenergyinternational.com/biogas/new-eba-report-shows-significant-growth-and-potential-for-biomethane (Accessed: 08.10.2021).

Bioplastics Magazine (2020) Newlight Technologies opens new commercial-scale AirCarbon production facility. 25.09.2020 https://www.bioplasticsmagazine.com/en/news/meldungen/20200925-Newlight-Technologies-opens-new-commercial-scale-AirCarbon-production-facility.php (Accessed: 08.09.2021)

Blunt, W., Levin, D.B. and Cicek, N. (2018) Bioreactor operating strategies for improved polyhydroxyalkanoate (PHA) productivity. *Polymers* **10**(11). doi:10.3390/polym10111197.

Boey, J.Y., Mohamad, L., Khok, Y.S., Tay, G.S. and Baidurah, S. (2021) A Review of the applications and biodegradation of polyhydroxyalkanoates and poly(lactic acid) and its composites. *Polymers* **13**(10). doi:10.3390/polym13101544.

Bugnicourt, E., Cinelli, P., Alvarez, V. and Lazzeri, A. (2014) Polyhydroxyalkanoate (PHA): Review of synthesis, characteristics, processing and potential applications in packaging. *EXPRESS Polym Lett* **8**, 791-808. doi:10.3144/expresspolymlett.2014.82.

Cal, A.J., Sikkema, W.D., Ponce, M.I., Franqui-Villanueva, D., Riiff, T.J., Orts, W.J., Pieja, A.J. and Lee, C.C. (2016) Methanotrophic production of polyhydroxybutyrate-co-hydroxyvalerate with high hydroxyvalerate content. *Int J Biol Macromol* **87**, 302-307. doi: 10.1016/j.ijbiomac.2016.02.056.

CalRecycle (2013) Bioplastics in California - Economic Assessment of Market Conditions for PHA/PHB Bioplastics Produced from Waste Methane, California, USA.https://www2.calrecycle.ca.gov/Publications/Download/1085.

Cantera, S., Bordel, S., Lebrero, R., Gancedo, J., García-Encina, P.A. and Muñoz, R. (2019) Bio-conversion of methane into high profit margin compounds: an innovative, environmentally friendly and cost-effective platform for methane abatement. *World J Microbiol Biotechnol* **35**(1), 16. doi:10.1007/s11274-018-2587-4.

Cantera, S., Estrada, J.M., Lebrero, R., García-Encina, P.A. and Muñoz, R. (2016a) Comparative performance evaluation of conventional and two-phase hydrophobic stirred tank reactors for methane abatement: Mass transfer and biological considerations. *Biotechnol Bioeng* **113**(6), 1203-1212. doi: 10.1002/bit.25897.

Cantera, S., Lebrero, R., García-Encina, P.A. and Muñoz, R. (2016b) Evaluation of the influence of methane and copper concentration and methane mass transport on the community structure and biodegradation kinetics of methanotrophic cultures. *J Environ Manage* **171**, 11-20. doi:10.1016/j.jenvman.2016.02.002.

Cantera, S., Muñoz, R., Lebrero, R., López, J.C., Rodríguez, Y. and García-Encina, P.A. (2018) Technologies for the bioconversion of methane into more valuable products. *Curr Opin Biotechnol* **50**, 128-135. doi: 10.1016/j.copbio.2017.12.021.

Castilho, L.R., Mitchell, D.A. and Freire, D.M. (2009) Production of polyhydroxyalkanoates (PHAs) from waste materials and by-products by submerged and solid-state fermentation. *Bioresour Technol* **100**(23), 5996-6009. doi:10.1016/j.biortech.2009.03.088.

EU (2020). Communication from the Commission to the European Parliament, the Council, the European Economic and Social Committee and the Committee of the Regions. Stepping up Europe's 2030 climate ambition. Investing in a climate-neutral future for the benefit of our people, Brussels, 17.9.2020. https://eur-lex.europa.eu/legal-content/EN/TXT/PDF/?uri=CELEX:52020DC0562&from=EN

Costa, S.S., Miranda, A.L., de Morais, M.G., Costa, J.A.V. and Druzian, J.I. (2019) Microalgae as source of polyhydroxyalkanoates (PHAs) — A review. *Int J Biol Macromol* **131**, 536-547. doi: 10.1016/j.ijbiomac.2019.03.099.

Cui, M., Ma, A., Qi, H., Zhuang, X. and Zhuang, G. (2015) Anaerobic oxidation of methane: an "active" microbial process. *MicrobiologyOpen* **4**(1), 1-11. doi: 10.1002/mbo3.232.

Chen, G.-Q. (2010) Plastics Completely Synthesized by Bacteria: Polyhydroxyalkanoates. In: Chen, G.G.-Q. (ed) Plastics from Bacteria: Natural Functions and Applications. Springer Berlin Heidelberg, Berlin, Heidelberg, 17-37. doi:10.1007/978-3-642-03287-5_2.

Choi, S.Y., Cho, I.J., Lee, Y., Kim, Y.J., Kim, K.J. and Lee, S.Y. (2020) Microbial polyhydroxyalkanoates and nonnatural polyesters. *Adv Mater* **32**(35), 1907138, 1-37. doi:10.1002/adma.201907138.

Directive (EU) 2019/904 of the European Parliament and of the Council of 5 June 2019 on the reduction of the impact of certain plastic products on the environment (OJ L *155*, 12.06.2019, p. 1-19).

Directive (EU) 2018/851 of the European Parliament and of the Council of 30 May 2018 amending Directive 2008/98/EC on waste (Text with EEA relevance) (OJ L *150*, 14.6.2018, p. 109-140).

Doi, Y., Kitamura, S. and Abe, H. (1995) Microbial synthesis and characterization of poly(3-hydroxybutyrate-co-3-hydroxyhexanoate). *Macromolecules* **28**(14), 4822-4828. doi:10.1021/ma00118a007.

Dunfield, P. and Knowles, R. (1995) Kinetics of inhibition of methane oxidation by nitrate, nitrite, and ammonium in a humisol. *Appl Environ Microbiol* **61**(8), 3129-3135. doi:10.1128/aem.61.8.3129-3135.1995.

EBA (2018) EBA Statistical Report 2018, European Biogas Association.https://www.europeanbiogas.eu/wp-content/uploads/2019/11/EBA_report2018_abriged_A4_vers12_220519_RZweb.pdf (Accessed: 03.10.2021).

EBA (2020) EBA Statistical Report 2020, European Biogas Association, Belgium.https://www.europeanbiogas.eu/eba-statistical-report-2020/ (Accessed: 03.10.2021).

EC (2020) Report from the Commission to the European Parliament and the Council on Progress of Clean Energy Competitiveness. Brussels, **953**. https://eur-lex.europa.eu/legal-content/EN/TXT/?uri=COM%3A2020%3A953%3AFIN.

Estrada, J.M., Lebrero, R., Quijano, G., Pérez, R., Figueroa-González, I., García-Encina, P.A. and Muñoz, R. (2014) Methane abatement in a gas-recycling biotrickling filter: Evaluating innovative operational strategies to overcome mass transfer limitations. *Chem Eng J* **253**, 385-393. doi: 10.1016/j.cej.2014.05.053.

EUBP (2018) What are bioplastics? Material types, terminology, and labels – an introduction, European Bioplastics, Berlin.

https://docs.european-bioplastics.org/publications/fs/EuBP_FS_What_are_bioplastics.pdf (Accessed: 23.08.21).

EUBP (2020a) Bioplastics - Facts and Figures, European Bioplastics.https://docs.european-bioplastics.org/publications/EUBP_Facts_and_figures.pdf (Accessed: 05.09.2021).

EUBP (2020b) Bioplastics market data, European Bioplastics.https://www.european-bioplastics.org/market/ (Accessed: 05.09.2021).

Fergala, A., AlSayed, A. and Eldyasti, A. (2018) Factors affecting the selection of PHB accumulating methanotrophs from waste activated sludge while utilizing ammonium as their nitrogen source. *J Chem Technol Biotechnol* **93**(5), 1359-1369. doi: 10.1002/jctb.5502.

García-Depraect, O., Bordel, S., Lebrero, R., Santos-Beneit, F., Borner, R.A., Borner, T. and Muñoz, R. (2021) Inspired by nature: Microbial production, degradation and valorization of biodegradable bioplastics for life-cycle-engineered products. *Biotechnol Adv*, 107772. doi:10.1016/j.biotechadv.2021.107772.

García-Pérez, T., López, J.C., Passos, F., Lebrero, R., Revah, S. and Muñoz, R. (2018) Simultaneous methane abatement and PHB production by *Methylocystis hirsuta* in a novel gas-recycling bubble column bioreactor. *Chem Eng J* **334**, 691-697. doi:10.1016/j.cej.2017.10.106.

Geyer, R., Jambeck Jenna, R. and Law Kara, L. (2017) Production, use, and fate of all plastics ever made. *Sci Adv* **3**(7), e1700782. doi:10.1126/sciadv.1700782.

Giacomazzi, M. 2021. Soil improvers for the European Union. *Fertilizer Focus*, 76-79 https://www.linkedin.com/posts/european-biogas-association_soil-improvers-for-the-european-union-activity-6845696388903370752-utoO (02-10-21).

Graham, D.W., Chaudhary, J.A., Hanson, R.S. and Arnold, R.G. (1993) Factors affecting competition between type I and type II methanotrophs in two-organism, continuous-flow reactors. *Microb Ecol* **25**(1), 1-17. doi:10.1007/BF00182126.

Helm, J., Wendlandt, K.D., Jechorek, M. and Stottmeister, U. (2008) Potassium deficiency results in accumulation of ultra-high molecular weight poly-β-hydroxybutyrate in a methane-utilizing mixed culture. *J Appl Microbiol* **105**(4), 1054-1061. doi:10.1111/j.1365-2672.2008.03831.x.

Helm, J., Wendlandt, K.D., Rogge, G. and Kappelmeyer, U. (2006) Characterizing a stable methane-utilizing mixed culture used in the synthesis of a high-quality biopolymer in an open system. *J Appl Microbiol* **101**(2), 387-395. doi:10.1111/j.1365-2672.2006.02960.x.

Henckel, T., Roslev, P. and Conrad, R. (2000) Effects of O_2 and CH_4 on presence and activity of the indigenous methanotrophic community in rice field soil. *Environ Microbiol* **2**(6), 666-679. doi: 10.1046/j.1462-2920.2000.00149.x.

IEA (2020) Outlook for Biogas and Biomethane. Prospects for Organic Growth, International Energy Agency, France. https://www.iea.org/reports/outlook-for-biogas-and-biomethane-prospects-for-organic-growth (Accessed: 06.10.2021).

Iglesias, R., Muñoz, R., Polanco, M., Díaz, I., Susmozas, A., Moreno, A.D., Guirado, M., Carreras, N. and Ballesteros, M. (2021) Biogas from anaerobic digestion as an energy vector: current upgrading development. *Energies* **14**(10). doi:10.3390/en14102742.

IRENA (2021) Renewable Capacity Statistics 2021, International Renewable Energy Agency (IRENA), Abu Dhabi. https://www.irena.org/publications/2021/March/Renewable-Capacity-Statistics-2021 (Accessed: 04.10.2021).

Jambeck, J.R., Geyer, R., Wilcox, C., Siegler, T.R., Perryman, M., Andrady, A., Narayan, R. and Law, K.L. (2015) Plastic waste inputs from land into the ocean. *Science* **347**(6223), 768. doi:10.1126/science.1260352.

Jiang, G., Hill, D.J., Kowalczuk, M., Johnston, B., Adamus, G., Irorere, V. and Radecka, I. (2016) Carbon sources for polyhydroxyalkanoates and an integrated biorefinery. *Int J Mol Sci* **17**(7). doi:10.3390/ijms17071157.

Kalyuzhnaya, M.G., Yang, S., Rozova, O.N., Smalley, N.E., Clubb, J., Lamb, A., Gowda, G.A.N., Raftery, D., Fu, Y., Bringel, F., Vuilleumier, S., Beck, D.A.C., Trotsenko, Y.A., Khmelenina, V.N. and Lidstrom,

M.E. (2013) Highly efficient methane biocatalysis revealed in a methanotrophic bacterium. *Nat Commun* **4**(1), 2785. doi:10.1038/ncomms3785.

Kaneka (2019) Completion of Kaneka Biodegradable Polymer PHBH™ Plant with annual production of 5,000 tons, pp. 1-2, Kaneka Corporation. https://www.kaneka.co.jp/en/topics/news/nr20191219/ (Accessed: 19.10.2021)

Kapoor, R., Ghosh, P., Tyagi, B., Vijay, V.K., Vijay, V., Thakur, I.S., Kamyab, H., Nguyen, D.D. and Kumar, A. (2020) Advances in biogas valorization and utilization systems: A comprehensive review. *J Clean Prod* **273**, 123052. doi: 10.1016/j.jclepro.2020.123052.

Karthikeyan, O.P., Chidambarampadmavathy, K., Cirés, S. and Heimann, K. (2015) Review of sustainable methane mitigation and biopolymer production. *Crit Rev Environ Sci Technol* **45**(15), 1579-1610. doi:10.1080/10643389.2014.966422.

Kaur, G. and Roy, I. (2015) Strategies for large-scale production of polyhydroxyalkanoates. *Chem Biochem Eng Q* **29**, 157-172. doi:10.15255/CABEQ.2014.2255.

Khatami, K., Perez-Zabaleta, M., Owusu-Agyeman, I. and Cetecioglu, Z. (2021) Waste to bioplastics: How close are we to sustainable polyhydroxyalkanoates production? *Waste Manag* **119**, 374-388. doi: 10.1016/j.wasman.2020.10.008.

Khmelenina, V.N., Colin Murrell, J., Smith, T.J. and Trotsenko, Y.A. (2018) Physiology and Biochemistry of the Aerobic Methanotrophs. In: Rojo, F. (ed) Aerobic Utilization of Hydrocarbons, Oils and Lipids. Springer International Publishing, Cham 1-25. doi:10.1007/978-3-319-39782-5_4-1.

Knief, C. (2015) Diversity and habitat preferences of cultivated and uncultivated aerobic methanotrophic bacteria evaluated based on pmoA as molecular marker. *Front Microbiol* **6**, 1346. doi:10.3389/fmicb.2015.01346.

Koller, M. (2018) A Review on established and emerging fermentation schemes for microbial production of polyhydroxyalkanoate (PHA) biopolyesters. *Fermentation* **4**(2), 30. doi:10.3390/fermentation4020030.

Koller, M., Atlić, A., Dias, M., Reiterer, A. and Braunegg, G. (2010) Microbial PHA Production from Waste Raw Materials. In Chen, G.G.-Q. (ed) Plastics from Bacteria: Natural Functions and Applications. Springer Berlin Heidelberg, Berlin, Heidelberg, 85-119. doi:10.1007/978-3-642-03287-5_5.

Kraakman, N.J.R., Rocha-Rios, J. and van Loosdrecht, M.C.M. (2011) Review of mass transfer aspects for biological gas treatment. *Appl Microbiol Biotechnol* **91**(4), 873-886. doi:10.1007/s00253-011-3365-5.

Lebrero, R., Hernández, L., Pérez, R., Estrada, J.M. and Muñoz, R. (2015) Two-liquid phase partitioning biotrickling filters for methane abatement: Exploring the potential of hydrophobic methanotrophs. *J Environ Manage* **151**, 124-131. doi: 10.1016/j.jenvman.2014.12.016.

Lebrero, R., López, J.C., Lehtinen, I., Pérez, R., Quijano, G. and Muñoz, R. (2016) Exploring the potential of fungi for methane abatement: Performance evaluation of a fungal-bacterial biofilter. *Chemosphere* 144, 97-106. doi: 10.1016/j.chemosphere.2015.08.017.

Lebreton, L. and Andrady, A. (2019) Future scenarios of global plastic waste generation and disposal. *Palgrave Commun* **5**(1), 6. doi:10.1057/s41599-018-0212-7.

Levett, I., Birkett, G., Davies, N., Bell, A., Langford, A., Laycock, B., Lant, P. and Pratt, S. (2016) Techno-economic assessment of poly-3-hydroxybutyrate (PHB) production from methane - The case for thermophilic bioprocessing. *J Environ Chem Eng* **4**, 3724-3733. doi: 10.1016/j.jece.2016.07.033.

Li, Z., Yang, J. and Loh, X.J. (2016) Polyhydroxyalkanoates: opening doors for a sustainable future. *NPG Asia Mater* **8**(4), e265-e265. doi:10.1038/am.2016.48.

Liebetrau, J., Kornatz, P., Baier, U., Wall, D. and Murphy, J.D. (2020) Integration of biogas systems into the energy system: Technical aspects of flexible plant operation, IEA Bioenergy, Task 37.

López, J.C., Arnáiz, E., Merchán, L., Lebrero, R. and Muñoz, R. (2018) Biogas-based polyhydroxyalkanoates production by *Methylocystis hirsuta*: A step further in anaerobic digestion biorefineries. *Chem Eng J* **333**, 529-536. doi: 10.1016/j.cej.2017.09.185.

López, J.C., Porca, E., Collins, G., Clifford, E., Quijano, G. and Muñoz, R. (2019a) Ammonium influences kinetics and structure of methanotrophic consortia. *Waste Manag* **89**, 345-353. doi: 10.1016/j.wasman.2019.04.028.

López, J.C., Quijano, G., Pérez, R. and Muñoz, R. (2014) Assessing the influence of CH_4 concentration during culture enrichment on the biodegradation kinetics and population structure. *J Environ Manage* **146**, 116-123. doi: 10.1016/j.jenvman.2014.06.026.

Lopez, J.C., Quijano, G., Souza, T.S., Estrada, J.M., Lebrero, R. and Muñoz, R. (2013) Biotechnologies for greenhouse gases (CH_4, N_2O, and CO_2) abatement: state of the art and challenges. *Appl Microbiol Biotechnol* **97**(6), 2277-2303. doi:10.1007/s00253-013-4734-z.

López, J.C., Rodríguez, Y., Pérez, V., Lebrero, R. and Muñoz, R. (2019b) CH_4-based polyhydroxyalkanoate production: a step further towards a sustainable bioeconomy. In Kalia, V.C. (ed) Biotechnological Applications of Polyhydroxyalkanoates. Springer Singapore, Singapore, 283-321. doi:10.1007/978-981-13-3759-8_11.

Luangthongkam, P., Strong, P.J., Syed Mahamud, S.N., Evans, P., Jensen, P., Tyson, G., Laycock, B., Lant, P.A. and Pratt, S. (2019) The effect of methane and odd-chain fatty acids on 3-hydroxybutyrate (3HB) and 3-hydroxyvalerate (3HV) synthesis by a *Methylosinus*-dominated mixed culture. *Bioresour Bioprocess* **6**(1). doi:10.1186/s40643-019-0285-1.

Mango Materials. https://www.mangomaterials.com/innovation/ (Accessed: 09.09.2021)

Matsuura, T., Rana, D., Rasool Qtaishat, M. and Singh, G. (2011) Recent advances in membrane science and technology in sea water desalination with technology development in the Middle East and Singapore Water and Wastewater Technologies. Encyclopedia of Life Support Systems (EOLSS), Oxford, UK.

Meereboer, K.W., Misra, M. and Mohanty, A.K. (2020) Review of recent advances in the biodegradability of polyhydroxyalkanoate (PHA) bioplastics and their composites. *Green Chem* **22**(17), 5519-5558. doi:10.1039/d0gc01647k.

Mozejko-Ciesielska, J. and Kiewisz, R. (2016) Bacterial polyhydroxyalkanoates: Still fabulous? *Microbiol Res* **192**, 271-282. doi:10.1016/j.micres.2016.07.010.

Mühlemeier, I.M., Speight, R. and Strong, P.J. (2018) Biogas, Bioreactors and Bacterial Methane Oxidation. In: Kalyuzhnaya, M.G. and Xing, X.-H. (eds) Methane Biocatalysis: Paving the Way to Sustainability. Springer International Publishing, Cham, 213-235. doi:10.1007/978-3-319-74866-5_14.

Muñoz, R., Meier, L., Diaz, I. and Jeison, D. (2015) A review on the state-of-the-art of physical/chemical and biological technologies for biogas upgrading. *Rev Environ Sci Biotechnol* **14**(4), 727-759. doi:10.1007/s11157-015-9379-1.

Murrell, J.C., Gilbert, B. and McDonald, I.R. (2000) Molecular biology and regulation of methane monooxygenase. *Arch Microbiol* **173**(5), 325-332. doi:10.1007/s002030000158.

Myung, J., Flanagan, J.C.A., Waymouth, R.M. and Criddle, C.S. (2016) Methane or methanol-oxidation dependent synthesis of poly(3-hydroxybutyrate-co-3-hydroxyvalerate) by obligate type II methanotrophs. *Process Biochem* **51**(5), 561-567. doi: 10.1016/j.procbio.2016.02.005.

Myung, J., Flanagan, J.C.A., Waymouth, R.M. and Criddle, C.S. (2017) Expanding the range of polyhydroxyalkanoates synthesized by methanotrophic bacteria through the utilization of omega-hydroxyalkanoate co-substrates. *AMB Express* **7**(1), 118. doi:10.1186/s13568-017-0417-y.

Myung, J., Galega, W.M., Van Nostrand, J.D., Yuan, T., Zhou, J. and Criddle, C.S. (2015) Long-term cultivation of a stable *Methylocystis*-dominated methanotrophic enrichment enabling tailored production of poly(3-hydroxybutyrate-co-3-hydroxyvalerate). *Bioresour Technol* **198**, 811-818. doi: 10.1016/j.biortech.2015.09.094.

Nyerges, G., Han, S.-K. and Stein Lisa, Y. (2010) Effects of ammonium and nitrite on growth and competitive fitness of cultivated methanotrophic bacteria. *Appl Environ Microbiol* **76**(16), 5648-5651. doi:10.1128/AEM.00747-10.

Pawlowska, M. (2014) Mitigation of landfill gas emissions, CRC Press/Balkema, London. ISBN: 0-429-22712-4

Pérez, R., Cantera, S., Bordel, S., García-Encina, P.A. and Muñoz, R. (2019) The effect of temperature during culture enrichment on methanotrophic polyhydroxyalkanoate production. *Int Biodeterior Biodegradation* **140**, 144-151. doi:10.1016/j.ibiod.2019.04.004.

Pérez, V., Lebrero, R. and Muñoz, R. (2020) Comparative evaluation of biogas valorization into electricity/heat and poly(hydroxyalkanoates) in waste treatment plants: Assessing the influence of local

commodity prices and current biotechnological limitations. *ACS Sustain Chem Eng* **8**(20), 7701-7709. doi:10.1021/acssuschemeng.0c01543.

Pfluger, A.R., Wu, W.M., Pieja, A.J., Wan, J., Rostkowski, K.H. and Criddle, C.S. (2011) Selection of Type I and Type II methanotrophic proteobacteria in a fluidized bed reactor under non-sterile conditions. *Bioresour Technol* **102**(21), 9919-9926. doi:10.1016/j.biortech.2011.08.054.

Pieja, A.J., Morse, M.C. and Cal, A.J. (2017) Methane to bioproducts: the future of the bioeconomy? *Curr Opin Chem Biol* **41**, 123-131. doi: 10.1016/j.cbpa.2017.10.024

Pieja, A.J., Rostkowski, K.H. and Criddle, C.S. (2011) Distribution and selection of poly-3-hydroxybutyrate production capacity in methanotrophic proteobacteria. *Microb Ecol* **62**(3), 564-573. doi:10.1007/s00248-011-9873-0.

Pieja, A.J., Sundstrom, E.R. and Criddle, C.S. (2012) Cyclic, alternating methane and nitrogen limitation increases PHB production in a methanotrophic community. *Bioresour Technol* **107**, 385-392. doi: 10.1016/j.biortech.2011.12.044.

Pittman, M.J., Bodley, M.W. and Daugulis, A.J. (2015) Mass transfer considerations in solid–liquid two-phase partitioning bioreactors: a polymer selection guide. *J Chem Technol Biotechnol* **90**(8), 1391-1399. doi:10.1002/jctb.4720.

PlasticsEurope (2013) Plastics – the Facts 2013. An analysis of European latest plastics production, demand and waste data PlasticsEurope. Association of European Manufacturers. https://www.plasticseurope.org/application/files/7815/1689/9295/2013plastics_the_facts_PubOct2013.pdf (Accessed: 10.08.2021).

PlasticsEurope (2020) Plastics - the Facts 2020, https://www.plasticseurope.org/en/resources/publications/4312-plastics-facts-2020 (Accessed: 10.08.2021).

Pol, A., Heijmans, K., Harhangi, H.R., Tedesco, D., Jetten, M.S.M. and Op den Camp, H.J.M. (2007) Methanotrophy below pH 1 by a new Verrucomicrobia species. *Nature* **450**(7171), 874-878. doi:10.1038/nature06222.

Poltronieri, P. and Kumar, P. (2019) Polyhydroxyalkanoates (PHAs) in Industrial Applications. In: Martínez, L.M.T., Kharissova, O.V. and Kharisov, B.I. (eds) Handbook of Ecomaterials. Springer International Publishing, Cham, 2843-2872. doi:10.1007/978-3-319-68255-6_70.

Porta, R. (2019) The plastics sunset and the bio-plastics sunrise. *Coatings* **9**(8), 526. doi:10.3390/coatings9080526.

Rahnama, F., Vasheghani-Farahani, E., Yazdian, F. and Shojaosadati, S.A. (2012) PHB production by *Methylocystis hirsuta* from natural gas in a bubble column and a vertical loop bioreactor. *Biochem Eng J* **65**, 51-56. doi: 10.1016/j.bej.2012.03.014.

Ravenstijn, J. (2021) Fast growing PHA demand and new capacities, but what about legislation? GO!PHA Global Organization for PHA, pp. 1-33.

REN21 (2020) Renewables 2020 Global Status Report, REN21 Paris, France ISBN: 978-3-948393-00-7. https://www.ren21.net/wp-content/uploads/2019/05/gsr_2020_full_report_en.pdf (Accessed: 02.10.21).

Riaz, S., Rhee, K.Y. and Park, S.J. (2021) Polyhydroxyalkanoates (PHAs): Biopolymers for biofuel and biorefineries. *Polymers* **13**(2). doi:10.3390/polym13020253.

Riedel, S.L. and Brigham, C.J. (2020) Inexpensive and Waste Raw Materials for PHA production. In: Koller, M. (ed) The Handbook of Polyhydroxyalkanoates: Microbial Biosynthesis and Feedstocks (1st ed.). . Vol 1, 1st edn. CRC Press. doi: 10.1201/9780429296611.

Rocha-Rios, J., Bordel, S., Hernández, S. and Revah, S. (2009) Methane degradation in two-phase partition bioreactors. *Chem Eng J* **152**(1), 289-292. doi: 10.1016/j.cej.2009.04.028.

Rocha-Rios, J., Kraakman, N.J.R., Kleerebezem, R., Revah, S., Kreutzer, M.T. and van Loosdrecht, M.C.M. (2013) A capillary bioreactor to increase methane transfer and oxidation through Taylor flow formation and transfer vector addition. *Chem Eng J* **217**, 91-98. doi: 10.1016/j.cej.2012.11.065.

Rocha-Rios, J., Muñoz, R. and Revah, S. (2010) Effect of silicone oil fraction and stirring rate on methane degradation in a stirred tank reactor. *J Chem Technol Biotechnol* **85**(3), 314-319. doi:10.1002/jctb.2339.

Rocha-Rios, J., Quijano, G., Thalasso, F., Revah, S. and Muñoz, R. (2011) Methane biodegradation in a two-phase partition internal loop airlift reactor with gas recirculation. *J Chem Technol Biotechnol* **86**(3), 353-360. doi:10.1002/jctb.2523.

Rodríguez, Y., Pérez, V., López, J.C., Bordel, S., Firmino, P.I.M., Lebrero, R. and Muñoz, R. (2020) Coupling Biogas with PHA Biosynthesis. In: Koller, M. (ed) The Handbook of Polyhydroxyalkanoates: Microbial Biosynthesis and Feedstocks. Vol 1, 1st edn. CRC Press. doi: 10.1201/9780429296611.

Rostkowski, K.H., Pfluger, A.R. and Criddle, C.S. (2013) Stoichiometry and kinetics of the PHB-producing Type II methanotrophs *Methylosinus trichosporium* OB3b and *Methylocystis parvus* OBBP. *Bioresour Technol* **132**, 71-77. doi:10.1016/j.biortech.2012.12.129.

Sahoo, K.K., Goswami, G. and Das, D. (2021) Biotransformation of methane and carbon dioxide into high-value products by methanotrophs: current state of art and future prospects. *Front Microbiol* **12**:636486 doi: 10.3389/fmicb.2021.636486

Sazinsky, M.H. and Lippard, S.J. (2015) Methane Monooxygenase: Functionalizing Methane at Iron and Copper. In Kroneck, P.M.H. and Sosa Torres, M.E. (eds) Sustaining Life on Planet Earth: Metalloenzymes Mastering Dioxygen and Other Chewy Gases. Springer International Publishing, Cham, 205-256. doi:10.1007/978-3-319-12415-5_6.

Scarlat, N., Dallemand, J.-F. and Fahl, F. (2018) Biogas: Developments and perspectives in Europe. *Renew Energy* **129**, 457-472. doi: 10.1016/j.renene.2018.03.006.

Semrau, J.D., DiSpirito, A.A., Gu, W. and Yoon, S. (2018) Metals and Methanotrophy. *Appl Environ Microbiol* **84**(6), 1-17. doi:10.1128/aem.02289-17.

Semrau, J.D., DiSpirito, A.A. and Yoon, S. (2010) Methanotrophs and copper. *FEMS Microbiol Rev* **34**(4), 496-531. doi:10.1111/j.1574-6976.2010.00212.x.

Singh, A.K. and Mallick, N. (2008) Enhanced production of SCL-LCL-PHA co-polymer by sludge-isolated *Pseudomonas aeruginosa* MTCC 7925. *Lett Appl Microbiol* **46**(3), 350-357. doi: 10.1111/j.1472-765X.2008.02323.x.

Singhaboot, P. and Kaewkannetra, P. (2015) A higher in value biopolymer product of polyhydroxyalkanoates (PHAs) synthesized by *Alcaligenes latus* in batch/repeated batch fermentation processes of sugar cane juice. *Ann Microbiol* **65**(4), 2081-2089. doi:10.1007/s13213-015-1046-9.

Stone, K.A., Hilliard, M.V., He, Q.P. and Wang, J. (2017) A mini review on bioreactor configurations and gas transfer enhancements for biochemical methane conversion. *Biochem Eng J* **128**, 83-92. doi:10.1016/j.bej.2017.09.003.

Strong, J.P., Laycock, B., Mahamud, N.S., Jensen, D.P., Lant, A.P., Tyson, G. and Pratt, S. (2016) The opportunity for high-performance biomaterials from methane. *Microorganisms* **4**(1). doi:10.3390/microorganisms4010011.

Sun, Z., Ramsay, J.A., Guay, M. and Ramsay, B.A. (2007) Fermentation process development for the production of medium-chain-length poly-3-hydroxyalkanoates. *Appl Microbiol Biotechnol* **75**(3), 475-485. doi:10.1007/s00253-007-0857-4.

Sundstrom, E.R. and Criddle, C.S. (2015) Optimization of methanotrophic growth and production of poly(3-hydroxybutyrate) in a high-throughput microbioreactor System. *Appl Environ Microbiol* **81**(14), 4767. doi:10.1128/AEM.00025-15.

Tan, D., Wang, Y., Tong, Y. and Chen, G.Q. (2021) Grand challenges for industrializing polyhydroxyalkanoates (PHAs). *Trends Biotechnol* **39**(9), 953-963. doi:10.1016/j.tibtech.2020.11.010.

Tullo, A. 2019. PHA: A biopolymer whose time has finally come. *Chemical & Engineering News*, **97**(35) https://cen.acs.org/business/biobased-chemicals/PHA-biopolymer-whose-time-finally/97/i35 (Accessed: 09.09.21).

UNEP (2014) UNEP YEAR BOOK 2014: Emerging issues in our global environment, United Nations Environment Programme, Nairobi, Kenya. https://wedocs.unep.org/handle/20.500.11822/9240 (Accessed: 10.08.21).

van den Oever, M., Molenveld, K., van der Zee, M. and Bos, H. (2017) Bio-based and biodegradable plastics - Facts and Figures, Wageningen UR, Wageningen. doi: 10.18174/408350

van Teeseling Muriel, C.F., Pol, A., Harhangi Harry, R., van der Zwart, S., Jetten Mike, S.M., Op den Camp Huub, J.M., van Niftrik, L. and Drake, H.L. (2014) Expanding the Verrucomicrobial methanotrophic world: description of three novel species of *Methylacidimicrobium* gen. nov. *Appl Environ Microbiol* **80**(21), 6782-6791. doi:10.1128/AEM.01838-14.

Vandi, L.-J., Chan, C.M., Werker, A., Richardson, D., Laycock, B. and Pratt, S. (2018) Wood-PHA composites: Mapping opportunities. *Polymers* **10**(7). doi:10.3390/polym10070751.

Vorholt, J.A. (2002) Cofactor-dependent pathways of formaldehyde oxidation in methylotrophic bacteria. *Arch Microbiol* **178**, 239-249. doi:10.1007/s00203-002-0450-2

WBA (2019) Global Potential of Biogas, World Biogas Association. https://www.worldbiogasassociation.org/wp-content/uploads/2019/09/WBA-execsummary-4ppa4_digital-Sept-2019.pdf (Accessed: 07.10.2021).

WBA (2021) Biogas: Pathways to 2030, World Biogas Association, London. https://www.worldbiogasassociation.org/biogas-pathways-to-2030-report/ (Accessed: 07.10.2021).

WEF (2016) The New Plastics Economy. Rethinking the future of plastics, World Economic Forum https://www3.weforum.org/docs/WEF_The_New_Plastics_Economy.pdf (Accessed: 15.08.2021).

Wellinger, A. (2017) Report on the practical experiences with the application of European Biomethane Standards, Biosurf Fuelling Biomethane. https://ec.europa.eu/research/participants/documents/downloadPublic?documentIds=080166e5b53edbc1&appId=PPGMS (Accessed: 02.10.2021).

Wendlandt, K.D., Jechorek, M., Helm, J. and Stottmeister, U. (2001) Producing poly-3-hydroxybutyrate with a high molecular mass from methane. *J Biotechnol* **86**(2), 127-133. doi: 10.1016/S0168-1656(00)00408-9.

Yamane, T. (1993) Yield of poly-D(-)-3-hydroxybutyrate from various carbon sources: A theoretical study. *Biotechnol Bioeng* **41**(1), 165-170. doi:10.1002/bit.260410122.

Yanez, L., Conejeros, R., Vergara-Fernandez, A. and Scott, F. (2020) Beyond intracellular accumulation of polyhydroxyalkanoates: Chiral hydroxyalkanoic acids and polymer secretion. *Front Bioeng Biotechnol* **8**, 248. doi:10.3389/fbioe.2020.00248.

Zhang, T., Zhou, J., Wang, X. and Zhang, Y. (2017) Coupled effects of methane monooxygenase and nitrogen source on growth and poly-β-hydroxybutyrate (PHB) production of *Methylosinus trichosporium* OB3b. *J Environ Sci* **52**, 49-57. doi: 10.1016/j.jes.2016.03.001.

Zhang, Y., Xin, J., Chen, L., Song, H. and Xia, C. (2008) Biosynthesis of poly-3-hydroxybutyrate with a high molecular weight by methanotroph from methane and methanol. *J Nat Gas Chem* **17**(1), 103-109. doi: 10.1016/S1003-9953(08)60034-1.

Zhang, Z.P., Rong, M.Z. and Zhang, M.Q. (2018) Polymer engineering based on reversible covalent chemistry: A promising innovative pathway towards new materials and new functionalities. *Prog Polym Sci* **80**, 39-93. doi: 10.1016/j.progpolymsci.2018.03.002.

2.

Aim and scope of the thesis

2.1 Justification of the thesis

In a global context of increasing energy demand and climate emergency, anaerobic digestion (AD) can play a crucial role in the transition towards carbon neutrality. AD turns organic waste into biogas, a renewable source of dispatchable energy with a relatively stable composition compared to the organic waste fed to the digesters. Thus, the biogas sector can tackle two major contemporary challenges: the reduction of todays' global dependence on fossil fuels and the mitigation of greenhouse gases emissions. Despite its enormous untapped potential, the rapid expansion of the biogas industry is limited by its low economic sustainability and huge dependence on fiscal incentives, which makes biogas unable to compete with cost-effective renewable energies such as solar or wind power. The development of an integrated biorefinery for the generation of added-value products from biogas has recently emerged as an opportunity to boost the economic viability of AD and overcome the current impasse of the sector. In this context, methanotrophs are regarded as a potential platform for the bioconversion of the CH_4 fraction of biogas into green chemicals such as polyhydroxyalkanoates (PHAs). These microbial storage materials, which are synthetized under unbalanced growth conditions by type II methanotrophs, constitute a nature-friendly alternative to traditional plastics. Nonetheless, the development of biogas-to-PHAs biotechnologies is challenged by a series of biological and operational drawbacks: i) poor CH_4 gas-liquid mass transfer rates due to the low aqueous solubility of CH_4 and the electron acceptor (O_2) and reduced concentration gradients resulting from biogas dilution in air, ii) low biomass productivities and reduced CH_4 elimination capacities mediated by the nutrient deprivation conditions that are necessary to induce PHA synthesis, iii) limited understanding of the mechanisms governing CH_4 uptake and nutrient assimilation during growth and PHA synthesis in type-II methanotrophs, and iv) limited knowledge about suitable operating strategies in high mass transfer systems devoted to PHA production via CH_4 bioconversion under continuous process operation.

2.2 Main objectives

The overall objective of this research was the development and optimization of biogas-to-PHA biotechnologies as a feasible platform for the production of biopolymers using type II methanotrophs. This global objective involved the design of novel operating strategies for improved PHA synthesis and the intensification of CH_4 gas-liquid mass transfer in gas-phase bioreactors. Special attention was given to the underlying mechanisms of methane bioconversion into PHB. More particularly, the specific objectives accomplished were:

I. Evaluation of the influence of key environmental factors on CH_4 biodegradation kinetics and polyhydroxybutyrate (PHB) accumulation by *M. hirsuta*.

II. Development of a mechanistic model that describes the processes underlying PHA synthesis by *M. hirsuta* CSC1.

III. Optimization of the operational conditions and evaluation of the potential for CH_4 utilization of novel operating strategies such as internal gas recirculation in a column bioreactor constructed with fine bubble diffusers using *M. hirsuta*

IV. Assessment of the feasibility, in terms of process stability and PHB productivity, of the simultaneous CH_4 conversion and PHB synthesis under sequential nitrogen feast-famine cycles (single-stage process) *vs* continuous regime (two-stage process) by the type-II methanotrophic bacterium *M. hirsuta*.

V. Design and optimization of the continuous and sequential cultivation strategies (nitrogen supply, duration of nitrogen feast:famine periods) to support a continuous production of PHB by the type-II methanotrophic bacterium *M. parvus* in a stirred tank bioreactor.

2.3 Thesis outline

In the present thesis work, biogas bioconversion coupled to polyhydroxyalkanoates production was investigated. More precisely:

Chapter 1 presents a comprehensive literature review of all scientific and technical fundamentals embraced in this thesis. The current chapter **(Chapter 2)** features the rationale of the work and main objectives, which are supported by a schematic overview of the work **(Fig. 2.1)**. **Chapters 3 to 7** are dedicated to the core investigation work of this PhD thesis. Thus, the elucidation of the influence of environmental conditions (O_2:CH_4 ratio, temperature and nitrogen source) on biogas-based growth and PHA synthesis of the strain *Methylocystis hirsuta* CSC1 was conducted batchwise in order to fulfill objective I **(Chapter 3)**. Additional batch tests (biomass decay and PHA utilization) were performed for the development and validation of a mechanistic model capable of describing processes involved in methanotrophic growth and PHA synthesis according to objective II **(Chapter 4).** Then, the optimization of a continuous bubble column bioreactor engineered with internal gas recirculation to support an enhanced methane biodegradation by *M. hirsuta* under sequential batch operation and nutrient sufficient growth conditions was conducted to fulfil objective III **(Chapter 5)**. Maximal resource utilization conditions were investigated via implementation of a cyclic feast:famine nitrogen regime for continuous PHB production in the aforementioned bubble column reactor in accordance with objective IV. This goal was also approached in **Chapter 6** via evaluation of a novel two-stage growth-accumulation configuration for PHB production under two nitrogen supply conditions in continuous mode. Finally, objective V was accomplished in **Chapter 7**, where a systematic comparison of process operation under decreasing nitrogen loading rates in continuous mode *vs.* sequential nitrogen feast:famine modes, and different feast:famine cycle configurations (24h:24h *vs*. 24h:48h), in terms of PHB productivity and methane biodegradation by *M. parvus* was carried out. Finally, concluding remarks and further research are presented in **Chapter 8**.

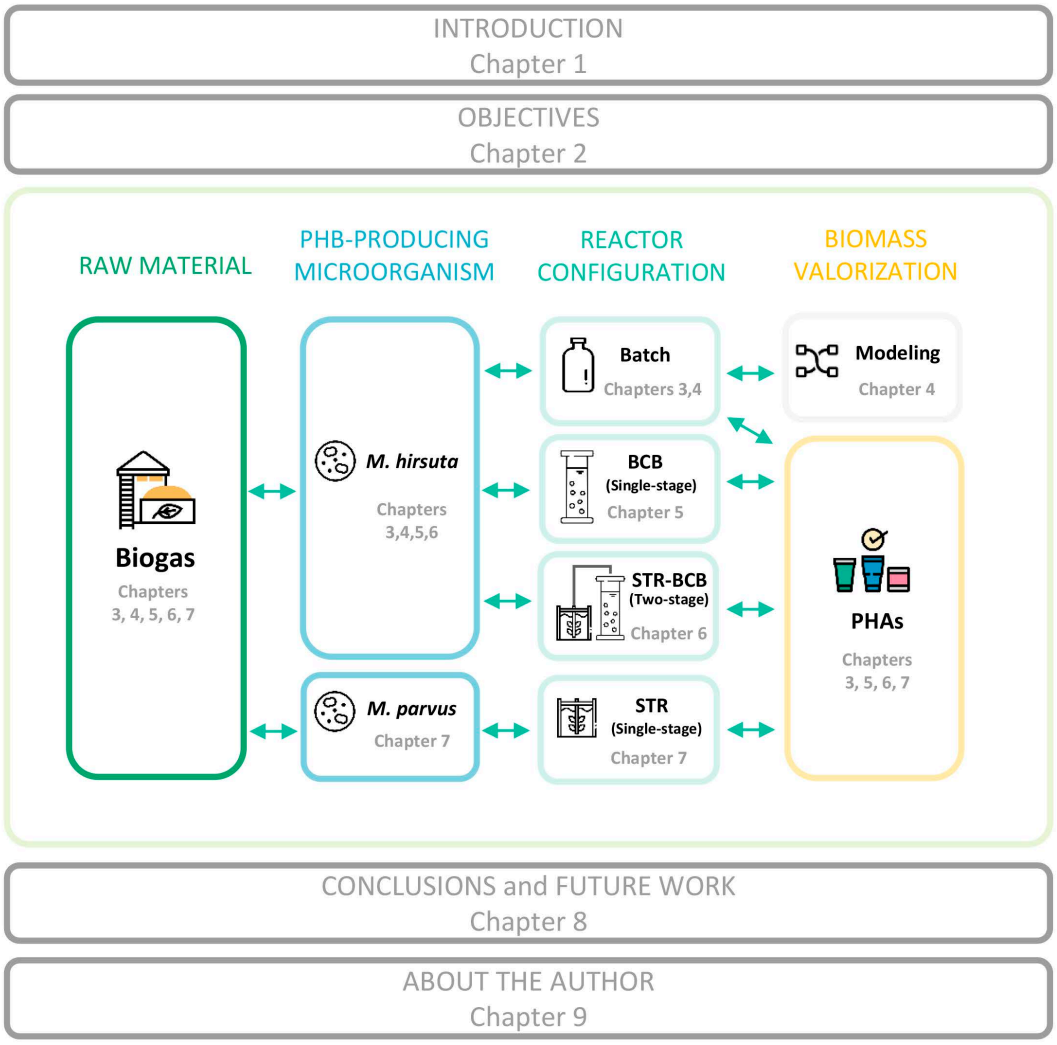

Fig. 2.1 *Pert chart of this thesis.*

3.

Elucidating the influence of environmental factors on biogas-based polyhydroxybutyrate production by *Methylocystis hirsuta* CSC1

This chapter was adapted after its publication in *Science of the Total Environment:*

Rodríguez, Y., Firmino, P.I.M., Arnáiz, E., Lebrero, R., Muñoz, R. (2020) Elucidating the influence of environmental factors on biogas-based polyhydroxybutyrate production by *Methylocystis hirsuta* CSC1. *Sci Total Environ*, 706, 135136. doi: 10.1016/j.scitotenv.2019.135136

Elucidating the influence of environmental factors on biogas-based polyhydroxybutyrate production by *Methylocystis hirsuta* CSC1

Yadira Rodríguez[a,b], Paulo Igor Milen Firmino[b,c], Esther Arnáiz[a,b], Raquel Lebrero[a,b], Raúl Muñoz[a,b,*]

[a] Department of Chemical Engineering and Environmental Technology, School of Industrial Engineering, University of Valladolid, Dr. Mergelina s/n, 47011 Valladolid, Spain

[b] Institute of Sustainable Processes, Dr. Mergelina s/n, 47011 Valladolid, Spain.

[c] Department of Hydraulic and Environmental Engineering, Federal University of Ceará, Fortaleza, Ceará, Brazil

* Corresponding author: mutora@iq.uva.es.

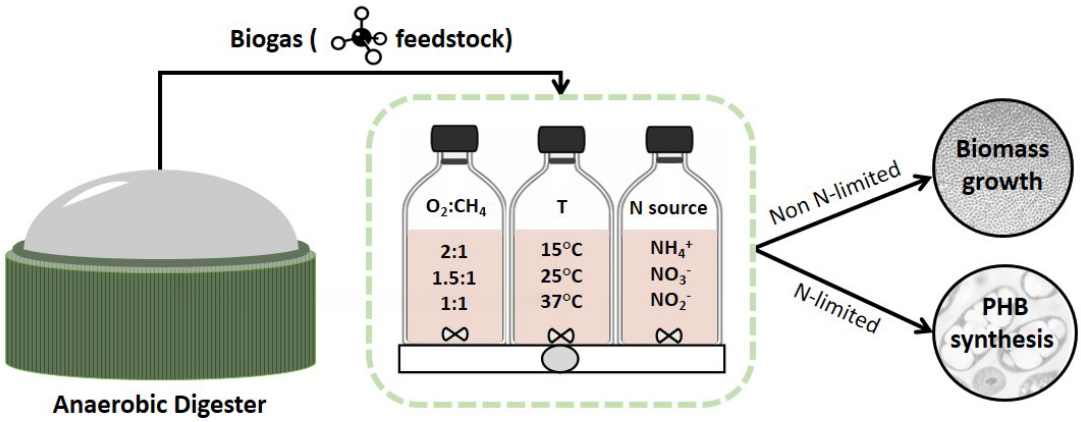

Graphical abstract

Abstract

The valorization of biogas as a feedstock for the generation of added-value bioproducts will play a key role on the sustainability of anaerobic digestion. The present work assessed the influence of key environmental parameters (O_2:CH_4 ratio, temperature and nitrogen source) on the growth and polyhydroxybutyrate (PHB) synthesis under nitrogen limiting conditions of the type II methanotroph *Methylocystis hirsuta* CSC1 using biogas as a feedstock. The O_2:CH_4 ratios tested (1:1, 1.5:1 and 2:1) did not affect significantly *M. hirsuta* CSC1 growth yields (≈5 g TSS mol^{-1} CH_4), although lower CH_4 removal rates were reached under O_2-limiting conditions (ratio 1:1). The highest PHB content (45 wt%) was achieved at a ratio 2:1 and was threefold higher than those obtained at lower ratios (≈15 wt%). The increase in temperature from 15 to 25ºC resulted in increases in the growth yield (from 5 to 6 g TSS mol^{-1} CH_4) and PHB content (from 32 to 40 wt%). Conversely, the lowest PHB content (30 wt%) was reached at 37ºC, together with a negligible growth under nutrient sufficient conditions. The nitrogen source also played a key role on both *M. hirsuta* CSC1 growth and PHB synthesis. Thus, ammonium resulted in the highest growth yield (7 g TSS mol^{-1} CH_4), although the maximum PHB content was achieved when biomass was previously grown in nitrate as the nitrogen source (41 wt%). Nitrite exerted an inhibitory effect on *M. hirsuta* CSC1 growth.

Keywords: biogas valorization, methane conversion, methanotrophs, *Methylocystis hirsuta*, microbial cell factories, polyhydroxybutyrate production

3.1 Introduction

Polyhydroxyalkanoates (PHAs) are microbial plastics that are naturally produced under nutrient limitation and carbon surplus by over 300 bacterial strains (Pieja et al., 2017; Strong et al., 2016). These biodegradable and biocompatible polyesters are regarded as promising candidates to substitute petroleum-derived plastics owing to their similarity to various conventional thermoplastics and elastomers (Choi & Lee, 1999). Approximately 24 companies are nowadays involved in PHA manufacturing, Metabolix (USA), Meredian (USA), Bio-on (Italy) and Tianjin Green Bioscience (China) corporations being at the forefront of poly-3-hydroxybutyrate (PHB) and poly(3-hydroxybutyrate-*co*-3-hydroxyvalerate) (PHBV) production worldwide (Chen, 2009; Singh et al., 2017). Despite the environmental advantages of bioplastics, the development of the PHA market (expected to reach up to $250 \cdot 10^3$ t $year^{-1}$ by 2021) is still hampered by their high costs of production and purification, which are currently 5-10 times higher than those associated with conventional plastics (nova-Institut, 2016; Raza et al., 2018). Research efforts are focused on reducing the operating costs associated with downstream PHA processing and the acquisition of the carbon source (the latter accounting for 30 – 40% of the total cost) (Cantera et al., 2018; Lee & Na, 2013) .

In this context, biogas has emerged as a potential low-cost substrate for PHA production due to its high content of methane (50 - 70%) (López et al., 2018). Biogas from the anaerobic microbial conversion of organic matter (i.e. agro-industrial residues, urban solid waste or sewage sludge) has been typically used for heat and power generation, upgraded into biomethane for grid injection, or simply flared. In the last decade, the number of biogas production facilities in Europe has increased by 186%, from 6227 in 2009 to 17783 units and a total installed electric capacity of 10532 MW by the end of 2017 (EBA, 2019).

Methane-oxidizing bacteria (MOB), also known as methanotrophs, are strict aerobic microorganisms that use methane as their sole carbon and energy source. Unlike other methanotrophs, type II MOB utilize the serine pathway for formaldehyde assimilation and

possess the ability to produce PHAs from dilute methane emissions or biogas under nutrient-limited (usually nitrogen) conditions (Hanson & Hanson, 1996; Lindner et al., 2007). Among the PHA-synthesizing methanotrophs, *Methylocystis*, *Methylosinus* and *Methylocella* are the most important genera, with PHA contents ranging from 20 to 60 wt% (Bordel et al., 2019a; Cantera et al., 2019). In particular, the strain *Methylocystis hirsuta* CSC1, isolated for the first time from an aquifer in CA (USA) in the mid-eighties (Lindner et al., 2007), exhibits a high PHA-accumulating capacity, with PHA contents of 43 and 52 wt% using biogas and natural gas (90% methane) as feedstock, respectively, and a high metabolic plasticity (López et al., 2018; Rahnama et al., 2012). PHA synthesis in methanotrophs depends on environmental factors such as pH, temperature, and the concentrations of methane, oxygen, carbon dioxide, macronutrients (nitrogen, phosphorous, etc.) and micronutrients (copper, cobalt, etc.) (Karthikeyan et al., 2015; Strong et al., 2016; Zhang et al., 2017). Unfortunately, there is still a limited understanding of the influence of most of these environmental factors on PHA accumulation by type II methanotrophs. In this regard, Rostkowski et al. (2013) reported that the oxygen requirements and the effect of the nitrogen source on the kinetics and stoichiometry of growth and PHB accumulation of type-II methanotrophs are highly organism-specific. Nitrate and ammonia, even gaseous N_2, can be assimilated by obligate methanotrophs (Murrell and Dalton, 1983). Nitrate and ammonium concentrations of up to 40 mM can support methane oxidation by the type-II MOB R-45379 (Hoefman et al., 2014). Despite the versatile nitrogen metabolism of methanotrophs, there is a limited number of studies about the nitrite detoxification ability of certain type-II microorganisms. This harmful compound can be produced either from nitrate reduction or from ammonia oxidation via hydroxylamine by some type-II methanotrophs (Bowman et al., 1993; Hoefman et al., 2014). On the other hand, the optimum growth temperature for most methanotrophic bacteria typically ranges from 25 to 35ºC (Hanson and Hanson, 1996), although some strains have been isolated from psychrophilic and thermophilic environments (Dunfield, 2009). Indeed, *Methylosinus trichosporium* OB3b and *Methylocystis parvus* OBBP were able to grow and accumulate PHB at 37ºC (Lindner et al., 2007).

This work aimed at assessing the influence of key environmental parameters such as the O_2:CH_4 ratio, the type of nitrogen source (NO_3^-, NO_2^- and NH_4^+) and the temperature on the growth and PHB synthesis of the type II methanotroph *Methylocystis hirsuta* CSC1 using biogas as the sole carbon and energy source.

3.2 Materials and methods

3.2.1 Microorganism and chemicals

The methanotrophic strain *Methylocystis hirsuta* CSC1, purchased from Leibniz-Institut DSMZ (DSM no. 18500), was inoculated (10% v/v) under sterile conditions in 125-mL crimp-sealed serum bottles containing 50 mL of nitrate mineral salt (NMS) medium. NMS medium (pH of 6.8) was composed of (g L^{-1}): 1.0 KNO_3, 1.1 $MgSO_4 \cdot 7H_2O$, 0.8 $Na_2HPO_4 \cdot 12H_2O$, 0.26 KH_2PO_4 and 0.2 $CaCl_2 \cdot 2H_2O$; and 1 mL of trace element solution (g L^{-1}): 0.3 $Na_2MoO_4 \cdot 2H_2O$, 0.3 $Na_2EDTA \cdot 2H_2O$, 1 $CuSO_4 \cdot 5H_2O$, 0.5 $FeSO_4 \cdot 7H_2O$, 0.4 $ZnSO_4 \cdot 7H_2O$, 0.03 $CoCl_2$, 0.02 $MnCl_2 \cdot 4H_2O$, 0.015 H_3BO_3, 0.01 $NiCl_2 \cdot 6H_2O$ and 0.38 Fe-EDTA. Subsequently, the bottles headspace (75 mL) was flushed under sterile conditions for 5 minutes with filtered oxygen (0.22 μm; Millex GP, Merck). Then, 25 mL of the oxygen headspace atmosphere were replaced by methane, which resulted in an O_2:CH_4 concentration ratio of 66.7:33.3% (v/v). The cultures were incubated at 30°C and 200 rpm in an orbital shaker (MaxQ 4000; Thermo Scientific, USA) for ~7 days. The headspace atmosphere of the bottles was replaced 5 times upon CH_4 depletion. Unless otherwise specified, this inoculum was prepared prior the start-up of i) the test series assessing the influence of environmental conditions on *M. hirsuta* CSC1 growth and ii) the growth of *M. hirsuta* CSC1 biomass for the tests series assessing the influence of the environmental conditions on PHA accumulation.

Gas cylinders of CH_4 (purity ≥ 99.995%), O_2 (≥ 99.5%), He (≥ 99.5%) and synthetic biogas (70% CH_4, 30% CO_2) were purchased from Abelló Linde S.A. (Barcelona, Spain). Potassium nitrate was obtained from Cofarcas S.A. (Burgos, Spain), whereas the rest of the

salts required for the preparation of the mineral medium were acquired from PanReac AppliChem (Barcelona, Spain). Commercial PHBV (with a PHV content of 12% mol) for the preparation of standard biopolymer solutions in chloroform was purchased from Sigma-Aldrich (St. Louis, MO, USA).

3.2.2 Experimental procedure

All tests described below were performed batchwise in duplicate in 2.2-L serum bottles (working volume of 0.4 L) capped with butyl-rubber stoppers and aluminum screw caps (Fig. 3.1). Unless otherwise specified, bottles were incubated under mesophilic conditions (25 °C) with an initial pH of 7.1 in a thermostated room and magnetically stirred at 300 rpm (Poly 15 Variomag, Thermo Fisher Scientific).

The CH_4, CO_2 and O_2 headspace concentrations were periodically monitored by gas chromatography coupled with a thermal conductivity detector (GC-TCD) in all tests. The characterization of the culture broth was carried out by withdrawing 4 mL-samples and determining biomass concentration via optical density measurement and PHB content via gas chromatography-mass spectrometry (GC-MSD). The latter was carried out exclusively during the accumulation assays. pH was recorded at the beginning and end of each test. Additionally, initial and final concentrations of total nitrogen (TN), $N\text{-}NO_2^-$ and $N\text{-}NO_3^-$ were analyzed in the Test series 3-G (see section 3.2.2.5).

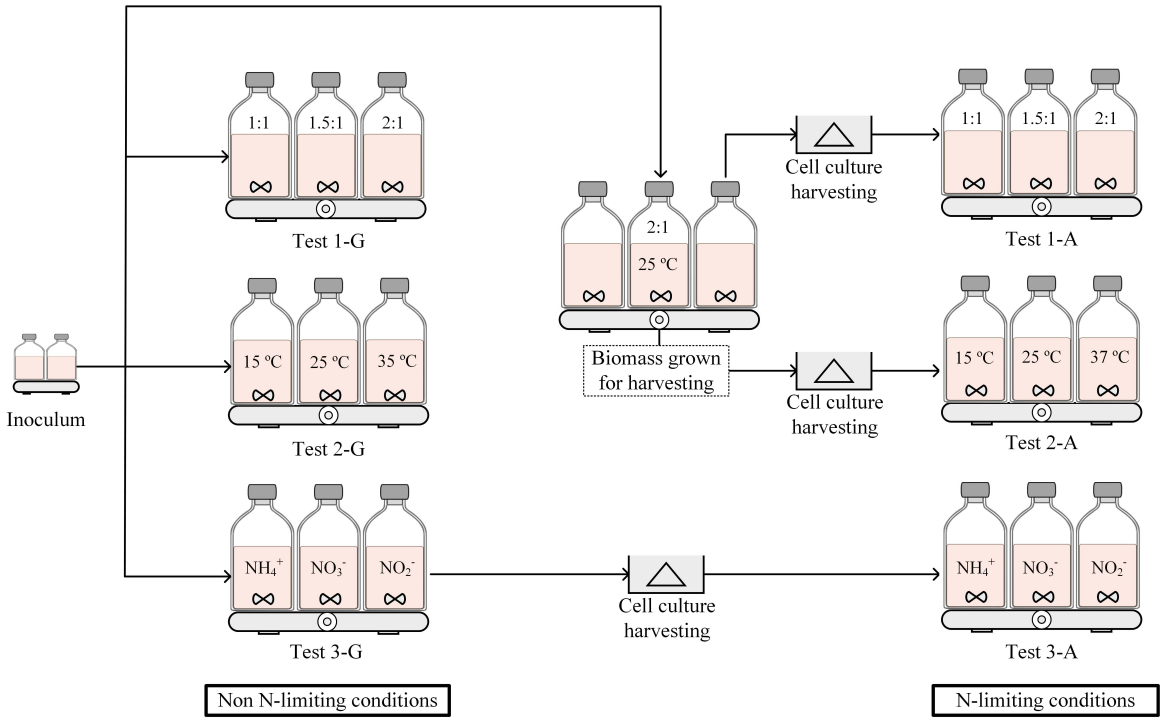

Fig. 3.1 *Outline of the experimental setup of the tests carried out and main conditions assayed.*

Three different headspace compositions (CH_4:O_2:CO_2:He) were tested in order to assess the influence of the O_2:CH_4 ratio on *M. hirsuta* CSC1 growth using biogas as a feedstock: 29.2:29.2:12.5:29.2%, 29.2:43.8:12.5:14.6% and 29.2:58.3:12.5:0.0%, which corresponded to O_2:CH_4 molar ratios of 1:1, 1.5:1 and 2:1, respectively. These headspace compositions were prepared by supplying the corresponding volumes from synthetic biogas, O_2 and He cylinders into 25-L Tedlar gas sampling bags. Then, these gas mixtures were pumped into the corresponding bottles headspace by a gas compressor (C5, Electro AD, Barcelona, Spain), ensuring a complete headspace replacement. Finally, the bottles were inoculated with fresh *M. hirsuta* CSC1 inoculum at 2.5% (v/v) and incubated over 2 weeks until CH_4 consumption ceased.

3.2.2.1 Test 1-A: Influence of the O_2:CH_4 ratio on PHB synthesis by M. hirsuta *CSC1*

The capacity of *M. hirsuta* CSC1 to synthesize PHB was assessed at O_2:CH_4 molar ratios of 1:1, 1.5:1 and 2:1. First, *M. hirsuta* CSC1 was grown at 25°C and 300 rpm in six 2.2-L serum bottles containing 400 mL of NMS medium under an O_2:CH_4 atmosphere of

66.7:33.3% until complete methane depletion (~10 days). Then, the biomass was harvested from the culture broth by centrifugation at 10000 rpm for 8 min (Sorvall Legend RT+; Thermo Scientific, USA) and re-suspended into 220 mL of nitrate-free mineral salt (NFMS) medium (prepared based on the NMS receipt described above without nitrate addition). An aliquot of 30 mL of this concentrated culture was inoculated (7.5% v/v) in each bottle resulting in an initial biomass concentration (estimated as total suspended solids, TSS) of 253.5 mg L^{-1}. Finally, the air headspace of the bottles was replaced with gas mixtures (prepared as above described) containing O_2:CH_4 molar ratios of 1:1, 1.5:1 and 2:1, and incubated until CH_4 consumption ceased (~3 weeks).

3.2.2.2 Test 2-G: Influence of the temperature on M. hirsuta *CSC1 growth*

M. hirsuta CSC1 growth on biogas was assessed at different temperatures (15, 25 and 37°C), which were controlled using either a thermostatic water bath (15 °C) or temperature-controlled rooms (25 and 37°C). The bottles were provided with an initial headspace CH_4:O_2:CO_2 atmosphere of 29.2:58.3:12.5% (O_2:CH_4 ratio of 2:1), inoculated with fresh *M. hirsuta* CSC1 inoculum at 2.5% (v/v) (initial TSS of 14 mg L^{-1}) and incubated until CH_4 consumption ceased (55, 16 and 30 days for 15, 25 and 37 °C, respectively).

3.2.2.3 Test 2-A: Influence of the temperature on PHB synthesis by M. hirsuta *CSC1*

The capacity of *M. hirsuta* CSC1 to synthesize PHB under nitrogen deprivation was assessed at 15, 25 and 37°C. First, *M. hirsuta* CSC1 biomass was grown at 25°C under an O_2:CH_4 headspace composition of 66.7:33.3% and harvested as previously described in section 3.2.2.2. The bottles in Test 2-A were initially provided with a headspace CH_4:O_2:CO_2 composition of 29.2:58.3:12.5% (O_2:CH_4 ratio of 2:1), inoculated with the harvested biomass at 7.5% (v/v) (initial TSS of 269.3 mg L^{-1}) and incubated at the target temperatures until CH_4 consumption ceased (~3 weeks).

3.2.2.4 *Test 3-G: Influence of the nitrogen source on* M. hirsuta *CSC1 growth*

The influence of the nitrogen source (NH_4Cl, $NaNO_3$ and $NaNO_2$) on *M. hirsuta* CSC1 growth on biogas was assessed by modifying the composition of the NMS medium accordingly, while maintaining a TN concentration of 138 mg N L^{-1}. The bottles (pH = 7.0 ± 0.1) were initially provided with a headspace CH_4:O_2:CO_2 composition of 29.2:58.3:12.5% (O_2:CH_4 ratio of 2:1), inoculated with fresh *M. hirsuta* CSC1 inoculum at 2.5% (v/v) (initial TSS of 21.3 mg L^{-1}) and incubated until CH_4 consumption ceased (≈2 weeks).

3.2.2.5 *Test 3-A: Influence of the nitrogen source during* M. hirsuta *CSC1 growth on PHB synthesis*

The influence of the nitrogen source (NH_4Cl, $NaNO_3$ and $NaNO_2$) during the growth phase on the capacity of *M. hirsuta* CSC1 to synthesize PHB was evaluated. Thus, the biomass grown in Test 3-G was harvested separately by centrifugation (at 10000 rpm for 8 min and re-suspended into 70 mL of NFMS per bottle). Then, the bottles were provided with an initial headspace CH_4:O_2:CO_2 composition of 29.2:58.3:12.5% (O_2:CH_4 ratio of 2:1), inoculated with the nitrogen-free cell suspension at 7.5% (v/v) (initial TSS of 192 ± 13 mg L^{-1}) and incubated until CH_4 consumption ceased (≈3 weeks).

3.2.3 Analytical methods

The gas concentrations of CH_4, O_2 and CO_2 were periodically monitored by using a Bruker 430 GC-TCD (Bruker Corporation, Palo Alto, USA) equipped with CP-PoraBOND Q and CP-Molsieve 5A columns as described by Estrada et al. (2014). pH and TSS in the culture broth were analyzed according to APHA (2015), whereas the optical density of the culture samples was determined at 600 nm (OD_{600}) by spectrophotometry (UV-2550; Shimadzu, Japan). NO_2^- and NO_3^- concentrations were quantified at the beginning and at the end of Test 3-G by high performance liquid chromatography-ion conductivity (HPLC-IC) according to Posadas et al. (2013). TN concentration was analyzed by chemiluminiscense using a TOC-V analyzer equipped with a TNM-1 unit (Shimadzu, Japan).

PHB extraction from *M. hirsuta* CSC1 biomass was conducted by modifying the method described by Zúñiga et al. (2011), which is based on the hydrolysis and propanolysis of the PHB. Two liquid samples (1.5 mL each) were centrifuged at 10000 rpm for 10 min. After discarding supernatant, 1 mL of propanol containing hydrochloric acid (80:20% (v/v)) and 2 mL of trichloromethane were added to the biomass pellets. Benzoic acid in propanol (10 µL) was used as internal standard solution (5 g L^{-1}). Then, samples were agitated by vortexing and incubated for 4h at 100ºC in a thermoreactor. After cooling down to room temperature, 1 mL of deionized water was added to the samples, which were agitated again. The organic phase was collected after phase separation and filtered (0.22 µm; Merck). The quantitative determination of PHB was carried out using an Agilent 7820A gas chromatograph (GC) coupled with a 5977E mass spectrometer detector (MSD) (Agilent Technologies, USA) and equipped with a DB-WAX column (Agilent Technologies, USA). The GC-MSD temperature program for PHB determination can be found elsewhere (López et al. 2014).

3.3 Results and discussion

3.3.1 Influence of the O_2:CH_4 ratio on *M. hirsuta* CSC1 growth

At the O_2:CH_4 ratios of 1.5:1 and 2:1, CH_4 (provided at an initial concentration of 161 ± 2 g m^{-3}) was fully depleted within the first 10 days (Fig. 3.2a). However, at the O_2:CH_4 ratio of 1:1, only 70% of the CH_4 initially present in the headspace was consumed as a result of O_2 limitation (Fig. 3.2a). In fact, methanotrophs require approximately 1.5 to 2 mol O_2 to oxidize 1 mol CH_4 (Karthikeyan et al., 2015). Therefore, biomass production (195 ± 6 mg TSS L^{-1}) at the lowest O_2:CH_4 ratio was approximately 23% lower than that obtained at O_2:CH_4 ratios of 1.5 and 2 (252 ± 4 mg TSS L^{-1}) (Fig. 3.2b). Nevertheless, comparable growth yields (Y_X/CH_4) were obtained at all O_2:CH_4 ratios tested (4.9 ± 0.2, 5.0 ± 0.1 and 5.2 ± 0.1 g TSS mol^{-1} CH_4 at ratios of 1:1, 1.5:1 and 2:1, respectively). Similarly, Rostkowski et al. (2013) also observed no significant difference in the growth yield of two type II methanotrophs – *Methylosinus trichosporium* OB3b (0.66 ± 0.03 g VSS g^{-1} CH_4) and *Methylocystis parvus* OBBP (0.55 ± 0.03 g VSS g^{-1} CH_4) – at different O_2:CH_4 ratios (from 0.37:1 to 1.47:1) with nitrate as the nitrogen source.

The O_2:CH_4 consumption molar ratios were similar at all tested conditions (1.4 ± 0.1, 1.5 ± 0.1 and 1.5 ± 0.0 mol O_2 mol^{-1} CH_4 at ratios of 1:1, 1.5:1 and 2:1, respectively). These values were close to the theoretical consumption molar ratio for type II methanotrophs growth (1.5 mol O_2 mol^{-1} CH_4) (Asenjo & Suk, 1986). Additionally, these results were in accordance with previous studies conducted with *M. trichosporium* OB3b, *M. parvus* OBBP and *M. hirsuta* CSC1, where O_2:CH_4 consumption molar ratios ranging from 1.3 to 1.5 mol O_2 mol^{-1} CH_4 were observed (López et al., 2018; Rostkowski et al., 2013; Zhang et al., 2017). Finally, it should be highlighted that O_2 availability severely influenced the maximum CH_4 removal rates (RRs). Thus, *M. hirsuta* CSC1 growth at an O_2:CH_4 ratio of 1:1 resulted in lower RR (26.5 ± 0.8 g CH_4 m^{-3} d^{-1}) than the cultivation at O_2:CH_4 ratios of 1.5 and 2 (34.0 ± 1.5 and 36.8 ± 0.7 g CH_4 m^{-3} d^{-1}, respectively). In this context, since the Henry´s law constants of O_2 and CH_4 ($H^{cp} = 1.4 \cdot 10^{-5}$ for methane and $H^{cp} = 1.3 \cdot 10^{-5}$ mol

m^{-3} Pa^{-1} for oxygen at 298.15 K (Sander, 2015)) are similar, low initial concentrations of O_2 in the gas phase entail low O_2 gas-liquid mass transfer rates, which can ultimately mediate O_2 limitation in the culture broth and reduced CH_4 RR.

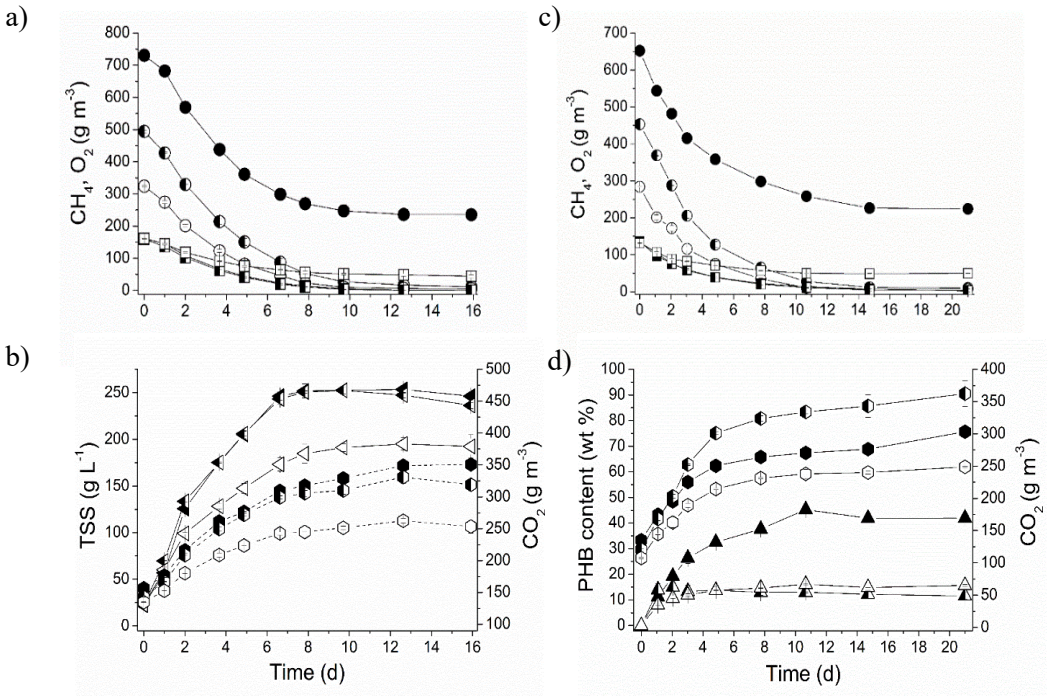

Fig. 3.2. *Time course of CH_4 (squares), O_2 (circles), CO_2 (hexagons), TSS (inverted triangles) and PHB (triangles) concentrations during the growth test 1-G (a, b) and the accumulation test 1-A (c, d). Empty, half-filled and filled symbols correspond to the experiments carried out under the O_2:CH_4 atmospheres of 1:1, 1.5 and 2:1, respectively.*

3.3.2 Influence of the O_2:CH_4 ratio on PHB synthesis by *M. hirsuta* CSC1

Under N-limiting conditions, O_2 and CH_4 consumption by *M. hirsuta* CSC1 exhibited the same pattern as in the growth assay at all tested O_2:CH_4 ratios (Fig. 3.2c). However, the O_2:CH_4 consumption molar ratios observed during PHB synthesis were higher than those recorded in the growth test (1.7 ± 0.0, 1.7 ± 0.1 and 1.6 ± 0.1 mol O_2 mol CH_4^{-1} at 1:1, 1.5:1 and 2:1 ratios, respectively) and also exceeded the theoretical value for PHB accumulation by type II methanotrophs (1.5 mol O_2 mol^{-1} CH_4) (Asenjo & Suk, 1986). Previous studies

with *M. trichosporium* OB3b, *M. parvus* OBBP and *M. hirsuta* CSC1 reported a decrease in the O_2:CH_4 consumption molar ratio under N-limiting conditions due to the electron deviation to PHB accumulation (López et al., 2018; Rostkowski et al., 2013). The maximum CH_4 RRs recorded in the assays carried out at 1:1, 1.5:1 and 2:1 O_2:CH_4 ratios were 22.9 ± 1.7, 28.4 ± 0.3 and 36.1 ± 1.7 g CH_4 m^{-3} d^{-1}, respectively.

M. hirsuta CSC1 reached the maximum PHB content within 5 and 2 days at the O_2:CH_4 ratios 1:1 and 1.5:1, while 8 days were needed at the ratio 2:1 (Fig. 3.2d). However, the latter condition resulted in a maximum PHB content threefold higher (45.3 ± 1.7 wt%) than those obtained at 1:1 and 1:5 ratios (16.1 ± 0.2 and 15.0 ± 1.8 wt%, respectively) (Fig. 3.2d). This corresponded to PHB yields (Y_{PHB/CH_4}) of 2.3 ± 0.0, 2.6 ± 0.1 and 6.9 ± 0.1 g PHB mol^{-1} CH_4 at 1:1, 1.5:1 and 2:1 ratios, respectively. At O_2:CH_4 ratios of 1:1 and 1.5:1, the analysis of the carbon mass balance (data not shown) suggests that carbon fluxes support a major mineralization rather than PHB synthesis through the serine cycle, i.e.: CH_4 is preferentially used for energy generation rather than PHB synthesis as a result of the metabolic stress caused by O_2 limitation in the assays. The results obtained at the O_2:CH_4 ratio of 2:1 were in agreement with those reported by López et al. (2018), who found a maximum PHB content of 45 ± 1 wt% (Y_{PHB/CH_4} = 7.0 ± 0.0g PHB mol^{-1} CH_4) when using biogas as a feedstock for biopolymer production by *M. hirsuta* CSC1 in batch assays at a similar O_2:CH_4 ratio (1.75:1). According to Karthikeyan et al. (2015), O_2 requirements during biopolymer synthesis depend on the methanotroph strain, and limiting O_2 concentrations can negatively affect PHB accumulation. Therefore, an O_2:CH_4 ratio higher than 1.5:1 is required to maximize PHB synthesis in *M. hirsuta* CSC1.

3.3.3 Influence of the temperature on *M. hirsuta* CSC1 growth

The growth of *M. hirsuta* CSC1 at three different temperatures (15, 25 and 37°C) was evaluated (Fig. 3.3a and b). CH_4 removals > 95% were achieved within 10 and 43 days at 25 and 15°C, respectively. Neither *M. hirsuta* CSC1 growth nor CH_4 consumption was recorded at 37ºC for the 30 days of experiment. Despite its relevance, the influence of temperature on *M. hirsuta* CSC1 growth has been scarcely studied in literature. For instance, Lindner et al. (2007) pointed out that *M. hirsuta* CSC1 grows optimally at 30ºC and is not able to grow at 37ºC. On the contrary, other species from the genus *Methylocystis*, such as *M. parvus* (15-37ºC) and *M. rosea* (5-37ºC), possess the ability to grow at 37ºC, although optimal values are similar to those reported for *M. hirsuta* (28-30ºC and 27ºC for *M. parvus* and *M. rosea*, respectively) (Tsyrenzhapova et al., 2007).

The O_2:CH_4 consumption molar ratios were not temperature dependent, with values of 1.5 ± 0.1 and 1.6 ± 0.1 mol O_2 mol CH_4^{-1} at 15 and 25ºC, respectively, similar to the theoretical ones previously discussed in section 3.3.1. Conversely, cultures grown at 25ºC exhibited a maximum RR of 36.5 ± 0.2 g CH_4 m^{-3} d^{-1} during the exponential phase, whereas, at 15ºC, *M. hirsuta* CSC1 supported a maximum RR of 6.2 ± 0.2 g CH_4 m^{-3} d^{-1} after a very long lag phase (≈22 d). Thus, the kinetics of methane biodegradation by *M. hirsuta* CSC1 exhibited a great sensitivity to temperature. Finally, maximum biomass concentrations of 198.5 ± 12.6 and 244.2 ± 3.8 mg TSS L^{-1} were recorded at 15 and 25ºC, respectively, which resulted in biomass yield coefficients (Y_{X/CH_4}) of 5.0 ± 0.2 and 5.8 ± 0.2 g TSS mol^{-1} CH_4, respectively.

3.3.4 Influence of the temperature on PHB synthesis by *M. hirsuta* CSC1

The temperature of cultivation did influence not only the extent of CH_4 oxidation, but also PHB synthesis in the absence of nitrogen (Fig. 3.3c and d). Methane conversion reached 60% within the first 15 days at 15ºC, while a nearly complete methane conversion (>90%) was achieved at 25 and 37ºC within 15 days, with maximum RRs of 38.8 ± 0.8 and

36.4 ± 2.8 g CH_4 m^{-3} d^{-1}, respectively. At 15ºC, the maximum CH_4 RR was approximately half of the RRs values recorded at 25 and 37ºC (17.7 ± 0.2 g CH_4 m^{-3} d^{-1}).

No significant influence of the temperature on the O_2:CH_4 consumption molar ratios was observed (1.5 ± 0.1, 1.6 ± 0.0 and 1.7± 0.2 mol O_2 mol CH_4^{-1} at 15, 25 and 37ºC, respectively).

On the other hand, the highest PHB content in *M. hirsuta* CSC1 was obtained at 25ºC with a PHB accumulation of 39.7 ± 0.2 wt%, followed by a 32.0 ± 0.1 wt% at 15ºC and 30.1 ± 0.5 wt% at 37ºC. This similar methane consumption at different PHB contents at 25 and 37ºC suggests that temperature exerts a significant impact on PHB yield. In this context, similar PHB yields of 6.6 ± 0.0 and 6.9 ± 0.3 g PHB mol^{-1} CH_4 were observed at 15 and 25ºC, respectively, whereas the PHB yield at 37ºC was 5.0 ± 0.5 g PHB mol^{-1} CH_4. Despite its sensitivity to temperature, *M. hirsuta* CSC1 exhibited a high PHB synthesis capacity within the range of temperatures tested. It should be stressed that PHB accumulation tests at different temperatures were carried out with biomass pre-cultivated at 25ºC. Interestingly, no lag phase was observed during the accumulation stage at any of the temperatures tested. Moreover, the 10 day pre-cultivation phase was unlikely to induce any temperature adaptation based on the fact that experiments were carried out with an axenic strain.

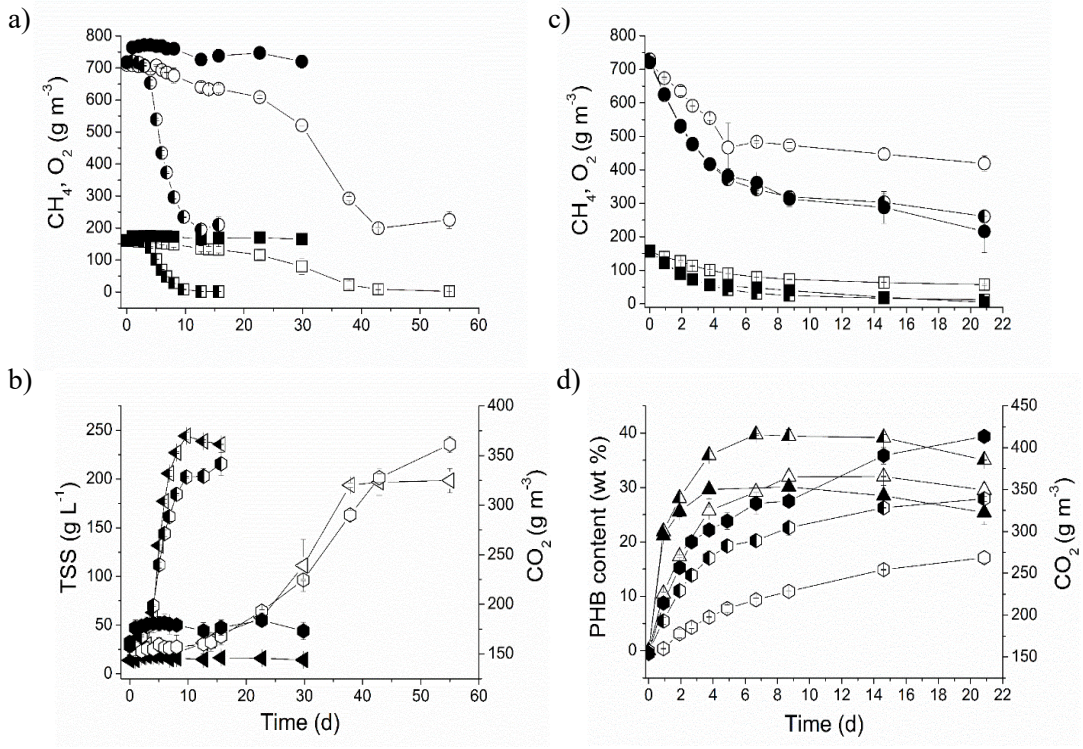

Fig. 3.3. *Time course of CH_4 (squares), O_2 (circles), CO_2 (hexagons), TSS (inverted triangles) and PHB (triangles) concentrations during the growth test 2-G (a, b) and the accumulation test 2-A (c, d). Empty, half-filled and filled symbols correspond to the experiments carried out at the temperatures of 15, 25 and 37°C, respectively.*

The PHB contents herein recorded were in good agreement with previous findings for *M. hirsuta* (42.5% at 30ºC (Rahnama et al., 2012) or 34.6% at 25ºC (García-Pérez et al., 2018)). In a recent study, Pérez et al. (2019) evaluated the PHB accumulation capacity of mixed cultures enriched from *Sphagnum* and *Sphagnum* + activated sludge at 25, 30 and 37ºC. Enrichments from *Sphagnum* at 25ºC resulted in the highest PHB contents (~18 wt%), which were mediated by the dominance of the *Methylocystis* genus (up to 46%) in the community. Interestingly, while *M. hirsuta* CSC1 in this study was not able to grow at 37ºC (likely due to the heat stress that did not enable DNA replication in cells and inhibited the activity of the base excision repair system) (Kantidze et al., 2016), this microorganism was able to synthetize PHB at such a high temperature. These outcomes are hardly comparable with literature since, to the best of the author's knowledge, no previous studies

have addressed the PHB synthesis capacity of pure methanotrophic cultures at different temperatures.

3.3.5 Influence of the nitrogen source on *M. hirsuta* CSC1 growth

Methane conversions of 80% and 100%, along with maximum RRs of 31.4 ± 1.3 and 35.6 ± 1.9 g CH_4 m^{-3} d^{-1}, were recorded when ammonium and nitrate, respectively, were used as the sole nitrogen source (Fig. 3.4a and b). The lower rate of methane oxidation in the presence of ammonium at 10 mM NH_4^+ evidenced a slight competitive inhibition between methane and ammonium for the enzyme particulate methane monooxygenase (pMMO) (Bordel et al., 2019a). In this regard, previous studies reported greater inhibitory effects on methane biodegradation at 5 mM ammonium on some type II MOB strains, such as *Methylocystis sp*. and *Methylosinus sporium* (Nyerges & Stein, 2009). This suggests that *M. hirsuta* CSC1 exhibits a significantly greater tolerance than its close relative species. Interestingly, a negligible growth was observed in the presence of nitrite (10 mM NO_2^-), which highlights the inhibitory effect of nitrite on *M. hirsuta* metabolism, more specifically on the formate dehydrogenase activity (Jollie & Lipscomb, 1990). Unfortunately, the mechanisms underlying this inhibition have not been yet elucidated (King and Schnell, 1994).

Nevertheless, the genome sequence of the *M. hirsuta* CSC1, which has recently been published, revealed that this strain possesses genes involved in denitrification, which would allow nitrite reduction to NO and further to N_2O (Bordel et al., 2019a). Thus, despite its detrimental effect on CH_4 oxidation, a certain tolerance was observed in previous works investigating the toxic effect of nitrite on mixed methanotrophic communities (Dunfield & Knowles, 1995) and pure cultures (NMS amended with nitrite (2mM) in *Methylocystis* sp.) (Nyerges & Stein, 2009).

M. hirsuta CSC1 cultures grown in nitrate supported greater biomass concentrations (TSS = 264.4 ± 0.7 mg L^{-1}) than those grown in ammonium (TSS = 239.3 ± 2.9 mg L^{-1}) as a result of the incomplete methane oxidation in the presence of the latter. Similarly, the

biomass yield depended on the nitrogen sources (Y_{X/CH_4} = 7.10 ± 0.10 and 5.80 ± 0.01 g TSS mol^{-1} CH_4 were estimated for ammonium and nitrate, respectively). Although biomass growth rates were quite similar using both media, ammonium seems to be the preferred N source for *M. hirsuta* CSC1 in terms of biomass yield. However, the influence of the nitrogen source on the metabolism of methanotrophs in strain dependent. For instance, ammonium mediated greater biomass yields than nitrate with concomitant lower growth rates for the type-II methanotrophs *Methylocystis* sp. Rockwell and *Methylocystis* sp. WRRC1 (Tays et al., 2018), whereas nitrate was the preferred nitrogen source in terms of biomass productivity for *M. trichosporium* OB3b (Rostkowski et al., 2013; Tays et al., 2018). Moreover, the results obtained in the present work were in agreement with Bordel et al. (2019b), who predicted (using a Genome Scale Metabolic Model for *M. hirsuta*) higher biomass yields when using ammonium owing to the fact that no reducing power is needed for the conversion of NH_4^+ to organic nitrogen. The final pH of the culture media was also affected by the nitrogen source, with a final pH value of 4.5 when using ammonium, and pH values of 6.3 and 6.2 in the presence of nitrate or nitrite, respectively. This decrease in pH during CH_4 biodegradation with NH_4^+ was likely due to the nitrification mediated by the enzyme pMMO. Indeed, when ammonium was used as a nitrogen source, an accumulation of nitrate up to 48.2 ± 8.0 mg L^{-1} occurred in the culture medium. In this sense, ammonium is initially oxidized by pMMO to hydroxylamine (NH_2OH) (Hanson & Hanson, 1996), which is a highly toxic intermediate further oxidized to nitrite (NO_2^-) due to the evolved ability of ammonia-oxidizing bacteria to encode the enzyme hydroxylamine oxidoreductase (HAO) (Stein & Klotz, 2011). Finally, nitrite is converted into NO_3^-.

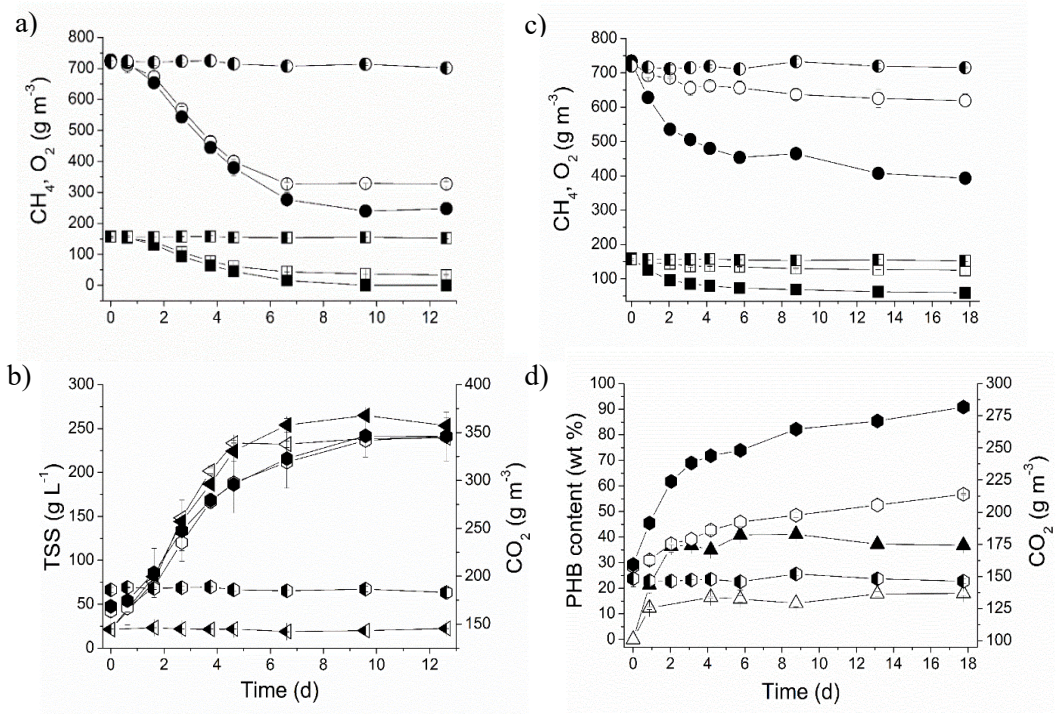

Fig. 3.4. *Time course of CH_4 (squares), O_2 (circles), CO_2 (hexagons), TSS (inverted triangles) and PHB (triangles) concentrations during the growth test 3-G (a, b) and the accumulation test 3-A (c, d). Empty, half-filled and filled symbols correspond to the experiments carried out with NH_4^+, NO_2^- and NO_3^- as nitrogen sources, respectively.*

3.3.6 Influence of the nitrogen source during *M. hirsuta* CSC1 growth on PHB synthesis

This test evaluated the PHB synthesis capacity of *M. hirsuta* CSC1 using biomass pre-grown in different nitrogen sources. The history and physiological status of the biomass influenced the capacity of the cells to oxidize CH_4 and accumulate PHB (Fig. 3.4c and d). Cultures previously grown in ammonium converted 21.9 ± 0.6% of the initial methane supplied, whereas those grown in nitrate achieved a total conversion of 62.8 ± 0.0% within 13 days of experiment (Fig. 3.4c). Similarly, nearly a threefold decrease in the methane removal rate was observed in cultures previously grown in ammonium (13.3 ± 0.9 g CH_4 m^{-3} d^{-1}) compared with cultures previously grown in nitrate (38.3 ± 2.4 g CH_4 m^{-3} d^{-1}). Similarly, the PHB content of cultures grown in nitrate accounted for 41.1 ± 0.1%, while a PHB content of 18.0 ± 0.7% was observed in biomass grown in ammonium (Fig. 3.4d).

These results are in agreement with those of Rostkowski et al. (2013) who reported higher PHB contents under N deprivation when *M. trichosporium* OB3b was previously grown in nitrate than in ammonium (29 versus 12%, respectively) at an O_2:CH_4 ratio of 1:1. However, the PHB contents achieved with species from the same genus (*M. parvus* OBBP) do not seem to support an overall pattern (60 wt% under ammonium limitation and 14 wt% under nitrate limitation).

The highest experimental yield in the present study was recorded under nitrate deprivation (Y_{PHB/CH_4} = 7.3 ± 0.1 g PHB mol^{-1} CH_4), which was close to the theoretical value (8.6 g mol^{-1}) estimated by Yamane (1993) and to other experimental values reported in literature (7.0 – 8.8 g PHB mol^{-1} CH_4 for *M. hirsuta* CSC1 and *Methylocystis sp.* GB 25, respectively) (López et al., 2018; Wendlandt et al., 2001). Under NH_4^+ limitation, the PHB yield herein obtained was substantially lower (Y_{PHB/CH_4} = 3.2 ± 0.1 g PHB mol^{-1} CH_4). The mechanism of influence on this counterproductive PHB may be ascribed to the acidic pH (4.5) of the culture broth at the end of the previous test, which negatively impacted the physiological status of *M. hirsuta* CSC1 (Test 3-G). According to Hanson and Hanson (1996), pH values ranging from 4.0 to 6.0 exert a detrimental effect on methane oxidation rates in methanotrophs. In order to uncouple the effects of the N source and pH on PHB synthesis, further investigation with pH control should be conducted in automated fermenters. Finally, the resulting O_2 demand for CH_4 conversion under nitrate deprivation correlated with the values reported in sections 3.3.2 and 3.3.4, under similar environmental conditions (≈1.7 mol O_2 mol CH_4^{-1}).

3.4 Conclusions

The different O_2:CH_4 ratios tested did not significantly influenced *M. hirsuta* growth yields, although lower CH_4 RRs were achieved under O_2-limiting conditions. O_2 limitation also induced lower PHB contents under N deprivation. Higher growth yields and PHB accumulations were recorded when temperature increased from 15 to 25ºC. Interestingly, while a negligible growth was observed at 37ºC, nitrogen limitation supported PHB contents up to 30 wt% at this temperature. Finally, ammonium resulted in higher growth yields compared to nitrate, while nitrite inhibited severely its growth. However, the PHB synthesis was higher for the culture previously grown in nitrate.

Acknowledgements

The authors acknowledge the financial support from the Spanish Ministry of Economy and Competitiveness (BES-2016-077160 contract and CTM2015-70442-R project), and the Regional Government of Castilla y León and the EU-FEDER (CLU 2017-09, VA281P18 and UIC 071). The authors are very grateful to J. Prieto and E. Marcos for their technical support.

References

APHA (2015) Standard Methods for the Examination of Water and Wastewater. 21st ed, American Public Health Association. Washington, D.C.

Asenjo, J.A., Suk, J.S. (1986) Microbial Conversion of Methane into poly-β-hydroxybutyrate (PHB): Growth and intracellular product accumulation in a type II methanotroph. *J Ferment Technol*, **64**(4), 271-278. doi: 10.1016/0385-6380(86)90118-4

Bordel, S., Rodríguez, E., Muñoz, R. (2019a) Genome sequence of *Methylocystis hirsuta* CSC1, a polyhydroxyalkanoate producing methanotroph. *MicrobiologyOpen*, **8**(6), 1-5. doi: 10.1002/mbo3.771

Bordel, S., Rodríguez, Y., Hakobyan, A., Rodríguez, E., Lebrero, R., Muñoz, R. (2019b) Genome scale metabolic modeling reveals the metabolic potential of three type II methanotrophs of the genus *Methylocystis*. *Metab Eng*, **54**, 191-199. doi: 10.1016/j.ymben.2019.04.001

Bowman, J., Lindsay, I., Nichols, P.D., Hayward, A.C. (1993) Revised taxonomy of the methanotrophs: Description of *Methylobacter* gen. nov., emendation of *Methylococcus*, validation of *Methylosinus* and *Methylocystis* species, and a proposal that the family *Methylococcaceae* includes only the group I methanotrophs. *Int J Syst Evol Microbiol*, **43**(4), 735-753. doi: 10.1099/00207713-43-4-735

Cantera, S., Bordel, S., Lebrero, R., Gancedo, J., García-Encina, P.A., Muñoz, R. (2019) Bio-conversion of methane into high profit margin compounds: an innovative, environmentally friendly and cost-effective platform for methane abatement. World *J Microbiol Biotechnol*, **35**(16), 1-10. doi: 10.1007/s11274-018-2587-4

Cantera, S., Muñoz, R., Lebrero, R., López, J.C., Rodríguez, Y., García-Encina, P.A. (2018) Technologies for the bioconversion of methane into more valuable products. *Curr Opin Biotechnol*, **50**, 128-135. doi: 10.1016/j.copbio.2017.12.021.

Chen, G.Q. (2009) A microbial polyhydroxyalkanoates (PHA) based bio- and materials industry. *Chem Soc Rev*, **38**(8), 2434-2446. doi: 10.1039/B812677C

Choi, J., Lee, S.Y. (1999) Factors affecting the economics of polyhydroxyalkanoate production by bacterial fermentation. *Appl Microbiol Biotechnol*, **51**(1), 13-21. doi: 10.1007/s002530051357

Dunfield, P., Knowles, R. (1995) Kinetics of inhibition of methane oxidation by nitrate, nitrite, and ammonium in a humisol. *Appl environ microbiol*, **61**(8), 3129-3135.

Dunfield, P.F. (2009) Methanotrophy in extreme environments. In: eLS, John Wiley & Sons Ltd. Chichester.

Estrada, J.M., Lebrero, R., Quijano, G., Pérez, R., Figueroa-González, I., García-Encina, P.A., Muñoz, R. (2014) Methane abatement in a gas-recycling biotrickling filter: Evaluating innovative operational strategies to overcome mass transfer limitations. *Chem Eng J*, **253**, 385-393. doi: 10.1016/j.cej.2014.05.053.

EBA (2019) EBA Statistical Report 2018. European Biogas Association. http://european-biogas.eu/wp-content/uploads/2019/05/EBA_report2018_abriged_A4_vers12_220519_RZweb.pdf (Accessed: 5.6.2019).

García-Pérez, T., López, J.C., Passos, F., Lebrero, R., Revah, S., Muñoz, R. (2018) Simultaneous methane abatement and PHB production by *Methylocystis hirsuta* in a novel gas-recycling bubble column bioreactor. *Chem Eng J*, **334**, 691-697. doi: 10.1016/j.cej.2017.10.106.

Hanson, R.S., Hanson, T.E. (1996) Methanotrophic bacteria. *Microbiol rev*, **60**(2), 439-471.

Hoefman, S., van der Ha, D., Boon, N., Vandamme, De Vos, P., Heylen, K. (2014) Niche differentiation in nitrogen metabolism among methanotrophs within an operational taxonomic unit. *BMC Microbiol*, **14**(83). doi: 10.1186/1471-2180-14-83

Jollie, D.R., Lipscomb, J.D. (1990) Formate dehydrogenase from *Methylosinus trichosporium* OB3b. *Methods Enzymol*, **188**, 331-334. doi: 10.1016/0076-6879(90)88051-B.

Kantidze, O.L., Velichko, A.K., Luzhin, A.V., Razin, S.V. (2016) Heat Stress-Induced DNA Damage. *Acta Naturae***. 8**(2): 75–78.

Karthikeyan, O.P., Chidambarampadmavathy, K., Cirés, S., Heimann, K. (2015) Review of sustainable methane mitigation and biopolymer production. *Crit Rev Environ Sci Technol*, **45**(15), 1579-1610. doi: 10.1080/10643389.2014.966422

King, G.M., Schnell, S. (1994) Effect of increasing atmospheric methane concentration on ammonium inhibition of methane oxidation by *Methylobacter albus* BG8 and *Methylosinus trichosporium* OB3b at low methane concentrations. *Appl Environ Microbiol* **60**(10), 3508-3513.

Lee, G.N., Na, J. (2013) Future of microbial polyesters. *Microbial Cell Factories*, **12**(54), 1-4. doi: 10.1186/1475-2859-12-54

Lindner, A.S., Pacheco, A., Aldrich, H.C., Costello Staniec, A., Uz, I., Hodson, D.J. (2007) *Methylocystis hirsuta* sp. nov., a novel methanotroph isolated from a groundwater aquifer. *Int J Syst Evol Microbiol*, **57**(8), 1891-1900. doi: 10.1099/ijs.0.64541-0

López, J.C., Arnáiz, E., Merchán, L., Lebrero, R., Muñoz, R. (2018) Biogas-based polyhydroxyalkanoates production by *Methylocystis hirsuta*: A step further in anaerobic digestion biorefineries. *Chem Eng J*, **333**, 529-536. doi: 10.1016/j.cej.2017.09.185.

López, J.C., Quijano, G., Pérez, R., Muñoz, R. (2014) Assessing the influence of CH_4 concentration during culture enrichment on the biodegradation kinetics and population structure. *J Environ Manage*, **146**, 116-123. doi: 10.1016/j.jenvman.2014.06.026

Murrell, J.C., Dalton H. (1983) Nitrogen-fixation in obligate methanotrophs. *J Gen Microbiol*, **129**, 3481-3486.

nova-Institute GmbH (2016) Bio-based building blocks and polymers global capacities and trends 2016 – 2021. http://bio-based.eu/downloads/bio-based-building-blocks-and-polymers-global-capacities-and-trends-2016-2021-2/ (Accessed: 2.3.2019).

Nyerges, G., Stein, L.Y. (2009) Ammonia cometabolism and product inhibition vary considerably among species of methanotrophic bacteria. *FEMS Microbiol Lett*, **297**(1), 131-136. doi: 10.1111/j.1574-6968.2009.01674.x

Pérez, R., Casal, J., Muñoz, R., Lebrero, R. (2019) Polyhydroxyalkanoates production from methane emissions in *Sphagnum* mosses: Assessing the effect of temperature and phosphorus limitation. *Sci Total Environ*, **688**, 684-690. doi: 10.1016/j.scitotenv.2019.06.296

Pieja, A.J., Morse, M.C., Cal, A.J. (2017) Methane to bioproducts: the future of the bioeconomy? *Curr Opin Chem Biol*, **41**, 123-131. doi: 10.1016/j.cbpa.2017.10.024.

Posadas, E., García-Encina, P.-A., Soltau, A., Domínguez, A., Díaz, I., Muñoz, R. (2013) Carbon and nutrient removal from centrates and domestic wastewater using algal–bacterial biofilm bioreactors. *Bioresour Technol*, **139**, 50-58. doi: 10.1016/j.biortech.2013.04.008

Rahnama, F., Vasheghani-Farahani, E., Yazdian, F., Shojaosadati, S.A. (2012) PHB production by *Methylocystis hirsuta* from natural gas in a bubble column and a vertical loop bioreactor. *Biochem Eng J*, **65**, 51-56. doi: 10.1016/j.bej.2012.03.014.

Raza, Z., Abid, S., Banat, I. (2018) Polyhydroxyalkanoates: Characteristics, production, recent developments and applications. *Int Biodeterior Biodegradation*, **126**, 45-56. doi: 10.1016/j.ibiod.2017.10.001

Rostkowski, K.H., Pfluger, A.R., Criddle, C.S. (2013) Stoichiometry and kinetics of the PHB-producing Type II methanotrophs *Methylosinus trichosporium* OB3b and *Methylocystis parvus* OBBP. *Bioresour Technol*, **132**, 71-77. doi: 10.1016/j.biortech.2012.12.129.

Sander, R. (2015) Compilation of Henry's law constants (version 4.0) for water as solvent. *Atmos. Chem. Phys*. **15**(8), 4399-4981. doi: 10.5194/acp-15-4399-2015

Singh, A., Sharma, L., Mallick, N., Mala, J. (2017) Progress and challenges in producing polyhydroxyalkanoate biopolymers from cyanobacteria. *J Appl Phycol*, **29**, 1213–1232. doi: 10.1007/s10811-016-1006-1

Stein, L.Y., Klotz, M.G. (2011) Nitrifying and denitrifying pathways of methanotrophic bacteria. *Biochem Soc Trans*, **39**(6), 1826-1831. doi: 10.1042/BST20110712

Strong, J.P., Laycock, B., Mahamud, N.S., Jensen, D.P., Lant, A.P., Tyson, G., Pratt, S. (2016) The Opportunity for High-Performance Biomaterials from Methane. *Microorganisms*, **4**(11), 1-20. doi: 10.3390/microorganisms4010011

Tays, C., Guarnieri M.T., Sauvageau D., Stein L.Y. (2018) Combined effects of carbon and nitrogen source to optimize growth of proteobacterial methanotrophs. *Front. Microbiol*. **9,** 2239. doi: 10.3389/fmicb.2018.02239

Tsyrenzhapova, I.S., Eshinimaev, B.Ts., Khmelenina, V.N., Osipov, G.A., Trotsenko, Yu.A. (2007) A new thermotolerant aerobic methanotroph from a thermal spring in Buryatia. *Microbiology* **76**, 118-121. doi:10.1134/S0026261707010171

Wendlandt, K.D., Jechorek, M., Helm, J., Stottmeister, U. (2001) Producing poly-3-hydroxybutyrate with a high molecular mass from methane. *J Biotechnol*, **86**(2), 127-133. doi: 10.1016/S0168-1656(00)00408-9.

Yamane, T. (1993) Yield of poly-D(-)-3-hydroxybutyrate from various carbon sources: A theoretical study. *Biotechnol Bioeng*, **41**(1), 165-170. doi: 10.1002/bit.260410122

Zhang, T., Zhou, J., Wang, X., Zhang, Y. (2017) Coupled effects of methane monooxygenase and nitrogen source on growth and poly-β-hydroxybutyrate (PHB) production of *Methylosinus trichosporium* OB3b. *J Environ Sci*, **52**, 49-57. doi: 10.1016/j.jes.2016.03.001

Zúñiga, C., Morales, M., Le Borgne, S., Revah, S. (2011) Production of poly-β-hydroxybutyrate (PHB) by *Methylobacterium organophilum* isolated from a methanotrophic consortium in a two-phase partition bioreactor. *Journal of Hazard Mater*, **190**(1), 876-882. doi: 10.1016/j.jhazmat.2011.04.011.

4.

Modeling of polyhydroxyalkanoate synthesis from biogas by *Methylocystis hirsuta*

This chapter was adapted after its publication in *ACS Sustainable Chemistry & Engineering*:

Chen, X., Rodríguez, Y., López, J.C., Muñoz, R., Ni, B.-J., Sin, G. (2020) Modeling of polyhydroxyalkanoates synthesis from biogas by *Methylocystis hirsuta*. *ACS Sustain Chem Eng* 8(9), 3906-3912. doi: 10.1021/acssuschemeng.9b07414

Modeling of polyhydroxyalkanoate synthesis from biogas by *Methylocystis hirsuta*

Xueming Chen[1,*], Yadira Rodríguez[2], Juan C. López[3], Raúl Muñoz[2], Bing-Jie Ni[4], Gürkan Sin[1]

[1]Process and Systems Engineering Center (PROSYS), Department of Chemical and Biochemical Engineering, Technical University of Denmark, 2800 Kgs. Lyngby, Denmark

[2]Institute of Sustainable Processes, University of Valladolid, Dr. Mergelina s/n, 47011 Valladolid, Spain

[3]Ainia Centro Tecnológico, Benjamin Franklin 5-11, 46980 Paterna, Valencia, Spain

[4]Centre for Technology in Water and Wastewater, School of Civil and Environmental Engineering, University of Technology Sydney, Sydney, NSW 2007, Australia

*Correspondence to

Xueming Chen, Tel: + 45 8194 8080, E-mail: xuem.chen@hotmail.com

---

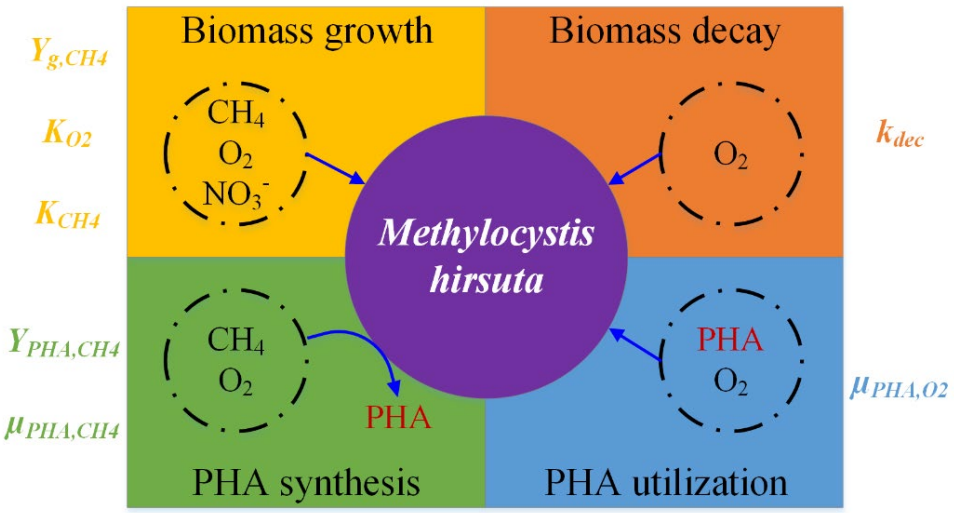

Graphical abstract

Abstract

Methylocystis hirsuta, a type II methanotroph, has been experimentally demonstrated to be able to efficiently synthesize polyhydroxyalkanoates (PHA) from biogas under nutrient-limited conditions. A mechanistic model capable of describing the relevant processes of *Methylocystis hirsuta*, which is currently not available, would therefore lay a solid foundation for future practical demonstration and optimization of the PHA synthesis technology using biogas. To this end, dedicated batch tests were designed and conducted to obtain experimental data for different mechanistic processes of *Methylocystis hirsuta*. Through utilizing the experimental data of well-designed batch tests and following a step-wise model calibration/validation protocol, the stoichiometrics and kinetics of *Methylocystis hirsuta* are reported for the first time, including the yields of growth and PHA synthesis on CH_4 (0.14±0.01 g COD g^{-1} COD and 0.25±0.02 g COD g^{-1} COD), the CH_4 and O_2 affinity constants (5.1±2.1 g COD m^{-3} and 4.1±1.7 g O_2 m^{-3}), the maximum PHA consumption rate (0.019±0.001 g COD g^{-1} COD d^{-1}) and the maximum PHA synthesis rate on CH_4 (0.39±0.05 g COD g^{-1} d^{-1}). Through applying the developed model, an optimal O_2:CH_4 molar ratio of 1.6 mol O_2 mol^{-1} CH_4 was found to maximize the PHA synthesis by *Methylocystis hirsuta*. Practically, the model and parameters obtained would not only benefit the design and operation of bioreactors performing PHA synthesis from biogas, but also enable specific research on selection for type II methanotrophs in diverse environments.

Keywords: biogas; modeling; polyhydroxyalkanoates (PHA); type II methanotrophs

4.1 Introduction

Polyhydroxyalkanoates (PHA) are biopolymers that could act as storage compounds for microorganisms under conditions of unbalanced growth (Anderson and Dawes, 1990; Burniol-Figols et al., 2018b). Some bacterial species are capable of producing PHA under conditions which restrict growth by nutrient limitation. Due to their biocompatibility, biodegradability, and thermal and mechanical properties similar to polyethylene and polypropylene, PHA have been regarded as a potential substitute for petrochemically-derived plastics, the production of which, however, often entails environmental concerns such as greenhouse gas emissions (López et al., 2018, Morgan-Sagastume et al., 2010; Wijeyekoon et al., 2018). Despite the currently small scale of industrial manufacturing of PHA worldwide, the continuous development of the PHA market is hindered by the high costs associated with the production from carbon source and the downstream processing, which are 4 - 9 times higher than those associated with the generation of conventional plastics (Burniol-Figols et al., 2018a; Chen, 2009; Reddy et al., 2003; Serafim et al., 2008; Singh et al., 2016; Venkata Mohan and Venkateswar Reddy, 2013; Wijeyekoon et al., 2018).

Under such circumstances, the CH_4 present in biogas could serve as a low-cost feedstock for PHA synthesis, especially considering its prevalent generation at wastewater treatment plants through waste activated sludge anaerobic digestion as well as the nature of methane itself as a greenhouse gas (Rostkowski et al., 2012, Strong et al., 2015). As discussed by López et al. (2018), the potential of biogas as a renewable energy source for heat and electricity generation which usually necessitates high investment on site and incentives might weaken due to the huge reserves of shale gas detected worldwide and the decreasing prices of solar and wind energy. Therefore, the bioconversion of biogas into PHA with high added-value is a promising technology that could also assist in combatting climate change.

Capable of using methane as the sole carbon and energy source, methanotrophs are typically classified into two types based on their metabolic and physiological differences. Different from type I methanotrophs, type II methanotrophs (e.g., *Methylocystis*, *Methylosinus* and *Methylocella* genera) are able to synthesize PHA from methane under nutrient-limited conditions (e.g., in the absence of nitrogen source needed for growth) (Hanson and Hanson, 1996, Pieja et al., 2011). Among the type II methanotrophs identified, *Methylocystis hirsuta* has been found to possess a high PHA-accumulating capacity, as evidenced by its highest PHA production from methane recorded (i.e., PHA content of 43 – 45 % w/w) (López et al., 2018, Rahnama et al., 2012). Despite the reported experimental research, to the best of our knowledge, there is no specific mechanistic modeling work on *Methylocystis hirsuta*. This gap needs to be filled if optimizing PHA synthesis is desired. In particular, if the feast-famine regime is applied to achieve continuous PHA production (e.g., through manipulating the availability of nitrogen source), a clear understanding and reliable quantification of the stoichiometric and kinetic features of all processes involved in *Methylocystis hirsuta* (i.e., biomass growth/decay and PHA synthesis/utilization) would significantly benefit the design of the specific operational strategy.

This work therefore aims to develop a mechanistic model to describe the relevant processes of *Methylocystis hirsuta*, which might lay the foundation for future practical demonstration and optimization of the PHA synthesis technology using biogas. To this end, dedicated batch tests were firstly designed and conducted to obtain experimental data for different mechanistic process(es) of *Methylocystis hirsuta*. The experimental data obtained together with the batch test data reported by López et al. (2018) were then used to calibrate and validate the model. Finally, the developed model was applied in a case study to optimize the PHA production under the studied conditions in batch mode.

4.2 Materials and methods

4.2.1 Development of the mechanistic model

As presented in **Table 4.1**, the mechanistic model describes the relevant processes of *Methylocystis hirsuta* metabolism, including biomass growth/decay and PHA synthesis/utilization, through the relationships among 4 components, i.e., methane (S_{CH4}), oxygen (S_{O2}), PHA (X_{PHA}), and active biomass (i.e., *Methylocystis hirsuta*, X_B). Based on the findings of López et al. (2018), with the supply of methane and oxygen, the biomass growth process (r1) only takes place in the presence of nitrogen source (i.e., nitrate in this work), while the PHA synthesis process (r2) is merely activated in the absence of nitrogen source. Yield coefficients (Y) link substrates consumption to biomass growth and PHA synthesis, the rates of which are modelled using dual-substrate Monod equations. Similar to Chen et al. (2017) and Chen et al. (2019), a coefficient lower than 1 (k) accounts for the electrons diverted to the accompanying generation of products associated with biomass growth (i.e., not all the electrons released from methane oxidation are used for biomass growth), which was not specifically investigated in this work. Based on the results of relevant batch tests conducted in this work (detailed in the following section), the PHA utilization process in the presence of oxygen (r3) is depicted by a rate equation with the single Monod term of oxygen, while the biomass decay process (r4) is expressed by a zero-order rate equation.

Table 4.1. *Stoichiometric and kinetic matrix of the model*

	Component process	S_{CH4} g COD m^{-3}	S_{O2} g O_2 m^{-3}	X_B g COD m^{-3}	X_{PHA} g COD m^{-3}	**Process rate equation**
r1	Biomass growth in the presence of NO_3^-	$\frac{-1}{Y_{g,CH4}}$	$\frac{Y_{g,CH4}-1}{Y_{g,CH4}}k$	k		$\mu_{g,CH4}\frac{S_{CH4}}{K_{CH4}+S_{CH4}}\frac{S_{O2}}{K_{O2}+S_{O2}}X_B$
r2	PHA synthesis in the absence of NO_3^-	$\frac{-1}{Y_{PHA,CH4}}$	$\frac{Y_{PHA,CH4}-1}{Y_{PHA,CH4}}$		1	$\mu_{PHA,CH4}\frac{S_{CH4}}{K_{CH4}+S_{CH4}}\frac{S_{O2}}{K_{O2}+S_{O2}}X_B$
r3	PHA consumption		-1		-1	$\mu_{PHA,O2}\frac{S_{O2}}{K_{O2}+S_{O2}}X_B$
r4	Biomass decay		-1	-1		$k_{Dec}X_B$

4.2.2 Experimental investigations

4.2.2.1 *Inocula*

The methanotrophic strain *Methylocystis hirsuta* (DSMZ no. 18500, Leibniz Institute, Germany) was inoculated (10% v/v) under sterile conditions in 125-mL crimp-sealed serum bottles containing 50 mL of nitrate mineral salt (NMS) medium with a pH of 6.8 prepared according to Bowman (2006). The 75-mL headspace of the bottles was filled with oxygen and methane supplied using gas cylinders of O_2 (≥ 99.5%) and CH_4 (≥ 99.995%) at an O_2:CH_4 ratio of 66.7:33.3% (v/v), and was replaced upon the depletion of CH_4. The serum bottles were incubated at 30 °C and 200 rpm in an orbital shaker for approximately 7 days.

4.2.2.2 *Batch tests.*

All batch tests described below were performed in duplicate in 2.2-L serum bottles with a liquid-phase working volume of 0.4 L. With an initial pH of around 7.0, the bottles were incubated at 25 °C and constantly mixed at 300 rpm. Gas and liquid samples were taken periodically for relevant analyses.

Batch tests for biomass growth were conducted at three different headspace compositions, with gas cylinders of O_2 (≥ 99.5%), He (≥ 99.5%) and synthetic biogas (70% CH_4, 30% CO_2) providing gas mixtures. The headspace CH_4:O_2:CO_2:He ratios of 29.2:29.2:12.5:29.2%, 29.2:43.8:12.5:14.6% and 29.2:58.3:12.5:0.0% corresponded to O_2:CH_4 molar ratios of 1:1, 1.5:1 and 2:1, respectively, which are termed Batch Test G1, G2 and G3 in this work. With 2.5% (v/v) of fresh *Methylocystis hirsuta* inocula in the 400-mL NMS medium, the bottles were incubated until the consumption of CH_4 and O_2 ceased.

Batch tests for biomass decay, termed Batch Test D, were performed in serum bottles with biomass previously grown at the O_2:CH_4 molar ratio of 2:1 for 2 weeks (i.e., Batch Test G3). The bottles were provided with an initial headspace O_2 concentration of 21%

(v/v) by flushing air for 5 minutes through the bottle headspace with a gas compressor, thus ensuring a complete headspace replacement.

Batch tests for PHA synthesis, termed Batch Test S, were carried out in serum bottles supplied with 400 mL of nitrate-free mineral salt (NFMS) medium, which were inoculated with biomass harvested from a culture broth grown as previously describes in Batch Test G3. The headspace of the bottles was supplied with a gas mixture containing an O_2:CH_4 molar ratio of 2:1. The bottles were incubated until the consumption of CH_4 and O_2 ceased.

Batch tests for PHA utilization, termed Batch Test U, were implemented as an extension of the previous PHA synthesis test (i.e., Batch Test S). Starting from the depletion of CH_4 in the bottle headspace, the bottles were incubated with the remaining O_2 for over 30 days.

4.2.3 Analytical methods

CH_4 and O_2 in the headspace of the bottles were measured by gas chromatography coupled with thermal conductivity detection according to Estrada et al. (2014) (the detailed method could be found in the supporting information (SI)). Total suspended solids (TSS) were analyzed according Lopez et al. (2014), whereas the optical density of the culture samples was determined at 600 nm by spectrophotometry. PHA extraction from *Methylocystis hirsuta* biomass was conducted referring to Lopez et al. (2014), while the determination of PHA concentration was carried out by gas chromatography coupled with mass spectrometry as detailed in the SI. The PHA content (%, in terms of weight) was referred to the total biomass concentration of the sample. For the convenience of model implementation, conversion factors of 1.67 and 1.42 (i.e., ratio between COD and TSS) were applied to determine PHA and biomass concentrations in terms of COD, respectively (by assuming the empirical formula of PHA and biomass as $C_4H_6O_2$ and $C_5H_7O_2N$, respectively).

4.2.4 Evaluations of the mechanistic model

The mass transfer of CH_4 and O_2 from the headspace to the liquid phase of the setup was described in the model using **Eq. 4.1**. To determine K_LaO_2, dedicated duplicate batch tests were conducted in the same serum bottles used in Section 4.2.2 where only O_2 was supplied in the headspace and no biomass was provided in the liquid phase. K_LaO_2 was calculated by analysing the initial linear decline of gas-phase O_2 and assuming a correction factor of 0.95 due to the presence of biomass (Tchobanoglous et al., 2003). The calculated K_LaO_2 was then used to infer K_LaCH_4 according to **Eq. 4.2.**

$$R_x = K_L a_x \left(\frac{S_{x,g}}{H_x} - S_{x,l}\right) \quad (4.1)$$

where R_x is the flux of gas x (i.e., CH_4 or O_2) from the headspace to the liquid phase (g m^{-3} d^{-1}), K_La_x is the mass transfer coefficient of gas x (d^{-1}), $S_{x,g}$ is the concentration of gas x in the headspace (g m^{-3}), $S_{x,l}$ is the concentration of gas x in the liquid phase (g m^{-3}), and H_x is the Henry's law constant (Sander, 2015).

$$\frac{K_L a_{CH4}}{K_L a_{O2}} = \sqrt{\frac{D_{CH4}}{D_{O2}}} \quad (4.2)$$

where K_LaCH_4 and K_LaO_2 are the mass transfer coefficients of CH_4 and O_2 (d^{-1}), and D_{CH4} and D_{O2} are the diffusion coefficients of CH_4 and O_2 in water (i.e., 1.84×10^{-9} m^2 s^{-1} and 2.42×10^{-9} m^2 s^{-1}, respectively) (Haynes, 2014).

The following stepwise protocol was adopted to rigorously calibrate and validate the model (i.e., **Table 4.1**) in the modeling and simulation environment AQUASIM (Reichert, 1998). Through following the secant algorithm, AQUASIM was used to estimate constant variables (i.e., parameters of interest listed in **Table 4.2**) by minimizing the sum of the squares of the weighted deviations between measurements and calculated model results (Ralston and Jennrich, 1978).

Step 1: The data of Batch Test D, which involved only process r4 in **Table 4.1**, were firstly used to estimate the biomass decay rate (i.e., k_{dec}).

Step 2: The data of Batch Test G1, G2 and G3, which involved both processes r1 and r4 in **Table 4.1**, were used to estimate the yield of growth on CH_4 (i.e., $Y_{g,CH4}$), CH_4 affinity constant (i.e., K_{CH4}) and O_2 affinity constant (i.e., K_{O2}). The value of the maximum growth rate on CH_4 (i.e., $\mu_{g,CH4}$) was directly taken from literature.

Step 3: The data of Batch Test U, which involved both processes r3 and r4 in **Table 4.1**, were used to estimate the maximum PHA consumption rate (i.e., $\mu_{PHA,O2}$).

Step 4: The data of Batch Test S, which involved processes r2, r3 and r4 in **Table 4.1**, were used to estimate the yield of PHA synthesis on CH_4 (i.e., $Y_{PHA,CH4}$) and maximum PHA synthesis rate on CH_4 (i.e., $\mu_{PHA,CH4}$).

Step 5: To further validate the results obtained in Step 4, the data of a reported, independent batch test (López et al., 2018) conducted in the same setup as Batch Test S but fed with different initial O_2 and CH_4 compositions, termed Batch Test E, were further tested using the developed model.

The developed model with parameters shown in **Table 4.2** was then used to optimize PHA production in batch mode. Referring to the conditions applied in the batch tests in **Section 4.2.2.2**, the initial biomass and CH_4 concentrations were set at 500 and 600 g COD m^{-3}, respectively. The initial O_2 concentration was adjusted between 300 and 900 g m^{-3}, thus forming simulation scenarios with an initial O_2:CH_4 molar ratio in the headspace from 1 to 3 mol O_2 mol^{-1} CH_4. The PHA content and utilization efficiencies of O_2 and CH_4 of different simulation scenarios were compared on the 20^{th} day.

Table 4.2. *Parameters of the model*

Parameter	Definition	Value	Unit	Source
Stoichiometric Parameters				
$Y_{g,CH4}$	Yield of growth on CH_4	0.14±0.01	g COD g^{-1} COD	This work
$Y_{PHA,CH4}$	Yield of PHA synthesis on CH_4	0.25±0.02	g COD g^{-1} COD	This work
i_{NXB}	Nitrogen content of biomass	0.07	g N g^{-1} COD	Henze et al. (2000)
k	Fraction of electrons used for biomass production	0.8	-	Chen et al. (2019), Chen et al. (2017)
Kinetic Parameters				
$\mu_{g,CH4}$	Maximum growth rate on CH_4	1.17	g COD g^{-1} COD d^{-1}	Arcangeli and Arvin (1997)
$\mu_{PHA,CH4}$	Maximum PHA synthesis rate on CH_4	0.39±0.05	g COD g^{-1} COD d^{-1}	This work
$\mu_{PHA,O2}$	Maximum PHA consumption rate	0.019±0.001	g COD g^{-1} COD d^{-1}	This work
k_{dec}	Biomass decay rate	0.0033±0.0002	d^{-1}	This work
K_{CH4}	CH_4 affinity constant	5.1±2.1	g COD m^{-3}	This work
K_{O2}	Oxygen affinity constant	4.1±1.7	g O_2 m^{-3}	This work

4.3 Results and discussion

4.3.1 Experimental results

Figure 4.1A, B and **C** depicts the measured results of the batch tests for biomass growth, i.e., Batch Test G1, G2 and G3, respectively. With the simultaneous consumption of O_2 and CH_4, biomass was gradually formed but stagnated on the 9th day due to substrate depletion. O_2 was firstly depleted at the O_2:CH_4 molar ratio of 1:1 (see **Figure 4.1A**), while CH_4 was firstly exhausted at the O_2:CH_4 molar ratio of 1.5:1 (see **Figure 4.1B**). At the highest O_2:CH_4 molar ratio of 2:1 studied in this work, ~35% of the O_2 provided remained unconverted (see **Figure 4.1C**). This observation means that an O_2:CH_4 molar ratio between 1:1 and 1.5:1 would lead to the complete consumption of O_2 and CH_4 in the process of biomass growth. However, this ratio is slightly lower than the theoretically calculated value of 1.5:1 reported by Asenjo and Suk (1986). The discrepancy might be related to the assumptions made by Asenjo and Suk (1986), e.g., using $C_4H_8O_2N$ to

represent biomass and applying a hypothetical yield. The measured results of the batch test for biomass decay (i.e., Batch Test D) are shown in **Figure 4.2**. Due to aerobic decay in the absence of CH_4, both the concentrations of O_2 and biomass decreased gradually.

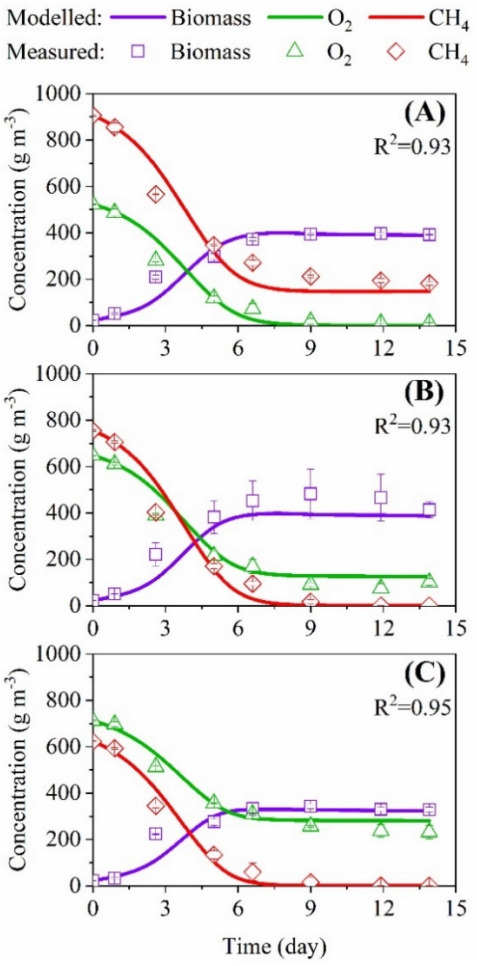

Fig. 4.1 *Comparison between modelled and measured results of Batch Test (**A**) G1, (**B**) G2, and (**C**) G3.*

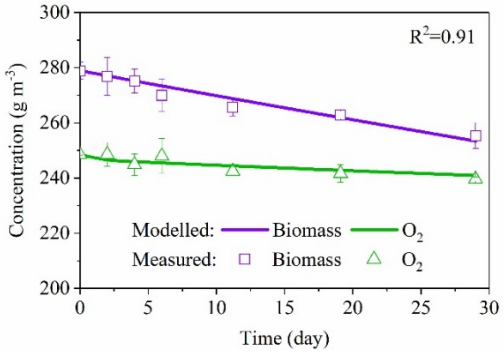

Fig. 4.2 *Comparison between modelled and measured results of Batch D*

Figure 4.3A illustrates the empirical results of the batch test for PHA synthesis (i.e., Batch Test S). The simultaneous consumption of O_2 and CH_4 led to the production of PHA. After CH_4 was depleted by day 11, the PHA formed started to be consumed aerobically. Therefore, both the concentrations of PHA and O_2 decreased gradually till the end of the batch test. The measured results of the batch test for PHA utilization (i.e., Batch Test U) are presented in **Figure 4.4**. The simultaneous decline of O_2 and PHA clearly confirmed the capability of *Methylocystis hirsuta* to utilize PHA as an energy source.

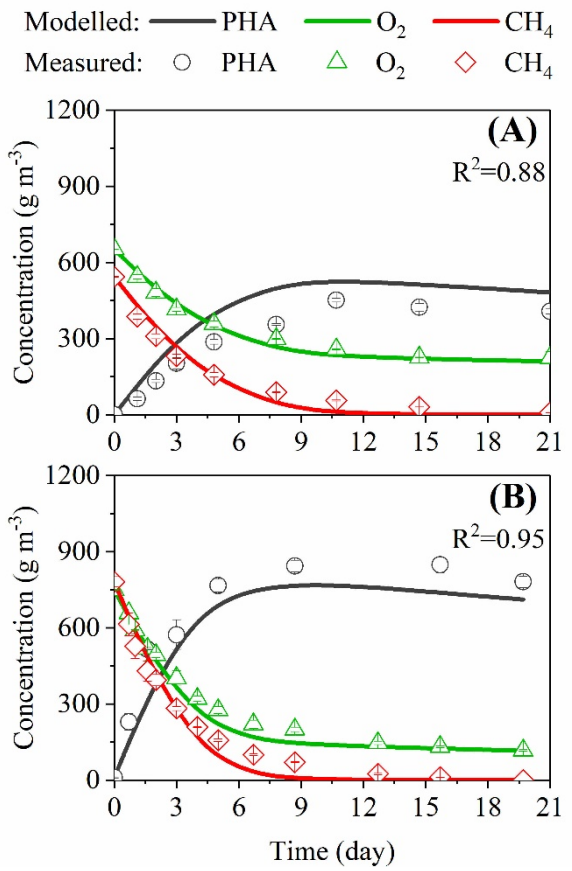

Fig. 4.3 *Comparison between modelled and measured results of Batch Test* ***(A)*** *S and* ***(B)*** *E*

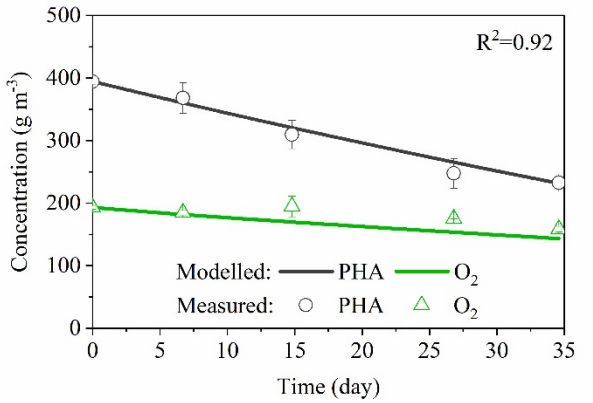

Fig. 4.4 *Comparison between modelled and measured results of Batch Test U*

4.3.2 Model evaluations

With a high coefficient of determination (i.e., R^2=0.91) between the modelled and measured results of Batch Test D shown in **Figure 4.2**, k_{dec} of process r4 was estimated at 0.0033±0.0002 d^{-1} in the first step. **Figure 4.1A and B** illustrates the second-step calibration results of processes r1 and r4 using the results of Batch Test G1 and G2. With the good agreement between the modelled and measured profiles of Batch Test G1 and G2 (i.e., R^2=0.93 in **Figure 4.1A and B**), $Y_{g,CH4}$, K_{CH4} and K_{O2} were estimated at 0.14±0.01 g COD g^{-1} COD, 5.1±2.1 g COD m^{-3} and 4.1±1.7 g O_2 m^{-3}, respectively. The value of $Y_{g,CH4}$ is lower than that reported for *Methylocystis hirsuta* by López et al. (2018) (i.e., 0.21 g COD g^{-1} COD) as well as those reported for different type II methanotrophs by Rostkowski et al. (2013) (i.e., 0.23 g COD g^{-1} COD for *Methylosinus trichosporium* OB3b and 0.20 g COD g^{-1} COD for *Methylocystis parvus* OBBP), which could be due to the different environmental conditions applied or the various microbial strains studied. The estimated standard deviations of K_{CH4} and K_{O2} are quite significant, being 40% of the estimated parameter values. This is due to the fact that K_{CH4} and K_{O2} are highly negatively correlated in the model structure, with a calculated correlation factor of -0.94. In this case, a further validation process is usually needed. Therefore, the results of Batch Test G3 which involved processes r1 and r4 were used in the second-step validation process. As

demonstrated in **Figure 4.1C**, the validity of the estimated K_{CH4}, K_{O2} and $Y_{g,CH4}$ of the developed model was verified by the good match between the modelled and measured trends (i.e., $R^2 = 0.95$).

As shown in **Figure 4.4** with R^2 of 0.92, $\mu_{PHA,O2}$ was estimated at 0.019±0.001 g COD g^{-1} COD d^{-1} in the third step using the data of Batch Test U which involved both processes r3 and r4. **Figure 4.3A** shows the fourth-step calibration results of processes r2, r3 and r4 using the results of Batch Test S. Through matching the modelled results to measured profiles of Batch Test S to a satisfactory level (i.e., R^2 of 0.88 in **Figure 4.3A**), $Y_{PHA,CH4}$ and $\mu_{PHA,CH4}$ were estimated at 0.25±0.02 g COD g^{-1} COD and 0.39±0.05 g COD g^{-1} COD d^{-1}. The value of $Y_{PHA,CH4}$ is higher than that reported for *Methylocystis hirsuta* by López et al. (2018) (i.e., 0.19 g COD g^{-1} COD) but lower than those reported for different type II methanotrophs by Rostkowski et al. (2013) (i.e., 0.47 g COD g^{-1} COD for *Methylosinus trichosporium* OB3b and 0.37 g COD g^{-1} COD for *Methylocystis parvus* OBBP), which could be ascribed to the difference in either environmental conditions applied or microbial strains studied. On top of the already acceptable uncertainty (i.e., with the estimated standard deviations being <15% of the estimated parameter values), the validity of the estimated $Y_{PHA,CH4}$ and $\mu_{PHA,CH4}$ of the developed model was further confirmed by the fifth-step validation results of processes r2, r3 and r4 using the additional results of Batch Test E. As demonstrated in **Figure 4.3B**, a high coefficient of determination (i.e., R^2=0.95) between the modelled and measured data was obtained.

4.3.3 Model-based optimization of PHA production

To elucidate the O_2:CH_4 molar ratio leading to the complete consumption of O_2 and CH_4 in the process of PHA synthesis, a case study was performed using the developed model, the results of which are illustrated in **Figure 4.5**. When the O_2:CH_4 molar ratio in the headspace increased from the lowest level studied (i.e., 1 mol O_2 mol^{-1} CH_4), the amount of PHA produced increased firstly. Under such conditions, CH_4 was in excess while O_2 was limiting. Therefore, the CH_4 utilization efficiency kept rising while the O_2 utilization

efficiency remained at ~100%. The PHA production peaked at the O_2:CH_4 molar ratio of 1.6 mol O_2 mol^{-1} CH_4, where nearly a complete utilization of O_2 (i.e., 97%) and CH_4 (i.e., 99%) was achieved. When the O_2:CH_4 molar ratio increased beyond 1.6 mol O_2 mol^{-1} CH_4, CH_4 became limited while O_2 was in excess. Consequently, the CH_4 utilization efficiency reached 100% while the O_2 utilization efficiency exhibited a declining trend, accompanied by a decreasing PHA production due to aerobic consumption. In summary, this case study showed that an O_2:CH_4 molar ratio of 1.6 mol O_2 mol^{-1} CH_4 would lead to the complete consumption of O_2 and CH_4 in the process of PHA synthesis. This value is slightly higher than the theoretically calculated value of 1.5 mol O_2 mol^{-1} CH_4 reported by Asenjo and Suk (1986). The difference might be caused by the additional O_2-consuming processes considered in this work, i.e., processes r3 (i.e., PHA consumption) and r4 (i.e., biomass decay). Practically, in order to avoid the negative impact of limited O_2 availability on PHA production (Karthikeyan et al., 2014), an optimal O_2:CH_4 molar ratio of 1.6 mol O_2 mol^{-1} CH_4 is needed to maximize the PHA synthesis by *Methylocystis hirsuta*.

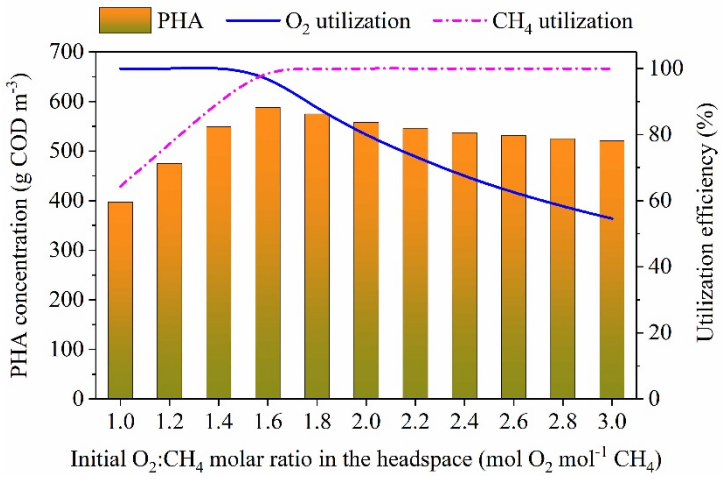

Fig. 4.5 *PHA content and utilization efficiencies of O_2 and CH_4 of simulation scenarios with an initial O_2:CH_4 molar ratio in the headspace ranging from 1 to 3 mol O_2 mol^{-1} CH_4.*

4.3.4 Implications of this work

This work reports for the first time the stoichiometrics and kinetics of all mechanistic processes related to *Methylocystis hirsuta*, including biomass growth/decay and PHA synthesis/utilization, based on the experimental data of well-designed batch tests. Therefore, this work represents a valuable contribution to the current knowledge base of stoichiometrics and kinetics of methanotrophs which is more oriented on mixed cultures. This work would also significantly facilitate the design and operation of bioreactors devoted to PHA synthesis from biogas. For example, the model and parameters could be implemented in relevant setup to model and optimize PHA production in bioreactors (e.g., bubble column bioreactor (Khosravi-Darani et al., 2019, Moradi et al., 2019)) under feast-famine regime, which has been reported as an ideal operational strategy for PHA accumulation (Pieja et al., 2012).

Moreover, the model and parameters obtained would also favor the practical selection for type II methanotrophs. For example, through applying a model integrating the stoichiometrics and kinetics of both type I and II methanotrophs in a fluidized bed reactor proposed by Pfluger et al. (2011), improvement of selection for type II methanotrophs and hence increased PHA production could be expected. As denitrifying anaerobic methane oxidation (DAMO) microorganisms and aerobic methane oxidation (AMO) microorganisms could thrive in environments suitable for the growth and PHA synthesis of type II methanotrophs (i.e., with O_2 and CH_4 in the presence/absence of nitrate), the model and parameters obtained in this work could be coupled with those reported for DAMO and AMO (e.g. Chen et al. (2014), Chen et al. (2016), Daelman et al. (2014)) to assess the interactions between type II methanotrophs and potential competitors, especially in mixed culture environments. These aspects are subject to future specific investigations.

4.4 Conclusions

In this work, through utilizing the experimental data of well-designed batch tests and following a step-wise model calibration/validation protocol, the stoichiometrics and kinetics of growth/decay and PHA synthesis/utilization processes of *Methylocystis hirsuta* are reported for the first time. Through applying the developed model, an optimal O_2:CH_4 molar ratio of 1.6 mol O_2 mol^{-1} CH_4 was found to maximize PHA synthesis by *Methylocystis hirsuta*. Practically, the model and parameters obtained would not only benefit the design and operation of bioreactors performing PHA synthesis from biogas, but also enable specific research on selection for type II methanotrophs in diverse environments.

Acknowledgements

X. C. acknowledges the financial support by the European Union's Horizon 2020 research and innovation programme through Marie Skłodowska-Curie Individual Fellowship under grant agreement No. 790231. B.-J. Ni acknowledges the Australian Research Council (ARC) through Future Fellowship FT160100195. This work was supported by the Regional Government of Castilla y León and the EU-FEDER programme (CLU-2017-09, UIC 71).

The authors are grateful to the research collaboration and declare no conflict of interest.

References

Anderson, A.J. and Dawes, E.A. (1990) Occurrence, metabolism, metabolic role, and industrial uses of bacterial polyhydroxyalkanoates. *Microbiol Rev* **54**(4), 450-472. doi: 10.1128/mmbr.54.4.450-472.1990

Arcangeli, J.-P. and Arvin, E. (1997) Modelling of the growth of a methanotrophic biofilm. *Water Science and Technology* **36**(1), 199-204. doi: 10.1016/S0273-1223(97)00353-3

Asenjo, J.A. and Suk, J.S. (1986) Microbial Conversion of Methane into poly-β-hydroxybutyrate (PHB): Growth and intracellular product accumulation in a type II methanotroph. *Journal of Fermentation Technology* **64**(4), 271-278. doi: 10.1016/0385-6380(86)90118-4

Bowman, J. (2006) The Prokaryotes: Volume 5: Proteobacteria: Alpha and Beta Subclasses. Dworkin, M., Falkow, S., Rosenberg, E., Schleifer, K.-H. and Stackebrandt, E. (eds), pp. 266-289, Springer New York, New York, NY. doi: 10.1007/0-387-30745-1_15

Burniol-Figols, A., Varrone, C., Daugaard, A.E., Le, S.B., Skiadas, I.V. and Gavala, H.N. (2018a) Polyhydroxyalkanoates (PHA) production from fermented crude glycerol: Study on the conversion of 1,3-propanediol to PHA in mixed microbial consortia. *Water Res* **128**, 255-266. doi: 10.1016/j.watres.2017.10.046

Burniol-Figols, A., Varrone, C., Le, S.B., Daugaard, A.E., Skiadas, I.V. and Gavala, H.N. (2018b) Combined polyhydroxyalkanoates (PHA) and 1,3-propanediol production from crude glycerol: Selective conversion of volatile fatty acids into PHA by mixed microbial consortia. *Water Res* **136**, 180-191. doi: 10.1016/j.watres.2018.02.029

Chen, G.Q. (2009) A microbial polyhydroxyalkanoates (PHA) based bio- and materials industry. *Chem Soc Rev* **38**(8), 2434-2446. doi: 10.1039/b812677c

Chen, X., Guo, J., Shi, Y., Hu, S., Yuan, Z. and Ni, B.J. (2014) Modeling of simultaneous anaerobic methane and ammonium oxidation in a membrane biofilm reactor. *Environ Sci Technol* **48**(16), 9540-9547. doi: 10.1021/es502608s

Chen, X., Lai, C.-Y., Fang, F., Zhao, H.-P., Dai, X. and Ni, B.-J. (2019) Model-based evaluation of selenate and nitrate reduction in hydrogen-based membrane biofilm reactor. *Chemical Engineering Science* **195**, 262-270. doi: 10.1016/j.ces.2018.11.032

Chen, X., Liu, Y., Peng, L. and Ni, B.-J. (2017) Perchlorate, nitrate, and sulfate reduction in hydrogen-based membrane biofilm reactor: Model-based evaluation. *Chemical Engineering Journal* **316**, 82-90. doi: 10.1016/j.cej.2017.01.084

Chen, X., Liu, Y., Peng, L., Yuan, Z. and Ni, B.J. (2016) Model-Based Feasibility Assessment of Membrane Biofilm Reactor to Achieve Simultaneous Ammonium, Dissolved Methane, and Sulfide Removal from Anaerobic Digestion Liquor. *Sci Rep* **6**(1), 25114. doi: 10.1038/srep25114

Daelman, M.R.J., Van Eynde, T., van Loosdrecht, M.C.M. and Volcke, E.I.P. (2014) Effect of process design and operating parameters on aerobic methane oxidation in municipal WWTPs. *Water Res* **66**, 308-319. doi: 10.1016/j.watres.2014.07.034

Estrada, J.M., Lebrero, R., Quijano, G., Pérez, R., Figueroa-González, I., García-Encina, P.A. and Muñoz, R. (2014) Methane abatement in a gas-recycling biotrickling filter: Evaluating innovative operational strategies to overcome mass transfer limitations. *Chemical Engineering Journal* **253**, 385-393. doi: 10.1016/j.cej.2014.05.053

Hanson, R.S. and Hanson, T.E. (1996) Methanotrophic bacteria. *Microbiol Rev* **60**(2), 439-471. doi: 10.1128/mmbr.60.2.439-471.1996

Haynes, W.M. (2014) CRC handbook of chemistry and physics, CRC press. ISBN:1482208687

Henze, M., Gujer, W., Mino, T., van Loosdrecht, M.C.M., Henze, M., Gujer, W., Mino, T. and van Loosdrecht, M.C.M. (2000) Activated sludge models ASM1, ASM2, ASM2d and ASM3, IWA Publishing. ISBN: 1-90022-224-8

Karthikeyan, O.P., Chidambarampadmavathy, K., Cirés, S. and Heimann, K. (2014) Review of Sustainable Methane Mitigation and Biopolymer Production. *Critical Reviews in Environmental Science and Technology* **45**(15), 1579-1610. doi: 10.1080/10643389.2014.966422

Khosravi-Darani, K., Yazdian, F., Babapour, F. and Amirsadeghi, A. (2019) Poly (3-hydroxybutyrate) Production from Natural Gas by a Methanotroph Native Bacterium in a Bubble Column Bioreactor. *Chemical and biochemical engineering quarterly* **33**(1), 69-77. doi: 10.15255/cabeq.2017.1263

López, J.C., Arnáiz, E., Merchán, L., Lebrero, R. and Muñoz, R. (2018) Biogas-based polyhydroxyalkanoates production by *Methylocystis hirsuta*: A step further in anaerobic digestion biorefineries. *Chemical Engineering Journal* **333**, 529-536. doi: 10.1016/j.cej.2017.09.185

Lopez, J.C., Quijano, G., Perez, R. and Munoz, R. (2014) Assessing the influence of CH_4 concentration during culture enrichment on the biodegradation kinetics and population structure. *J Environ Manage* **146**, 116-123. doi: 10.1016/j.jenvman.2014.06.026

Moradi, M., Rashedi, H., Mofradnia, S.R., Khosravi-Darani, K., Ashouri, R. and Yazdian, F. (2019) Polyhydroxybutyrate Production from Natural Gas in A Bubble Column Bioreactor: Simulation Using COMSOL. *Bioengineering* **6**(3), 84. doi: 10.3390/bioengineering6030084

Morgan-Sagastume, F., Karlsson, A., Johansson, P., Pratt, S., Boon, N., Lant, P. and Werker, A. (2010) Production of polyhydroxyalkanoates in open, mixed cultures from a waste sludge stream containing high levels of soluble organics, nitrogen and phosphorus. *Water Res* **44**(18), 5196-5211. doi: 10.1016/j.watres.2010.06.043

Pfluger, A.R., Wu, W.M., Pieja, A.J., Wan, J., Rostkowski, K.H. and Criddle, C.S. (2011) Selection of Type I and Type II methanotrophic proteobacteria in a fluidized bed reactor under non-sterile conditions. *Bioresour Technol* **102**(21), 9919-9926. doi: 10.1016/j.biortech.2011.08.054

Pieja, A.J., Rostkowski, K.H. and Criddle, C.S. (2011) Distribution and selection of poly-3-hydroxybutyrate production capacity in methanotrophic proteobacteria. *Microb Ecol* **62**(3), 564-573. doi: 10.1007/s00248-011-9873-0

Pieja, A.J., Sundstrom, E.R. and Criddle, C.S. (2012) Cyclic, alternating methane and nitrogen limitation increases PHB production in a methanotrophic community. *Bioresour Technol* **107**, 385-392. doi: 10.1016/j.biortech.2011.12.044

Rahnama, F., Vasheghani-Farahani, E., Yazdian, F. and Shojaosadati, S.A. (2012) PHB production by *Methylocystis hirsuta* from natural gas in a bubble column and a vertical loop bioreactor. *Biochemical Engineering Journal* **65**, 51-56. doi: 10.1016/j.bej.2012.03.014

Ralston, M.L. and Jennrich, R.I. (1978) Dud, A Derivative-Free Algorithm for Nonlinear Least Squares. *Technometrics* **20**(1), 7-14. doi: 10.2307/1268154

Reddy, C.S., Ghai, R., Rashmi and Kalia, V.C. (2003) Polyhydroxyalkanoates: an overview. *Bioresour Technol* **87**(2), 137-146. doi: 10.1016/s0960-8524(02)00212-2

Reichert, P. (1998) AQUASIM 2.0-Computer program for the identification and simulation of aquatic systems, EAWAG, Dubendorf, Switzerland.

Rostkowski, K.H., Criddle, C.S. and Lepech, M.D. (2012) Cradle-to-gate life cycle assessment for a cradle-to-cradle cycle: biogas-to-bioplastic (and back). *Environ Sci Technol* **46**(18), 9822-9829. doi: 10.1021/es204541w

Rostkowski, K.H., Pfluger, A.R. and Criddle, C.S. (2013) Stoichiometry and kinetics of the PHB-producing Type II methanotrophs *Methylosinus trichosporium* OB3b and *Methylocystis parvus* OBBP. *Bioresour Technol* **132**, 71-77. doi: 10.1016/j.biortech.2012.12.129

Sander, R. (2015) Compilation of Henry's law constants (version 4.0) for water as solvent. *Atmospheric Chemistry and Physics* **15**(8), 4399-4981. doi: 10.5194/acp-15-4399-2015

Serafim, L.S., Lemos, P.C., Albuquerque, M.G. and Reis, M.A. (2008) Strategies for PHA production by mixed cultures and renewable waste materials. *Appl Microbiol Biotechnol* **81**(4), 615-628. doi: 10.1007/s00253-008-1757-y

Singh, A.K., Sharma, L., Mallick, N. and Mala, J. (2016) Progress and challenges in producing polyhydroxyalkanoate biopolymers from cyanobacteria. *Journal of Applied Phycology* **29**(3), 1213-1232. doi: 10.1007/s10811-016-1006-1

Strong, P.J., Xie, S. and Clarke, W.P. (2015) Methane as a resource: can the methanotrophs add value? *Environ Sci Technol* **49**(7), 4001-4018. doi: 10.1021/es504242n

Tchobanoglous, G., Burton, F.L. and Stensel, H.D. (2003) Metcalf & Eddy wastewater engineering: treatment and reuse. *International Edition. McGrawHill* **4**, 361-411

Venkata Mohan, S. and Venkateswar Reddy, M. (2013) Optimization of critical factors to enhance polyhydroxyalkanoates (PHA) synthesis by mixed culture using Taguchi design of experimental methodology. *Bioresour Technol* **128**, 409-416. doi: 10.1016/j.biortech.2012.10.037

Wijeyekoon, S., Carere, C.R., West, M., Nath, S. and Gapes, D. (2018) Mixed culture polyhydroxyalkanoate (PHA) synthesis from nutrient rich wet oxidation liquors. *Water Res* **140**, 1-11. doi: 10.1016/j.watres.2018.04.017

Appendix A. Supplementary Material

Modeling of Polyhydroxyalkanoate Synthesis from Biogas by *Methylocystis hirsuta*

[1]Process and Systems Engineering Center (PROSYS), Department of Chemical and Biochemical Engineering, Technical University of Denmark, 2800 Kgs. Lyngby, Denmark

[2]Institute of Sustainable Processes, University of Valladolid, 47011 Valladolid, Spain

[3]AINIA, Parque Tecnológico de Valencia, 46980 Paterna, Valencia, Spain

[4]Centre for Technology in Water and Wastewater, School of Civil and Environmental Engineering, University of Technology Sydney, Sydney, New South Wales 2007, Australia

***Correspondence to**

Xueming Chen, Tel: + 45 8194 8080, E-mail: xuem.chen@hotmail.com

Available at: https://pubs.acs.org/doi/10.1021/acssuschemeng.9b07414.

Method for CH_4 and O_2 concentrations determination

CH_4 and O_2 in the headspace of the bottles were measured by gas chromatography (Bruker 430 gas chromatography (GC), Palo Alto, USA) coupled with thermal conductivity detection (TCD). The GC was equipped with CP-Molsieve 5Å (15m × 0.53 mm × 15 μm) and a CP-PoraBOND Q (25m × 0.53 mm × 10 μm) columns (Agilent, Santa Clara, USA). The carrier gas (He) flow was set at 13.7 mL min^{-1}, and the temperatures of the injector, oven and detector were kept at 150, 45 and 200ºC, respectively. Gas samples of 100 μL were taken using a gas-tight syringe (Hamilton Company, NV, USA). Gas calibration cylinders with CH_4 concentrations of 55, 70, 99.995% (v/v) and O_2 concentrations of >99.5% were purchased from Abelló Linde S.A. (Barcelona, Spain). Figure S4.1A and B presents the GC-TCD analysis report at the beginning and the end of one batch test for PHA synthesis conducted, respectively.

Method for PHA concentration determination

The PHA extraction from cells was accomplished by first adding 1 mL of 1-propanol and hydrochloric acid (80:20%) to the biomass pellets obtained from 1.5 mL of culture sample. After vortexing, samples were transferred to test tubes and 2 mL of chloroform and 10 µL of an internal standard solution (5 g L^{-1} of benzoic acid in propanol) were added. Then, samples were agitated again and subjected to a 4h-digestion at 100ºC in a thermoreactor. Once samples were cooled down to room temperature, 1 mL of deionized water was added and the mixture was agitated again. Finally, the organic phase after liquid phase separation was collected and filtered for analysis through a 0.22 µm filter (Merck). The quantification of PHA concentration was conducted in an Agilent 7820A GC equipped with a DB-WAX column (30 m × 0.25 mm × 0.25 µm) (Agilent, Santa Clara, USA) and coupled with an Agilent 5977E mass spectrometer (MS) unit. The injector temperature was maintained at 250ºC while the oven temperature was initially held at 40ºC for 5 min, then programmed to rise up to 200ºC at 10ºC min^{-1}, maintained at 200ºC for 2 min and finally increased up to 240ºC at 5ºC min^{-1}. Injection volume was 1 µL and each run lasted for 31 min. Figure S4.2A and B shows the GC-MS analysis report at the beginning and the end of one of the batch tests for PHA synthesis at O_2:CH_4 ratio of 2:1, respectively.

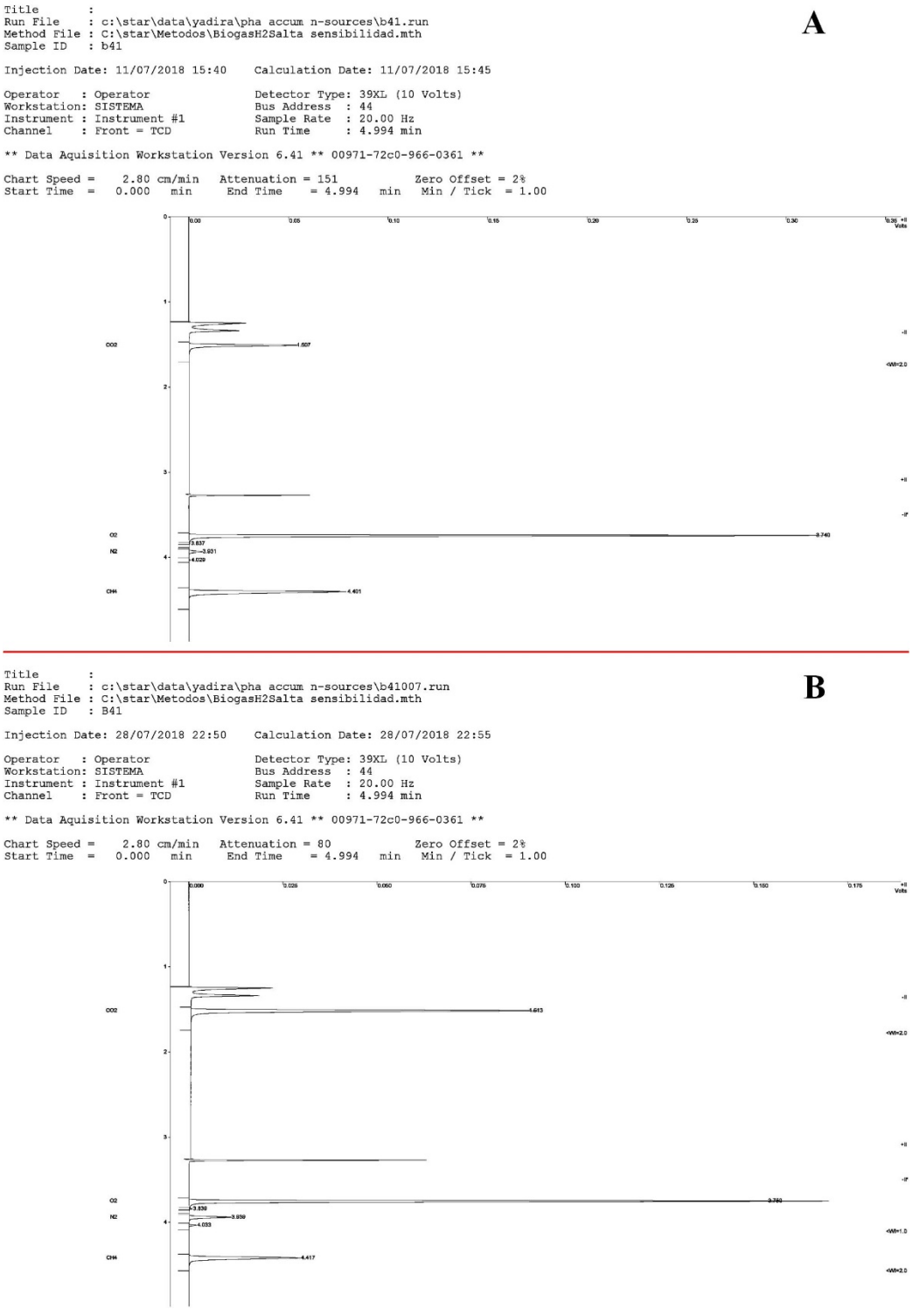

Figure S4.1. *GC-TCD analysis report at (**A**) the beginning and (**B**) the end of one batch test for PHA synthesis conducted.*

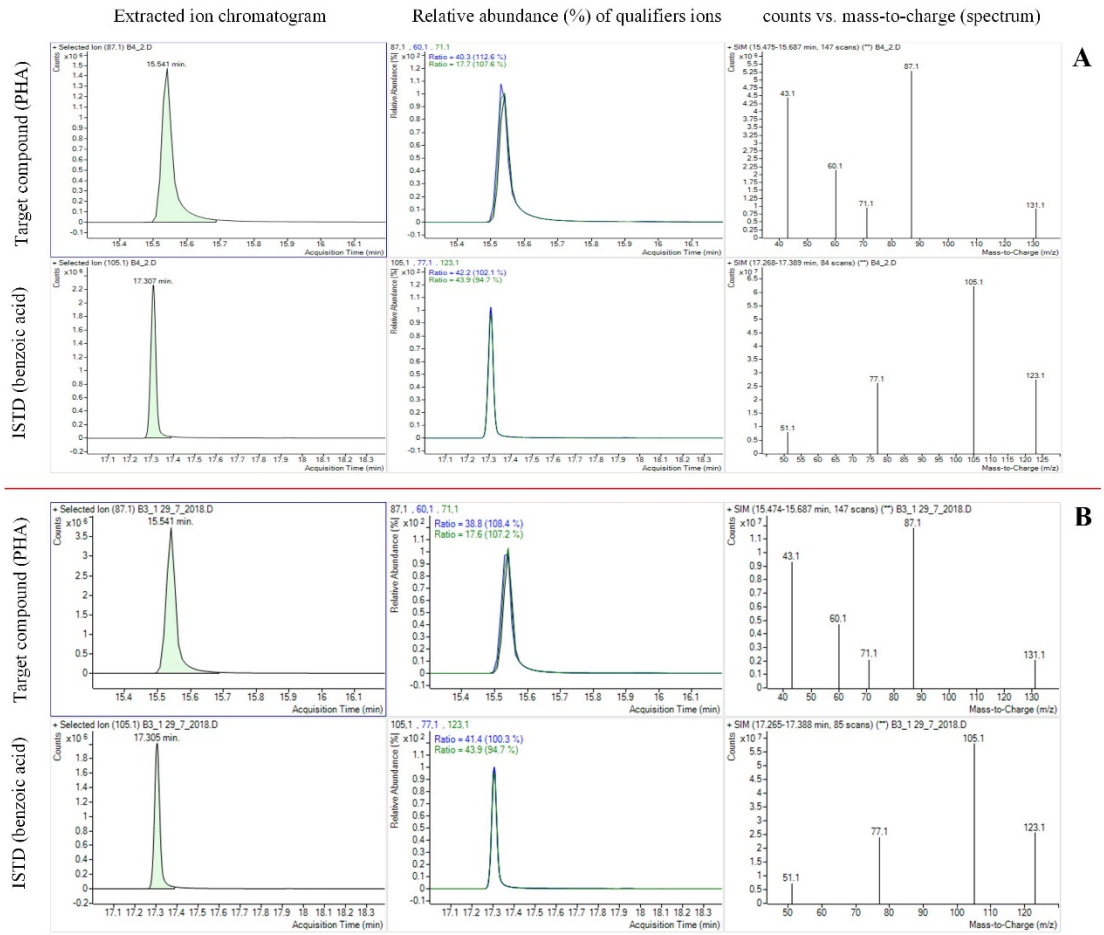

***Figure S4.2**. GC-MS analysis report at (**A**) the beginning and (**B**) the end of one of the batch tests for PHA synthesis at O_2:CH_4 ratio of 2:1*

5.

Biogas valorization via continuous polyhydroxybutyrate production by *Methylocystis hirsuta* in a bubble column bioreactor

This chapter was adapted after its publication in *Waste Management*:

Rodríguez, Y., Firmino, P.I.M., Pérez, V., Lebrero, R., Muñoz, R. (2020) Biogas valorization via continuous polyhydroxybutyrate production by *Methylocystis hirsuta* in a bubble column bioreactor. *Waste Manage*, 113, 395-403. doi: 0.1016/j.wasman.2020.06.009

Biogas valorization via continuous polyhydroxybutyrate production by *Methylocystis hirsuta* in a bubble column bioreactor

Yadira Rodríguez[a,b], Paulo Igor Milen Firmino[b,c], Víctor Pérez[a,b], Raquel Lebrero[a,b], Raúl Muñoz[a,b,*]

[a] Department of Chemical Engineering and Environmental Technology, School of Industrial Engineering, University of Valladolid, Dr. Mergelina s/n, 47011 Valladolid, Spain

[b] Institute of Sustainable Processes, Dr. Mergelina s/n, 47011 Valladolid, Spain.

[c] Department of Hydraulic and Environmental Engineering, Federal University of Ceará, Fortaleza, Ceará, Brazil

* Corresponding author: mutora@iq.uva.es.

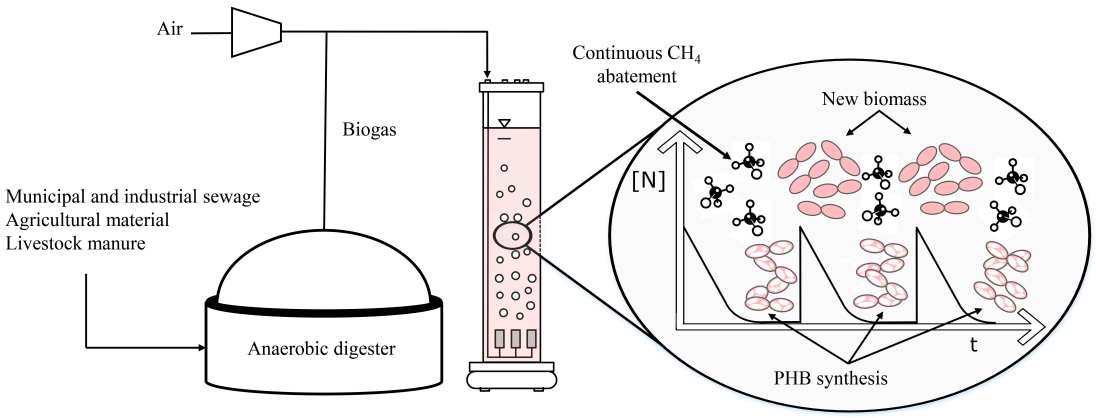

Graphical abstract

Abstract

Creating additional value out of biogas during waste treatment has become a priority in past years. Biogas bioconversion into valuable bioproducts such as biopolymers has emerged as a promising strategy. This work assessed the operational feasibility of a bubble column bioreactor (BCB) implemented with gas recirculation and inoculated with a polyhydroxybutyrate (PHB)-producing strain using biogas as substrate. The BCB was initially operated at gas empty bioreactor residence times (EBRTs) ranging from 30 to 120 min and gas recirculation ratios (R) from 0 to 30 to assess the gas-to-liquid mass transfer and bioconversion of CH_4. Subsequently, the BCB was continuously operated at a R of 30 and an EBRT of 60 min under excess of nitrogen and nitrogen feast-famine cycles of 24h:24h to trigger PHB synthesis. Gas recirculation played a major role in CH_4 gas-liquid transfer, providing almost fourfold higher CH_4 elimination capacities (≈41 g CH_4 m^{-3} h^{-1}) at the highest R and EBRT of 60 min. The long-term operation under N excess conditions entailed nitrite accumulation (induced by O_2 limiting conditions) and concurrent methanotrophic activity inhibition above ≈60 mg N-NO_2^- L^{-1}. Adjusting the N-NO_3^- supply to match microbial N demand successfully prevented nitrite accumulation. Finally, the N feast-famine 24h:24h strategy supported a stable CH_4 conversion with a removal efficiency of 70% along with a continuous PHB production, which yielded PHB accumulations of 14.5 ± 2.9% (mg PHB mg^{-1} total suspended solids × 100). These outcomes represent the first step towards the integration of biogas biorefineries into conventional anaerobic digestion plants.

Keywords: bioplastics; biorefinery; gas-liquid mass transfer; methane conversion; methanotrophic bacteria; polyhydroxyalkanoate production

5.1 Introduction

Polyhydroxyalkanoates (PHAs), which exhibit similarity in their mechanical properties to polypropylene and polyethylene, are regarded as an attractive alternative for replacing oil-based plastics due to the striving necessity of meeting the increasing societal demand for more environmentally friendly materials (Lee & Na, 2013). These renewable biopolyesters, with the added advantages of biocompatibility and biodegradability, are synthetized intracellularly as carbon and energy storage by a broad collection of microorganisms under nutrient deprivation and carbon surplus conditions (Castilho et al., 2009; Myung et al., 2017; Narancic et al., 2018). Although the market size of PHA is foreseen to quadruple by 2023, it is still relatively small. Indeed, PHA represented only 1.4% of the global biopolymer market by 2018, which accounted for 2.1 million tonnes (European Bioplastics, 2018). Its expansion is currently hampered by the significant contribution of the carbon feedstock (usually sugars, vegetable oils and fatty acids) acquisition to the total production costs (up to 50%) (Koller et al., 2017). Thus, PHAs prices (4 to 20 € kg-1) are nowadays up to fifteen-fold higher than those of their fossil counterparts (Blunt et al., 2018; Cantera et al., 2018).

On this scenario, the use of industrial by-products or wastes such as biogas as a feedstock represents an opportunity to decrease the cost of PHAs production (Cal et al., 2016; Strong et al. 2016). Biogas resulting from the anaerobic decomposition of the biodegradable fraction of organic waste in anaerobic digestion plants or landfills is primarily made up of methane (30-70%), carbon dioxide (20-50%) and hydrogen sulfide (< 2%) (Nikiema et al., 2007; Muñoz et al., 2015). Gasification and methanation of wood or recalcitrant organic waste can also generate a biomethane with CH_4 concentration higher than 90% (IEA, 2018). Methane, aside from being a potent greenhouse gas, has been traditionally regarded as a green energy vector and is increasingly used as a C source in industrial biotechnology. Indeed, the integration of biogas into biorefineries for manufacturing high added value bioproducts such as PHA, protein or ectoine is

increasingly drawing attention due to the recent stabilization of the biogas industry expansion (Mühlemeier et al., 2018).

PHA biosynthesis from CH_4 relies on the ability of type II-methane oxidizing bacteria (MOB), also referred as methanotrophs, to synthetize PHA granules under growth limiting conditions (Pieja et al., 2011a; Rostkowski et al., 2013; Zhang et al., 2017). Type II-MOB metabolize methane and one-carbon compounds via the serine cycle (Pieja et al., 2011a). When methane is used as the sole C and energy feedstock, cells naturally synthesize the short-chain-length PHA poly-3-hydroxybutyrate (PHB). Among type II-methanotrophs, the strain *Methyloscystis hirsuta* CSC1 has drawn interest due to its high PHB-accumulating ability and metabolic plasticity (Bordel et al., 2019b). In a recent work, López et al. (2018) obtained comparable cell growth and PHB accumulation (43%) when synthetic biogas rather than CH_4 was used as carbon source in *M. hirsuta* regardless of the presence of hydrogen sulfide. Nevertheless, to the best of the authors' knowledge, the potential of biogas as a feedstock for the continuous production of PHB and the constraints associated to a long-term continuous operation have not been yet reported.

The major operational constraint associated to CH_4/biogas bioconversion technologies is the poor mass transfer of O_2 and CH_4 (Henry´s law constants (k_H) of $1.3 \cdot 10^{-3}$ and $1.4 \cdot 10^{-3}$ M atm^{-1} at standard conditions, respectively) (Sander, 2015). In this regard, turbulent contactors such as bubble column bioreactors (BCBs) engineered with innovative gas-liquid mass transfer strategies (i.e. the utilization of a non-aqueous phase or the implementation of internal gas recirculation) can support an enhanced methane biodegradation (Cantera et al., 2016; Rocha-Rios et al., 2011). Moreover, this type of suspended-growth bioreactors allows an easy biomass harvesting and bioproduct downstream processing (López et al., 2019).

This study aims at optimizing the biogas residence time and the internal recirculation rate to maximize CH_4 mass transfer and at assessing the long-term (> 4 weeks of stable

operation) production of PHB from biogas by *M. hirsuta* in a continuous BCB equipped with gas recirculation.

5.2 Materials and methods

To fulfill the above-mentioned objectives, the experimental research was structured into two main assays that were carried out in a bubble column bioreactor whose configuration was described in section 5.2.2.1. A first approach pursued the optimization of operating parameters through a mass transfer test in which 18 different conditions for EBRT and R (5.2.2.2) were assayed. A second approach aimed at investigating the process stability (5.2.2.3) under non-nutrient limited conditions prior the implementation of sequential nitrogen feast-famine cycles (5.2.2.4) to induce the PHB synthesis. Sections 5.2.2.3 and 5.2.2.4 were performed at the same EBRT and R conditions.

5.2.1 Chemicals, culture media and inoculum

5.2.1.1 *Chemicals.*

The chemicals used for PHB extraction (trichloromethane (≥ 99%), 1-propanol (99.7%), benzoic acid (≥ 99.5%), and hydrochloric acid (37% w/v)) and for the culture medium preparation were acquired from PanReac AppliChem (Spain), except KNO_3, which was purchased from COFARCAS (Spain). Poly(3-hydroxybutyrate-co-3-hydroxyvalerate) (PHBV) with a mole fraction 3HB/3HV of 88/12 (≥ 99.99%) was acquired from Sigma-Aldrich (USA). O_2 (≥ 99.5%), CH_4 (≥ 99.995%), He (≥ 99.5%), and a synthetic biogas mixture containing 70% of CH_4 and 30% of CO_2 were provided by Abelló Linde S.A. (Spain).

5.2.1.2 *Culture medium.*

Unless otherwise specified, a nitrate mineral salt (NMS) medium containing the following macronutrients (g L^{-1}) was employed: 0.2 $CaCl_2 \cdot 2H_2O$, 1.0 KNO_3, 1.1 $MgSO_4 \cdot 7H_2O$ and the following trace elements (mg L^{-1}): 0.01 $NiCl_2 \cdot 6H_2O$, 0.02 $MnCl_2 \cdot 4H_2O$, 0.03 $CoCl_2$, 0.015 H_3BO_3, 0.38 Fe-EDTA, 0.3 $Na_2EDTA \cdot 2H_2O$, 0.4 $Na_2MoO_4 \cdot 2H_2O$, 0.4 $ZnSO_4 \cdot 7H_2O$, 0.5 $FeSO_4 \cdot 7H_2O$ and 1.0 $CuSO_4 \cdot 5H_2O$. The NMS was stored in borosilicate glass bottles and autoclaved (121 °C, 30 min). After cooling the sterile NMS down to room temperature, 10 mL of a sterile buffer solution (72 g L^{-1} $Na_2HPO_4 \cdot 12H_2O$ and 26 g L^{-1} KH_2PO_4) per liter of NMS medium were added to adjust its pH to 6.8.

5.2.1.3 *Strain and inoculum preparation.*

A stock culture of *Methylocystis hirsuta* CSC1 (DSM 18500) was purchased from Leibniz-Institut DSMZ (Germany) and stored at 4ºC until use. The cultivation of *M. hirsuta*, which was grown up to a concentration of 0.54 ± 0.03 g L^{-1} prior to inoculation of the bioreactors, was conducted in two stages under strictly sterile conditions based on López et al. (2018) procedure. Initially, gastight serum vials of 125 mL containing 50 mL of NMS medium were inoculated from the DSMZ vial at 10% ($v\ v^{-1}$) under an O_2:CH_4 atmosphere (66.7:33.3% ($v\ v^{-1}$)). The cultures were incubated in an orbital shaker at 200 rpm and 30°C for 8 days. Once the cultures were metabolically active, the headspace atmosphere was restored systematically up to a maximum of 5 times every 24 h. To that end, filtered oxygen was gassed for 5 min and replaced (25 mL) with methane afterwards with a 50 mL gastight syringe (Hamilton 1050 TLL, USA). Finally, aliquots of 10 mL of this active culture were transferred to sterile serum bottles (2.2 L) containing 0.4 L of NMS medium sealed with aluminum caps and chlorobutyl rubber stoppers under an O_2:CH_4:CO_2 atmosphere of 58.3:29.2:12.5% ($v\ v^{-1}$). The headspace atmosphere was obtained by flushing for 3 min a gas mixture composed of biogas and oxygen with the above mentioned composition from a 100 L-Tedlar gas sampling bag (Sigma-Aldrich, USA). The cultures

were grown under continuous stirring at 300 rpm (Thermo Scientific Variomag Multipoint 6, USA) and 25ºC in a thermostated room for 10-12 days until complete methane depletion.

5.2.2 Experimental procedure

5.2.2.1 *Experimental set-up*

The study herein presented was carried out in a bench-scale bubble column bioreactor (BCB) implemented with gas recirculation to ensure a high CH_4 and O_2 mass transfer to the cultivation broth **(Fig. 5.1)**. The bioreactor, with a working volume of 2.5 L, was equipped with a set of three micropore stainless steel diffusers (2 μm, Supelco, USA) and a magnetic stirrer (Agimatic S, JP Selecta, Spain, 500 rpm) located at the bottom of the column to ensure an adequate mixing throughout the column. A gas mixture composed of atmospheric air and synthetic biogas was continuously sparged into the bioreactor through the diffusers. The biogas stream was regulated by a mass flow controller (GFC17, Aalborg™, USA), whereas the atmospheric air was supplied by an air compressor and controlled by a rotameter to deliver a gas mixture with O_2:CH_4 ratios ranging from 1.5:1 to 2:1. A condenser (maintained at 10°C) was installed at the internal gas recirculation line in order to prevent operational problems derived from water condensation. The BCB was operated at 25ºC in a temperature-controlled room.

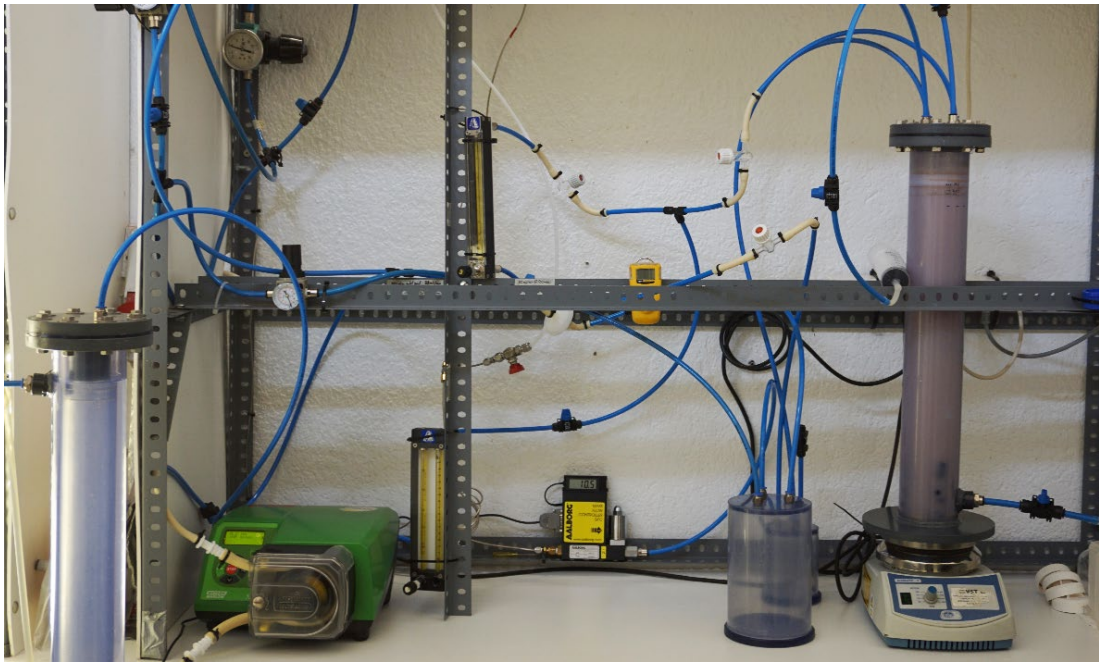

(a)

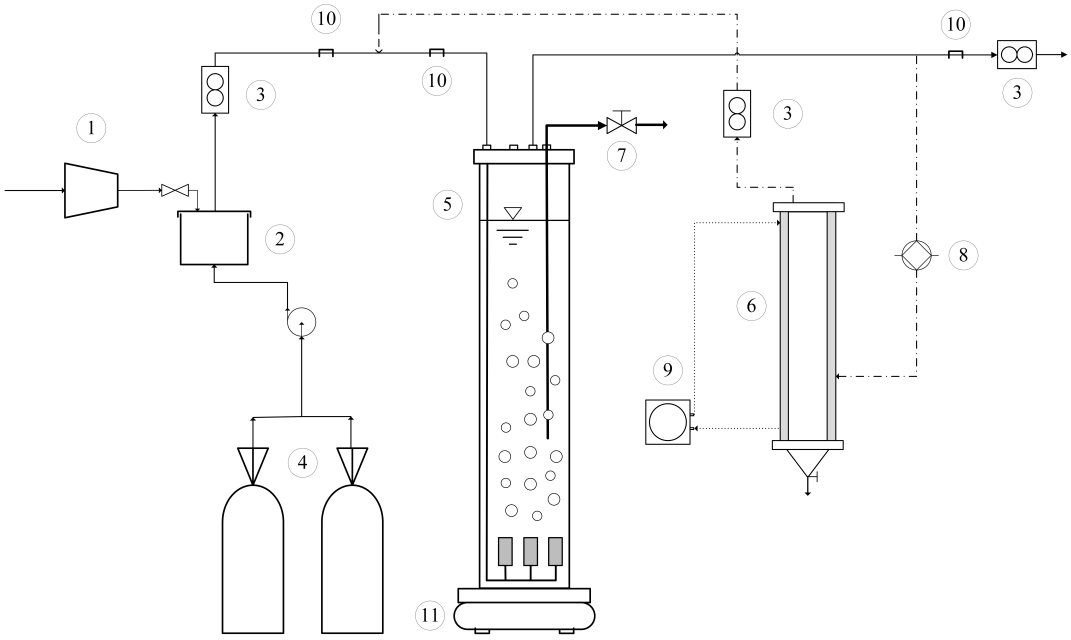

(b)

Fig.5.1 (a) *Image and* ***(b)*** *Schematic representation of the experimental set-up. (1) Air compressor, (2) Mixing chamber, (3) Rotameters, (4) Biogas cylinders, (5) Bubble column bioreactor, (6) Condenser, (7) Liquid sampling port, (8) Gas recirculation pump, (9) Thermostatic bath, (10) Gas sampling ports, (11) Magnetic stirrer, (12) Mass flow controller.*

5.2.2.2 *CH_4/O_2 mass transfer optimization test.*

The bioreactor was first inoculated with a fresh *Methylocystis hirsuta* CSC1 culture resulting in an initial total suspended solids (TSS) concentration of 0.5 g L^{-1}. The BCB was initially operated at an EBRT of 30 min with a CH_4 content of 90 ± 8 g CH_4 m^{-3} (14 ± 1 % *v* v^{-1}) and without gas recirculation for four weeks. In this period, biomass concentration reached 3 g L^{-1}, a concentration that was maintained under all operational conditions tested to guarantee that the process was not biologically limited. For this purpose, aliquots of 500 mL of culture broth from the BCB were daily centrifuged (10000 rpm, 8 min) and replaced by fresh NMS. In order to maintain a constant biomass concentration of ≈3.5 g TSS L^{-1} in the culture broth, the harvested biomass was either partially returned to the system or discarded. The diffusers were replaced when the pressure drop exceeded 0.5 bar. The nitrogen concentration of the NMS supplied was adjusted from 1 to 7 g L^{-1} KNO_3 at each operational condition tested to avoid nitrogen limitation in the culture broth. Subsequently, the influence of the EBRT and the gas recirculation ratio (hereinafter referred to as R) on CH_4 biodegradation under balanced growth conditions was assessed **(Table 5.1)**. Each operational condition was maintained for a period of 5-8 days, which ensured steady state operation regarding the liquid and gas phases.

Table 5.1. *Operational conditions during the CH_4 mass transfer optimization test.*

Test No.	EBRT (min)	Inlet gas flow (ml min^{-1})	R	Virtual EBRT (min)	Inlet load (g CH_4 m^{-3} h^{-1})	Organic loading rate (g COD $L^{-1}d^{-1}$)
1.1	30	83	0	30	202 ± 22	19.4 ± 2.1
1.2			2.5	9		
1.3			5	5		
1.4			10	3		
1.5			15	2		
1.6			30	1		
2.1	60	42	0	60	86 ± 6	8.3 ± 0.6
2.2			2.5	17		
2.3			5	10		
2.4			10	5		
2.5			15	4		
2.6			30	2		
3.1	120	21	0	120	51 ± 4	4.9 ± 0.4
3.2			2.5	34		
3.3			5	20		
3.4			10	11		
3.5			15	8		
3.6			30	4		

5.2.2.3 *Methane biodegradation under nitrogen surplus conditions in the BCB*

The bioreactor was inoculated with the above mentioned strain at 90 ± 10 mg TSS L^{-1} and operated under the optimum operational conditions selected in the previous test (EBRT of 60 min, R = 30, methane inlet load of 68 ± 8 g CH_4 m^{-3} h^{-1} and an O_2:CH_4 molar ratio of 1.8 ± 0.3) in order to identify long-term microbial and mechanical limitations during continuous CH_4 abatement. Thus, CH_4 biodegradation was investigated under nitrogen excess for 50 days (from day 0 to day 35, and from day 51 to day 66) and nitrogen limiting conditions for 15 days (from day 36 to day 50) using a modified NMS medium with N-NO_3^- concentrations of 552 and 276 mg L^{-1}, respectively. During the first week of operation, the biomass contained in 500 mL of culture broth was daily collected and returned to the BCB re-suspended into 500 mL of fresh NMS. From day 8 onwards, no biomass was returned to the BCB so that the biomass concentration was maintained at ≈3 g L^{-1}.

5.2.2.4 *Biogas utilization coupled to continuous PHB production in the BCB*

This test aimed at assessing the continuous PHB biosynthesis from biogas by *M. hirsuta*. The system was initially inoculated at 190 ± 0 mg TSS L^{-1} with *M. hirsuta* and operated at an EBRT of 60 min, a R of 30 and a methane inlet load of 60 ± 3 g CH_4 m^{-3} h^{-1} (corresponding to an O_2:CH_4 ratio of 2.1 ± 0.1). CH_4 biodegradation was initially investigated under nitrogen-balanced conditions for 32 days of operation (using a NMS with a N-NO_3^- content of 345 mg L^{-1}). By day 33, a nitrogen-free mineral salt (NFMS) medium was supplied to deplete the nitrogen in the BCB, and subsequently 15 sequential nitrogen feast-famine cycles of 48 h (i.e. 24 h under nitrogen balanced growth conditions followed by 24 h under nitrogen starvation) were applied to trigger PHB biosynthesis. To this end, 500 mL d^{-1} of modified NMS medium (345 mg N-NO_3^- L^{-1}) or NFMS medium were alternatively provided corresponding to a dilution rate of 0.2 d^{-1}.

Gas flow rate, pressure drop in the gas diffusers and gas composition in the inlet and outlet streams (CH_4, CO_2 and O_2) were monitored daily. Total dissolved nitrogen (TN), NO_2^- and NO_3^- in the culture broth were also recorded. Culture samples (40 mL) were collected for the determination of TSS, pH and PHAs. The pellets from the centrifugation of 3 mL of culture broth samples (10000 rpm, 10 min) were stored at -20ºC prior PHAs analysis.

5.2.3 Analytical procedures

CH_4, CO_2 and O_2 gas concentrations were measured in duplicate in a gas chromatograph coupled with a thermal conductivity detector (Bruker 430, Bruker Corporation, USA) and equipped with CP-Molsieve 5A and CP-PoraBOND Q columns. The pressure drop in the BCB was monitored with a pressure sensor (PI1696, Ifm Electronic, Germany). Outlet gas flow rate was estimated by using the water displacement method.

Biomass concentration, expressed as TSS, was determined according to the 2540 method (APHA, 2017) using 0.45 μm pore size filters (Merck, Germany). Biomass density was also estimated using optical density measurements at 600 nm with a UV-2550 spectrophotometer (Shimadzu, Japan). A Basic 20 pH meter (Crison, Spain) was used for the measurement of pH.

NO_2^- and NO_3^- concentrations were analyzed by ion chromatography using a Waters 432 HPLC conductivity detector (Waters Corporation, USA). TN and total organic carbon (TOC) concentrations were quantified simultaneously in a TOC-V analyzer equipped with a Shimadzu TNM-1 unit.

The biopolymer extraction procedure for PHB quantification via gas chromatography-mass spectrometry (GC-MS) was conducted according to Rodríguez et al. (2020).

5.2.4 Calculation

5.2.4.1 *Performance indicators of the BCB*

The elimination capacity ($CH_4 - EC$), removal efficiency ($CH_4 - RE$) and the volumetric carbon dioxide production rate (PCO_2) are defined as:

$$CH_4 - EC = \frac{Q \cdot (C_{CH_4,in} - C_{CH_4,out})}{V_R} \quad (5.1)$$

$$CH_4 - RE\ (\%) = \frac{C_{CH_4,in} - C_{CH_4,out}}{C_{CH_4,in}} x100 \quad (5.2)$$

$$PCO_2 = \frac{Q \cdot (C_{CO_2,out} - C_{CO_2,in})}{V_R} \quad (5.3)$$

where C_{in} and C_{out} are the inlet and outlet concentration (g m^{-3}), respectively, Q is the inlet gas flow ($m^3\ h^{-1}$) and V_R (m^3) is the working volume of the bioreactor.

5.2.4.2 *Stoichiometry and theoretical PHB productivity in the BCB*

According to literature, the theoretical biomass and PHB yields in type-II methanotrophs are 0.46 g biomass g^{-1} CH_4 (using nitrate as nitrogen source) (Asenjo and Suk, 1986) and 0.54 g PHB g^{-1} CH_4, respectively (Yamane, 1993; Khosravi-Darani et al., 2013).

The overall equations for biomass growth and PHB accumulation supporting these yields are given below.

$$CH_4 + 1.55\,O_2 + 0.07\,HNO_3 \rightarrow 0.07\,C_4H_8O_2N\,(biomass) + 0.71\,CO_2 + 1.75\,H_2O \quad (5.4)$$

$$CH_4 + 1.55\,O_2 \rightarrow 0.10\,C_4H_6O_2\,(PHB) + 0.60\,CO_2 + 1.70\,H_2O \quad (5.5)$$

The sum of Eqs. (5.4) and (5.5) taking into consideration the duration of both growth and accumulation phases within the cycles (1/2) gives the theoretical PHB yield (Y_{PHB}^{th}) of the global process.

Thus, the theoretical PHB productivity (P_{th}) for a 24h:24h growth:accumulation cycle was estimated using the following formula:

$$P_{PHB}^{th}(kg\,m^{-3}d^{-1}) = \frac{(1/2)\cdot 0.54\cdot CH_4EC\cdot 24\,(h/d)}{1000\,(g/kg)} \quad (5.6)$$

where 0.54 is the Y_{PHB}^{th} (g PHB produced g^{-1} CH_4 removed) and CH_4EC is the methane elimination capacity (g CH_4 m^{-3} h^{-1}).

5.3 Results and discussion

5.3.1 CH_4 mass transfer optimization in the BCB: Influence of the gas empty bioreactor residence time and the gas recirculation on CH_4 degradation

BCB operation at EBRTs of 30, 60 and 120 min with no internal gas recirculation showed CH_4-elimination capacities (CH_4-ECs) of 29.8 ± 2.0, 11 ± 1.7 and 6.9 ± 1.8 g CH_4 m^{-3} h^{-1}, with associated CH_4-removal efficiencies (CH_4-REs) of 13.3 ± 0.6, 12.3 ± 1.7 and 12.7 ± 1.2%, respectively (**Fig. 5.2a and b**). This suggests that the enhancement in the turbulence of the cultivation broth mediated by the decrease in the EBRT caused a positive effect on the volumetric mass transfer coefficient (K_La_{CH4}) and consequently, on the CH_4-EC.

Internal gas recirculation has been reported as a promising strategy for enhancing CH_4-biodegradation in biotrickling filters (> 2.5 times) and BCBs (> 2.1 times) during the treatment of CH_4-diluted air emissions (Estrada et al., 2014; García-Pérez et al., 2018). This approach allows decoupling the actual gas residence time in the reactor from the liquid turbulence in the bioreactor. Thus, at an EBRT of 30 min, the CH_4-EC increased to 42.2 ± 1.0, 55.1 ± 1.7, 54.3 ± 1.6, 57.6 ± 1.4 and 73.8 ± 2.1 g CH_4 m^{-3} h^{-1} at R of 2.5, 5, 10, 15 and 30, respectively (**Fig. 5.2a**). Consequently, CH_4-REs increased to 20.5 ± 0.8, 25.0 ± 1.4, 27.1 ± 3.5, 32.7 ± 2.0 and 39.0 ± 3.6% at these R values (**Fig. 5.2b**). Similarly, Rocha-Rios et al. (2011) reported an enhancement of 51% in the CH_4 biodegradation performance of an airlift loop bioreactor by increasing the gas recirculation rate from 0 to 1 volumes per minute (vvm).

At EBRTs of 60 and 120 min, the CH_4-EC increased by a factor of 3.7 (from 11.0 ± 1.7 to 41.1 ± 0.4 g CH_4 m^{-3} h^{-1}) and 3.2 (from 6.9 ± 1.8 to 22.2 ± 0.7 g CH_4 m^{-3} h^{-1}), respectively (**Fig. 5.2b**), at the highest R applied. A similar behavior was observed during the biodegradation of CH_4-laden emissions (4% v v^{-1}) in a BCB with internal gas recirculation.

However, the lower CH_4 gas-liquid gradients during the biodegradation of diluted CH_4 emissions resulted in lower CH_4-ECs (i.e.: 35.2 ± 0.4 g CH_4 m^{-3} h^{-1} at an EBRT of 30 and R of 15) (García-Pérez et al., 2018).

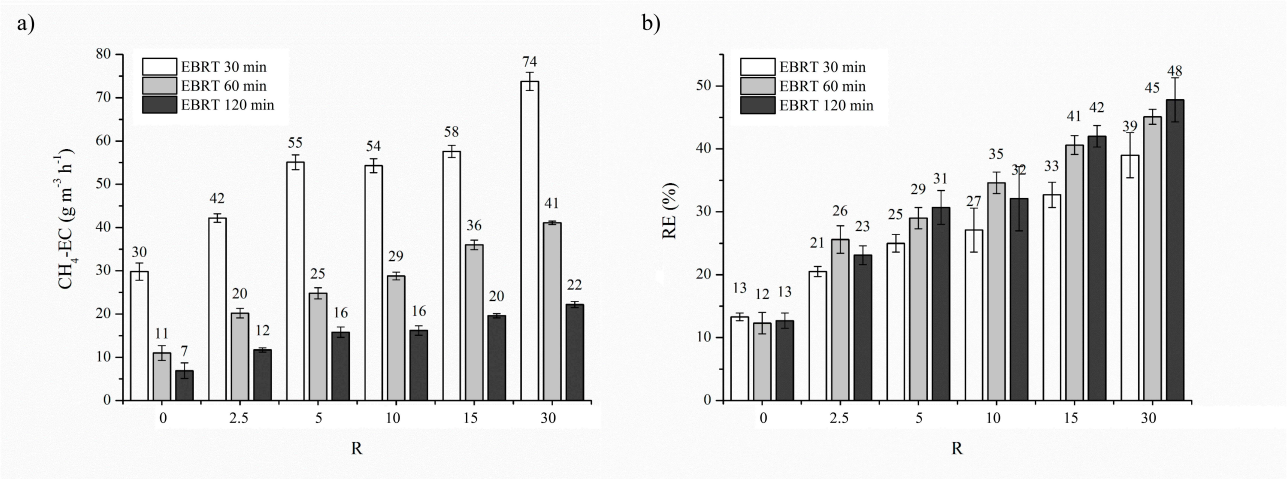

Fig. 5.1 *Influence of R on the (a) CH_4-EC and on the (b) CH_4-RE at EBRTs of 30 min, 60 min and 120 min.*

It can be inferred that internal gas recirculation induces opposite effects by increasing system turbulence at the expense of reducing CH_4 gas-liquid gradient in the column. Results in **Fig. 5.3** indicates that shorter gas contact times in the system mediated greater elimination capacities despite the negative effects which may be associated to a high turbulence such as bubble coalescence or *eddies* (Stone et al., 2017). The correlation observed is explained by the fact that the input of energy into the system reduces the liquid film and enhance the superficial contact area by breaking the bubbles (Kraakman et al., 2011). For instance, the operation of the BCB in the absence of gas recirculation at an EBRT of 30 min and at an EBRT of 120 min with R of 2.5 showed similar virtual EBRTs (30 and 34.3 min, respectively), but a different CH_4-degradation performance with ECs of 29.8 ± 2.0 and 11.7 ± 0.5 g CH_4 m^{-3} h^{-1} and CH_4-REs of 13.3 ± 0.6 and 23.1 ± 1.5%, respectively.

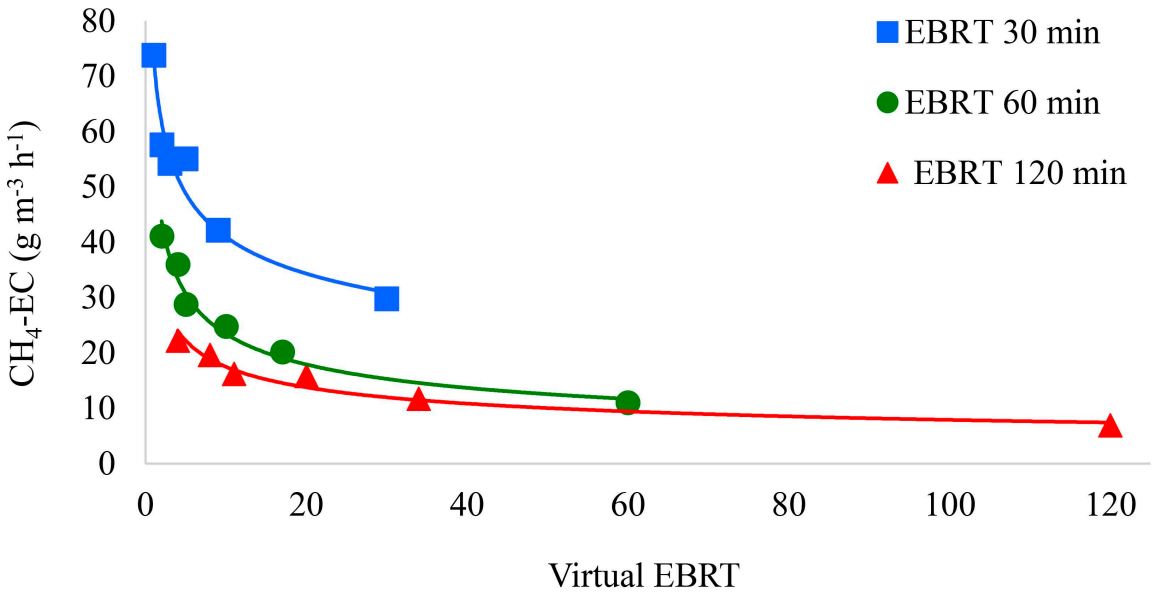

Fig. 5.2 *Influence of the virtual gas residence time on the CH_4-EC.*

Overall, the elimination capacities herein recorded were superior to the ≈20 g m^{-3} h^{-1} achieved in an internal loop airlift reactor (Rocha et al., 2011). Furthermore, there was a satisfactory match with the ≈75 and 22 g m^{-3} h^{-1} (REs of 34 and 15%) achieved in a stirred tank reactor (at 800 rpm) and a trickling bed reactor both operated with a similar methane load. Conversely, the supplementation of the stirred tank reactor with 10% silicon oil resulted in a higher EC (106 g m^{-3} h^{-1}) than the maximum EC reached in this work (74 g m^{-3} h^{-1}) (Rocha et al., 2009). Despite having proved to enhance the gas-liquid transfer at high stirring rates in turbulent contactors (Kraakman et al., 2011), the addition of a non-aqueous phase is up to date not suitable for biomass valorization (Stone et al., 2017).

The highest CH_4-REs were targeted as selection criteria in order to maximize the utilization of CH_4 from biogas as a substrate for PHB biosynthesis (Pérez et al., 2019). Therefore, EBRTs of 60 and 120 min with R of 30 exhibited the highest potential for CH_4 bioconversion with CH_4-REs of 45.1 ± 1.2 and 47.8 ± 3.5% and CH_4-ECs of 41.1 ± 0.4 and 22.2 ± 0.7 g CH_4 m^{-3} h^{-1}, respectively. In the light of the similar CH_4-REs at both EBRTs, the operation at an EBRT of 60 min with a R of 30 was selected as the most appropriate condition for PHB production given the higher CH_4-EC, which would ultimately result in

a significant reduction of equipment costs and enhanced bioreactor productivities. This selection was also supported by a carbon footprint analysis **(Fig. S5.2)**, in which the selected operating conditions mediated the largest CO_2 equivalents reduction (30%) compared to a scenario where the biogas was vented.

The mass transfer experiments here presented were performed with a sufficiently high biomass concentration (>3 g TSS L^{-1}) to guarantee that CH_4 gas-liquid mass transfer was the limiting step of the process. Likewise, the high dilution rate applied prevented nutrient-limiting conditions and secondary metabolites accumulation, which could negatively affect CH_4 biodegradation performance. In this regard, the minimum TN (41.56 ppm) and maximum TOC (74.6 ppm) concentrations corresponded to the maximum CH_4-ECs achieved at an EBRT of 30 min and R of 30. Accordingly, the CH_4 mineralization ratio, expressed as the volumetric CO_2 production rate to methane elimination capacity ratio (PCO_2/CH_4-EC), remained constant at 2.4 ± 0.2, 2.2 ± 0.2 and 2.4 ± 0.3 at EBRTs of 30, 60 and 120 min, respectively, which suggested a balanced methanotrophic metabolism along the entire experiment.

5.3.2 Effect of the N supply on the continuous CH_4 abatement

The CH_4-EC rapidly increased up to 53.0 ± 2.3 g CH_4 m^{-3} h^{-1} concomitantly with an increase in PCO_2 up to 119.9 ± 0.1 g CO_2 m^{-3} h^{-1} following BCB inoculation (**Fig. 5.4a**). Both CH_4-EC and PCO_2 remained stable at 57.1 ± 3.6 g CH_4 m^{-3} h^{-1} and 128.7 ± 11.4 g CO_2 m^{-3} h^{-1}, respectively, during the first 20 days. Biomass concentration increased up to 4.8 ± 0.1 g L^{-1} by day 8 and steadily decreased to 2.4 ± 0.0 g L^{-1} by day 20 (**Fig. 5.4c**). Unexpectedly, CH_4-EC and PCO_2 experienced a slight decrease by day 20 **(Fig. 5.4a)**.

Thus, all biomass was collected by centrifugation and resuspended into fresh NMS medium on day 23 to prevent the culture from a potential accumulation of non-desired metabolites. Despite the system showed an almost complete recovery within the two next days, a sharp drop in CH_4 biodegradation performance occurred again. A new steady state

with CH_4-EC of 7.4 ± 1.5 g CH_4 m^{-3} h^{-1} and PCO_2 of 21.5 ± 4.2 g CO_2 m^{-3} h^{-1} was recorded from day 26 to 36 concomitantly with a gradual biomass wash-out **(Fig. 5.4c).**

The BCB was reinoculated by day 36 with *M. hirsuta* resuspended into NMS medium prepared with half of the nitrogen concentration (276 mg N-NO_3^- L^{-1}). As shown in **Fig. 5.4a**, a consistent steady state was rapidly achieved and maintained for the next 14 days under no excess of nitrogen. When the N-NO_3^- concentration of the NMS medium was restored to 552 mg N-NO_3^- L^{-1}, and the system was no longer nitrogen limited, the CH_4-EC remained constant for four days and eventually dropped from 41.1 ± 2.7 to 5.2 ± 0.7 g CH_4 m^{-3} h^{-1}. PCO_2 was correlated to CH_4-EC with a mineralization of 79.2 ± 7.6% during both steady states achieved.

The analysis of the N species prevailing in the cultivation broth revealed that nitrate reduction to nitrite occurred from day 11 onwards, resulting in nitrite accumulation in the liquid broth, with a maximum concentration of 83.3 mg N-NO_2^- L^{-1} by day 22. It can be inferred that nitrite accumulation (mediated by the O_2 limiting conditions in the cultivation broth at the low O_2:CH_4 ratios used; 1.3:1-1.7:1) induced the inhibition of the methanotrophic metabolism, leading to a deterioration of the system performance despite the high NMS medium dilution rate applied (0.2 d^{-1}). Nitrite formation rapidly occurred again along with a decrease in CH_4-EC after biomass resuspension into fresh NMS medium. Interestingly, when N supply was limited from day 36 to day 50, this accumulation did not occur, which allowed maintaining a stable process operation throughout this period. By day 51, the increase in N loading triggered again the accumulation of nitrite. This confirmed that nitrite accumulation and process inhibition was inherent to N surplus conditions.

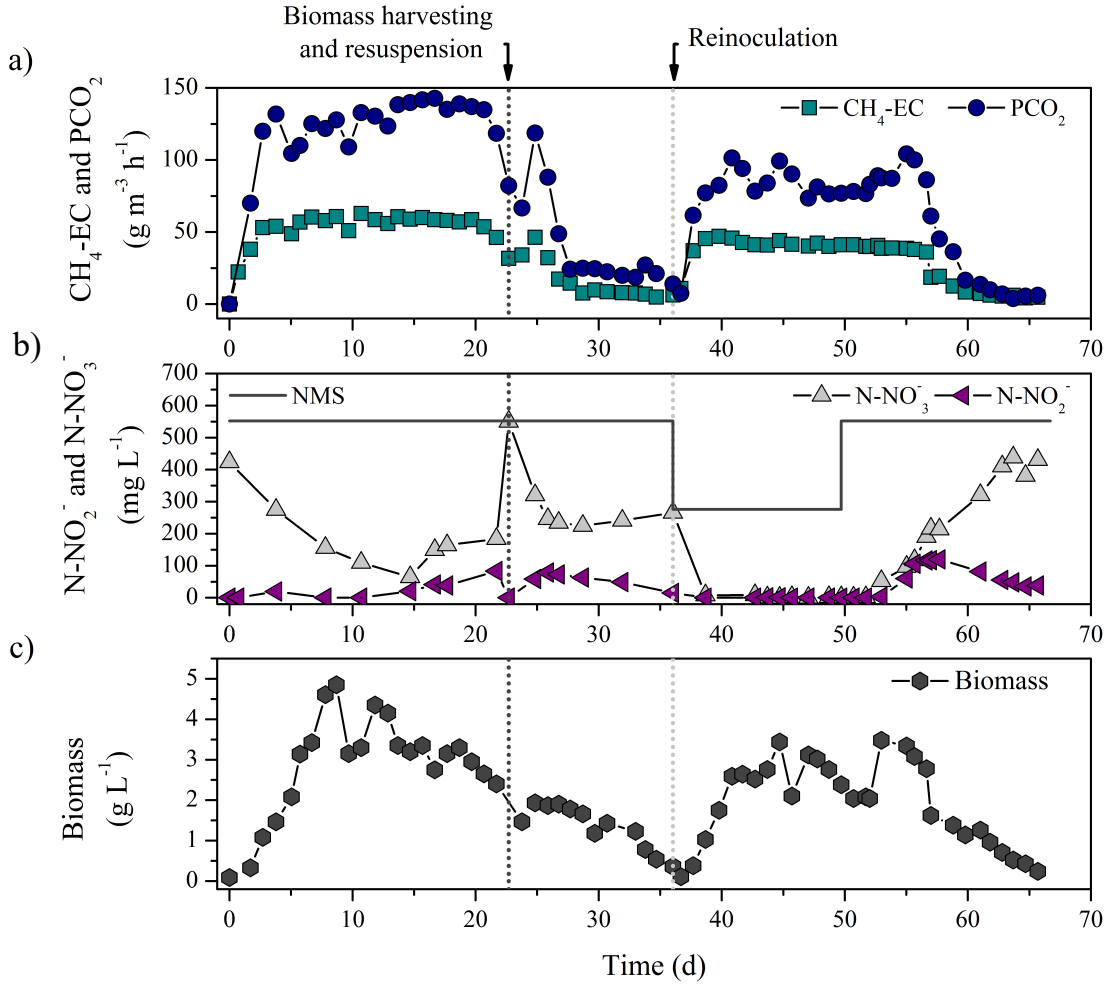

Fig. 5.3 *Time course of (a) CH_4-EC and PCO_2; (b) N-NO_2^- and N-NO_3^- concentration in the culture broth, and N-NO_3^- concentration in the mineral salt medium; (c) biomass concentration expressed as TSS.*

In this context, the batchwise cultivation of *M. hirsuta* CSC1 in mineral salt medium prepared with nitrite as a nitrogen source (138 mg N-NO_2^- L^{-1}) resulted in a complete growth inhibition (Rodríguez et al., 2020). The inhibitory effect of nitrite in type II-MOB was already reported in a previous study, where *Methylocystis* sp. growing in both nitrate- and ammonium-containing growth medium increased its doubling time by 65 and 51%, respectively, when supplemented with 2.5 mM $NaNO_2$ (35 mg N-NO_2^- L^{-1}) (Nyerges et al., 2010). Conversely, the type I strain *Methylomicrobium album* maintained similar doubling times and CH_4 removal rates to those of the control tests under identical conditions, with

additional nitrous oxide production. Interestingly, the genome sequence of *Methylocystis hirsuta* CSC1 recently elucidated revealed that this strain possesses the mechanisms to conduct partially the denitrification pathway (Bordel et al., 2019a). To the best of the author´s knowledge, this phenomenon has not been previously reported in continuous bioreactors devoted to methane abatement. In this regard, N supply limitation strategies can overcome this concurrent nitrite accumulation while inducing PHB synthesis in *M. hirsuta* (Rodríguez et al., 2020).

Finally, the pH of the cultivation broth during the stationary states achieved (7.2 ± 0.1) suggests that the oxidation of methane releases basic metabolites that maintained the pH above the pH of the mineral salt medium (6.8 ± 0.1) despite the presence of buffer and the solubilization of the CO_2 inherently present in biogas.

5.3.3 Biogas utilization coupled to continuous PHB production in the BCB

The BCB was continuously operated under the optimum operational parameters determined in the previous tests (EBRT of 60 min, R of 30 and a N supply of 69 mg $N\text{-}NO_3^-$ d^{-1} L^{-1}) to achieve a steady CH_4 abatement along with a simultaneous biopolymer production. Within the first two days of operation, the system achieved a stable CH_4-EC of 40.2 ± 2.3 g CH_4 m^{-3} h^{-1} corresponding to a CH_4-RE of 70.1 ± 2.7% (**Fig. 5.5a**). These CH_4-EC values, which are in accordance with those achieved during the CH_4/O_2 mass transfer test under comparable operational conditions (41.1 ± 0.4 g CH_4 m^{-3} h^{-1}), supported a PCO_2 of 78.5 ± 6.3 g CO_2 m^{-3} h^{-1} along with a mineralization of 70.5 ± 4.7%. As discused in Section 5.3.1, the performance indicators of this study were comparable to those typically reported for poorly water soluble compounds (< 70%) (Kraakman et al., 2011).

Additionally, the observed O_2:CH_4 molar consumption at this stage was 1.5 ± 0.1, which corresponded to the theoretical value (≈1.5-2) reported by Karthikeyan et al. (2015). The pH remained stable at 7.2 ± 0.2 throughout the whole operation and the presence of nitrite was not detected, thus avoiding culture inhibition **(Fig. 5.5b)**. This supports the

hypothesis that dissimilatory nitrate reduction, where NO_3^- is used as the electron acceptor for energy production, did not prevail over assimilatory nitrate reduction when N consumption and N supply are balanced. These outcomes have important implications for the application of this biotechnology at pilot or industrial scale under long-term operation. Biomass concentration was maintained at 3.0 ± 0.9 g TSS L^{-1} from day 10 onwards, accounting for a biomass production of 20.0 ± 8.3 g TSS m^{-3} h^{-1} **(Fig. 5.5c)**.

Process operation under sequential N feast-famine cycles from day 35 onward supported a stable CH_4-EC of 40.5 ± 1.4 g CH_4 m^{-3} h^{-1} over 15 cycles. Remarkably, the N starvation periods (24 h) did not entail a significant decrease in the system performance as previously reported by García-Pérez et al. (2018). These authors observed a deterioration in the EC from the fifth cycle onwards when longer N deprivation periods were applied (48 h) during the treatment of diluted CH_4 emissions in a BCB. Interestingly, an increase in the mineralization ratio (from 2.1 ± 0.1 to 2.3 ± 0.1 g CO_2 g^{-1} CH_4) was recorded during the N-deprivation periods **(Fig. 5.5a)**, which suggested a higher carbon flux towards formaldehyde oxidation to CO_2 for the regeneration of reducing equivalents needed in the PHB pathway (Khosravi-Darani et al., 2013).

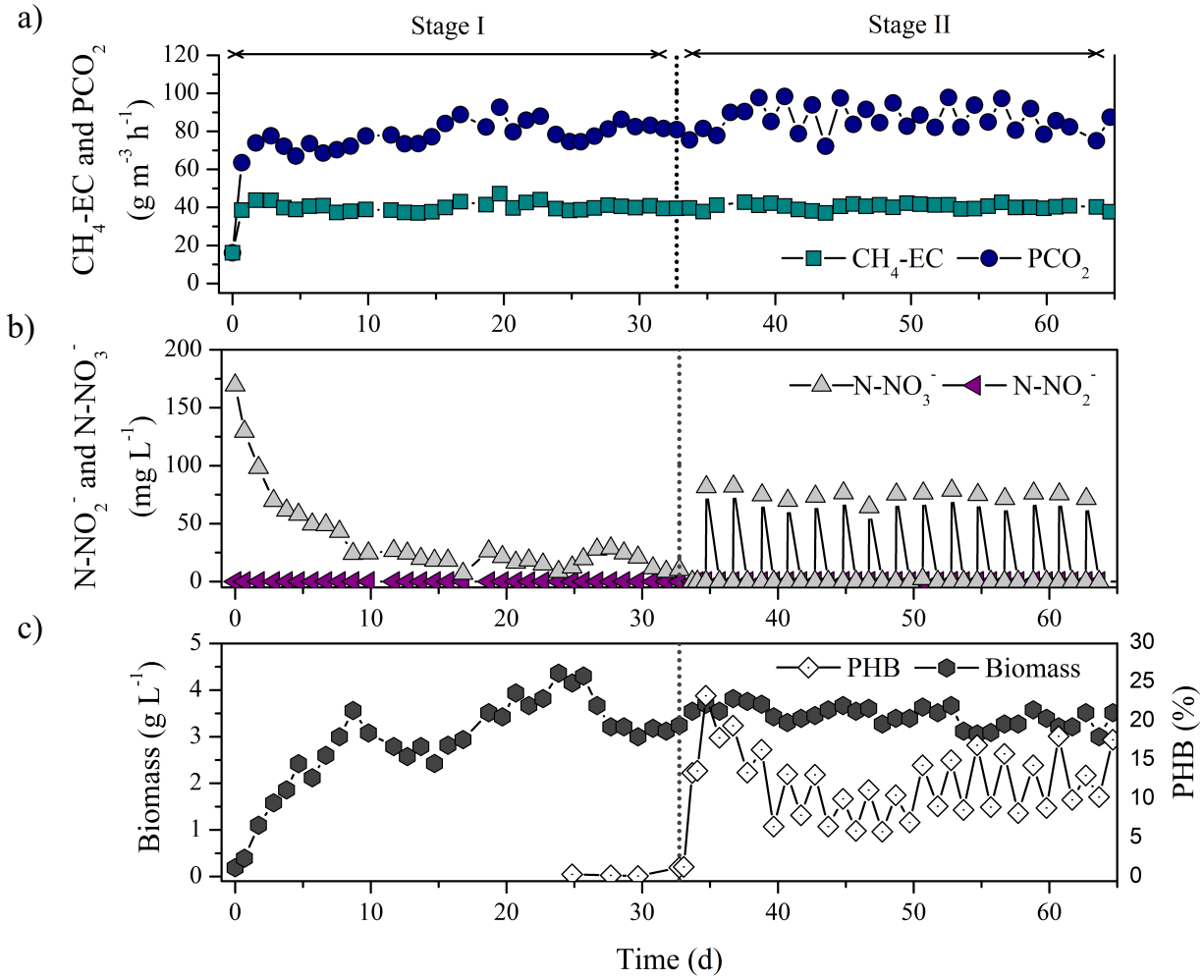

Fig. 5.4 *Time course of* ***(a)*** *CH_4-EC and PCO_2;* ***(b)*** *$N\text{-}NO_2^-$ and $N\text{-}NO_3^-$ concentration in the culture broth,* ***(c)*** *PHB (%) and biomass concentration expressed as TSS).*

The implementation of feast-famine N cycles was initiated after a first limitation period lasting 48 h, which induced a PHB accumulation up to 23.2 ± 0.3% (mg PHB mg^{-1} TSS × 100) in the cells. **Fig. 5.5b** illustrates the dynamics of N addition and rapid N uptake by *M. hirsuta* during the 15 cycles. The implementation of 15 N feast-famine cycles supported an average PHB accumulation of 14.5 ± 2.9% (**Fig. 5.5c**). The determination of the partitioning coefficients revealed that most of the electrons derived from methane were used for energy production by the cells (f_e = 0.80) during the accumulation phase **(Table S5.1)**. Although values ranging 0.52-0.94 were reported by López et al. (2018) when cultures were supplemented with volatile fatty acids, the f_e found in batch assays were

typically lower (≈0.32). During each cycle, the presence of N in the cultivation broth triggered the co-consumption of PHB and CH_4, which entailed a decrease of ≈5% in PHB accumulation (up to 9.1 ± 3.5%).

According to Bordel et al. (2019c), the depletion of the stored PHB in the presence of both CH_4 and nitrogen occurs through anaplerotic reactions. These reactions provide intermediates that are necessary for the synthesis of building blocks such as glyoxylate and succinyl-CoA into the serine and TCA cycle, respectively. In this context, a previous work demonstrated that the consumption of the accumulated PHB by *Methylocystis parvus* did not support growth in the absence of CH_4 (Pieja et al., 2011b). In fact, it has been reported that PHB storage in the presence of CH_4 could provide bacteria a competitive advantage.

Repeated N cycles of 24-h in a sequencing batch reactor resulted in a similar PHB content in a methanotrophic mixed culture (≈15%) (Pieja et al., 2012). Although the figures recorded were nearly a third than those achieved batchwise by *M. hirsuta* using biogas as CH_4 source (up to 45%) (López et al., 2018; Rodríguez et al., 2020), no previous study has been carried out under strictly continuous operation mode aiming at biogas valorization. It must be emphasized that the carbon mass balance conducted presented errors of 0.4 and 5.4% during the growth and accumulation phase, respectively, which validated the results and analyses carried out **(Table S5.1)**.

PHB productivities ranging from 0.04 to 0.06 kg PHB m^{-3} d^{-1}, corresponding to non-N limited and N limiting conditions, respectively, were obtained. An estimation based on the global stoichiometry of the process and the CH_4 uptake rate (Eq. 6) led to a theoretical productivity value of ≈0.26 kg PHB m^{-3} d^{-1}. The productivities herein recorded remained below this value likely due to the substantial impact observed from PHB consumption during the growth phase on the overall yield of the process. In this regard, PHB consumption lowered this value nearly by 60%, i.e. from 0.12 (expected) to 0.05 g PHB produced g^{-1} CH_4 **(Table S5.1)**. Thus, PHB depletion would result in a PHB productivity of 0.10 kg PHB m^{-3} h^{-1}, which would match satisfactorily with the experimental results. In

addition, productivities slightly below the theoretical figures could be also explained by the short time available for methanotrophs to accumulate PHB during the N deprived period applied. A previous study using a similar gas-liquid contactor in batch mode and natural gas as a CH_4 source found that the maximum PHB accumulation (30.5%) occurred over 84 h (Rahnama et al., 2012). In this context, a strategy with an extended N limiting period was carried out (24h with N:48 without N). However, process operation with such long N limitation resulted in an EC and PHB content decrease after the first complete cycle (data not shown), which ultimately resulted in system collapse.

In a biorefinery context, in which a medium size municipal solid waste (MSW) plant treats over 300 ton d^{-1} of residues with an organic fraction of 46% (IEA Bioenergy), 1 ton of VS typically would yield 121.7 m^3 CH_4. Thus, considering repeated N cycles of 24h:24h, a removal efficiency of 70% and a PHB yield of 0.54 g PHB g^{-1} CH_4, it can be predicted that 72.1 ton of MSW would be necessary for the production of 1 ton of PHB. This is, 6.9 kg of PHB can be produced out of 1 ton of MSW. In this regard, a recent geographical analysis conducted by Pérez et al. (2020) revealed that a combined scenario, i.e. PHB and cogeneration from biogas, in countries in which energy costs are high, would achieve PHB production costs as low as 1.5 euro kg^{-1}. It also came out that in those regions where energy production is not economically favorable, biogas could be fully exploited for PHB production with competitive production costs (4.1 euro kg^{-1}).

Finally, it is also worth mentioning that methane content in the exhaust gas from the reactor was 3.0 ± 0.0 % *v* v^{-1} as a result of the high dilution ratio when using air as O_2 source. Therefore, this CH_4 content would not match the minimum concentration required for CH_4 combustion, which is above 35-40% (Haubrichs and Widmann, 2006).

5.4 Conclusions

This work demonstrated for the first time the technical feasibility of PHB production from biogas in a continuous bubble column bioreactor equipped with internal gas recirculation. This work provided valuable insights into the operational conditions supporting a sustained CH_4 bioconversion into PHB. The implementation of internal gas recirculation led to the decoupling of the turbulence in the cultivation broth and gas EBRT, providing outstanding CH_4-ECs and CH_4-REs with values up to 4 times higher than in the absence of gas recirculation. An EBRT of 60 min and a R of 30 were identified as the optimal conditions for maximizing substrate utilization. N-NO_3^- supply to the culture broth must match N demand when using biogas as a CH_4 source in order to prevent nitrite accumulation and the subsequent inhibition of methanotrophic activity. Finally, the N feast-famine strategy applied for PHB production (24h:24h) under optimal mass transfer conditions conferred a stable CH_4 oxidation (stage I) and a continuous PHB production (stage II) with a CH_4-RE of 70% and PHB productivities up to 0.06 kg PHB m^{-3} d^{-1}. These findings highlight the potential of methanotrophic bacteria as an effective/feasible platform for PHB production within a biogas bio-refinery concept. Furthermore, the use of biogas as a low-cost and "green" alternative to conventional carbon sources for biopolymer production would boost their viability in terms of environmental and economic impact. Further studies should explore process robustness under N limiting conditions ranging from 24 to 48 h to achieve higher PHB accumulations.

Acknowledgements

This work was supported by the Spanish Ministry of Science and Innovation (grant number BES-2016-077160, project CTM2015-70442-R). The Regional Government of Castilla y León and the EU-FEDER programme (CLU 2017-09, UIC 071 and VA281P18) are also acknowledged. J.C. López, E. Marcos, A. Crespo and B. Muñoz are gratefully acknowledged for their practical assistance.

References

APHA (2017). Standard Methods for the Examination of Water and Wastewater. 23rd ed, American Public Health Association. Washington, D.C.

Asenjo, J.A., Suk, J.S. (1986) Microbial conversion of methane into poly-β-hydroxybutyrate (PHB): Growth and intracellular product accumulation in a type II methanotroph. *J Ferment Technol*, **64**(4), 271-278. doi: 10.1016/0385-6380(86)90118-4

Blunt, W., Levin, B.D., Cicek, N. (2018) Bioreactor operating strategies for improved polyhydroxyalkanoate (PHA) productivity. *Polymers*, **10**(11). doi: 10.3390/polym10111197

Bordel, S., Rodríguez, E., Muñoz, R. (2019a) Genome sequence of *Methylocystis hirsuta* CSC1, a polyhydroxyalkanoate producing methanotroph. *MicrobiologyOpen*, **8**(6), 1-5. doi: 10.1002/mbo3.771

Bordel, S., Rodríguez, Y., Hakobyan, A., Rodríguez, E., Lebrero, R., Muñoz, R. (2019b) Genome scale metabolic modeling reveals the metabolic potential of three Type II methanotrophs of the genus *Methylocystis*. *Metab Eng*, **54**, 191-199. doi: 10.1016/j.ymben.2019.04.001

Bordel, S., Rojas, A., Muñoz, R., (2019c) Reconstruction of a genome scale metabolic model of the polyhydroxybutyrate producing methanotroph *Methylocystis parvus* OBBP. *Microb Cell Fact*, **18**(104). doi: 10.1186/s12934-019-1154-5

Cal, A.J., Sikkema, W.D., Ponce, M.I., Franqui-Villanueva, D., Riiff, T.J., Orts, W.J., Pieja, A.J., Lee, C.C., (2016) Methanotrophic production of polyhydroxybutyrate-co-hydroxyvalerate with high hydroxyvalerate content. *Int J Biol Macromol*, **87**, 302-307. doi: 10.1016/j.ijbiomac.2016.02.056

Cantera, S., Estrada, J.M., Lebrero, R., García-Encina, P.A., Muñoz, R. (2016) Comparative performance evaluation of conventional and two-phase hydrophobic stirred tank reactors for methane abatement: Mass transfer and biological considerations. *Biotechnol Bioeng*, **113**(6), 1203-1212. doi: 10.1002/bit.25897

Cantera, S., Muñoz, R., Lebrero, R., López, J.C., Rodríguez, Y., García-Encina, P.A. (2018). Technologies for the bioconversion of methane into more valuable products. *Curr Opin Biotechnol*, **50**, 128-135. doi: 10.1016/j.copbio.2017.12.021

Castilho, L.R., Mitchell, D.A., Freire, D.M.G. (2009) Production of polyhydroxyalkanoates (PHAs) from waste materials and by-products by submerged and solid-state fermentation. *Bioresour Technol*, **100**(23), 5996-6009. doi: 10.1016/j.biortech.2009.03.088

Estrada, J.M., Lebrero, R., Quijano, G., Pérez, R., Figueroa-González, I., García-Encina, P.A., Muñoz, R., (2014) Methane abatement in a gas-recycling biotrickling filter: Evaluating innovative operational strategies to overcome mass transfer limitations. *Chem Eng J*, **253**, 385-393. doi: 10.1016/j.cej.2014.05.053

European Bioplastics (2018) Bioplastics market data 2018. Global production capacities of bioplastics 2018–2023. https://www.european-bioplastics.org/wp-content/uploads/2016/02/Report_Bioplastics-Market-Data_2018.pdf (Accessed: 15.12.2019).

García-Pérez, T., López, J.C., Passos, F., Lebrero, R., Revah, S., Muñoz, R. (2018) Simultaneous methane abatement and PHB production by *Methylocystis hirsuta* in a novel gas-recycling bubble column bioreactor. *Chem Eng J*, **334**, 691-697. doi: 10.1016/j.cej.2017.10.106

Haubrichs, R., Widmann, R. (2006) Evaluation of aerated biofilter systems for microbial methane oxidation of poor landfill gas. *Waste Manage*, **26**, 408-416. doi: 10.1016/j.wasman.2005.11.008

IEA (2013) AD of the organic fraction of MSW. System overview for source and central separate waste. https://www.ieabioenergy.com/wp-content/uploads/2013/09/AD-of-the-organic-fraction-of-MSW-Baxter.pdf (Accessed: 08.05.2020).

IEA (2018) Green Gas. Facilitating a future green gas grid through the production of renewable gas. IEA Bioenergy 2018. http://task37.ieabioenergy.com/files/daten-redaktion/download/Technical Brochures/green_gas_web_end.pdf (Accessed: 15.05.2020).

Karthikeyan, O.P., Chidambarampadmavathy, K., Nadarajan, S., Lee, P.K.H., Heimann, K. (2015) Effect of CH_4/O_2 ratio on fatty acid profile and polyhydroxybutyrate content in a heterotrophic–methanotrophic consortium. *Chemosphere*, **141**, 235-242. doi: 10.1016/j.chemosphere.2015.07.054

Khosravi-Darani, K., Mokhtari, Z.-B., Amai, T., Tanaka, K. (2013) Microbial production of poly(hydroxybutyrate) from C1 carbon sources. *Appl Microbiol Biotechnol*, **97**(4), 1407-1424. doi: 10.1007/s00253-012-4649-0

Koller, M., Maršálek, L., de Sousa Dias, M.M., Braunegg, G. (2017) Producing microbial polyhydroxyalkanoate (PHA) biopolyesters in a sustainable manner. *New Biotechnol*, **37**, 24-38. doi: 10.1016/j.nbt.2016.05.001

Kraakman, N.J.R., Rocha-Rios, J., van Loosdrecht, M.C.M. (2011) Review of mass transfer aspects for biological gas treatment. *Appl Microbiol Biotechnol*, **91**(4), 873-886. doi: 10.1007/s00253-011-3365-5

Lee, G.N., Na, J. (2013) Future of microbial polyesters. *Microb Cell Fact*, **12**(54). doi: 10.1186/1475-2859-12-54

López, J., Rodríguez, Y., Pérez, V., Lebrero, R., Muñoz, R. (2019) CH_4-based polyhydroxyalkanoate production: a step further towards a sustainable bioeconomy, in: Kalia, V.C., (Eds), Biotechnological Applications of Polyhydroxyalkanoates. Springer Singapore, Singapore, pp. 283-321.

López, J.C., Arnáiz, E., Merchán, L., Lebrero, R., Muñoz, R. (2018) Biogas-based polyhydroxyalkanoates production by *Methylocystis hirsuta*: A step further in anaerobic digestion biorefineries. *Chem Eng J*, **333**, 529-536. doi: 10.1016/j.cej.2017.09.185

Mühlemeier, I.M., Speight, R., Strong, P.J. (2018) Biogas, bioreactors and bacterial methane oxidation, in: Kalyuzhnaya, M.G., Xing, X.-H. (Eds), Methane biocatalysis: Paving the way to sustainability. Springer International Publishing AG, pp. 213-235. doi: 10.1007/978-3-319-74866-5_1

Muñoz, R., Meier, L., Diaz, I., Jeison, D. (2015) A review on the state-of-the-art of physical/chemical and biological technologies for biogas upgrading. *Rev Environ Sci Biotechnol*, **14**(4), 727-759. doi: 10.1007/s11157-015-9379-1

Myung, J., Flanagan, J.C.A., Waymouth, R.M., Criddle, C.S. (2017) Expanding the range of polyhydroxyalkanoates synthesized by methanotrophic bacteria through the utilization of omega-hydroxyalkanoate co-substrates. *AMB Express*, **7**(1). doi: 10.1186/s13568-017-0417-y

Narancic, T., Verstichel, S., Reddy Chaganti, S., Morales-Gamez, L., Kenny, S.T., De Wilde, B., Babu Padamati, R., O'Connor, K.E. (2018) Biodegradable Plastic Blends Create New Possibilities for End-of-Life Management of Plastics but They Are Not a Panacea for Plastic Pollution. *Environ Sci Technol*, **52**(18), 10441-10452. doi: 10.1021/acs.est.8b02963

Nikiema, J., Brzezinski, R., Heitz, M. (2007) Elimination of methane generated from landfills by biofiltration: a review. Rev Environ Sci Biotechnol, 6, 261–284. doi: 10.1007/s11157-006-9114-z

Nyerges, G., Han, S.-K., Stein, L.Y. (2010) Effects of Ammonium and Nitrite on Growth and Competitive Fitness of Cultivated Methanotrophic Bacteria. *Appl Environ Microbiol*, **76**(16), 5648. doi: 10.1128/AEM.00747-10

Pérez, R., Cantera, S., Bordel, S., García-Encina, P.A., Muñoz, R. (2019) The effect of temperature during culture enrichment on methanotrophic polyhydroxyalkanoate production. *Int Biodeterior Biodegrad*, **140**, 144-151. doi: 10.1016/j.ibiod.2019.04.004

Pérez, V., Lebrero, R., Muñoz, R. (2020) Comparative evaluation of biogas valorization into electricity/heat and polyhydroxyalkanoates in waste treatment plants: Assessing the influence of local commodity prices and current biotechnological limitations. *ACS Sustain Chem Eng* **8**(20), 7701-7709. doi: 10.1021/ acssuschemeng.0c01543

Pieja, A.J., Rostkowski, K.H., Criddle, C.S. (2011a) Distribution and selection of poly-3-hydroxybutyrate production capacity in methanotrophic proteobacteria. *Environ Microbiol*, **62**, 564-573. doi: 10.1007/s00248-011-9873-0

Pieja, A.J., Sundstrom, E.R., Criddle, C.S. (2011b) Poly-3-hydroxybutyrate metabolism in the type II methanotroph *Methylocystis parvus* OBBP. *Appl Environ Microbiol*, **77**(17), 6012-6019. doi: 10.1128/AEM.00509-11

Pieja, A.J., Sundstrom, E.R., Criddle, C.S. (2012) Cyclic, alternating methane and nitrogen limitation increases PHB production in a methanotrophic community. *Biores Technol* **107**: 385-392. doi: 10.1016/j.biortech.2011.12.044

Rahnama, F., Vasheghani-Farahani, E., Yazdian, F., Shojaosadati, S.A. (2012) PHB production by *Methylocystis hirsuta* from natural gas in a bubble column and a vertical loop bioreactor. *Biochem Eng J*, **65**, 51-56. doi: 10.1016/j.bej.2012.03.014.

Rocha-Rios, J., Bordel, S., Hernández, S., Revah, S. (2009) Methane degradation in two-phase partition bioreactors. Chem Eng J, 152(1): 289-292. doi: 10.1016/j.cej.2009.04.028

Rocha-Rios, J., Quijano, G., Thalasso, F., Revah, S., Muñoz, R. (2011) Methane biodegradation in a two-phase partition internal loop airlift reactor with gas recirculation. *J Chem Technol Biotechnol*, **86**(3), 353-360. doi: 10.1002/jctb.2523

Rodríguez, Y., Firmino, P.I.M., Arnáiz, E., Lebrero, R., Muñoz, R. (2020) Elucidating the influence of environmental factors on biogas-based polyhydroxybutyrate production by *Methylocystis hirsuta* CSC1. *Sci Total Environ*, **706**, 135136. doi: 10.1016/j.scitotenv.2019.135136

Rostkowski, K.H., Pfluger, A.R., Criddle, C.S. (2013) Stoichiometry and kinetics of the PHB-producing Type II methanotrophs *Methylosinus trichosporium* OB3b and *Methylocystis parvus* OBBP. *Bioresour Technol*, **132**, 71-77. doi: 10.1016/j.biortech.2012.12.129

Sander, R. (2015) Compilation of Henry's law constants (version 4.0) for water as solvent. *Atmos. Chem. Phys*, **15**(8), 4399-4981. doi: 10.5194/acp-15-4399-2015

Stone, K.A., Hilliard, M.V., He, Q.P., Wang, J (2017) A mini review on bioreactor configurations and gas transfer enhancements for biochemical methane conversion. *Biochem Eng J*, **128**, 83-92 doi: 10.1016/j.bej.2017.09.003

Strong, J.P., Laycock, B., Mahamud, N.S., Jensen, D.P., Lant, A.P., Tyson, G., Pratt, S. (2016) The Opportunity for High-Performance Biomaterials from Methane. *Microorganisms*, **4**(11). doi: 10.3390/microorganisms4010011

Yamane, T. (1993) Yield of poly-D(-)-3-hydroxybutyrate from various carbon sources: A theoretical study. *Biotechnol Bioeng* **41**, 165-170. doi: 10.1002/bit.260410122

Zhang, T., Zhou, J., Wang, X., Zhang, Y. (2017) Coupled effects of methane monooxygenase and nitrogen source on growth and poly-β-hydroxybutyrate (PHB) production of *Methylosinus trichosporium* OB3b. *J Environ Sci*, **52**, 49-57. doi: 10.1016/j.jes.2016.03.001

Appendix B. Supplementary Material

Biogas valorization via continuous polyhydroxybutyrate production by *Methylocystis hirsuta* in a bubble column bioreactor

Yadira Rodríguez[a,b], Paulo Igor Milen Firmino[b,c], Víctor Pérez[a,b], Raquel Lebrero[a,b], Raúl Muñoz[a,b,*]

[a] Department of Chemical Engineering and Environmental Technology, School of Industrial Engineering, University of Valladolid, Dr. Mergelina s/n, 47011 Valladolid, Spain
[b] Institute of Sustainable Processes, Dr. Mergelina s/n, 47011 Valladolid, Spain.
[c] Department of Hydraulic and Environmental Engineering, Federal University of Ceará, Fortaleza, Ceará, Brazil

* Corresponding author: mutora@iq.uva.es

Material and methods

S1. Electric power demand

The power demand of the internal gas recirculation and air compressors for each operational condition at the mass transfer test (5.2.2.2) was estimated according to the following formula (Estrada et al. 2011):

$$P\ (kW) = \frac{\Delta P \cdot (Q + Q_R)}{\eta} \qquad \text{(S5.1)}$$

where ΔP represents the pressure drop (kPa), $Q + Q_R$ represent the real flow entering the column (inlet gas flow and internal recirculation flow, respectively) and η stands for the efficiency of both compressors (70%).

S2. Carbon footprint emissions

Two scenarios were evaluated to study the environmental impact in terms of CO_2 equivalents (kg CO_2 y^{-1}) of direct and indirect emissions on a 1-year basis: (1) The biogas produced in the anaerobic digester was completely vented; (2) The biogas produced in the anaerobic digester was treated in the BCB. Both scenarios were assessed at the different operating conditions of the mass transfer test.

Conversion factors for methane emission and electricity production of 25 kg CO_2 kg^{-1} CH_4 and 0.35 kg CO_2 kWh^{-1} were used, respectively.

$$Carbon\ footprint\ reduction\ (\%) = \frac{CO_2\ eq_{(1)} - CO_2\ eq_{(2)}}{CO_2\ eq_{(1)}} \quad \text{(S5.2)}$$

S3. Substrate partitioning coefficients (f_e and f_s) and carbon distribution

As described by Rostkowski et al. (2012), cell synthesis in methanotrophs occurs in three half reactions: (1) the reduction of the electron acceptor (O_2) into H_2O (eq. S5.3); (2) the oxidation of the electron donor (CH_4) into CO_2 (eq. S5.4) and (3) cell growth. The latter has been adjusted according to the formula used for cell mass ($C_4H_8O_2N$) (Khosravi-Darani et al., 2013) in the present work (eq. S5.5).

$$f_e\ (1/4\ [O_2 + 4H^+ + 4e^- \rightarrow 2H_2O]) \quad \text{(S5.3)}$$

$$1/4\ [CH_4 + O_2 \rightarrow CO_2 + 4H^+ + 4e^-] \quad \text{(S5.4)}$$

$$f_s\ (1/27\ [4CO_2 + NO_3^- + 28H^+ + 27e^- \rightarrow C_4H_8O_2N + 10H_2O]) \quad \text{(S5.5)}$$

The global reaction for cell mass synthesis using NO_3^- as a nitrogen source is given by Eq. S5.6.

$$1/4\ CH_4 + (1/4 + f_e/4)O_2 + (f_s/27)NO_3^- + (28/27 f_s + f_e - 1)H^+ \rightarrow (1/4 - 4f_s/28)CO_2 + (f_e/2 + 11f_s/27)H_2O + (f_s/27)C_4H_8O_2N \quad \text{(S5.6)}$$

f_e and f_s represent the fraction of electrons from the substrate that are utilized for energy generation and for biomass synthesis, respectively. The sum of f_e and f_s is equal to 1.

Likewise, biopolymer ($C_4H_6O_2$) synthesis can be expressed as:

$$1/4\ CH_4 + (1/4 + f_e/4)O_2 \rightarrow (1/4 - 2f_s/9)CO_2 + (f_e/2 + f_s/3)H_2O + (f_s/18)C_4H_6O_2 \quad \text{(S5.7)}$$

Results and discussion

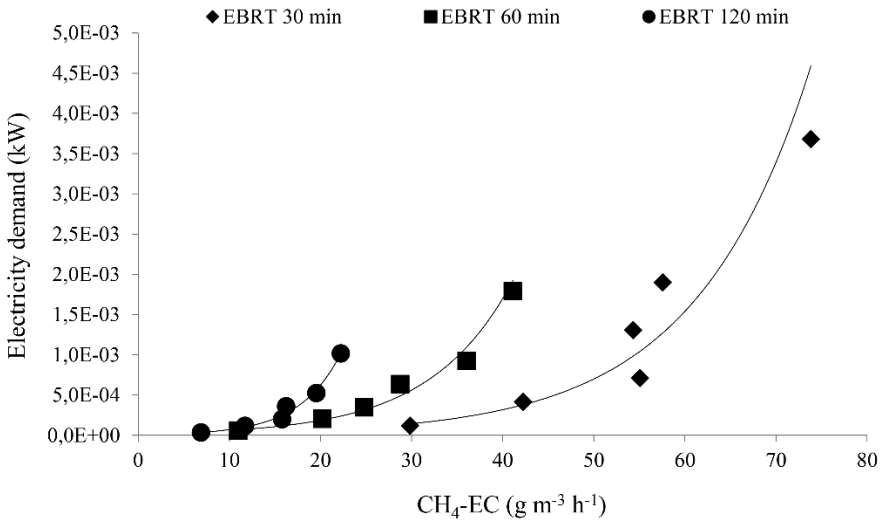

Fig. S5.1. *Power demand at different EBRTs. Each point of the curve represents the different internal recirculation rates assayed (from left to right: 0, 2.5, 5, 10, 15 and 30).*

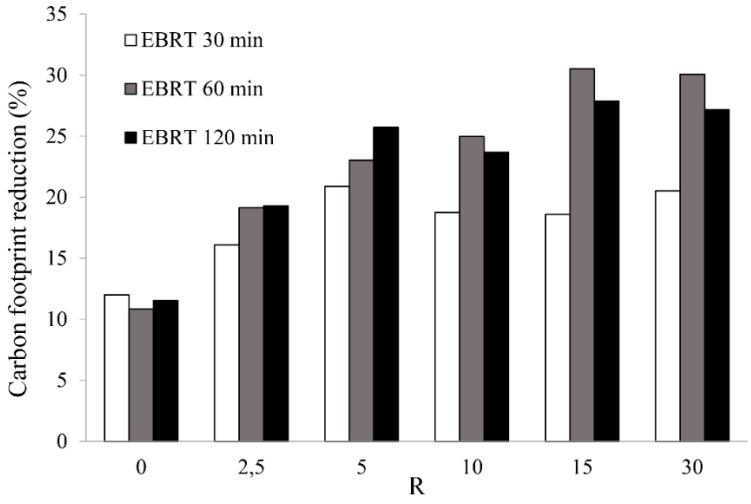

Fig. S5.2. *Carbon footprint mitigation (%) resulting from the biological treatment at lab scale of biogas (comparison between Scenario 1 and 2).*

Table S5.1. Electron fractions (f_e and f_s) and carbon distribution during a N feast-famine cycle (24h:24h)

Phase	f_e	f_s	Y_X ($g_{biomass}$ g^{-1}_{CH4}) Y_{PHB} (g_{PHB} g^{-1}_{CH4})	Carbon balances (C-g)							
				$CH_{4\ (in)}$	$CO_{2\ (in)}$	$CH_{4\ (out)}$	$CO_{2\ (out)}$	Biomass $_{(out)}$	PHB $_{(out)}$	TOC $_{(out)}$	Balance error (%)
Growth	0.44	0.56	0.55	2.70 ± 0.11	1.07 ± 0.03	0.89 ± 0.03	2.41 ± 0.11	0.64 ± 0.06	-0.19 ± 0.02	0.04 ± 0.00	0.45
Accumulation	0.80	0.20	0.24	2.73 ± 0.07	1.05 ± 0.04	0.90 ± 0.02	2.55 ± 0.13	0.21 ± 0.01	0.32 ± 0.04	0.00 ± 0.00	5.38

References

Estrada, J.M., Kraakman, N.J.R., Muñoz, R., Lebrero, R. (2011) A comparative analysis of odour treatment technologies in wastewater treatment plants. *Environ Sci Technol*, **45**, 1100-1106 DOI: 10.1021/es103478j

Khosravi-Darani, K., Mokhtari, Z.-B., Amai, T., Tanaka, K. (2013) Microbial production of poly(hydroxybutyrate) from C1 carbon sources. *Appl Microbiol Biotechnol*, **97**(4), 1407-1424. DOI: 10.1007/s00253-012-4649-0

Rostkowski, K.H., Pfluger, A.R., Criddle, C.S. (2013) Stoichiometry and kinetics of the PHB-producing Type II methanotrophs *Methylosinus trichosporium* OB3b and *Methylocystis parvus* OBBP. *Bioresour Technol*, **132**, 71-77. DOI: 10.1016/j.biortech.2012.12.129

6.

Continuous polyhydroxybutyrate production from biogas in an innovative two-stage bioreactor configuration

Rodríguez Y, García S, Lebrero R, Muñoz R. Continuous polyhydroxybutyrate production from biogas in an innovative two-stage bioreactor configuration (In preparation)

Continuous polyhydroxybutyrate production from biogas in an innovative two-stage bioreactor configuration

Yadira Rodríguez[a,b], Silvia García[a,b], Raquel Lebrero[a,b], Raúl Muñoz[a,b,*]

[a] Department of Chemical Engineering and Environmental Technology, School of Industrial Engineering, University of Valladolid, Dr. Mergelina, s/n, 47011 Valladolid, Spain

[b] Institute of Sustainable Processes, Dr. Mergelina, s/n, 47011 Valladolid, Spain.

* Corresponding author: mutora@iq.uva.es

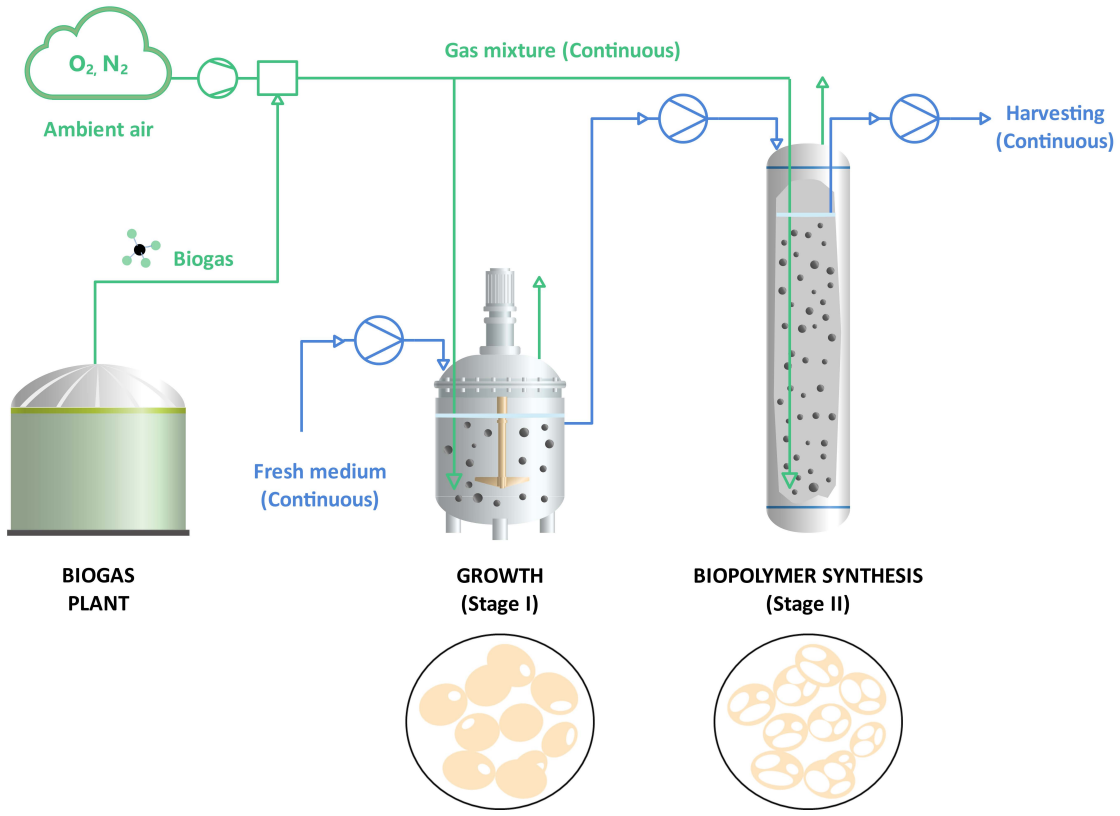

Graphical abstract

Abstract

The concept of biogas biorefineries opens up new horizons beyond heat and electricity production in the anaerobic digestion sector. In this context, added-value products such as polyhydroxyalkanoates (PHAs), which are environmentally benign and potential candidates to replace conventional plastics, can be generated from biogas. This work investigated the potential of a two-stage growth-accumulation system for the continuous production of biogas-based polyhydroxybutyrate (PHB) using *Methylocystis hirsuta* CSC1 as cell factory. The system comprised two turbulent bioreactors in series to enhance methane and oxygen mass transfer: a continuous stirred tank reactor (CSTR) and a bubble column bioreactor (BCB) with internal gas recirculation. The CSTR was intended for methanotrophic growth under nitrogen balanced growth conditions and the BCB targeted PHB production under nitrogen limiting conditions. Two different operational approaches under different nitrogen loading rates and dilution rates were investigated. A balanced nitrogen loading rate along with a dilution rate of 0.3 d^{-1} resulted in the most stable operating conditions and a PHB productivity of ~53 g PHB m^{-3} d^{-1}. However, higher PHB productivities (~127 g PHB m^{-3} d^{-1}) were achieved using nitrogen excess at a D = 0.2 d^{-1}. Overall, the high PHB contents (up to 48% w/w) obtained in the CSTR under theoretically nutrient balanced conditions and the lack of sustained stability challenges the hypothetical advantages conferred by multi-stage *vs* single-stage process configurations for long-term PHB production.

Keywords: Biopolymers; Biogas biorefinery concept; Methane oxidation; Methanotrophic bacteria; Multi-stage system; Polyhydroxyalkanoate production

6.1 Introduction

The production of virgin plastics has risen exponentially since the 1950s, thus intensifying the accumulation of plastic waste in natural environment and landfills (Geyer et al., 2017;UNEP, 2021). Recent studies have highlighted that plastic pollution and climate change, the major threat nowadays, are intrinsically interconnected. Therefore, both environmental challenges should be addressed jointly: the engagement in finding solutions to plastic problem reinforces actions on climate change mitigation (Ford et al., 2022). Therefore, besides reducing their widespread utilization, substituting conventional plastics by biodegradable bioplastics can significantly contribute to decrease the environmental damage caused by mismanaged plastic waste and to reduce greenhouse gases (GHG) footprint.

Natural polymers such as polyhydroxyalkanoates (PHAs) can be synthetized intracellularly (forming spherical inclusions) by different prokaryotic microorganisms, typically when subjected to nutrient limitation (nitrogen, phosphorous, magnesium, etc.) in the presence of carbon excess (Kourmentza and Plácido, 2017;Urtuvia et al., 2014). PHAs are biocompatible, and readily biodegradable, in most of aerobic (marine, soil and compost) and anaerobic (landfills, digesters and sewage sludge) environments (Doi, 1990;Meereboer et al., 2020). With similar properties to those of polypropylene (PP), poly(3-hydroxybutyrate) (P3HB) along with its copolymer poly(3-hydroxybutyrate-co-3-hydroxyvalerate (P(3HB-*co*-3HV)), are the most representative of this family of biopolyesters, which encompasses over 150 different monomeric units (Koller et al., 2010;Li et al., 2016;Steinbüchel and Valentin, 1995). The global production of PHAs accounted for only 1.7% of the bioplastics market (2.1 million tonnes) in 2020 (EUBP, 2020).. Currently, the increasing PHA demand exceeds supply (Ravenstijn, 2021). Unfortunately, PHAs are not competitively priced in comparison with their petroleum-based counterparts, since the high carbon feedstock related costs dominate process costs

(up to 50%), which limits PHA commercialization (e.g. PHB prices average up to 6-fold higher than PP) (Riedel et al., 2015{van den Oever, 2017 #34;Vandi et al., 2018)}.

The need to identify low-cost, non-food based materials (e.g. wastewater, C1 gases, lignocellulose or waste plant oils) to replace sugars and vegetable oils as a feedstock has triggered an intensive research during the last decade (Jiang et al., 2016;Riedel and Brigham, 2020). Particularly, biogas-based PHB production has emerged as a promising alternative to sugar-based PHB synthesis owing to its high content in methane (50 – 70%), which can boost the economic sustainability and the environmental benefits of conventional anaerobic digestion (Kapoor et al., 2020;Pieja et al., 2017;Strong et al., 2016). Unlike other renewables energies such as solar photovoltaic or onshore wind, whose levelized electricity costs have declined by 85% and 56% (USD 0.057 and 0.039 kWh^{-1} in 2020) during last decade, respectively, the levelized cost of electricity from biogas has remained constant (USD 0.095-0.19 kWh^{-1}) (IRENA, 2021). Furthermore, developing the biogas sector through the exploitation of its vast untapped potential (1040 Mtoe) could contribute to the reduction of up to 12% of GHG emissions (WBA, 2019). In addition, methane can be generated from PHA anaerobic digestion, which creates a closed-loop carbon cycle (Yoon and Oh, 2021). Companies such as Mango Materials or Newlight Technologies are US-based and relatively new companies with a focus on the development of microbial fermentation paths to produce PHAs out of waste biogas.

The ability to synthetize PHAs out of methane correspond to type-II methane oxidizing bacteria (MOB), also known as methanotrophs. These microorganisms aerobically degrade methane (as the sole energy and carbon source) for its assimilation as formaldehyde through the serine pathway (Hanson and Hanson, 1996;Kalyuzhnaya et al., 2019). Within this bacterial group, *Methylocystis hirsuta* CSC1 has been recently pointed out as a workhorse for PHA production (Bordel et al., 2019b;López et al., 2018). In contrast to closely related species (e.g. *Methylocystis* sp. SC2), *M. hirsuta* CSC1 exhibits a truncated denitrification pathway (Bordel et al., 2019a). The strain was found to grow on biogas and synthetize PHB optimally at 25ºC under an O_2:CH_4 atmosphere of 1.6:1 (Chen et al., 2020;Rodríguez et al.,

2020a). PHB contents ranging from 43 to 52% have been reported when using biogas and natural gas as carbon substrates, respectively, under batch cultivation (López et al., 2018;Rahnama et al., 2012;Rodríguez et al., 2020a).

The industrialization of biogas bioconversion into PHA is nowadays challenged by the inherent poor gas-liquid CH_4 mass transfer and the reduced growth rate of methanotrophs under nutrient limiting conditions (Fei, 2015;Jawaharraj et al., 2020). Methane elimination capacities of up to 91.1 and 74 g m^{-3} h^{-1} have been achieved in turbulent contactors such as stirred tank and bubble column bioreactors, respectively (Cantera et al., 2016;Rodríguez et al., 2020b). Unfortunately, limited research devoted to achieve high PHAs contents concomitantly with high bacterial productivities is available in literature (Blunt et al., 2018;Koller, 2018). In this context, two-stage processes engineered with a continuous biogas-based cultivation under non nutrient limiting conditions to maximize methanotrophic growth, coupled to a nutrient limited stage devoted to maximize PHA accumulation represents a promising approach that has never been explored in literature.

This work investigated for the first time the potential of a novel two-stage system composed of a continuous stirred tank reactor operated under nitrogen sufficient conditions and a nitrogen-deprived bubble column bioreactor engineered with internal gas recirculation to maximize the continuous production of biogas-based PHB by *M. hirsuta* CSC1. The influence of N loading rates (i.e. excess and balanced N conditions) and of the dilution rate under balanced nitrogen conditions on process performance was evaluated.

6.2 Materials and methods

6.2.1 Methanotrophic strain and culture medium

Methylocystis hirsuta CSC1 (DSMZ 18500), acquired from Leibniz-Institut DSMZ (Germany), was used as model methanotrophic strain. Subcultures were performed in autoclaved 125-mL serum vials containing 45 mL of mineral medium and an oxygen:methane headspace (2:1 molar ratio), inoculated at 10% (v/v), and incubated at 250 rpm and 30ºC in a rotary shaker (Thermo Fisher Scientific Inc., USA) for 7-10 days. The gas headspace was periodically restored upon depletion by flushing filtered O_2 and injecting 25 mL with CH_4.

Inoculum preparation and the subsequent experiments were carried out with a mineral salt solution (NMS), unless otherwise stated, containing (mg L^{-1}): KNO_3 (1000); $MgSO_4 \cdot 7H_2O$ (1100); $Na_2HPO_4 \cdot 12H_2O$ (828); KH_2PO_4 (260); $CaCl_2 \cdot 2H_2O$ (200); $CuSO_4 \cdot 5H_2O$ (1); $FeSO_4 \cdot 7H_2O$ (0.5); $ZnSO_4 \cdot 7H_2O$ (0.4); $Na_2MoO_4 \cdot 2H_2O$ (0.4); Fe-EDTA (0.38); $Na_2EDTA \cdot 2H_2O$ (0.3); $CoCl_2$ (0.03); $MnCl_2 \cdot 4H_2O$ (0.02); H_3BO_3 (0.015) and $NiCl_2 \cdot 6H_2O$ (0.01). The mineral salt medium was adjusted to a pH of 6.8.

6.2.2 Chemicals

The aforementioned chemicals and most of the reagents required for PHB analysis (chloroform (≥ 99%), 1-propanol (99.7%), hydrochloric acid 37% (w/v) and benzoic acid ≥ 99.5%) were purchased from PanReac AppliChem (Spain). Poly(3-hydroxybutyrate-co-3-hydroxyvalerate) containing 14% w/w of HV was acquired from Sigma-Aldrich (USA). KNO_3 was supplied by COFARCAS (Spain). Synthetic biogas with a CH_4:CO_2 composition of 70:30% (v/v), O_2 (≥ 99.5%) and CH_4 (≥ 99.995%) were supplied by Abelló Linde S.A. (Spain).

6.2.3 Experimental set-up

The experiments were conducted in a two-stage system consisting of a stirred tank bioreactor (R1) (Biostat®A, Sartorius Stedim Biotech GmbH, Germany) and a bubble column bioreactor (R2) (Plasthermar, Spain), with individual working volumes of 2.5 L. R1 was equipped with an automated system for NMS supply and pH, temperature and volume control. Both systems were interconnected by a liquid pump that continuously fed R2 with R1 effluent, maintaining both dilution rates equal. An additional pump (Watson Marlon 120S, UK) was periodically activated every 15 min to remove effluent from R2 and maintain a constant volume in the bioreactor. A synthetic mixture of O_2:CH_4 (18%:9% v/v) was continuously supplied to both bioreactors at 42 mL min^{-1} via stainless steel porous spargers (2 µm-pore, Supelco, USA) arranged as shown in **Fig. 6.1**. The gas mixture was obtained by adjusting the flowrate of compressed ambient air and synthetic biogas (70:30% v/v CH_4:CO_2) with a rotameter and a mass flow controller (GFC17, Aalborg^{TM}, USA), respectively. The operating temperature was maintained at 32ºC and 25ºC in R1 and R2, respectively, whereas the pH was kept at 7.0 with the addition of NaOH (4 N). The Rushton impeller agitation speed in R1 and magnetic agitation in R2 were set at 600 and 500 rpm, respectively.

a)

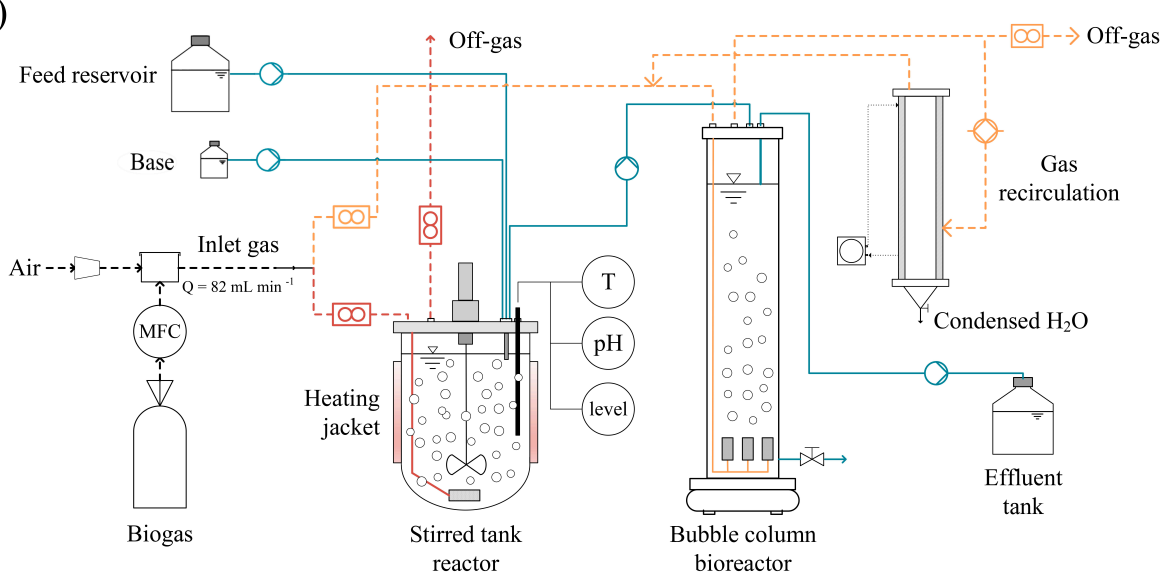

b)

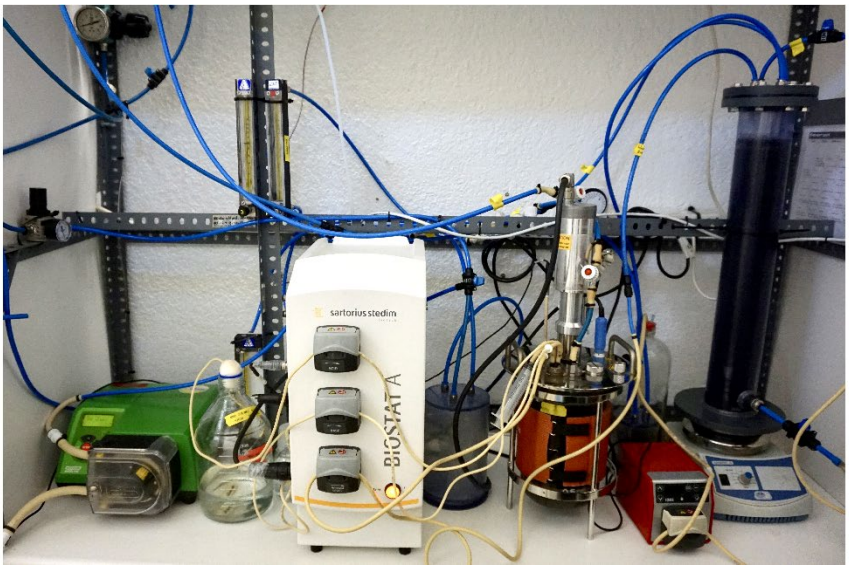

Fig. 6.1 (a) *Schematic representation and* ***(b)*** *picture of the two-stage bioreactor configuration. Continuous line (blue) represents the liquid stream whereas dashed lines represent gas streams for R1 (red) and R2 (yellow)*

6.2.4 Experimental procedure

6.2.4.1 *Test 1 – Nitrogen feeding at a high loading rate*

Nitrogen in the form of KNO_3 was provided in excess compared to N demand in R1, thereby supporting a partial *M. hirsuta* growth in R2 (Table 6.1). R1 was initially inoculated under strictly sterile conditions at 2% v/v with *M. hirsuta,* resulting in a biomass concentration of 8 mg L^{-1}. After an initial batch phase of 9 days, where the culture was grown in 276 mg $N\text{-}NO_3^-$ L^{-1}, autoclaved mineral media with the same $N\text{-}NO_3^-$ concentration was fed at a flow rate of 0.5 L d^{-1} in R1, corresponding to a nitrogen loading rate of 0.14 g $N\text{-}NO_3^-$ d^{-1}. At that point, the bubble column bioreactor containing 2 L of nitrogen-free NMS was interconnected to R1. Both bioreactors were operated at a constant dilution rate of 0.2 d^{-1} for 8 days.

6.2.4.2 *Test 2 - Nitrogen feeding at a balanced loading rate*

The nitrogen loading matched the nitrogen demand of the system, thus uncoupling completely growth and synthesis conditions in both bioreactors (Table 6.1). R1 was initially inoculated under strictly sterile conditions with *M. hirsuta* resulting in an initial biomass concentration of 22 mg L^{-1}. The continuous operation was carried out in two different stages. After an initial batch phase of 3 days where the culture was grown in 86 mg $N\text{-}NO_3^-$ L^{-1}, autoclaved NMS with a $N\text{-}NO_3^-$ concentration of 215 mg L^{-1} was fed at a flow rate of 0.5 L d^{-1} in R1, corresponding to a nitrogen loading rate of 0.11 g $N\text{-}NO_3^-$ d^{-1}. Simultaneously, the bubble column bioreactor containing 2 L of nitrogen-free mineral medium was coupled to the system. Both bioreactors were operated at a constant dilution rate of 0.2 d^{-1} for 20 days (Stage I). From day 23 onwards, a second stage (Stage II) with a dilution rate of 0.3 d^{-1} but similar nitrogen loading rate was operated.

Table 6.1 *Detailed operating conditions for the tests conducted*

Test	Stage	Continuous operation (d)	D (d^{-1})	N- NO_3^- NMS (mg L^{-1})	N- NO_3^- Loading Rate (mg L^{-1} d^{-1})	N- NO_3^- Supply (%)
1	I	8	0.2	276	56	130
2	I	20	0.2	215	44	100
	II	26	0.3	138	44	100

A daily characterization of the inlet and outlet gas and liquid streams in both bioreactors was performed. The outlet gas flowrates, pressure drops and composition of the inlet and outlet gas streams were measured. Monitoring of the liquid phase (30 mL aliquots) comprised the determination of the pH, optical density (OD) and total suspended solids (TSS) concentration. Moreover, biomass pellets obtained by centrifuging (10000 rpm, 10 min) 1.5 mL samples (in duplicate) were stored at -20ºC for PHB analyses. Filtered samples (0.22 μm) were used for the quantification of the total dissolved nitrogen (TN), total organic carbon (TOC), and nitrite/nitrate, phosphate and sulphate ions concentration.

6.2.5 Analytical procedures

PHB cell content was determined through gas chromatography-mass spectrometry (GC-MS) using a 7820A gas chromatograph coupled to a 5977E mass spectrometer (Agilent Technologies, USA). The PHB extraction methodology and GC-MS conditions can be found elsewhere (Chen et al. 2020). Biomass concentration was quantified using Standard Methods (APHA 2018) as total suspended solids and culture absorbance using a SPECTROstar Nano at 600 nm (BMG LABTECH, Germany). pH measurements were performed using a pH meter Basic 20 (Crison, Spain). Ion-exchange liquid chromatography with conductivity detection (Waters 432, Waters Corporation, USA) was used for the determinations of nitrite, nitrate, sulphate and phosphate concentrations. Total organic carbon and total nitrogen concentrations were determined in a Shimadzu TOC-$L_{CSH/CSN}$ analyser equipped with a TNM-1 unit (Shimadzu, Japan). Gas flowrates were measured using the water displacement method, whereas CH_4, CO_2 and O_2 concentrations were analyzed in a Bruker 430 gas chromatograph (GC) coupled with a thermal conductivity detector (TCD) (Bruker Corporation, USA) according to Estrada et al. (2014). An electronic pressure sensor PN7097 (Ifm Electronic, Germany) was used to monitor pressure drop.

6.2.6 Calculations

The methane elimination capacity (CH_4-EC), methane removal efficiency (CH_4-RE) and volumetric production of CO_2 (PCO_2) were herein used as key performance indicators to assess the performance of both bioreactors:

$$CH_4 - EC = \frac{Q \cdot (C_{CH_4,in} - C_{CH_4,out})}{V_R} \quad (6.1)$$

$$CH_4 - RE\ (\%) = \frac{C_{CH_4,in} - C_{CH_4,out}}{C_{CH_4,in}} x100 \quad (6.2)$$

$$PCO_2 = \frac{Q \cdot (C_{CO_2,out} - C_{CO_2,in})}{V_R} \quad (6.3)$$

where C_{in} and C_{out} are the inlet and outlet concentration (g m^{-3}), respectively, Q is the inlet gas flow (m^3 h^{-1}) and V_R (m^3) is the working volume of the bioreactor.

6.3 Results and discussion

6.3.1 Test 1 – Continuous operation at a high nitrogen loading rate.

Following a lag phase period of two days, N-NO_3^- was assimilated in R1 at a rate of 42.4 mg L^{-1} d^{-1} (R = 0.99), being completely assimilated by day 8 (**Fig. 6.2A**). Total nitrogen followed a similar consumption pattern, although a background TN concentration of ≈40 mg L^{-1} was recorded in the culture broth of R1. The presence of N-NO_2^- during batch cultivation was negligible. The continuous supply of NMS in R1 during stage I resulted in the accumulation of nitrate at a rate of 12.1 mg N-NO_3^- L^{-1} d^{-1} (R = 0.99) from day 10 onwards. A gradual accumulation of N-NO_2^- was also observed in R1 by day 14 (at concentrations >54 mg N-NO_3^- L^{-1}), reaching a final concentration of 31.1 mg of N-NO_2^- L^{-1} by day 17 **(Fig. 6.2A)**. On the other hand, the organic residual nitrogen content was of 38.2 ± 1.8 mg L^{-1} during the Stage I in R1. In the BCB, neither nitrate nor nitrite concentration was recorded in R2 during Test 1 (**Fig. 6.2B**). A noticeable accumulation of residual organic nitrogen occurred in R2, likely attributed to the nitrogen-rich effluent from R1.

Cultivation under batch conditions in R1 resulted in a biomass concentration of 2.3 g TSS L^{-1} by day 9, and a biomass productivity of 0.32 g L^{-1} d^{-1}. In this context, the maximum specific growth rate of *M. hirsuta* was of 0.21 d^{-1} (R = 0.998) from day 5 to 8. The biomass concentration remained constant from day 9 to 15 (Stage I), averaging 2.2 ± 0.1 g L^{-1}. However, a decrease in the biomass productivity with a subsequent biomass loss was observed during the last two days of operation, when biomass concentration dropped to 1.8

± 0.0 g TSS L^{-1} (**Fig. 6.2C**). Interestingly, synthesis of PHB was observed during the batch cultivation period in spite of the non-nitrogen limiting conditions. Indeed, PHB synthesis was initiated 3-4 days after inoculation, reaching a final content of 15.1 ± 0.6% at the end of the batch period. It can be hypothesized that the culture experience from day 3-4 growth limiting conditions generated by factors others than nitrogen availability (i.e. high temperature and high shear stress). Process operation under continuous mode entailed a slight decrease in PHB content during the first 24 hours. However, from day 10 onwards PHB cell content steadily increased up to 30.7% by day 17 despite nitrogen availability. These results agreed with the observations of Rahnama et al. (2012), who claimed that PHB is as a growth associated metabolite in *M. hirsuta*, unlike in other type II methanotrophs. These authors observed an increasing PHB production concomitant with an increasing growth rate using a modified NMS. These observations differs markedly with the majority of studies on PHB synthesis by *M. hirsuta,* where growth-associated PHB production did not occur (López et al., 2018;Rodríguez et al., 2020a). These discrepancies highlight the complexity of the regulatory mechanisms underlying PHB production in methanotrophs and evidence the need for further research. On the other hand, R2 exhibited higher values of biomass concentration (2.6 ± 0.0 g L^{-1} by day 16) than R1, likely due to the complete utilization of the nitrogen received from R1 **(Fig. 6.2D)**. Similarly, higher PHB values were observed in R2 during continuous operation. Thus, PHB cell content increased from 15.1 ± 0.6% (day 9) up to 30.2 ± 0.5% (day 12), remaining constant afterwards (30.6 ± 0.1%), which entailed a PHB productivity of 126.7 ± 18.2 g PHB m^{-3} d^{-1} **(Fig. 6.2D)**. The productivity herein recorded were 2-3 fold higher than the values obtained in a single-stage BCB under N feast-famine cycles (40 – 60 g PHB m^{-3} d^{-1}) using *M. hirsuta* (Rodríguez et al., 2020b). Unfortunately, the system did not support a stable PHB productivity since PHB content decreased to 22.6 ± 1.0% by day 16.

R1 initially exhibited a rapid increase in CH_4-EC, overcoming biological limitation by day 3 and reaching a stable value of 29.6 ± 1.2 g m^{-3} h^{-1} from day 3 to 8 of batch operation, which corresponded to a removal efficiency of 54.8 ± 3.3% **(Fig. 6.2E)**. Similarly, PCO_2

averaged 59.8 ± 6.4 g m^{-3} h^{-1} in the aforementioned period. By day 9, both CH_4-EC and PCO_2 values dropped sharply to 10.5 g CH_4 m^{-3} h^{-1} and 28.1 g CO_2 m^{-3} h^{-1}, respectively, as a result of the lack of assimilable nitrogen (i.e. NO_3^-) in the culture broth. At this point, the mineralization ratio (PCO_2/EC) increased from 2.0 ± 0.2 (days 3-8) to 2.7 g CO_2 g^{-1} CH_4. Both CH_4-EC and PCO_2 were restored following the continuous supply of NMS, achieving values of 32.5 ± 0.6 g CH_4 m^{-3} h^{-1} and 72.4 ± 6.0 g CO_2 m^{-3} h^{-1}, respectively, from day 10 to 15. Surprisingly, from day 15 onwards, process performance decreased by nearly 5 times in R1 (**Fig. 6.2E)**, supporting a CH_4-EC of 6.8 g CH_4 m^{-3} h^{-1}, which corresponded to a removal efficiency of 11.4%, by the end of Test 1. It might be inferred that nitrate denitrification prevailed over assimilatory pathways when PHB contents are high (>25%) in presence of nitrogen excess, nitrate causing a severe non-reversible inhibition of the methanotrophic metabolism. In R2, CH_4-EC of 19.5 ± 3.1 g CH_4 m^{-3} h^{-1} were achieved from day 12 onwards, while PCO_2 increased steadily up to 52.1 ± 1.7 g CO_2 m^{-3} h^{-1} by the end of Test 1.

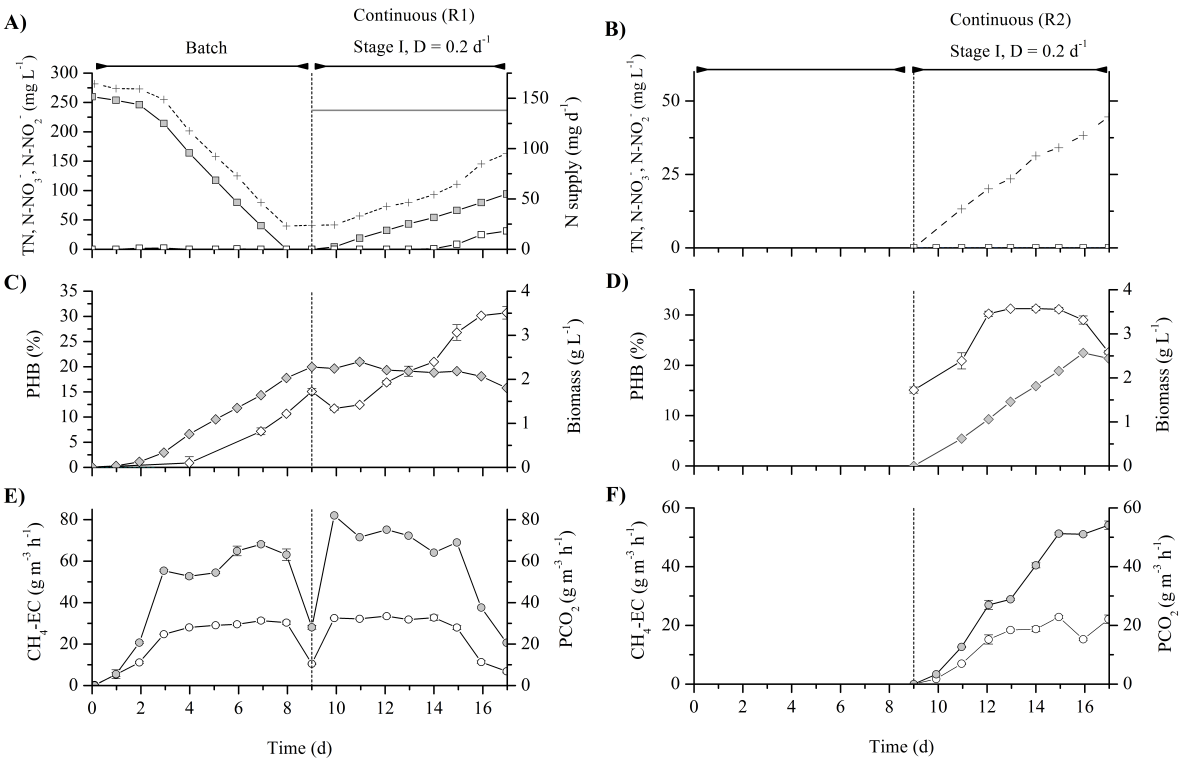

Fig. 6.2 *Time course of* ***(A, B)*** *Total nitrogen (crosses), N-NO_3^- (solid squares) and N-NO_2^- (empty squares) concentrations, N supply (continuous line);* ***(C, D)*** *PHB content (empty diamonds) and biomass concentration (solid diamonds), and* ***(E, F)*** *CH_4-EC (empty circles) and PCO_2 (solid circles) in R1* ***(left)*** *and R2* ***(right)*** *during Approach 1. Vertical dashed lines separate the different operational stages.*

6.3.2 Test 2 – Continuous operation at a balanced nitrogen loading rate.

Approximately 46% of the initial nitrate concentration was consumed during batch cultivation, reaching a final concentration of 49.5 mg L^{-1} N-NO_3^- with no nitrite accumulation observed by day 3 **(Fig. 6.3A)**. Unlike test 1, the total nitrogen present in the culture broth corresponded solely to nitrogen in the form of nitrate. Nitrate remained constant at 48.8 ± 0.9 mg N-NO_3^- L^{-1} from day 3 to 7 in R1 during process operation at D = 0.2 d^{-1} **(Fig. 6.3A).** Subsequently, a decrease in the nitrate concentration to 18.1 mg L^{-1} occurred from day 7 to 12, followed by a period of accumulation where N-NO_3^- increased up to 76.0 mg L^{-1}. These fluctuations in the nitrogen consumption might be related to shifts in the N demand during polyhydroxybutyrate synthesis/consumption (see **Fig. 6.3C**). The

increase in the dilution rate up to 0.3 d^{-1} resulted in a stabilization of the $N\text{-}NO_3^-$ concentration at 72.6 ± 3.0 mg L^{-1}, except from day 35 to 45 when fluctuated between this value and 31.3 mg L^{-1} **(Fig. 6.3A).** The decrease observed in the aforementioned period was probably due to a higher methanotrophic activity mediated by PHB consumption. Only minor peaks of nitrite (<3.6 mg L^{-1} $N\text{-}NO_2^-$) were recorded, whereas the residual organic nitrogen ranged from 9 to 23 mg L^{-1} during Test 2. On the other hand, nitrate concentration in R2 remained below 6 mg L^{-1} $N\text{-}NO_3^-$ from day 3 to 19, which indicated an almost complete assimilation **(Fig. 6.3B)**. Conversely, an increase in $N\text{-}NO_3^-$ concentration was observed by day 20 (Stage I) induced by the deterioration in the system performance and the concomitant nitrate accumulation in R1 **(Fig. 6.3A and E).** Nitrate concentration in R2 increased until day 28 of operation (Stage II) up to 44.0 mg L^{-1}. From day 37 onwards, R2 exhibited again a complete removal of nitrate. No significant accumulation of nitrite occurred along this test in R2 (<3.5 mg L^{-1} $N\text{-}NO_2^-$). At the end of Stage I, the residual organic nitrogen concentration achieved a maximum value of ≈45 mg L^{-1}, while process operation at 0.3 d^{-1} maintained the residual organic nitrogen at 11 mg L^{-1} by the end of Stage II **(Fig. 6.3B).**

Biomass concentration increased from 0.02 ± 0.00 to 0.37 ± 0.01 g TSS L^{-1} by day 3 in R1, and continued increasing during continuous operation at D = 0.2 d^{-1} up to a concentration of 1.69 ± 0.00 g L^{-1} **(Fig. 6.3C)**. The increase in the dilution rate, along with the deterioration in methane biodegradation performance, resulted in a steady decrease of biomass concentration from day 23 to 30, stabilizing from day 31 onwards at 0.79 ± 0.13 g L^{-1} in R1. Synthesis of PHB was rapidly initiated after inoculation, a PHB content of 25.9% being recorded by day 3 despite nitrogen availability **(Fig. 6.3C)**. During Stage I, PHB content increased up to 42.1% until day 5, but rapidly declined to 3.9% w/w by day 11. Interestingly, PHB synthesis was resumed again, reaching a maximum PHB content of 48.2% by day 22 likely due to the low nitrogen concentrations (18.1 mg $N\text{-}NO_3^-$ L^{-1}). Process operation at D = 0.3 d^{-1} resulted in a slight decrease in PHB content followed by a stabilization at 33.4 ± 7.8% during the rest of the experiment. On the other hand, biomass

concentrations in R2 remained below those values recorded in R1 during Stage I, suggesting biomass decay especially from day 11 to 15 when the culture was subjected to more severe nitrate limiting conditions in R2 **(Fig. 6.3D)**. After a steady decrease at the beginning of Stage II caused by the higher dilution rate, biomass concentration increased and stabilized at values of 1.43 ± 0.14 g L^{-1}. PHB contents in R2 during Stage I followed a similar trend to the one observed in R1, although superior PHB contents were only exhibited by day 8 (47.1%). In this period, PHB productivities ranged from to 89.1 to 3.5 g PHB m^{-3} d^{-1}. PHB contents during process operation at D = 0.3 d^{-1} remained low until day 37 (5.6 ± 2.4%) and increased from day 37 to 43 up to 20.5 ± 1.8%, which corresponded to PHB productivities of 53.2 ± 4.8 g PHB m^{-3} d^{-1}.

The methane elimination capacity and volumetric CO_2 production in R1 steeply increased up to 20.2 ± 1.4 g CH_4 m^{-3} h^{-1} and 34.4 ± 1.8 g CO_2 m^{-3} h^{-1}, respectively, during batch cultivation **(Fig. 6.3E)**. Both parameters remained stable during Stage I, averaging 25.7 ± 1.2 g CH_4 m^{-3} h^{-1} (corresponding to a RE of 44.4 ± 1.9%) and 51.6 ± 2.8 g CO_2 m^{-3} h^{-1} for CH_4-EC and PCO_2, respectively. From day 21 to 23, a deterioration of the biodegradation performance of R1 was observed, which resulted in CH_4-EC and PCO_2 of 17.8 ± 0.3 and 34.4 ± 0.1 g m^{-3} h^{-1}, respectively. Nonetheless, the mineralization ratio (PCO_2/EC) remained constant at 2.0 ± 0.1 g CO_2 g^{-1} CH_4 throughout Stage I. This decrease in biodegradation performance corresponded to the period that exhibited both the highest PHB accumulation (48% w/w) and highest accumulation of total organic carbon (TOC) (≈124 mg L^{-1}). Further investigations are required to rule out the possibility of inhibition caused by carbon intermediates such as formaldehyde, which is regarded as the most toxic among aldehydes for methylotrophs (Marx et al., 2020). The increase in the dilution rate up to 0.3 d^{-1} entailed steady state CH_4-EC and PCO_2 of 15.8 ± 1.4 g m^{-3} h^{-1} and 29.1 ± 2.9 g m^{-3} h^{-1}, corresponding to a PCO_2/EC of 1.8 ± 0.1 g CO_2 g^{-1} CH_4. This stable process operation may be attributed to the further reduction of TOC concentration (down to ≈60 mg L^{-1}) caused the higher mineral medium renewal. Interestingly, CH_4-EC increased up to 28.6 ± 1.1 g m^{-3} h^{-1} by day 39 concomitantly with

PHB utilization and an increase in biomass growth **(Fig. 6.3E).** On the other hand, CH_4-EC and PCO_2 in R2 fluctuated according to biomass concentration. Thus, CH_4-EC averaged 11.1 ± 0.9 g CH_4 m^{-3} h^{-1} from days 5 to 10, corresponding to a RE of 42.4% and a PCO_2 of 42.2 ± 2.0 g CO_2 m^{-3} h^{-1} **(Fig. 6.3F).** Afterwards, PCO_2 and CH_4-EC fluctuated from 20 to 64 g CO_2 m^{-3} h^{-1} and from 4 to 24 g CH_4 m^{-3} h^{-1}, respectively, during Stage I. Process operation at a dilution rate of 0.3 d^{-1} stabilized CH_4-EC and PCO_2 at 22.9 ± 3.3 g CH_4 m^{-3} h^{-1} and 58.3 ± 9.6 g CO_2 m^{-3} h^{-1}, respectively, by the end of stage II **(Fig. 6.3F).** Microscopic images of the culture in this period **(Fig S6.1)** revealed the presence of protozoa in R2, which could explain the low values of CH_4-EC recorded in spite of the high biomass concentration.

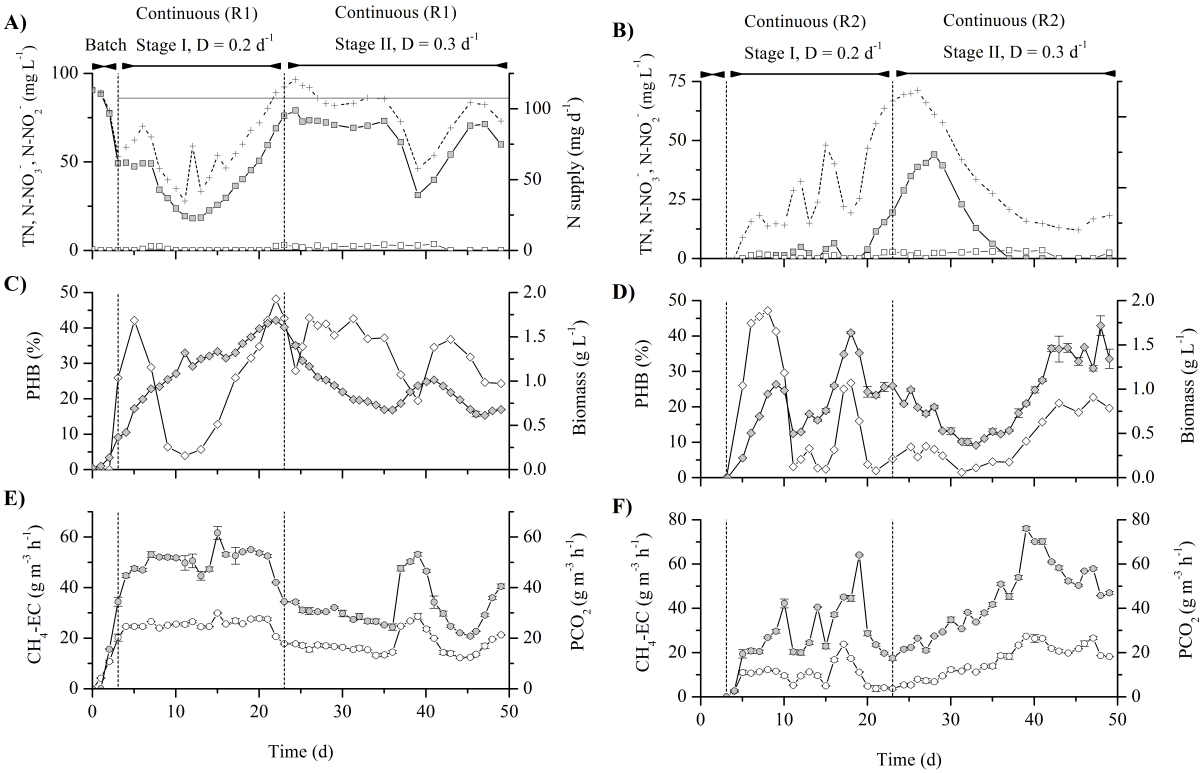

Fig. 6.3 *Time course of* ***(A, B)*** *total nitrogen (crosses), N-NO_3^- (solid squares) and N-NO_2^- (empty squares) concentrations, N supply (continuous line);* ***(C, D)*** *PHB content (empty diamonds) and biomass concentration (solid diamonds), and* ***(E, F)*** *CH_4-EC (empty circles) and PCO_2 (solid circles) in R1* ***(left)*** *and R2* ***(right)*** *during Test 2. Vertical dashed lines separate the different operational stages.*

6.4 Conclusions

This work constitutes the first attempt to continuously produce PHB from biogas using a two-stage growth-accumulation strategy. Continuous cultivation of *M. hirsuta* in the stirred tank reactor at 600 rpm and 32ºC likely mediated a physiological stress that induced PHB synthesis under nitrogen availability. Nonetheless, process operation at higher dilution rate supported a stable process performance at the expense of reduced methane elimination capacities (≈16 g CH_4 m^{-3} h^{-1}) and PHB productivities of ≈53 g PHB m^{-3} d^{-1}. The tests performed clearly demonstrated the high capacity of *M. hirsuta* CSC1 to accumulate PHB (up to 48% w/w) using biogas as carbon and energy source. However, further investigations are required to improve process robustness under continuous operation.

Acknowledgements

This research was funded by the Spanish Ministry of Science and Innovation under BES-2016-077160 contract and CTM2015-70442-R project. The support from the EU-FEDER programme and the regional government of Castilla y León (UIC 315, CLU 2017-09) is acknowledged. Authors would like to thank J. Prieto and E. Marcos for their practical support during PHA extraction and GC-MS analyses, respectively.

References

Blunt, W., Levin, D.B. and Cicek, N. (2018) Bioreactor Operating Strategies for Improved Polyhydroxyalkanoate (PHA) Productivity. *Polymers* **10**(11). doi: 10.3390/polym10111197.

Bordel, S., Rodríguez, E. and Muñoz, R. (2019a) Genome sequence of *Methylocystis hirsuta* CSC1, a polyhydroxyalkanoate producing methanotroph. *MicrobiologyOpen* **8**(6), e00771. doi:10.1002/mbo3.771.

Bordel, S., Rodriguez, Y., Hakobyan, A., Rodriguez, E., Lebrero, R. and Munoz, R. (2019b) Genome scale metabolic modeling reveals the metabolic potential of three type II methanotrophs of the genus *Methylocystis. Metab Eng* **54**, 191-199. doi:10.1016/j.ymben.2019.04.001.

Cantera, S., Estrada, J.M., Lebrero, R., García-Encina, P.A. and Muñoz, R. (2016) Comparative performance evaluation of conventional and two-phase hydrophobic stirred tank reactors for methane abatement: Mass transfer and biological considerations. *Biotechnol Bioeng* **113**(6), 1203-1212. doi: 10.1002/bit.25897.

Chen, X., Rodríguez, Y., López, J.C., Muñoz, R., Ni, B.-J. and Sin, G. (2020) Modeling of Polyhydroxyalkanoate Synthesis from Biogas by *Methylocystis hirsuta*. *ACS Sustain Chem Eng* **8**(9), 3906-3912. doi:10.1021/acssuschemeng.9b07414.

Doi, Y. (1990) Microbial polyesters. VCH, New York. ISBN: 0895737469

Estrada, J.M., Lebrero, R., Quijano, G., Pérez, R., Figueroa-González, I., García-Encina, P.A. and Muñoz, R. (2014) Methane abatement in a gas-recycling biotrickling filter: Evaluating innovative operational strategies to overcome mass transfer limitations. *Chemical Engineering Journal* **253**, 385-393. doi: 10.1016/j.cej.2014.05.053.

EUBP (2020) Bioplastics market data, European Bioplastics.https://www.european-bioplastics.org/market/ (Accessed: 05.09.2021).

Fei, Q. (2015) Benefits and hurdles for biological methane upgrading. Sustainable Chemicals & Plastics Adoptions & Applications Summit, San Diego, California. https://www.nrel.gov/docs/fy15osti/64878.pdf (Accessed: 15.11.2011)

Ford, H.V., Jones, N.H., Davies, A.J., Godley, B.J., Jambeck, J.R., Napper, I.E., Suckling, C.C., Williams, G.J., Woodall, L.C. and Koldewey, H.J. (2022) The fundamental links between climate change and marine plastic pollution. *Sci Total Environ* **806**, 150392. doi: 10.1016/j.scitotenv.2021.150392.

Fraunhofer (2021) Levelized Cost of Electricity Renewable Energy Technologies. FRAUNHOFER Institute for Solar Energy Systems ISE. https://www.ise.fraunhofer.de/en/publications/studies/cost-of-electricity.html (Accessed: 15.11.2021)

Geyer, R., Jambeck Jenna, R. and Law Kara, L. (2017) Production, use, and fate of all plastics ever made. *Sci Adv* **3**(7). doi:10.1126/sciadv.1700782.

Hanson, R.S. and Hanson, T.E. (1996) Methanotrophic bacteria. *Microbiol rev* **60**(2), 439-471.

IRENA (2021) RENEWABLE POWER GENERATION COSTS IN 2020, International Renewable Energy Agency.https://www.irena.org/publications/2021/Jun/Renewable-Power-Costs-in-2020 (Accessed: 20.11.2021).

Jawaharraj, K., Shrestha, N., Chilkoor, G., Dhiman, S.S., Islam, J. and Gadhamshetty, V. (2020) Valorization of methane from environmental engineering applications: A critical review. *Water Res* **187**, 116400. doi: 10.1016/j.watres.2020.116400.

Jiang, G., Hill, D.J., Kowalczuk, M., Johnston, B., Adamus, G., Irorere, V. and Radecka, I. (2016) Carbon Sources for Polyhydroxyalkanoates and an Integrated Biorefinery. *Int J Mol Sci* **17**(7). doi:10.3390/ijms17071157.

Kalyuzhnaya, M.G., Gomez, O.A. and Murrell, J.C. (2019) The Methane-Oxidizing Bacteria (Methanotrophs). In: McGenity, T.J. (ed) Taxonomy, Genomics and Ecophysiology of Hydrocarbon-Degrading Microbes. Springer International Publishing, Cham. doi:10.1007/978-3-319-60053-6_10-1.

Kapoor, R., Ghosh, P., Tyagi, B., Vijay, V.K., Vijay, V., Thakur, I.S., Kamyab, H., Nguyen, D.D. and Kumar, A. (2020) Advances in biogas valorization and utilization systems: A comprehensive review. *J Clean Prod* **273**, 123052. doi: 10.1016/j.jclepro.2020.123052.

Koller, M. (2018) A Review on Established and Emerging Fermentation Schemes for Microbial Production of Polyhydroxyalkanoate (PHA) Biopolyesters. Fermentation **4**(2), 30. doi: 10.3390/fermentation4020030.

Koller, M., Atlić, A., Dias, M., Reiterer, A. and Braunegg, G. (2010) Microbial PHA Production from Waste Raw Materials. In Chen, G.G.-Q. (ed) Plastics from Bacteria: Natural Functions and Applications. Springer Berlin Heidelberg, Berlin, 85-119. doi:10.1007/978-3-642-03287-5_5.

Kourmentza, C., Plácido, J., Venetsaneas, N., Burniol-Figols, A., Varrone, C., Gavala, H.N., Reis, M.A.M. (2017) Recent Advances and Challenges towards Sustainable Polyhydroxyalkanoate (PHA) Production. *Bioengineering* **4**(2), 55. doi:10.3390/bioengineering4020055.

Li, Z., Yang, J. and Loh, X.J. (2016) Polyhydroxyalkanoates: opening doors for a sustainable future. *NPG Asia Mater* **8**(4), e265. doi:10.1038/am.2016.48.

López, J.C., Arnáiz, E., Merchán, L., Lebrero, R. and Muñoz, R. (2018) Biogas-based polyhydroxyalkanoates production by *Methylocystis hirsuta*: A step further in anaerobic digestion biorefineries. *Chem Eng J* **333**, 529-536. doi:https://doi.org/10.1016/j.cej.2017.09.185.

Meereboer, K.W., Misra, M. and Mohanty, A.K. (2020) Review of recent advances in the biodegradability of polyhydroxyalkanoate (PHA) bioplastics and their composites. *Green Chem* **22**(17), 5519-5558. doi: 10.1039/d0gc01647k.

Pieja, A.J., Morse, M.C. and Cal, A.J. (2017) Methane to bioproducts: the future of the bioeconomy? *Curr Opin Chem Biol* **41**, 123-131. doi: 10.1016/j.cbpa.2017.10.024

Rahnama, F., Vasheghani-Farahani, E., Yazdian, F. and Shojaosadati, S.A. (2012) PHB production by *Methylocystis hirsuta* from natural gas in a bubble column and a vertical loop bioreactor. *Biochem Eng J* **65**, 51-56. doi: 10.1016/j.bej.2012.03.014.

Ravenstijn, J. (2021) Fast growing PHA demand and new capacities, but what about legislation? pp. 1-33.

Riedel, S.L. and Brigham, C.J. (2020) Inexpensive and Waste Raw Materials for PHA production. In Koller, M. (ed) The Handbook of Polyhydroxyalkanoates: Microbial Biosynthesis and Feedstocks (1st ed.). Vol 1, 1st edn. CRC Press. doi: 10.1201/9780429296611.

Riedel, S.L., Jahns, S., Koenig, S., Bock, M.C., Brigham, C.J., Bader, J. and Stahl, U. (2015) Polyhydroxyalkanoates production with *Ralstonia eutropha* from low quality waste animal fats. *J Biotechnol* **214**, 119-127. doi:10.1016/j.jbiotec.2015.09.002.

Rodríguez, Y., Firmino, P.I.M., Arnaiz, E., Lebrero, R. and Munoz, R. (2020a) Elucidating the influence of environmental factors on biogas-based polyhydroxybutyrate production by *Methylocystis hirsuta* CSC1. *Sci Total Environ* 706, 135136. doi:10.1016/j.scitotenv.2019.135136.

Rodríguez, Y., Firmino, P.I.M., Pérez, V., Lebrero, R. and Muñoz, R. (2020b) Biogas valorization via continuous polyhydroxybutyrate production by *Methylocystis hirsuta* in a bubble column bioreactor. *Waste Manag* **113**, 395-403. doi: 10.1016/j.wasman.2020.06.009.

Steinbüchel, A. and Valentin, H.E. (1995) Diversity of bacterial polyhydroxyalkanoic acids. *FEMS Microbiol Lett* **128**(3), 219-228. doi: 10.1016/0378-1097(95)00125-O.

Strong, J.P., Laycock, B., Mahamud, N.S., Jensen, D.P., Lant, A.P., Tyson, G. and Pratt, S. (2016) The Opportunity for High-Performance Biomaterials from Methane. *Microorganisms* **4**(1). doi:10.3390/microorganisms4010011.

UNEP (2021) Drowning in Plastics - Marine Litter and Plastic Waste Vital Graphs, United Nations Environment Programme (UNEP) https://www.unep.org/resources/report/drowning-plastics-marine-litter-and-plastic-waste-vital-graphics (Accessed: 14.11.2021).

Urtuvia, V., Villegas, P., González, M. and Seeger, M. (2014) Bacterial production of the biodegradable plastics polyhydroxyalkanoates. *Int J Biol Macromol* **70**, 208-213. doi: 10.1016/j.ijbiomac.2014.06.001.

Vandi, L.-J., Chan, C.M., Werker, A., Richardson, D., Laycock, B. and Pratt, S. (2018) Wood-PHA Composites: Mapping Opportunities. Polymers **10**(7). doi:10.3390/polym10070751.

WBA (2019) Global Potential of Biogas, World Biogas Association.https://www.worldbiogasassociation.org/wp-content/uploads/2019/09/WBA-execsummary-4ppa4_digital-Sept-2019.pdf (Accessed: 07.10.2021).

Yoon, J. and Oh, M.-K. (2021) Strategies for Biosynthesis of C1 Gas-derived Polyhydroxyalkanoates: A review. *Bioresour Technol*, **344**, 126307. doi: 10.1016/j.biortech.2021.126307.

Appendix C. Supplementary Material

Continuous polyhydroxybutyrate production from biogas in an innovative two-staged bioreactor configuration

Yadira Rodríguez[a,b], Silvia García[a,b], Raquel Lebrero[a,b], Raúl Muñoz[a,b,*]

[a] Department of Chemical Engineering and Environmental Technology, School of Industrial Engineering, University of Valladolid, Dr. Mergelina, s/n, 47011 Valladolid, Spain

[b] Institute of Sustainable Processes, Dr. Mergelina, s/n, 47011 Valladolid, Spain.

* Corresponding author: mutora@iq.uva.es

Results and discussion

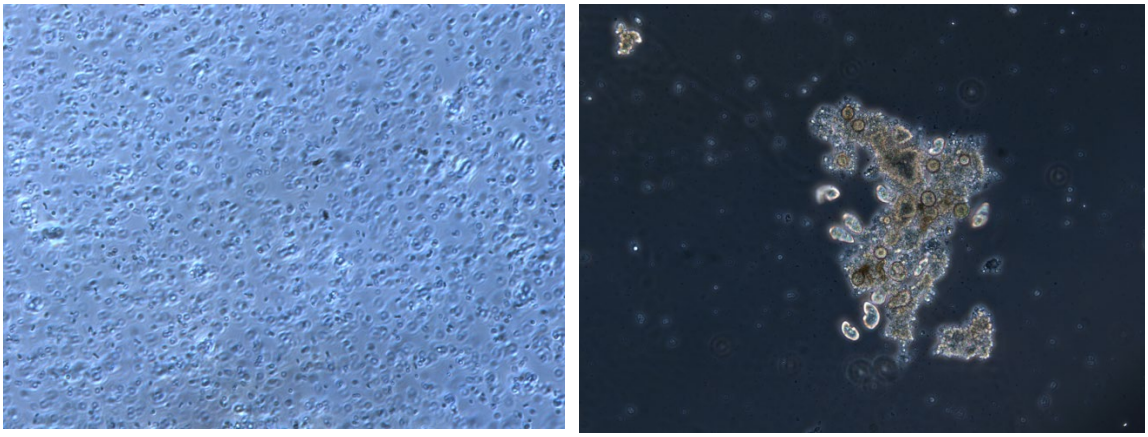

(a) (b)

Fig. S6.1. *Microscopic images of the culture broth in a) R1 at 20× magnification and b) R2 at 10× magnification at day 40 in Test 2 (Leica DM4000B microscope equipped with a Leica DFC300FX)*

7.

Optimization of nitrogen feeding strategies for improving polyhydroxybutyrate production from biogas by *Methylocystis parvus* in a stirred tank reactor

The content of this chapter has been submitted for publication in *Chemosphere*:

Rodríguez, Y., García, S., Pérez, R., Lebrero, R., Muñoz, R. Optimization of nitrogen feeding strategies for improving polyhydroxyalkanoate production from biogas by *Methylocystis parvus* in a stirred tank reactor.

Optimization of nitrogen feeding strategies for improving polyhydroxybutyrate production from biogas by *Methylocystis parvus* OBBP in a stirred tank reactor

Yadira Rodríguez[a,b], Silvia García[a,b], Rebeca Pérez[a,b], Raquel Lebrero[a,b], Raúl Muñoz[a,b,*]

[a] Department of Chemical Engineering and Environmental Technology, School of Industrial Engineering, University of Valladolid, Dr. Mergelina, s/n, 47011 Valladolid, Spain

[b] Institute of Sustainable Processes, Dr. Mergelina, s/n, 47011 Valladolid, Spain.

* Corresponding author: mutora@iq.uva.es

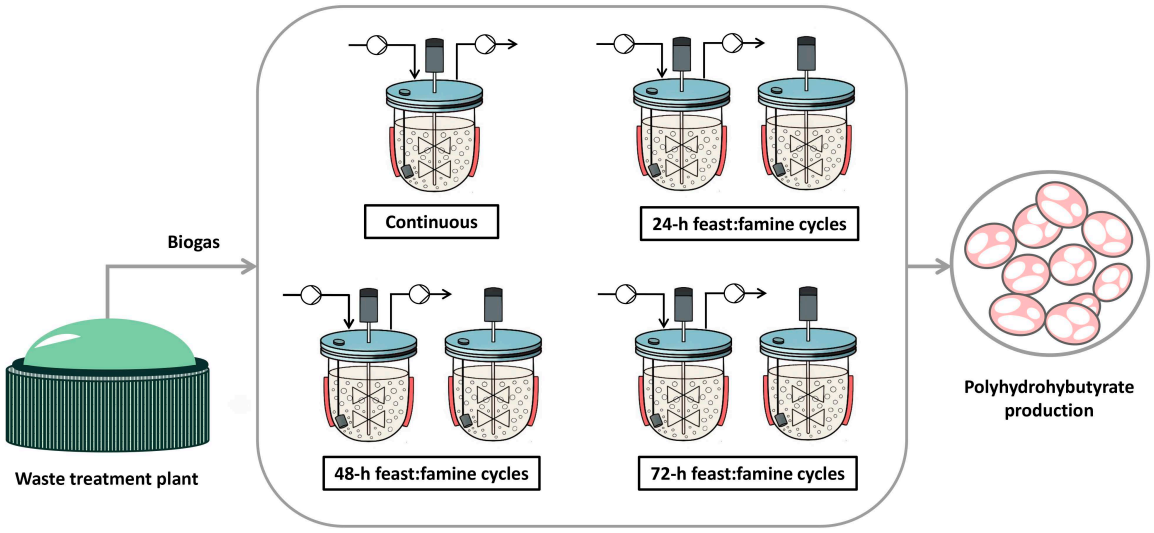

Graphical abstract

Abstract

Designing efficient cultivation strategies could boost bioplastics production from a renewable source like biogas. In this work, biogas-based polyhydroxybutyrate (PHB) production and CH_4 biodegradation performance was investigated in a stirred tank bioreactor inoculated with *Methylocystis parvus* OBBP. Decreasing nitrogen loading rates in continuous mode and alternating feast:famine regimes of 24h-cycles (75, 54, 41 and 27 mg d^{-1}, corresponding to 110%, 80%, 60% and 40% of the stoichiometric nitrogen requirements, respectively), and alternating feast:famine regimes of 24h:24h and 24h:48h were tested. Continuous N feeding did not support an effective PHB production despite the occurrence of nitrogen limiting conditions. Feast-famine cycles of 24h:24h (with 50% stoichiometric nitrogen supply) supported the maximum PHB production (20 g-PHB m^{-3} d^{-1}) without compromising the CH_4-elimination capacity (25 g m^{-3} h^{-1}) of the system. Feast:famine duration ratios ≤ 1:2 entailed the deterioration of process performance at stoichiometric nitrogen inputs ≤ 60%.

Keywords: Bioplastics; Biorefinery concept; Feeding regime; Methane oxidation; Methanotrophic bacteria; Polyhydroxyalkanoate production

7.1 Introduction

Nowadays, plastic pollution has become one of the major global environmental challenges (Heidbreder et al., 2019). The steady increase in plastic demand, which ramped up to 50.7 Mton by 2019 in Europe, and the global environmental problems derived from the lax plastic management policies in some countries, require an urgent reduction of our overdependence on petroleum-based plastics (Lebreton & Andrady, 2019; PlasticsEurope, 2020). Naturally synthetized polyesters constitute promising substitutes to conventional plastics (Sagong et al., 2018). These biodegradable and biocompatible thermoplastics, such as poly(3-hydroxybutyrate) (P3HB) homopolymer and its copolymer poly(3-hydroxybutyrate-co-3-hydroxyvalerate (P(3HB-*co*-3HV)), are biopolyesters that can be tuned targeting a broad range of applications (Myung et al., 2017; Steinbüchel & Valentin, 1995). Today, the commercial production of polyhydroxyalkanoates (PHAs) is hampered by the high cost of sugar-based feedstocks, which accounts for up to ≈50% of the overall production costs (Riedel et al., 2015; Van Wegen et al., 1998). In 2020, the PHA global production represented only 1.7% (+ 0.3% than 2018) of the bioplastics market (2.1 million tonnes) (EuropeanBioplastics & novaInstitute, 2020). With PHB selling prices ranging from 5 to 6 € kg^{-1}, PHAs cannot yet compete with their petroleum-based counterparts (1.0 and 1.5 € kg^{-1} for polypropylene and polyethylene, respectively) (Khatami et al., 2021; van den Oever et al., 2017; Vandi et al., 2018).

Thus, significant efforts are being directed to find cost-effective carbon sources for PHA production (whey, molasses, crude glycerol, fatty acids, etc.) (Riedel & Brigham, 2020). Beyond its use as a renewable gas fuel, biogas has recently attracted much attention as a low-cost carbon source for the manufacturing of PHA and other value-added products based on its high content of CH_4 (50-70%) (Cantera et al., 2019; López et al., 2018; Mühlemeier et al., 2018; Muñoz et al., 2015). A recent geographical analysis demonstrated that integrating PHB production with heat and power cogeneration from biogas results in a cost-competitive production of PHA (with selling prices as low as 1.5 € kg^{-1}). Additionally,

when biogas is entirely devoted to PHA production, production costs are viable (4.1 € kg^{-1}) in countries with more affordable energy prices (Pérez et al., 2020). Hence, integrated biorefineries involving alternative uses of biogas can potentially contribute to rise the biogas sector from the standstill experienced during the last three years (EBA, 2020).

PHA biosynthesis using biogas is based on the ability of type-II aerobic methane oxidizing bacteria, namely methanotrophs, to form biopolymer inclusions under growth-essential nutrient deprivation (e.g. nitrogen or phosphorous) and methane availability (Asenjo & Suk, 1986; Hanson & Hanson, 1996). Among methanotrophs, the strain *Methylocystis parvus* OBBP is regarded as a highly PHB-productive microorganism (Bordel et al., 2019b; Jiang et al., 2016; Sundstrom & Criddle, 2015). This strain was first isolated in 1970 by Whittenbury et al. (1970). Despite lacking soluble methane monoxygenase activity, *M. parvus* is a representative of type-II methanotrophs, with capability to fix nitrogen and to assimilate carbon through the serine pathway (del Cerro et al., 2012; Vecherskaya et al., 2009). There is a strong consensus in literature about the high PHB accumulation capacity of this strain, which can achieve PHB contents of up to 49.4% following culture media optimization (Sundstrom & Criddle, 2015) or up to 46% and 50% after ammonium and nitrate limitation, respectively (Pieja et al., 2011; Rostkowski et al., 2013). In the presence of the limiting growth factor in the culture broth, the accumulated PHB provides *M. parvus* a competitive advantage for rapid growth, with a specific growth rate of 0.154 h^{-1} (1.4 times higher than the specific growth rate on methane) (Bordel et al., 2019b; Pieja et al., 2011).

Continuous suspended-growth chemostat processes in fermenters are regarded as the optimum platform for PHA production from biogas since they enable the control of environmental conditions and nutrient feed, process operation under sterile conditions and an effective CH_4 mass transfer and biomass harvesting (AlSayed et al., 2018; Koller & Muhr, 2014; López et al., 2019). However, prior large scale implementation, methanotrophic growth under nutrient balanced conditions and PHA biosynthesis under

unbalanced conditions need to be optimized by adapting process design to the physiological characteristics of the biological system (Kaur & Roy, 2015; Koller, 2018).

This work reports for the first time a comparative analysis of different nitrogen supply strategies implemented to optimize PHB production coupled with continuous biogas utilization in a stirred tank bioreactor using the strain *Methylocystis parvus* OBBP. More specifically, the influence of (i) decreasing nitrogen loading rate (110%, 80%, 60% and 40% of the stoichiometric nitrogen requirements) under continuous mode and alternating feast:famine periods under discontinuous mode (24-h cycles), and (ii) 24h:24h and 24h:48h feast:famine cycles supplementing the stoichiometric nitrogen requirements, on PHB productivity and CH_4 biodegradation was systematically assessed.

7.2 Materials and methods

7.2.1 Culture media and chemicals

Mineral salt medium containing nitrogen in the form of potassium nitrate (hereinafter referred to as NMS), or alternatively nitrogen free mineral salt medium (NFMS), were used. Nitrogen concentration was modified depending on the nitrogen supplementation strategy of each test series. Unless otherwise stated, the NMS (pH 6.8) contained (per liter of distilled water): KNO_3, 1 g; $MgSO_4 \cdot 7H_2O$, 1.1 g; $CaCl_2 \cdot 2H_2O$, 0.2 g; $CuSO_4 \cdot 5H_2O$, 1 mg; $FeSO_4 \cdot 7H_2O$, 0.5 mg; $ZnSO_4 \cdot 7H_2O$, 0.4 mg; $Na_2MoO_4 \cdot 2H_2O$, 0.4 mg; Fe-EDTA, 0.38 mg; $Na_2EDTA \cdot 2H_2O$, 0.3 mg; $CoCl_2$, 0.03 mg; $MnCl_2 \cdot 4H_2O$, 0.02 mg; H_3BO_3, 0.015 mg and $NiCl_2 \cdot 6H_2O$, 0.01 mg. A phosphate buffer solution containing 72 g L^{-1} $Na_2HPO_4 \cdot 12H_2O$ and 26 g L^{-1} KH_2PO_4 was added to the corresponding mineral salt medium (10 mL per liter) following autoclave sterilization at 121ºC for 21 min and subsequent cooling.

All chemicals above mentioned and reagents/solvents for PHB analysis (chloroform ≥ 99%, 1-propanol 99.7%, hydrochloric acid 37% w/v and benzoic acid ≥ 99.5% as internal

standard) were purchased from PanReac AppliChem (Spain) unless otherwise specified. Potassium nitrate was obtained from COFARCAS (Spain). Poly(3-hydroxybutyrate-co-3-hydroxyvalerate) (PHBV) with a 3HB fraction of 88% was provided by Sigma-Aldrich (USA). Synthetic biogas (70/30% v/v CH_4:CO_2), oxygen (≥ 99.5%) and methane (≥ 99.995%) were supplied by Abelló Linde S.A. (Spain).

7.2.2 Bacterial strain and inocula preparation

Cryopreserved cells of *Methylocystis parvus* OBBP in glycerol at -80ºC were kindly supplied by Biopolis S.L. (Valencia, Spain). The bacterium was first cultivated in NMS in an oxygen and methane atmosphere for a period of two weeks followed by pre-inoculum preparation. The pre-inoculum was prepared by transferring 5 mL of *M. parvus* culture into NMS (50 mL) contained in 125 mL serum bottles closed with butyl rubber stoppers and aluminum caps. The headspace of the serum bottles was supplied with an oxygen and methane gas mixture at a 2:1 molar ratio, which was restored on a daily basis to support methanotrophic growth by gassing pure oxygen for 5 min and replacing 25 mL with pure methane. Pre-inoculum cultures were grown at 25ºC and 250 rpm in a rotary shaker (Thermo Fisher Scientific Inc., USA) for a week. Then, five sterile gas-tight bottles (2.2 L) containing 386 mL of NMS were supplemented with 4 mL of the buffer solution and inoculated with 10 mL of *M. parvus* pre-inoculum. Chlorobutyl septa and aluminium screw caps were used to maintain gas-tightness in the 2.2 L bottles. A 100 L Tedlar® bag (Sigma-Aldrich, USA) with an O_2:CH_4 composition of 66.7:33.3% (v/v) was used to provide the desired headspace atmosphere by flushing the gas mixture with a compressor for nearly 3 min. The bottles were incubated under controlled temperature and mixing conditions (25ºC, 300 rpm) on a Variomag Multipoint 6 magnetic stirrer (Thermo Scientific, USA) for ≈10 days. The headspace of the bottles was replaced with the above described gas mixture three days prior cells harvesting, which was carried out by centrifugation (10000 rpm, 8 min) in sterile centrifuge tubes. Biomass pellets were re-suspended either into fresh NMS or NFMS (depending on the nitrogen feeding strategy) and concentrated to deliver a

250 mL-inoculum with a total solids concentration ranging from 5.4 to 6.1 g L^{-1}. All these procedures were carried out under sterile conditions.

7.2.3 Bioreactor set-up

All experiments were performed in a bench-top borosilicate glass Biostat®A bioreactor (Sartorius Stedim Biotech GmbH, Germany) with a working volume of 2.5 L (**Fig. 7.1**). The bioreactor enabled process control and real-time monitoring of pH, temperature and dilution rate. For that purpose, the vessel was fitted with a temperature sensor and digital pH and level probes. The bioreactor was constructed with a 2 μm-pore stainless steel gas diffuser (Supelco, USA), which was placed at the bottom of the vessel to sparge the air:biogas mixture at 42 mL min^{-1} (corresponding to 60 min of gas residence time). The gas composition resulting from the mixture of synthetic biogas and pressurized air was adjusted to a O_2:CH_4 concentration of 16%:8% *v/v* by using a mass flow controller (GFC17, Aalborg^{TM}, USA) and a rotameter for the biogas and air streams, respectively. Continuous stirring at 600 rpm was provided with a six-blade Rusthon turbine to ensure enough turbulence without cell damage, whereas a heating blanket was used to maintain the operating temperature at 30ºC. The pH of the culture broth was maintained at 7.0 by addition of 4N NaOH.

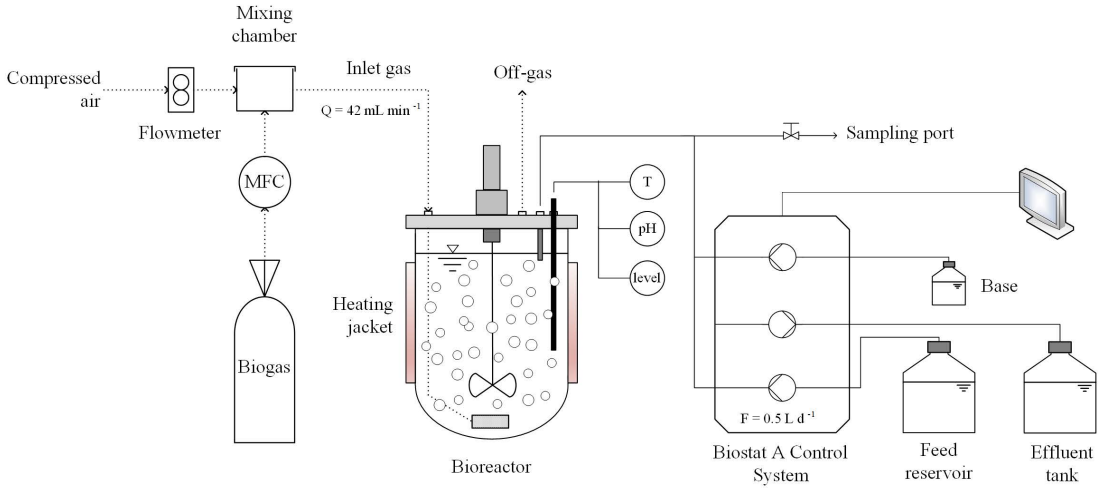

Fig. 7.1 *Schematic representation of the experimental set-up*

7.2.4 Experimental procedure

7.2.4.1 *Test series 1 - CH_4 biodegradation and PHB production under continuous nitrogen feeding.*

This test series assessed PHB accumulation under continuous NMS supply at decreasing nitrogen loading rates (NLR) below stoichiometric nitrogen requirements. The chemostat was initially inoculated with 50 mL of *M. parvus* pre-inoculum resulting in a biomass concentration of 20 mg L^{-1} and operated under batch mode with an initial concentration of 276 mg $N\text{-}NO_3^-$ L^{-1} in NMS until nitrogen depletion by day 9. Then, the bioreactor was operated for 90 days at a continuous dilution rate of 0.008 h^{-1} (below the critical dilution rate, D_{crit} = 0.017 h^{-1}) under decreasing NLR in four different stages. NLRs of 75, 54, 41 and 27 mg d^{-1} were set during stages I, II, III and IV, respectively, which corresponded to 110%, 80%, 60% and 40% of the stoichiometric nitrogen requirements based on *M. parvus* composition and yield, and the previously determined CH_4 mass transfer capacity of the bioreactor a 600 rpm. On average, each stage was run for 25 days (five times the hydraulic retention time), except for stage I that lasted 10 days.

7.2.4.2 *Test series 2 - CH_4 biodegradation and PHB production under different feast-famine regimes (24h cycles, discontinuous feeding)*

Following autoclave sterilization of the bioreactor, *M. parvus* was inoculated at an initial biomass concentration of 540 mg L^{-1}. The bioreactor was initially operated under batch cultivation and nitrogen deprived conditions for 72 h in order to initiate PHB synthesis. Then, the culture was subjected to a cyclic nitrogen feast-famine regime at varying feeding profiles. The operation was conducted in four different stages of seven feast-famine 24 h cycles. To this end, NMS containing a $N\text{-}NO_3^-$ concentration of 331 mg L^{-1} was supplied at feeding rates of 0.5 and 0 L d^{-1} corresponding to the growth and PHB accumulation phases, respectively. NMS feeding periods of 11, 8, 6 and 4 h were set in

stages I, II, III and IV, respectively, which corresponded to the same NLRs set in Test series 1 (75, 54, 41 and 27 mg $N\text{-}NO_3^-$ per cycle) (**Table 7.1**).

7.2.4.3 *Test series 3 - CH_4 biodegradation and PHB production under a 24h-24h feast-famine regime.*

The bioreactor was inoculated at an initial biomass concentration of 560 mg L^{-1} and operated under nitrogen limiting conditions in batch mode for 72 h. Batch cultivation was followed by 12 sequential feast-famine cycles consisting of continuous NMS feeding at 0.5 L d^{-1} for 24 h followed by 24 h of discontinuous operation under nitrogen deprived conditions. The nitrogen load of each cycle was 68 mg $N\text{-}NO_3^-$, which corresponded to the stoichiometric N requirements. The bioreactor was operated for 24 days under feast and famine conditions (**Table 7.1**).

7.2.4.4 *Test series 4 - CH_4 biodegradation and PHB production under a 24h-48h feast-famine regime.*

M. parvus was inoculated at an initial biomass concentration of 610 mg L^{-1}. Then, the bioreactor was batchwise operated under nitrogen limiting conditions for 72 h as described in Test series 2 and 3. Sequential feast-famine cycles of 24h-48h were implemented for 21 days (comprising a total of 7 cycles) via continuous NMS feeding at a flowrate of 0.5 L d^{-1} for 24 h followed by 48 h of batch incubation without mineral medium supply. The nitrogen load per cycle was set at 68 mg $N\text{-}NO_3^-$ per cycle.

Process monitoring was conducted at the end of both the growth and accumulation phases in Tests series 2, 3 and 4, or periodically (every 2-3 days) during continuous operation in Test series 1. Gas samples were withdrawn in duplicate with a 100 μL Hamilton gas-tight syringe from the inlet and outlet gas sampling points to monitor the concentration of CH_4, O_2 and CO_2. The outlet gas flowrate and the pressure drop caused by the gas diffuser were also measured. Aliquots of 40 mL of the culture broth were withdrawn from the bioreactor for the determination of the optical density (OD), total suspended solids

Table 7.1 *Detailed operating conditions for the different continuous and cyclic feeding strategies tested*

Test	Stage	Period (days)	Operation Mode	Feast-famine cycles (h:h)	N- NO_3^- Feed Concentration (mg L^{-1})	N- NO_3^- Loading Rate (mg $cycle^{-1}$) (mg d^{-1})*	N- NO_3^- Supply (%)
1	I	10	Continuous	-	150	75*	110
	II	25	Continuous	-	108	54*	80
	III	25	Continuous	-	82	41*	60
	IV	25	Continuous	-	54	27*	40
2	I	7	Cyclic	11:13	328	75	110
	II	7	Cyclic	8:16	328	54	80
	III	7	Cyclic	6:18	328	41	60
	IV	7	Cyclic	4:20	328	27	40
3	I	24	Cyclic	24:24	135	68	50
4	I	20	Cyclic	24:48	135	68	33

(TSS) concentration and pH. Culture broth (1.5 mL in duplicate) was centrifuged at 10000 rpm for 10 min and stored at -20ºC after supernatant decanting for PHB analysis. Filtrate collected from TSS determination was used for the analysis of the total dissolved nitrogen (TN), total organic carbon (TOC), NO_2^- and NO_3^- concentrations.

7.2.5 Analytical procedures

Microbial PHB was quantified in an Agilent 7820A gas chromatograph (GC) coupled to an Agilent 5977E mass spectrometer (MS) (Agilent Technologies, USA) following hydrochloric acid propanolysis (Rodríguez et al., 2020a). Gas chromatographic conditions are detailed elsewhere (Chen et al., 2020). Biomass concentration was determined as grams of TSS per liter of cell culture according to Standard Methods (2540 Solids, APHA 2018) using Merck MF Millipore (0.45 μm pore size) membrane filters (Merck, Germany). A SPECTROstar Nano (BMG LABTECH, Germany) spectrophotometer was used to monitor bacterial growth at 600 nm. pH measurements were carried out with a Basic 20 pH meter (Crison, Spain). The quantification of nitrite and nitrate concentrations was performed by ion-exchange liquid chromatography (IC) with conductivity detection (Waters 432, Waters Corporation, USA). TOC and TN measurements in filtered samples were performed simultaneously in a TOC-$L_{CSH/CSN}$ analyser coupled with a TNM-1 unit (Shimadzu, Japan). The inlet and outlet gas composition (CH_4, CO_2 and O_2) was analyzed in a Bruker 430 gas chromatograph (GC) coupled with a thermal conductivity detector (TCD) (Bruker Corporation, USA). The GC-TCD was equipped with CP-Molsieve 5A and CP-PoraBOND Q columns. Pressure drops were recorded using a PN7097 electronic pressure sensor (Ifm Electronic, Germany). Finally, the outlet gas flowrate was determined using the water displacement method.

7.2.6 Data treatment

The methane elimination capacity (CH_4-EC), the methane removal efficiency (CH_4-RE) and the volumetric production of CO_2 (PCO_2) were used as the main performance indicators of the bioreactor and calculated as described elsewhere (Rodríguez et al., 2020b). All results are presented as average values with standard deviations of duplicates analyses, except for TN and anions. Statistical analysis was performed using one-way ANOVA with a significance $P \leq 0.05$. Software OriginPro 8.5.0 SR1 (OriginLab Corp.) was used for data treatment and graphics preparation.

7.3 Results

7.3.1 Test series 1 – CH_4 biodegradation and PHB production under continuous nitrogen feeding.

Under batch cultivation, *M. parvus* supported a maximum N-NO_3^- consumption rate of 64.0 mg L^{-1} d^{-1} (R^2=0.997) (from day 5 to day 8) and a complete N-NO_3^- removal by day 9 (**Fig. 7.2a)**. During this initial stage, an almost negligible denitrification activity was observed, with N-NO_2^- concentrations ranging from 0.6 to 1.1 mg L^{-1}. From day 9 onwards, the bioreactor was operated under steady decreasing nitrogen loading rates. Neither the presence of nitrate nor nitrite in the culture broth was recorded regardless of the operating stages, whereas a residual total nitrogen content of 6.1 ± 1.7 mg L^{-1} was always observed. The pH of the cultivation broth remained constant at 7.05 ± 0.26 along the different stages. The maximum biomass concentration recorded at the end of the batch phase (1.43 ± 0.04 g L^{-1}, day 9) levelled off and remained at 1.35 ± 0.06 g L^{-1} in stage I (**Fig. 7.2b)**. The reduction of the nitrogen load from 75 to 54 mg d^{-1} (stage II) resulted in a sharp drop in the biomass concentration within the first seven days of stage II, which finally stabilized at 0.86 ± 0.04 g L^{-1}. In the following operating stages (stages III and IV), the biomass concentrations averaged 0.91 ± 0.07 g L^{-1} and 1.06 ± 0.13 g L^{-1}, respectively. On the other hand, process operation under nitrogen sufficient conditions in stage I resulted in

PHB contents of 1.0 ± 0.6%, while N feeding below the stoichiometric requirements resulted in PHB contents of 2.1 ± 2.2, 1.8 ± 1.3 and 2.2 ± 1.0% (corresponding to PHB productivities of 4, 3 and 5 g-PHB m^{-3} d^{-1}) in stages II, III and IV, respectively.

A maximum CH_4-EC of 47.9 ± 0.5 g m^{-3} h^{-1} was reached at the end of the initial batch period (day 7) followed by a decrease and stabilization at 26.4 ± 0.5 g m^{-3} h^{-1} (corresponding to a CH_4-RE of 47 ± 1%) when continuous operation was initiated (stage I) (**Fig. 7.2c)**. The EC remained similar in the subsequent operating stages, with CH_4-ECs of 25.5 ± 2.3, 25.2 ± 2.1 and 24.2 ± 2.9 g m^{-3} h^{-1} (corresponding to methane removal efficiencies of 43.5 ± 2.3, 43.2 ± 3.4 and 43.5 ± 4.2%) recorded in stages II, III and IV, respectively. Similarly, the bioreactor achieved a maximum PCO_2 of 110.8 ± 2.0 g m^{-3} h^{-1} by day 7 at the end of the exponential growth phase. Then, PCO_2 dropped sharply during the first two days stabilizing at 64.9 ± 7.2, 60.3 ± 7.0, 57.1 ± 5.8 and 61.7 ± 7.2 g m^{-3} h^{-1} in stages I, II, III and IV, respectively. Along with the reduction of the nitrogen load throughout the different stages, no statistically differences were observed in the methane mineralization ratio (PCO_2/CH_4-EC), which averaged 2.5 ± 0.2, 2.4 ± 0.4, 2.3 ± 0.2 and 2.6 ± 0.3 g CO_2 (g CH_4)$^{-1}$ during stages I, II, III and IV, respectively. Likewise, the consumed O_2 to CH_4 ratio remained constant at 1.58 ± 0.09 throughout the entire experiment.

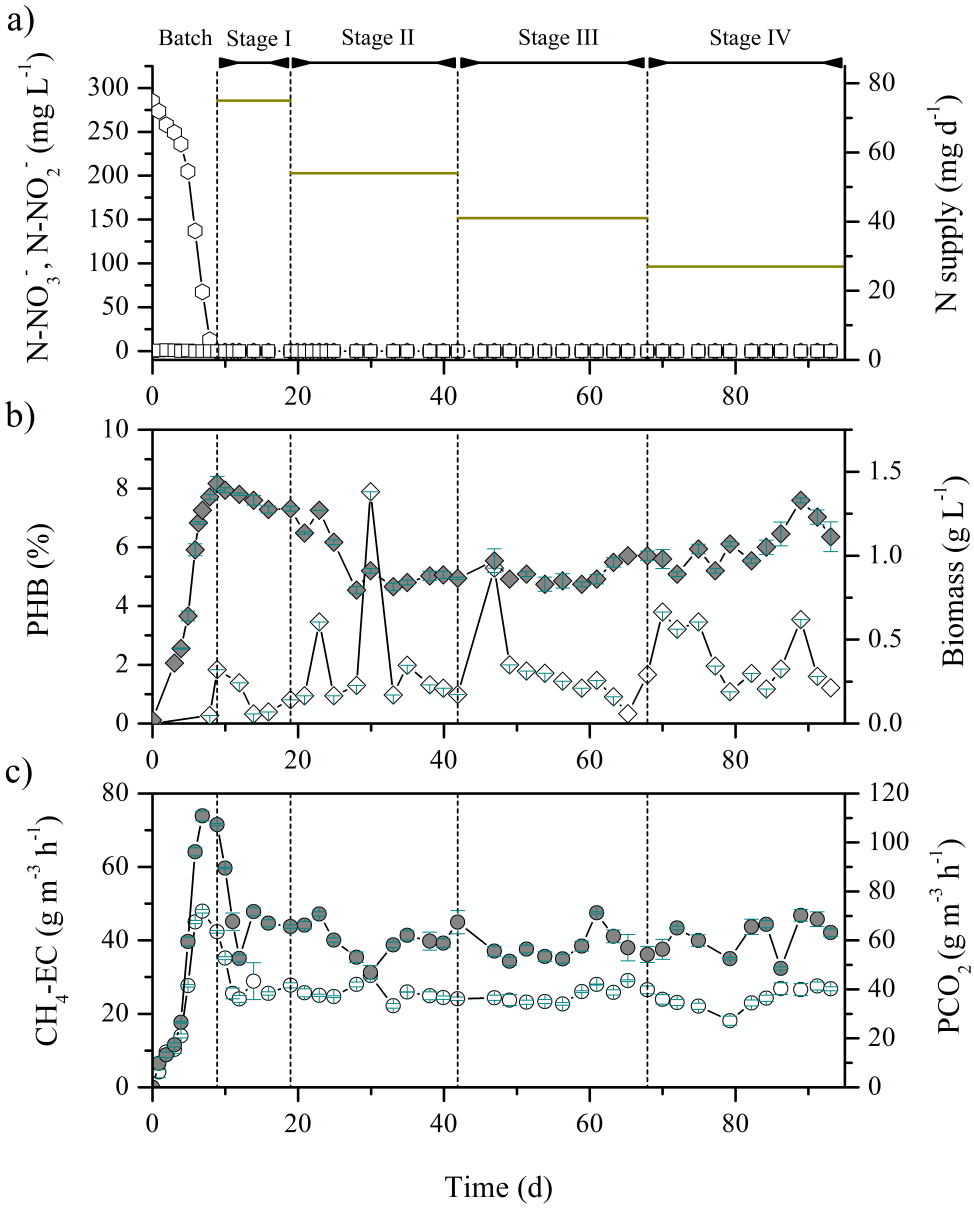

Fig. 7.2 *Time course of* ***(a)*** *NO3-N (hexagons) and NO2-N (squares), N supply (continuous line)* ***(b)*** *PHB content (empty diamonds) and biomass concentration (solid diamonds), and* ***(c)*** *CH4-EC (empty circles) and PCO2 (solid circles) in Test series 1. Vertical dashed lines separate the different operating stages.*

7.3.2 Test series 2 – CH_4 biodegradation and PHB production under different feast-famine regimes (24-h cycles, discontinuous feeding).

At the end of the feeding periods, $N\text{-}NO_3^-$ concentrations of 13.7 ± 1.8, 10.0 ± 1.9, 6.1 ± 1.5 and 7.9 ± 2.8 mg L^{-1} were observed in stages I, II, III and IV, respectively (**Fig. 7.3a**). By the end of the limitation periods, complete removal of $N\text{-}NO_3^-$ was achieved in stages I and II, with partial elimination (≈60%) in stage III. From cycle 18 (stage III) onwards, the $N\text{-}NO_3^-$ concentration in the cultivation broth at the end of the cycles gradually increased, reaching a concentration of 10.1 mg L^{-1} by the end of the experiment (stage IV). Low concentrations of $N\text{-}NO_2^-$ (≤4.5 mg L^{-1}) were observed throughout the test. However, from cycle 27 onwards (stage IV) $N\text{-}NO_2^-$ remained in the system with a concentration of 3.8 ± 0.5 mg L^{-1} (**Fig. 7.3a**). In addition, the presence of residual total nitrogen increased from 8.1 ± 6.0 (stage I) to 63.0 ± 12.8 mg L^{-1} (stage IV). Cultivation broth pH of 6.9 ± 0.1, 7.0 ± 0.1, 7.1 ± 0.0 and 7.2 ± 0.0 were recorded in stages I, II, III and IV, respectively. Following inoculation, biomass concentration steadily increased throughout the cycles until the end of stage II, where a maximum concentration of 2.38 ± 0.01 g L^{-1} was reached. Afterwards, biomass concentration levelled off at 2.19 ± 0.12 g L^{-1} during stage III, whereas cell concentration in stage IV dropped to values below 1.90 ± 0.04 g L^{-1} from cycle 25 onwards (**Fig. 7.3b**). Batch cultivation under N deprivation and presence of methane resulted in an initial PHB content of 7.1 ± 1.4% in stage I, which gradually decreased to 0.4 ± 0.0% by the end of stage I with the implementation of the cyclic operation. *M. parvus* exhibited a greater PHB accumulation during stage II, where PHB content varied from 1.9 ± 0.9% (cycle 8) to 7.5 ± 0.7% (cycle 14), corresponding to a volumetric PHB productivity of 12 g-PHB m^{-3} d^{-1} at the end of the stage. During these two first stages, both PHB consumption and accumulation phases in each cycle were clearly differentiated regarding PHB content, as shown in **Fig. 7.3b**. In stage III, the PHB content remained stable at 8.0 ± 1.0%, corresponding to a volumetric PHB productivity of 9 g-PHB m^{-3} d^{-1}. Finally, PHB content in cells during stage IV dropped below 4.5% from cycle 25 onwards.

Following batch cultivation (day 3), the system exhibited a CH_4-EC and a PCO_2 of 25.3 ± 1.1 and 70.8 ± 2.3 g m^{-3} h^{-1}, respectively **(Fig. 7.3c)**. Subsequently, CH_4-EC averaged 25.3 ± 1.4 g m^{-3} h^{-1} (corresponding to removal efficiencies of 42.9 ± 2.1%) in stages I and II, and during the first four cycles of stage III (cycles 15-18). From cycle 19 (stage III) to cycle 25 (stage IV), a sharp decrease in CH_4-EC was observed, which eventually stabilized at 8.8 ± 1.4 g m^{-3} h^{-1}. Similarly, PCO_2 did not vary significantly among stages I, II and III with values of 59.4 ± 5, 65.4 ± 4.6 and 61.9 ± 13.2 g m^{-3} h^{-1}, respectively, while a gradual decrease to stable values of 24.7 ± 3.4 g m^{-3} h^{-1} was recorded in stage IV. The reduction in the nitrogen loading rates induced a slight increase in PCO_2/CH_4-EC from 2.4 ± 0.2 g CO_2 g^{-1} CH_4 (stage I) to 2.7 ± 0.3 g CO_2 g^{-1} CH_4 in stages III and IV. Likewise, the consumed O_2 to CH_4 ratio in stage I (1.48 ± 0.08) significantly differed from those values observed in the subsequent stages (1.55 ± 0.05, 1.63 ± 0.10 and 1.69 ± 0.12 in stages II, III and IV, respectively).

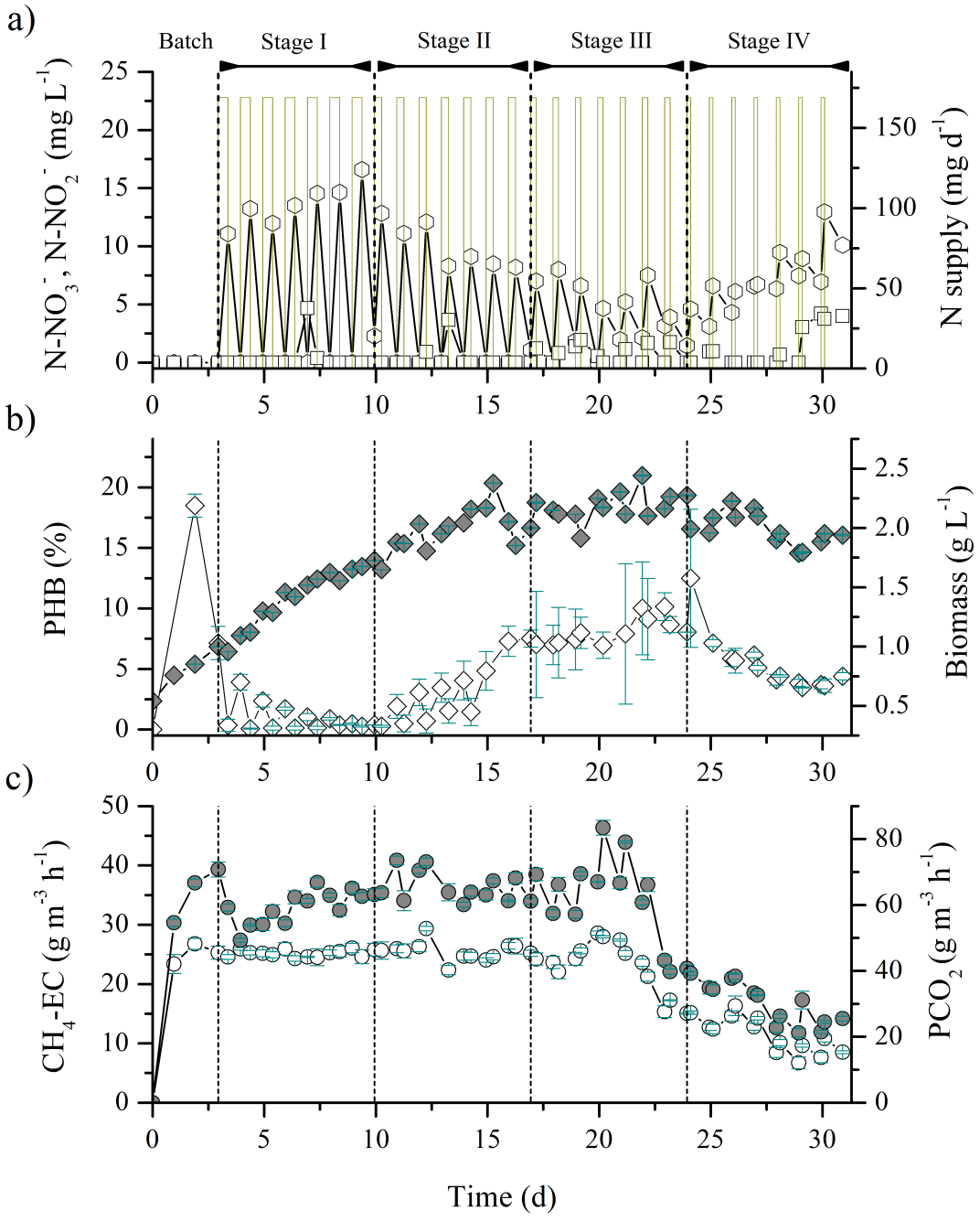

Fig. 7.3 *Time course of* ***(a)*** *NO_3-N (hexagons) and NO_2-N (squares), N supply (continuous line)* ***(b)*** *PHB content (empty diamonds) and biomass concentration (solid diamonds), and* ***(c)*** *CH_4-EC (empty circles) and PCO_2 (solid circles) in Test series 2. Vertical dashed lines separate the different operating stages.*

7.3.3 Test series 3 – CH_4 biodegradation and PHB production under a 24h-24h feast-famine regime.

After the initial cultivation period under N limiting conditions, the culture was subjected to a 24h:24h cyclic operation (**Fig. 7.4a**). The bioreactor supported a complete removal of nitrogen in the form of nitrate from the first cycle until the end of the test, with no formation of nitrite observed. On the other hand, a residual nitrogen concentration in the culture broth of 7.9 ± 3.2 mg L^{-1} was observed, while the pH remained stable at 6.82 ± 0.10 during the entire experiment. Following inoculation, the biomass concentration increased up to 1.33 ± 0.01 g L^{-1} by the end of batch cultivation. Biomass concentration in the culture broth progressively increased alternating decreases and increases after each feast and famine phase, respectively, reaching a final concentration of 2.55 ± 0.01 g L^{-1} by the end of the cycles. The PHB content, which accounted for 34.3 ± 2.4% at the end of the batch cultivation, steadily decreased to 1.8 ± 0.2% by cycle 7 with the implementation of the feast-famine regime. However, from the famine phase of cycle 7 onwards (day 16), the PHB content in *M. parvus* exhibited a gradual increase to finally stabilize during the last two cycles at average PHB contents ranging from 13.7 ± 1.5 to 21.6 ± 2.8% in the feast and famine phases, respectively (which represented a PHB productivity of 20 g-PHB m^{-3} d^{-1}).

During batch cultivation, the system supported an initial CH_4-EC of 23.3 ± 1.0 g m^{-3} h^{-1}, which decreased to 9.0 ± 2.0 g m^{-3} h^{-1} by day 3 of operation. CH_4-ECs fluctuated from ≈11 to ≈23 g m^{-3} h^{-1} during cycle 1, while from cycle 2 onwards CH_4-ECs remained stable at 24.9 ± 1.5 g m^{-3} h^{-1} (**Fig. 7.4c)** (corresponding to CH_4-REs of 44 ± 2%). Similarly, PCO_2 fluctuated between ≈24 and ≈59 g m^{-3} h^{-1} at the beginning of the cyclic operation, and rapidly stabilized at 64.5 ± 3.8 g m^{-3} h^{-1}. Moreover, no significant differences were observed neither in CH_4-ECs (24.5 ± 1.5 and 25.2 ± 1.6 g m^{-3} h^{-1}) nor in PCO_2 (64.5 ± 4.3 and 64.1 ± 3.6 g m^{-3} h^{-1}) at the corresponding feast and famine phases during the steady state. These values resulted in an average mineralization ratio of 2.6 ± 0.2 g CO_2 g^{-1} CH_4 and in a consumed O_2 to CH_4 ratio of 1.60 ± 0.07.

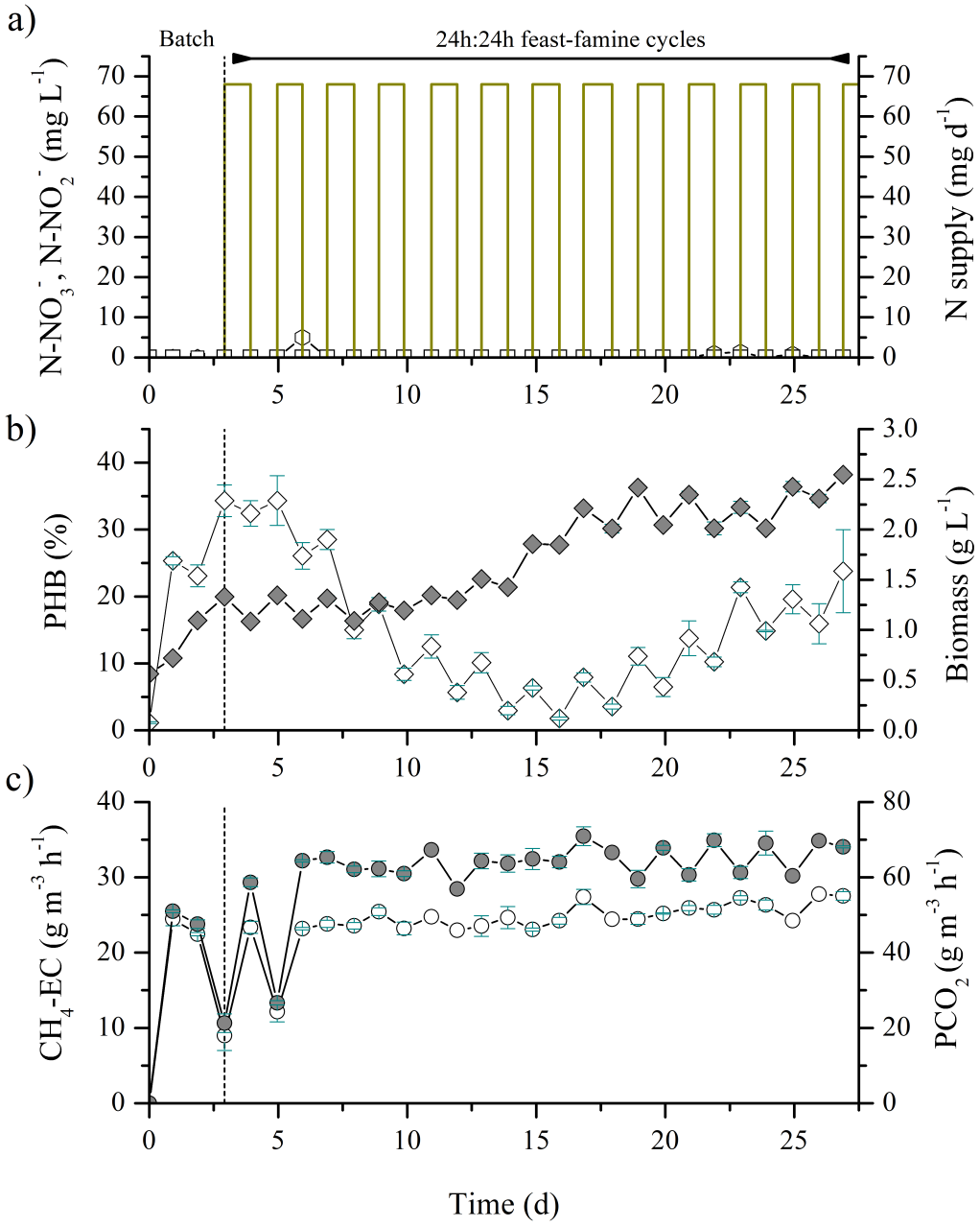

Fig. 7.4 *Time course of* ***(a)*** *NO_3-N (hexagons) and NO_2-N (squares), N supply (continuous line)* ***(b)*** *PHB content (empty diamonds) and biomass concentration (solid diamonds), and* ***(c)*** *CH_4-EC (empty circles) and PCO_2 (solid circles) in Test series 3. Vertical dashed line separates batch from continuous operation.*

7.3.4 Test series 4 – CH_4 biodegradation and PHB production under a 24h-48h feast-famine regime.

Following batch operation, nitrate was completely consumed only within the first two feast-famine cycles. From cycle 3 onwards, accumulations of nitrate (up to ≈38 mg L^{-1} N-NO_3^- by day 22) and, to a lesser extent of nitrite (1.6 ± 0.6 mg L^{-1} N-NO_2^-), were observed (**Fig. 7.5a**). Furthermore, a residual nitrogen content in the culture broth of 4.3 ± 2.0 mg L^{-1} was recorded. The pH of the cultivation broth averaged 7.0 ± 0.6, regardless of the feast and famine phases. Initially, a biomass concentration of 0.91 ± 0.00 g L^{-1} was reached during batch cultivation, which steadily increased (despite marked fluctuations) up to 1.26 ± 0.0 g L^{-1} by the end of cycle 3 (**Fig. 7.5b)**. From cycle 4 onwards, biomass concentration gradually decreased leading to a final concentration of 0.89 ± 0.0 g L^{-1}. Similarly, PHB accumulation, which accounted for 41.7 ± 3.4% at the beginning of the feast-famine operation, ranged from 27.2 ± 2% to 35.5 ± 1% within the first three cycles. These figures corresponded to a PHB productivity of 21 g-PHB m^{-3} d^{-1}. PHB content steadily decreased afterwards from 35.0 ± 0.3% to 26.1 ± 0.5% by the end of the experiment.

Following inoculation, the system reached a CH_4-EC of 26.3 ± 0.8 g m^{-3} h^{-1} by day 1, which dropped to 5.6 ± 0.3 g m^{-3} h^{-1} in the following two days. With the implementation of the 24h:48h feast-famine regime, CH_4-EC markedly fluctuated from 4.8 ± 0.6 to 24.6 ± 0.3 g m^{-3} h^{-1} during the first two cycles (corresponding to REs of 8 ± 1 and 40 ± 1%, respectively). Less sharp fluctuations were observed during cycles 3 and 4, stabilizing from cycle 5 onwards at 7.7 ± 1.2 g m^{-3} h^{-1} (corresponding to a CH_4-RE of 12.5 ± 2.0%) (**Fig. 7.5c)**. Likewise, PCO_2 fluctuated between ≈9 and ≈52 g m^{-3} h^{-1} in the first two cycles. From cycle 3 onwards, PCO_2 decreased from 41.3 ± 3.5 g m^{-3} h^{-1} by day 9 to 15.6 ± 1.7 g m^{-3} h^{-1} at the end of the experimentation period. Throughout the feast-famine regime the mineralization ratio averaged 2.5 ± 0.6 g CO_2 (g CH_4)$^{-1}$, with values > 3 g CO_2 (g CH_4)$^{-1}$ being occasionally recorded at the end of the cycle. Finally, the consumed O_2 to CH_4 ratio was 1.60 ± 0.2 regardless of the operational phase.

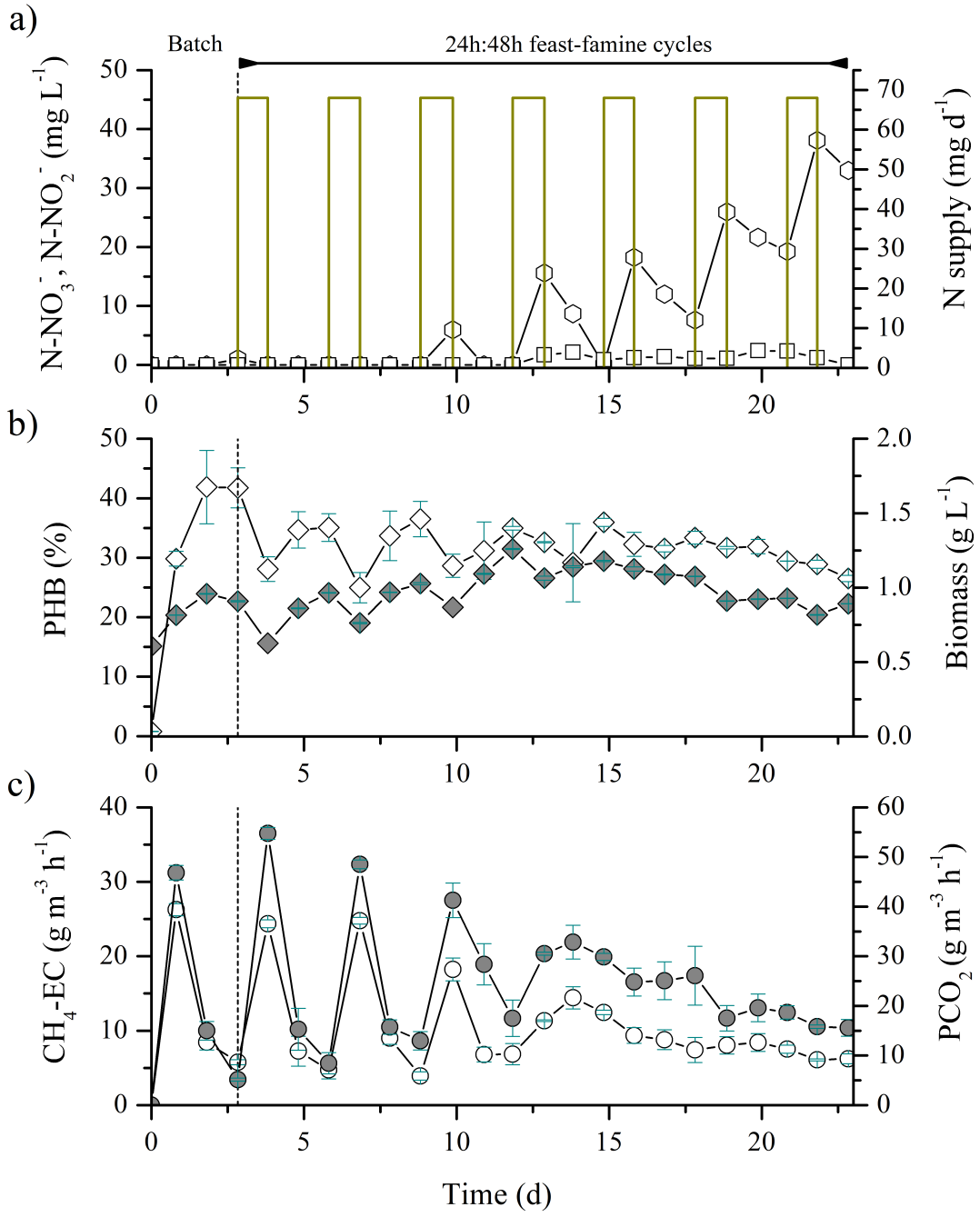

Fig. 7.5 *Time course of* ***(a)*** *NO_3-N (hexagons) and NO_2-N (squares), N supply (continuous line)* ***(b)*** *PHB content (empty diamonds) and biomass concentration (solid diamonds), and* ***(c)*** *CH_4-EC (empty circles) and PCO_2 (solid circles) in Test series 4. Vertical dashed line separates batch from cyclic operation.*

7.4 Discussion

The operational criteria for a cost-effective PHB production in a single-stage process should not only rely on the biopolymer content accumulated in the cells, but also provide favourable environmental conditions for a sustained methanotrophic activity in the long term operation. In this context, only process operation with a continuous nitrogen supply (Test Series 1) and 24h:24h feast:famine cycles (Test Series 3) supported a steady methane abatement (≈25 g m^{-3} h^{-1}) and a complete nitrate removal. The methane elimination capacities here recorded were comparable with those reported in other STRs using methanotrophic consortia, which ranged from 20 ± 3 to 33 ± 1 g m^{-3} h^{-1} at 500 and 800 rpm, respectively (Rocha-Rios et al., 2010), although lower than those reported by Muñoz et al. (2018) at a similar stirring velocity (42.5 ± 5.4 g m^{-3} h^{-1}). Despite gas bubble disruption caused by the mechanical agitation (herein supported by a Rushton turbine) typically increases biocatalytic activity by enhancing CH_4 bioavailability in the cultivation broth, preliminary works in our lab (data not shown) suggested that high stirring rates (>600 rpm) negatively impacted CH_4-ECs likely due to the high shear stress on *M. parvus* cell membrane. Similar CH_4-ECs (24.8 ± 1.3 g m^{-3} h^{-1}) were obtained by *Methylocystis hirsuta* in a bubble column bioreactor fed with air:biogas mixtures and operated with internal gas recirculation at the same gas residence time (60 min) and a gas recirculation ratio of 5 (Rodríguez et al., 2020b). Nitrate was not found to be inhibitory per se for *M. parvus* at any of the N concentrations of the present work, which remained always below the concentration found to alter methanotrophic activity (280 mg L^{-1} $N\text{-}NO_3^-$) in other type II-methanotroph such as *Methylosinus* sp. (R-45379) (Hoefman et al., 2014). Cell biosynthesis under continuous nitrogen supply (Test Series 1) and 24h:24h feast:famine cycles (Test Series 3) evidenced assimilative nitrogen uptake, as only small transient peaks of nitrite were detected. This assimilatory pathway involves nitrate reduction to nitrite and further to ammonia, which are mediated by nitrate and nitrite reductases, respectively, (Cai et al., 2016) and N assimilation via the glutamate cycle, a general characteristic of the *Alphaproteobacteria* class (Trotsenko & Murrell, 2008).

During Test Series 2, nitrogen feast-famine cycles of 11h:13h (110% N supply – stage I) and 8h:16h (80% N supply – stage II) supported comparable results in terms of bioreactor performance, with a stable methane biodegradation (≈25 g m^{-3} h^{-1}) and total nitrogen uptake. However, under more severe nitrogen limiting conditions such as those applied in stages III and IV in Test Series 2 with a feast-famine cyclic operation of 6h:18h (60% N supply) and 4h:20h (40% N supply), respectively, and in Test Series 4 with a cyclic nitrogen deprivation phase of 48h (33% N supply), nitrate levels in the culture broth increased with a concomitant accumulation of nitrite and a gradual deterioration of the CH_4-EC (accounting for a 65 and 69% CH_4-EC reduction in Test Series 2 and 4, respectively, by the end of the experiment). A recent paper, reporting the Genome Scale Metabolic Model of *M. parvus* OBBP, elucidated that nitrite can be produced not only via assimilatory and dissimilatory nitrate reduction during CH_4 degradation (Hoefman et al., 2014), but also via internal PHB consumption coupled to denitrification under anoxic conditions (Bordel et al., 2019b). This suggests a tentative explanation for nitrite formation in Test Series 2 and 4 (with N-NO_2^- concentrations of 3.8 ± 0.5 mg L^{-1} and 1.6 ± 0.6 mg L^{-1}, respectively), where the stored PHB could have been likely used as an energy source under oxygen limiting conditions. Indeed, the 2:1 O_2:CH_4 ratio present in the inlet gas stream was likely not sufficient to cope with the additional oxygen demand of PHB oxidation. *M. parvus* inability to assimilate nitrite and the concomitant deterioration of the methanotrophic activity observed under these nitrogen limiting conditions could be tentatively explained by the fact that nitrite inhibits the enzyme formate dehydrogenase (King & Schnell, 1994). This inhibition limits the generation of the reducing power required to reduce nitrite into ammonia (3 mol of NADH per 1 mol NO_2^-) via the NADH-dependent nitrite reductases. Even though the inhibitory effects of nitrite on methanotrophs are widely known (King & Schnell, 1994; Nyerges & Stein, 2009), genome sequences of closely related species, such as *Methylocystis* sp. SC2 and *Methylocystis hirsuta*, revealed the potential to cope with its toxicity through partial and complete denitrification pathways, respectively (Bordel et al., 2019a). Although nitrous oxide was not analysed in this study, the results herein obtained did not support an active detoxification mechanism by *M. parvus.*

The CH_4 mineralization ratios under all nitrogen supply strategies investigated (2.3 ± 0.2 - 2.7 ± 0.3 g CO_2 (g CH_4)$^{-1}$) remained above those reported under balanced growth conditions (<2.2 g CO_2 (g CH_4)$^{-1}$) (García-Pérez et al., 2018; Rodríguez et al., 2020b) at a similar gas residence time in the bioreactor. This discrepancy may be attributed to the co-utilization of the stored PHB and CH_4 to aid NADH regeneration (4 CO_2 per $C_4H_6O_2$), particularly noticeable under severe nitrogen stress conditions (≤40% N supply) (Pieja et al., 2011; Sipkema et al., 2000). For instance, PHB content decreased by nearly 45% during the operating stage under feast-famine cycles of 4h:18h (stage IV - Test Series 2). However, it is also worth noting that mineralization ratios peaked occasionally above 2.8 g CO_2 (g CH_4)$^{-1}$ (corresponding to mineralization ratios above 100%), suggesting also an active endogenous cell respiration (García-Pérez et al., 2018), very likely in scenarios with longer N deprived conditions (24h:48h cycles - Test Series 4), where PHB exhibited only a decrease by 25% at lower ECs. Overall, the observed O_2:CH_4 consumption ratios (≈1.6) were remarkably consistent with those reported by Chen et al. (2020), Karthikeyan et al. (2015) and Pieja et al. (2011) for PHB production, who estimated ratios of 1.6 (mechanistic model), 1.5 (stoichiometry) and 1.5 (empirical for *M. parvus*), respectively. Nevertheless, an increasing trend was observed under progressive nitrogen limiting conditions in Test Series 2 (e.g.: from 1.48 ± 0.08 (stage I) to 1.69 ± 0.12 (stage IV)), which could be likely attributed to the occurrence of other O_2-consuming processes such as the co-consumption of PHB and dissolved organic matter (excreted metabolites or cell lysis).

Nitrogen starvation for 72h under batch operation initially yielded PHB contents ranging from 7 – 42%, which were consistent with those reported for *M. parvus* OBBP (14-50%) under nitrate limitation in serum bottles (Pieja et al., 2011; Rostkowski et al., 2013). The continuous cultivation of *M. parvus* (Test Series 1) at decreasing nitrogen loads yielded low P(3HB) accumulations (≈2%) with no significant differences among stages. Interestingly, stepwise reductions in the nitrogen loading rate did not progressively boost PHB accumulation in the cultivation broth (as moderate intracellular PHB contents were only sporadically observed). Nonetheless, *M. parvus* was able to thrive on biogas regardless

of the nitrogen loading rate as demonstrated by a steady elimination capacity and a constant biomass productivity. These results suggest that process operation under continuous nitrogen limiting supply enabled concomitantly biopolymer synthesis and consumption, as PHB (in the presence of an exogenous carbon source and nitrogen) (Pieja et al., 2011) may serve as a reducing power source to cover the great energy demand of MMO, allowing pMMO activity and nitrogen assimilation. In addition, this study suggested that *M. parvus* was capable of utilizing gas N_2 as nitrogen source concomitantly with NO_3^- assimilation. Indeed, biomass yields of 0.41 ± 0.05, 0.31 ± 0.06, 0.30 ± 0.02 and 0.37 ± 0.05 g biomass $(g\ CH_{4\ degraded})^{-1}$ were recorded under N-NO_3^- loading rates representing 110, 80, 60 and 40% of the theoretical nitrogen demand at the empirical CH_4-EC. At this point, it should be stressed that continuous PHB production systems are still quite unexplored in comparison with batch and fed-batch PHB production systems (Blunt et al., 2018; Koller, 2018).

Nevertheless, the volumetric PHB productivities herein recorded (3 – 5 g-PHB $m^{-3}\ d^{-1}$) were below those reported to date by other PHB-accumulating bacteria under continuous culture. For instance, Ramsay et al. (1990) reported a productivity of 7.2 kg-PHBV $m^{-3}\ d^{-1}$ using sucrose and propionic acid as a carbon source by *Azohydromonas lata* in a single-stage CSTR. In addition to the limited bioavailability of the carbon source in the liquid phase for methanotrophs, a possible explanation to this discrepancy is that, unlike other PHB-producing microorganism, PHB synthesis by *M. parvus* is not growth-associated (Bordel et al., 2019b; Rostkowski et al., 2013). Conversely, identical N loading rates to Test Series 1 with chronological separation of both growth and accumulation phases (24h-cycles in Test Series 2) featured different outcomes in terms of PHB accumulation. Thus, PHB consumption prevailed over PHB accumulation under an 110% N supply (11h:13h cycles - stage I) whereas cycles providing a larger N limitation (i.e. 8h:16h cycles – stage I and 6h:18h cycles – stage II corresponding to N supplies of 80 and 60%, respectively) boosted the accumulation of PHB in the cultivation broth (while maintaining a good system performance throughout the entire test only in stage II). Therefore, the volumetric PHB

productivities (12 g-PHB m^{-3} d^{-1}) corresponding to the end of stage II in Test Series 2 increased by a factor of ≈4 compared to continuous cultivation. These results evidenced the need of decoupling both growth and PHB synthesis phases to achieve improved PHB productivities. The assessment of the long-term operation under N feast-famine cycles of 8h:16h (stage II) would be required as microbial stability might be affected in the long-term by the low dilution rate and the accumulation of dissolved metabolites (up to 120 mg-TOC L^{-1} were measured by the end of the stage II). The 24h:24h feast-famine strategy (50% N supply – Test Series 3) featured PHB contents of 22% and the highest PHB productivity (20 g-PHB m^{-3} d^{-1}), almost doubling the PHB productivities achieved during shorter cycles (Test Series 2) with a stable methane elimination capacity. These productivities were comparatively lower than those reported for *M. hirsuta* (≈50 g-PHB m^{-3} d^{-1}) by Rodríguez et al. (2020b), who operated a bubble column bioreactor under 24h:24h cycles with higher CH_4-ECs and alternating supply of NMS and NFMS. On the other hand, a further increase to 48h of N limitation (33% N supply – Test Series 4) resulted in PHB-rich cells (35.5%) and similar volumetric PHB productivities (21 g-PHB m^{-3} d^{-1}). Unfortunately, the process collapsed following 3 cycles of 24h:48h nitrogen feast:famine operation. Previous works subjecting *Methylocystis hirsuta* to N-deprivation periods of 48h under continuous supply of methane/biogas also entailed a deterioration of the microbial activity followed by an eventual system collapse (García-Pérez et al., 2018; Rodríguez et al., 2020b). These outcomes underlined the need of optimizing the period under nitrogen limitation to guarantee a sustained CH_4 abatement and a maximum PHB content.

7.5 Conclusions

This work constitutes the first study assessing strategies for a continuous biogas-based PHB production by *M. parvus*. Nitrogen feast-famine cycles of 8h:16h and 24h:24h (representing stoichiometric nitrogen inputs of 80 and 50%, respectively) supported an effective PHB production without compromising process stability. Conversely, exposures to nitrogen-limiting periods 2-folds higher than the duration of the nitrogen feeding phase entailed a deterioration in methanotrophic activity at nitrogen inputs ≤60%. The design of the feast-famine phases and mineral medium were crucial to sustain stable biogas utilization and PHB production. Surprisingly, continuous N feeding did not facilitate an effective PHB production despite nitrogen limitation.

Acknowledgements

Authors gratefully acknowledge the financial support by the Spanish Ministry of Science and Innovation under grant agreement no. BES-2016-077160 (CTM2015-70442-R project). The support from the EU-FEDER programme and the regional government of Castilla y León (UIC 071, CLU 2017-09) is also acknowledged. Authors sincerely thank V. Pérez for providing practical help with the experimental setup.

References

AlSayed, A., Fergala, A., Eldyasti, A. (2018) Sustainable biogas mitigation and value-added resources recovery using methanotrophs intergrated into wastewater treatment plants. *Rev Environ Sci Biotechnol*, **17**(2), 351-393. doi: 10.1007/s11157-018-9464-3

Asenjo, J.A., Suk, J.S. (1986) Microbial conversion of methane into poly-β-hydroxybutyrate (PHB): Growth and intracellular product accumulation in a type II methanotroph. *J Ferment Technol*, **64**(4), 271-278. doi: 10.1016/0385-6380(86)90118-4

Blunt, W., Levin, D.B., Cicek, N. (2018) Bioreactor operating strategies for improved polyhydroxyalkanoate (PHA) Productivity. *Polymers*, **10**(11). doi: 10.3390/polym10111197

Bordel, S., Rodriguez, Y., Hakobyan, A., Rodriguez, E., Lebrero, R., Munoz, R. (2019a) Genome scale metabolic modeling reveals the metabolic potential of three Type II methanotrophs of the genus *Methylocystis*. *Metab Eng*, **54**, 191-199. doi: 10.1016/j.ymben.2019.04.001

Bordel, S., Rojas, A., Munoz, R. (2019b) Reconstruction of a Genome Scale Metabolic Model of the polyhydroxybutyrate producing methanotroph *Methylocystis parvus* OBBP. *Microb Cell Fact*, **18**(1), 104. doi: 10.1186/s12934-019-1154-5

Cai, Y., Zheng, Y., Bodelier, P.L.E., Conrad, R., Jia, Z. (2016) Conventional methanotrophs are responsible for atmospheric methane oxidation in paddy soils. *Nature Communications*, **7**(1), 11728. doi: 10.1038/ncomms11728

Cantera, S., Bordel, S., Lebrero, R., Gancedo, J., García-Encina, P.A., Muñoz, R. (2019) Bio-conversion of methane into high profit margin compounds: an innovative, environmentally friendly and cost-effective platform for methane abatement. *World J Microbiol Biotechnol*, **35**(1), 16. doi: 10.1007/s11274-018-2587-4

Chen, X., Rodríguez, Y., López, J.C., Muñoz, R., Ni, B.J., Sin, G. (2020) Modeling of Polyhydroxyalkanoate Synthesis from Biogas by *Methylocystis hirsuta*. *ACS Sustain Chem Eng*, **8**(9), 3906-3912. doi: 10.1021/acssuschemeng.9b07414

del Cerro, C., García, J.M., Rojas, A., Tortajada, M., Ramón, D., Galán, B., Prieto, M.A., García, J.L. (2012) Genome sequence of the methanotrophic poly-β-hydroxybutyrate producer *Methylocystis parvus* OBBP. *J Bacteriol*, **194**(20), 5709. doi: 10.1128/jb.01346-12

EBA (2020) EBA Statistical Report. European Biogas Association. https://www.europeanbiogas.eu/wp-content/uploads/2021/01/EBA_StatisticalReport2020_abridged.pdf (Accessed: 03.05.2021)

EuropeanBioplastics, novaInstitute (2020) Bioplastics market data. https://www.european-bioplastics.org/market/ (Accessed: 05.05.2021)

García-Pérez, T., López, J.C., Passos, F., Lebrero, R., Revah, S., Muñoz, R. (2018) Simultaneous methane abatement and PHB production by *Methylocystis hirsuta* in a novel gas-recycling bubble column bioreactor. *Chem Eng J*, **334**, 691-697. doi: 10.1016/j.cej.2017.10.106

Hanson, R.S., Hanson, T.E. (1996) Methanotrophic bacteria. *Microbiol rev*, **60**(2), 439-471. doi: 10.1128/mr.60.2.439-471.1996

Heidbreder, L.M., Bablok, I., Drews, S., Menzel, C. (2019) Tackling the plastic problem: A review on perceptions, behaviors, and interventions. *Sci Total Environ*, **668**, 1077-1093. doi: 10.1016/j.scitotenv.2019.02.437

Hoefman, S., van der Ha, D., Boon, N., Vandamme, P., De Vos, P., Heylen, K. (2014) Niche differentiation in nitrogen metabolism among methanotrophs within an operational taxonomic unit. *BMC Microbiol*, **14**(1), 83. doi: 10.1186/1471-2180-14-83

Jiang, G., Hill, D.J., Kowalczuk, M., Johnston, B., Adamus, G., Irorere, V., Radecka, I. (2016) Carbon Sources for Polyhydroxyalkanoates and an Integrated Biorefinery. *Int J Mol Sci*, **17**(7). doi: 10.3390/ijms17071157

Karthikeyan, O.P., Chidambarampadmavathy, K., Cirés, S., Heimann, K. (2015) Review of Sustainable Methane Mitigation and Biopolymer Production. *Crit Rev Environ Sci Technol*, **45**(15), 1579-1610. doi: 10.1080/10643389.2014.966422

Kaur, G., Roy, I. (2015) Strategies for large-scale production of polyhydroxyalkanoates. *Chem Biochem Eng Q*, **29**, 157-172. doi: 10.15255/cabeq.2014.2255

Khatami, K., Perez-Zabaleta, M., Owusu-Agyeman, I., Cetecioglu, Z. (2021) Waste to bioplastics: How close are we to sustainable polyhydroxyalkanoates production? *Waste Manage*, **119**, 374-388. doi: 10.1016/j.wasman.2020.10.008

King, G.M., Schnell, S. (1994) Ammonium and Nitrite Inhibition of Methane Oxidation by *Methylobacter albus* BG8 and *Methylosinus trichosporium* OB3b at Low Methane Concentrations. *Appl Environ Microbiol*, **60**(10), 3508. doi: 10.1128/aem.60.10.3508-3513.1994

Koller, M. (2018) A Review on established and emerging fermentation schemes for microbial production of polyhydroxyalkanoate (PHA) biopolyesters. *Fermentation*, **4**(2), 30. doi: 10.3390/fermentation4020030

Koller, M., Muhr, A (2014) Continuous production mode as a viable process-engineering tool for efficient poly(hydroxyalkanoate) (PHA) bio-production. *Chem Biochem Eng Q*, **28**(1), 65-77.

Lebreton, L., Andrady, A. (2019) Future scenarios of global plastic waste generation and disposal. *Palgrave Commun*, **5**(1), 6. doi: 10.1057/s41599-018-0212-7

López, J.C., Arnáiz, E., Merchán, L., Lebrero, R., Muñoz, R. (2018) Biogas-based polyhydroxyalkanoates production by *Methylocystis hirsuta*: A step further in anaerobic digestion biorefineries. *Chem Eng J*, **333**, 529-536. doi: 10.1016/j.cej.2017.09.185

López, J.C., Rodríguez, Y., Pérez, V., Lebrero, R., Muñoz, R. (2019) CH_4-based polyhydroxyalkanoate production: A step further towards a sustainable bioeconomy. In: Biotechnological Applications of Polyhydroxyalkanoates, (Ed.) V.C. Kalia, Springer Singapore. Singapore, pp. 283-321. doi: 10.1007/978-981-13-3759-8_11

Mühlemeier, I.M., Speight, R., Strong, P.J. (2018) Biogas, Bioreactors and Bacterial Methane Oxidation. in: *Methane Biocatalysis: Paving the Way to Sustainability*, (Eds.) M.G. Kalyuzhnaya, X.-H. Xing, Springer International Publishing. Cham, pp. 213-235. doi: 10.1007/978-3-319-74866-5_14

Muñoz, R., Meier, L., Diaz, I., Jeison, D. (2015) A review on the state-of-the-art of physical/chemical and biological technologies for biogas upgrading. *Rev Environ Sci Biotechnol*, **14**(4), 727-759. doi: 10.1007/s11157-015-9379-1

Muñoz, R., Soto, C., Zuñiga, C., Revah, S. (2018) A systematic comparison of two empirical gas-liquid mass transfer determination methodologies to characterize methane biodegradation in stirred tank bioreactors. *J Environ Manage,* **217**, 247-252. doi: 10.1016/j.jenvman.2018.03.097

Myung, J., Flanagan, J.C.A., Waymouth, R.M., Criddle, C.S. (2017) Expanding the range of polyhydroxyalkanoates synthesized by methanotrophic bacteria through the utilization of omega-hydroxyalkanoate co-substrates. *AMB Express*, **7**(1), 118. doi: 10.1186/s13568-017-0417-y

Nyerges, G., Stein, L.Y. (2009) Ammonia cometabolism and product inhibition vary considerably among species of methanotrophic bacteria. *FEMS Microbiol Lett*, **297**(1), 131-136. doi: 10.1111/j.1574-6968.2009.01674.x

Pérez, V., Lebrero, R., Muñoz, R. (2020) Comparative Evaluation of Biogas Valorization into Electricity/Heat and Poly(hydroxyalkanoates) in Waste Treatment Plants: Assessing the Influence

of Local Commodity Prices and Current Biotechnological Limitations. *ACS Sustain Chem Eng*, **8**(20), 7701-7709. doi: 10.1021/acssuschemeng.0c01543

Pieja, A.J., Sundstrom, E.R., Criddle, C.S. (2011) Poly-3-hydroxybutyrate metabolism in the type II methanotroph *Methylocystis parvus* OBBP. *Appl Environ Microbiol,* **77**(17), 6012-9. doi: 10.1128/AEM.00509-11

PlasticsEurope (2020) Plastics - the Facts 2020. https://www.plasticseurope.org/en/resources/publications/4312-plastics-facts-2020 (Accessed: 07.05.2021)

Ramsay, B.A., Lomaliza, K., Chavarie, C., Dubé, B., Bataille, P., Ramsay, J.A. (1990) Production of poly-(beta-hydroxybutyric-co-beta-hydroxyvaleric) acids. *Appl Environ Microbiol,* **56**(7), 2093-2098. doi: 10.1128/aem.56.7.2093-2098.1990

Riedel, S.L., Brigham, C.J.(2020) Inexpensive and Waste Raw Materials for PHA production. 1st ed. in: *The Handbook of Polyhydroxyalkanoates: Microbial Biosynthesis and Feedstocks (1st ed.)* (Ed.) M. Koller, Vol. 1, CRC Press. doi: 10.1201/9780429296611

Riedel, S.L., Jahns, S., Koenig, S., Bock, M.C.E., Brigham, C.J., Bader, J., Stahl, U. (2015) Polyhydroxyalkanoates production with *Ralstonia eutropha* from low quality waste animal fats. *Journal of Biotechnology*, **214**, 119-127. doi: 10.1016/j.jbiotec.2015.09.002

Rocha-Rios, J., Muñoz, R., Revah, S. (2010) Effect of silicone oil fraction and stirring rate on methane degradation in a stirred tank reactor. *Journal of Chemical Technology & Biotechnology*, **85**(3), 314-319. doi: 10.1002/jctb.2339

Rodríguez, Y., Firmino, P.I.M., Arnáiz, E., Lebrero, R., Muñoz, R. (2020a) Elucidating the influence of environmental factors on biogas-based polyhydroxybutyrate production by *Methylocystis hirsuta* CSC1. Science of the Total Environment, **706**, 135136. doi: 10.1016/j.scitotenv.2019.135136

Rodríguez, Y., Firmino, P.I.M., Pérez, V., Lebrero, R., Muñoz, R. (2020b) Biogas valorization via continuous polyhydroxybutyrate production by *Methylocystis hirsuta* in a bubble column bioreactor. *Waste Management*, **113**, 395-403. doi: 0.1016/j.wasman.2020.06.009

Rostkowski, K.H., Pfluger, A.R., Criddle, C.S. (2013) Stoichiometry and kinetics of the PHB-producing Type II methanotrophs *Methylosinus trichosporium* OB3b and *Methylocystis parvus* OBBP. *Bioresour Technol*, **132**, 71-7. doi: 10.1016/j.biortech.2012.12.129

Sagong, H.-Y., Son, H.F., Choi, S.Y., Lee, S.Y., Kim, K.-J. (2018) Structural Insights into Polyhydroxyalkanoates Biosynthesis. *Trends in Biochemical Sciences*, **43**(10), 790-805. doi: 10.1016/j.tibs.2018.08.005

Sipkema, E.M., de Koning, W., Ganzeveld, K.J., Janssen, D.B., Beenackers, A.A.C.M. (2000) NADH-regulated metabolic model for growth of *Methylosinus trichosporium* OB3b. Model presentation, parameter estimation, and model validation. *Biotechnol Prog*, **16**(2), 176-188. doi: 10.1021/bp9901567

Steinbüchel, A., Valentin, H.E. (1995) Diversity of bacterial polyhydroxyalkanoic acids. *FEMS Microbiol Lett*, **128**(3), 219-228. doi: 10.1016/0378-1097(95)00125-O

Sundstrom, E.R., Criddle, C.S. (2015) Optimization of methanotrophic growth and production of poly(3-hydroxybutyrate) in a high-throughput microbioreactor system. *Appl Environ Microbiol*, **81**(14), 4767. doi: 10.1128/AEM.00025-15

Trotsenko, Y.A., Murrell, J.C. (2008) Metabolic Aspects of aerobic obligate methanotrophy. In: Advances in applied microbiology, Vol. **63**, *Academic Press*, pp. 183-229. doi: 10.1016/S0065-2164(07)00005-6

van den Oever, M., Molenveld, K., van der Zee, M., Bos, H. (2017) Bio-based and biodegradable plastics - Facts and Figures. *Wageningen UR*. 1722. doi: 10.18174/408350

Van Wegen, R.J., Ling, Y., Middelberg, A.P.J. (1998) Industrial Production of Polyhydroxyalkanoates Using *Escherichia Coli*: An Economic Analysis. *Chem Eng Res Des*, **76**(3), 417-426. doi: 10.1205/026387698524848

Vandi, L.-J., Chan, C.M., Werker, A., Richardson, D., Laycock, B., Pratt, S. (2018) Wood-PHA Composites: Mapping Opportunities. *Polymers*, **10**(7). doi: 10.3390/polym10070751

Vecherskaya, M., Dijkema, C., Saad, H.R., Stams, A.J.M. (2009) Microaerobic and anaerobic metabolism of a *Methylocystis parvus* strain isolated from a denitrifying bioreactor. *Environ Microbiol Rep*, **1**(5), 442-449. doi: 10.1111/j.1758-2229.2009.00069.x

Whittenbury, R., Phillips, K.C., Wilkinson, J.F. (1970) Enrichment, Isolation and Some Properties of Methane-utilizing Bacteria. *Microbiology*, **61**(2), 205-218. doi: 10.1099/00221287-61-2-205

8.

Conclusions and future work

Conclusions and future work

A battery of bioreactor configurations and operating strategies were investigated with the overall aim of maximizing the production of PHB and methane utilization using biogas as feedstock and strains from the genus *Methylocystis* as workhorse. The results herein obtained demonstrated the feasibility of biogas-to-PHA biotechnologies as an innovative platform for the generation of biopolymers, paving the way towards a biogas biorefinery concept.

Aerobic methane oxidation by the type-II methanotrophic bacterium *M. hirsuta* was found to be greatly influenced by the environmental conditions evaluated in **Chapter 3**. More specifically, temperature was confirmed to play a key role and to be highly process specific. Thus, *M. hirsuta* showed its ability to accumulate PHB at 37ºC but was not able to thrive on biogas at the same temperature. Nonetheless, the optimal temperature supporting higher CH_4 removal rates and yields for growth and PHB synthesis was 25ºC. Likewise, the selection of the nitrogen source was also a key process factor, as the utilization of NH_4^+ mediated acidic conditions (due to nitrification processes) in the culture media and altered the synthesis capacity of the strain, while nitrite was toxic to *M. hirsuta*. Moreover, the O_2:CH_4 molar ratio of the gas mixture significantly impacted on the PHB synthesis, yielding maximal accumulations (45% w/w) at O_2:CH_4 ratios of 2:1. A step-wise model calibration/validation protocol for PHA synthesis by *M. hirsuta* was developed for the first time (**Chapter 4**). The model-based optimization of PHB predicted an optimal O_2:CH_4 ratio of 1.6:1 for a utilization efficiency of CH_4 and O_2 of nearly 100%. Overall, the results obtained in **Chapters 3** and **4** aided in the selection of the required conditions to approach successfully the transition towards continuous operation.

Then, the potential of a novel operating strategy based on the implementation of internal gas recirculation was explored in **Chapter 5** in order to overcome methane mass transfer limitations in bubble columns**.** This strategy allowed to decouple the real gas residence time from turbulence and methane mass transfer rates into the cultivation broth, attaining

elimination capacities of up to 4 times higher than in the absence of gas recirculation. Maximal methane utilization (CH_4-EC = 42 g m^{-3} h^{-1} and CH_4-RE = 70%) in the absence of additional limitations such as biomass stripping or poor mixing conditions in the column bioreactor, was identified at a gas residence time of 60 min and a recirculation ratio of 30. These results, which would entail improved biomass productivities and significant equipment costs reduction, were reinforced by the carbon footprint analysis carried out.

Nitrite-mediated inhibition arose as one of the major additional limitations to support a sustained CH_4 utilization under the aforementioned conditions under long-term operation. In this context, **Chapter 5** presented valuable insights related to the nitrogen supplementation strategy in the mineral medium for attaining a successful start-up and robustness operation during continuous biogas bioconversion into PHB. Besides, this chapter also showed a successful proof of concept of the continuous production of biopolymers from biogas. Thus, under optimized mineral medium and mass transfer conditions, the implementation of a 24h:24h cyclic nitrogen feast-famine strategy supported a stable methane removal efficiency of 70% and average biopolymer productivities of ≈50 g PHB m^{-3} d^{-1} (15% w/w).

Chapter 6 proposed a two-stage growth-accumulation configuration as an innovative approach for PHB production. Interestingly, PHB synthesis was triggered in the biomass cultivation bioreactor, where *M. hirsuta* exhibited a high PHB accumulating capacity with intracellular contents of 48% w/w in the presence of nitrogen. The shear stress and the high temperatures in the suspended growth stirred tank reactor likely induced the stress required for PHB synthesis under nitrogen sufficient conditions. In this context, the increase in the dilution rate from 0.2 to 0.3 d^{-1} allowed for a process stabilization at the expense of a lower methane elimination capacity (≈16 g CH_4 m^{-3} h^{-1}) with overall PHB productivities in the system of ≈53 g PHB m^{-3} d^{-1}. Under the conditions applied, the second step bioreactor did not support significantly enhanced PHB accumulations. Based on these results, a cyclic nitrogen feast-famine strategy in a single-stage bubble column bioreactor would constitute

a more reliable and effective approach for PHB synthesis by *M. hirsuta* using biogas as a carbon and energy source.

Finally, **Chapter 7** explored the PHB synthesis potential of continuous *vs.* step-feeding strategies by a close relative species, *Methylocystis parvus* OBBP, in a stirred tank reactor. Unlike previous test, none of the N feeding stages induced significant PHB production (3 – 5 g-PHB m^{-3} d^{-1}) under a continuous mode. An effective PHB production (12-20 g-PHB m^{-3} d^{-1}) without compromising process stability was supported under nitrogen feast-famine cycles of 8h:16h and 24h:24h, evidencing the need of decoupling both balanced and unbalanced growth conditions. Conversely, exposures to nitrogen-deprivation periods 2-folds higher than the duration of the nitrogen feeding phase entailed a deterioration in the microbial activity at N inputs below 60%.

Despite the substantial advances and promising results obtained in this thesis on the bioconversion of biogas into PHAs, there is still much room for process optimization. In brief, further research on PHA production via biogas derived-methane oxidation should focus on:

- Optimization of N feast:famine cycles to achieve higher PHB accumulations and productivities in the column bioreactor.
- Optimization of the two-stage growth-accumulation configuration with other bioreactor and/or other type II methanotrophs
- Engineering alternative high mass transfer bioreactors for an effective CH_4 bioconversion (e.g. pressurized systems)
- Evaluation of the effect of trace compounds contained in biogas on the effectiveness of the process.
- Study of the continuous production of copolymers (e.g. PHBV) with enhanced mechanical properties via supplementation of co-substrates such as valeric acid.
- Scale-up of the operational strategies that allowed sustained CH_4 abatement and PHB production

9.

About the author

Biography

Yadira Rodríguez Muñoz (Vélez-Málaga, 1981) studied Chemical Engineering at the University of Málaga (Spain). During her studies, she participated in national (Sicue-Séneca) and international (Erasmus) mobility programs with stays at the University Rey Juan Carlos (2005/06) and the University of Chemical Technology of Prague (UCT Prague, Czech Republic) (2010/2011), respectively. Between 2011 and 2013, she collaborated with the Department of Water Technology and Environmental Engineering of UCT Prague under the supervision of Dr. Jan Bartáček, and the Center for Environmental and Sustainability Research (CENSE, Universidade Nova de Lisboa, Portugal) supervised by Dr. Alexandra Ribeiro. In 2013, Yadira was awarded with a Erasmus Mundus scholarship from the European Commission (2013/2015) to study the International MSc in Environmental Technology and Engineering (IMETE), jointly offered by Ghent University (UGent, Belgium), UNESCO-IHE Institute for Water Education (UNESCO-IHE, Delft, The Netherlands), and UCT Prague. During the MSc, she did an internship in FARMTEC (Jistebnice, Czech Republic), a leading supplier of biogas plants where she was in charge of giving support to the field engineer. Her MSc thesis, which focused on the bio-H_2 production from VFA-rich effluents via photo-fermentation, was conducted under the supervision of Dr. Gonzalo Ruiz-Filippi at the School of Biochemical Engineering (EIB-PUCV) (Valparaíso, Chile). After completing the MSc, she obtained a Master's degree in Teacher Training (spec. Physics and Chemistry) from the University of Málaga. In 2017, Yadira was awarded a FPI fellowship by the Spanish Ministry of Science and Innovation and joined the VOC and Microalgae Research Group headed by Full Professor Raúl Muñoz in the Environmental Technology Research Group (Institute of Sustainable Processes - University of Valladolid) to undertake a PhD on biogas bioconversion into polyhydroxyalkanoates (PHAs) supervised by Dr. Raúl Muñoz and Dr. Raquel Lebrero. Her research focused on the design of operational strategies aiming at simultaneous biogas utilization and PHA production, and understanding the mechanisms underlying methane oxidation during growth and PHA synthesis.

Publications in ISI-indexed journals

- Within the scope of this PhD thesis:

Rodríguez, Y., García, S., Lebrero, R., Muñoz, R. Continuous polyhydroxybutyrate production from biogas in an innovative two-stage bioreactor configuration (In preparation).

Rodríguez, Y., García, S., Pérez, R., Lebrero, R., Muñoz, R. Optimization of nitrogen feeding strategies for improving polyhydroxybutyrate production from biogas by *Methylocystis parvus* OBBP in a stirred tank reactor (Submitted for publication in Chemosphere).

Rodríguez, Y., Firmino, P.I.M., Pérez, V., Lebrero, R., Muñoz, R. (2020). Biogas valorization via continuous polyhydroxybutyrate production by *Methylocystis hirsuta* in a bubble column bioreactor. Waste Management 113, 395-403 https://doi.org/10.1016/j.wasman.2020.06.009

Chen, X., **Rodríguez, Y.**, López, J.C., Muñoz, R., Ni, B.-J., Sin, G. (2020). Modelling of Polyhydroxyalkanoates Synthesis from Biogas by *Methylocystis hirsuta*. ACS Sustainable Chemistry & Engineering 8(9), 3906-3912. https://dx.doi.org/10.1021/acssuschemeng.9b07414

Rodríguez, Y., Firmino, P.I.M., Arnáiz, E., Lebrero, R., Muñoz, R. (2020). Elucidating the influence of environmental factors on biogas-based polyhydroxybutyrate production by *Methylocystis hirsuta* CSC1. Science of the Total Environment 706, 135136. https://doi.org/10.1016/j.scitotenv.2019.135136

- Out of the scope of this PhD thesis:

Marycz, M., **Rodríguez, Y.**, Gębicki, J., Muñoz, R. Systematic comparison of a biotrickling filter and a conventional filter for the removal of a mixture of hydrophobic VOCs by *Candida subhashii* (In preparation).

Yáñez, L., **Rodríguez, Y**., Scott, F., Vergara-Fernández, A., Muñoz, R. In vivo depolymerization of intracelular poly-3-hydroxybutyrate in *Methylocystis parvus*. (In preparation).

Bordel, S., **Rodríguez, Y.**, Hakobyan, A., Rodríguez, E., Lebrero, R., Muñoz, R. (2019). Genome scale metabolic modeling reveals the metabolic potential of three Type II methanotrophs of the genus *Methylocystis*. Metabolic Engineering 54, 191–199. https://doi.org/10.1016/j.ymben.2019.04.001

Cantera, S., Muñoz, R., Lebrero, R., López, J.C., **Rodríguez, Y.**, García-Encina, P.A. (2018) Technologies for the bioconversion of methane into more valuable products. Current Opinion in Biotechnology 50, 128–135. https://doi.org/10.1016/J.COPBIO.2017.12.021

Guedes, P., Mateus, E.P., Couto, N., **Rodríguez, Y.**, Ribeiro, A.B. (2014) Electrokinetic remediation of six emerging organic contaminants from soil. Chemosphere 117: 124-131 http://dx.doi.org/10.1016/j.chemosphere.2014.06.017

Procházková, L., **Rodríguez-Muñoz, Y.**, Procházka, J., Wanner, J. (2013) Simple spectrophotometric method for determination of polyvinylalcohol in different types of wastewater. International Journal of Environmental Analytical Chemistry 94: 399-410 http://dx.doi.org/10.1080/03067319.2013.853761

Book Chapters

Rodríguez, Y., Pérez, V., López, J.C., Bordel, S., Firmino, P.I.M., Lebrero, R., Muñoz, R. (2020). Coupling biogas (CH_4) with PHA biosynthesis. In: Koller, M. (Ed.), The Handbook of Polyhydroxyalkanoates, CRC press, UK https://doi.org/10.1201/9780429296611

López, J.C., **Rodríguez, Y.,** Pérez, V., Lebrero, R., Muñoz, R. (2019). CH_4-Based polyhydroxyalkanoate production: A step further towards a sustainable bioeconomy. In: Kalia, V.C. (Ed.), Biotechnological Applications of Polyhydroxyalkanoates. Springer Singapore, Singapore, pp. 283–321. ISBN 978-981-13-3758-1. https://doi.org/10.1007/978-981-13-3759-8_11

Conference Proceedings

- Oral communications:

Raúl Muñoz, Silvia García, Raquel Lobo, María del Rosario Rodero, **Yadira Rodríguez,** Raquel Lebrero. Recent advances in biological biogas upgrading and valorization. 3rd International Conference on Chemical Engineering. 22-23 September 2021, Jamshoro (Pakistan).

Rodríguez, Y., Firmino, P.I.M., Pérez, V., López, J.C., Lebrero, R., Muñoz, R. Innovative biogas valorization strategies to boost the economic feasibility of anaerobic digestion. Biotechniques19 - 8th International Conference on Biotechniques for Air Pollution Control & Bioenergy. 28-30 August 2019, Galway (Ireland).

Guedes, P., Mateus, E.P., Couto, N., **Rodríguez, Y.,** Ribeiro, A.B. Electrokinetic remediation of emerging organic contaminants – preliminary results, 30th International Conference on the Society for Environmental Geochemistry and Health, 30 June – 4 July 2014, Newcastle (UK).

Lenka Vacková, Jindřich Procházka, **Yadira Rodríguez Muñoz**, Jan Bartáček, Jiří Wanner. Stanovení polyvinylalkoholu v různých typech vod. 4. Konference HYDROANALYTIKA 2011, Sept 13-14 2011 Hradec Králové (Czech Republic)

- Poster communications:

Estela Tapia, Fernando Silva, **Yadira Rodríguez**, Sean Smith, Pilar Valderrama, Lorena Jorquera, M. Cristina Schiappacasse, Gonzalo Ruiz-Filippi. Energy balance of coupled processes in bioenergy production from glycerol. XII DAAL Symposium and Workshop Latin America Anaerobic Digestion, 23-27 October 2016, Cusco (Perú)

Paula Guedes, Eduardo P. Mateus, **Yadira Rodríguez**, Nazaré Couto, Alexandra B. Ribeiro. Potential of electrokinetic process for the remediation of estrogens in soil. The International Conference on Interfaces against Pollution (IAP), May 25-28 2014, De Harmonie, Leeuwarden (The Netherlands)

P. Guedes, E.P. Mateus, N. Couto, **Y. Rodríguez**, A.B. Ribeiro Remediation of triclosan in soil through electrokinetics. ELKIN 2014 11th International Symposium on Electrokinetic Phenomena, 20-23 May 2014, Ghent (Belgium)

Rodríguez, Y., Procházka, J., Procházková, L., Bartácek, J., Rodríguez-Maroto, J.M. Determination of anaerobic biodegradation of poly(vinyl alcohol) in batch tests. 13th World Congress on Anaerobic Digestion, 25-28 June 2013, Santiago de Compostela (Spain)

Participation in Research Projects

Procesos biológicos avanzados para la purificación de aire interior (BIOPURAIR)

Main researchers: Raúl Muñoz, Raquel Lebrero

Funding: RETOS 2018. Ministry of Science, Innovation & Universities, 2019 – 2021

Biogas Bioconversion to Commodities and High-Added Value Products: Exploring new strategies for biogas valorization (CTM2015-70442-R).

Main researchers: Raúl Muñoz, Raquel Lebrero (University of Valladolid)

Funding: Spanish Ministry of Economy and Competitiveness (MINECO). 2016-2019

GRAIL project: Glycerol Biorefinery Approach for the Production of High Quality Products of Industrial Value (Grant agreement ID: 613667)

Main researcher: Gonzalo Ruiz-Filippi (Pontificia Universidad Católica de Valparaíso)

Funding: 7th Framework Programme (FP7-KBBE). European Commission, 2013-2017

ELECTROACROSS - Electrokinetics across disciplines and continents: an integrated approach to finding new strategies for sustainable development (Grant agreement: 269289)

Main researcher: Alexandra Ribeiro (Universidade Nova de Lisboa)

Funding: Seventh Framework Programme (FP7-PEOPLE-2010-IRSES). European Commission, 2011-2015

Teaching

Lecturer in "Tecnología Ambiental y de Procesos" at the Department of Chemical Engineering and Environmental Technology (UVa) during three academic years (2017/18, 2018/19 and 2019/20). Total teaching hours: 34 h.

Co-supervision / Mentoring

- Final year projects:

Co-supervisor of Silvia García Casado, student of BSc in Chemical Engineering at University of Valladolid. Project title: Optimización de la producción de biopolímeros a partir de gases de efecto invernadero. Academic year 2020/21. Grade: 9.9

Co-supervisor of José Luis López Herreros, student of BSc in Chemical Engineering at University of Valladolid. Project title: Estrategias de enriquecimiento de metanótrofos acumuladores de biopolímeros a partir de biogás. Academic year 2019/20. Grade: 9.5

Co-supervisor of Laura Merchán Catalina, student of MSc in Environmental Engineering at University of Valladolid. Project title: Biodegradación de metano en un biorreactor de columna de burbujeo con recirculación interna acoplado a la producción de biopolímeros. Academic year 2017/18. Grade: 9.0

- Research internships:

Miren Erquicia Bolivar, student of BSc in Chemical Engineering (150 h) 2020-2021

Silvia García Casado, student of BSc in Chemical Engineering (113 h) 2019-2020

Committee membership

Member of the Institute of Sustainable Processes (ISP) of the University of Valladolid since 2018.

Member of the Organizing Committee of the "IV Conferencia Internacional sobre Gestión de Olores y COVs en el medio ambiente". 20-21 September 2017. Valladolid, Spain

Reviewer Experience

Reviewer in Journal of Environmental Management - JEMA (IF: 6.789) since January 2021.

Specialized Courses & Workshops

Workshop "Anaerobic digestion, Quo vadis?" (4.5h) 21st October 2021. Institute of Sustainable Processes (University of Valladolid, Spain)

"Gas-liquid mass transfer modeling" (4.5 h). 26-30 July 2021. Institute of Sustainable Processes, University of Valladolid. Lecturer: Dr. Sergio Bordel (UVa, Spain)

"Introduction to Next-Generation Sequencing Technologies" (5 h - online). 10-11 December 2020. School of Industrial Engineering, University of Valladolid. Lecturer: Dr. Sara Cantera (Wageningen University and Research Center, The Netherlands)

"Gestión de la información. Gestores bibliográficos y bibliografía" (20h). Actividades Formativas Transversales de la Escuela de Doctorado Universidad de Valladolid (EsDUVa), entre el 27 de mayo y 09 de junio de 2020.

"Eficiencia y viabilidad de nuevas tecnologías en procesos de tratamiento de aguas residuales" (10h). 09-13 March 2020. School of Industrial Engineering, University of Valladolid. Lecturer: Dr. Francesc Hernández (University of Valencia, Spain)

Curso "A happy PhD": Productividad y Bienestar del Doctorando (6h). 20-22 January 2020. Actividades Formativas Transversales de la Escuela de Doctorado Universidad de Valladolid (EsDUVa). Lecturers: Dr. Luis P. Prieto, Dr. Paula Odriozola-González, Dr. Yannis Dimitriadis, Dr. Tobias Ley, Dr. María Jesús Rodríguez-Triana (Tallinn University).

"Iniciación al análisis de secuencias 16 S Illumina® MiSeq para el estudio de comunidades bacterianas" (14 h). 16-19 December 2019. School of Industrial Engineering, University of Valladolid. Lecturer: Dr. Sara Cantera (Wageningen University and Research Center, The Netherlands)

"Fundamentals of Bioengineering" (8h). 25-28 March 2019. School of Industrial Engineering, University of Valladolid. Lecturer: Dr. José Martínez Ruiz (DTU, Denmark)

"Gas Chromatography basic course" (6h). 14 and 21 of February of 2019. School of Industrial Engineering, University of Valladolid. Lecturer: Dr. Jon Sanz Landaluze (Complutense University of Madrid, Spain)

"Life Cycle Assessment. CcaLC Software" (8h). 17-19 December 2018. School of Industrial Engineering, University of Valladolid. Lecturer: Dr. Alejandro Gallego (University of Manchester, UK)

Course “Taller práctico sobre Técnicas analíticas físico-químicas e instrumentales” (8.5h) 06-16 November 2018. University of Valladolid.

“Odours, science and engineering” (8h). 20-23 November 2017. School of Industrial Engineering, University of Valladolid. Lecturer: Selena Sironi (Politecnico di Milano, Italy).

“Inglés C1 para doctorandos” (51h). 06/10/2017 – 20/12/2017. Centro de Idiomas Universidad de Valladolid.

Training School in “Modelling and Decision Support Systems (DSS) for Sustainable Wastewater Treatment” (36h). Water_2020 COST Action. 25-29 April 2016. Catalan Institute for Water Research (ICRA), Girona, Spain

Summer School in “Resource Recovery from Wastewater” (40h). 8-12 Sept 2014. Ghent University, Belgium. Coordinated by Dr. Korneel Rabaey, Dr. Lars Angenent, and Dr. Gijs Du Laing.

“Innovative Sludge Pre-treatments”. Pre-AD13 World Congress Specialized Short Courses (12h). 23-24 June 2013. Environmental Technology Group of the University of Valladolid. (Valladolid, Spain).

Grants

- FPI 2016 fellowship, State Research Agency. Spanish Ministry of Economy and Competitiveness (BES-2016-077160) (2017-2021).
- Training School. Water_2020 COST Action. Catalan Institute for Water Research (ICRA), Girona, Spain (25-29 April 2016).
- Erasmus Mundus scholarship. International MSc in Environmental Technology and Engineering (IMETE). EACEA, European Commission (2013-15).
- Erasmus Exchange Programme at UCT Prague, Czech Republic (2010-11).
- National Mobility Programme SICUE-SÉNECA at ESCET-URJC, Madrid (2005-06)

Acknowledgements / Agradecimientos

Quisiera expresar mi más sincero agradecimiento a todas aquellas personas que han contribuido de alguna forma a esta Tesis Doctoral que ahora ve su fin. En especial:

A mis directores, Raúl y Raquel por haberme brindado la oportunidad de embarcarme en esta aventura junto a ellos. Agradezco la dedicación con la que me habéis guiado, con un acompañamiento cercano e incansable, enriqueciendo tanto el trabajo como mi aprendizaje con atentas y valiosas orientaciones. Gracias por vuestro ejemplo y motivación, así como por no dejarme caer en el desánimo en los momentos difíciles. También por vuestra paciencia, y por vuestro empuje para crecer afrontando nuevos retos, depositando toda vuestra confianza en mí, lo que alejó miedos e incertidumbres. Espero que estas palabras hayan sabido transmitir toda mi gratitud y el orgullo que siento.

A todo el Departamento de Ingeniería Química y Medio Ambiente, en especial al grupo de Tecnología Ambiental, en el que me he sentido muy a gusto desde mi llegada. Gracias a todas y cada una de las personas que lo integran.

Echando la vista atrás, quisiera empezar dando las gracias a Juanqui tanto por trasladarme su pasión hacia el mundo metanótrofo, como por enseñarme con todo el esmero del mundo. Mi suerte ha sido doble al iniciar este camino junto a Víctor, inigualable anfitrión y *compi*. Gracias a los dos por las risas, por poner siempre el contrapunto y por vuestra amistad. ¡Larga vida al PHA club de fans!

A todos los compañeros VOC & Microalgae con los que he compartido tanto, y que han contribuido a amenizar y enriquecer esta travesía: algunos se marcharon demasiado pronto, Ilker, Sara y Dimas; y otros me acompañaron en las infatigables horas de *lab* y oficina (*afterwork included*) todos estos años, Chari (mi conexión sureña), David, Pelitos, y Javi ¡gracias por todo! A Roxi y Celia, por estar siempre ahí, por los paseos, vinitos y tantos momentos inolvidables, pero nunca suficientes. También gracias a las chicas de otros grupos que son sin duda parte de esto, Javiera, Johanna, Judit, Thiago, Cenit, María y Erika; y a los que están ya en plena batalla Fanny, Lois, Eva, Leo… A todos los investigadores

con los que he tenido la oportunidad de trabajar de cerca y de los que he aprendido tanto, gracias muy especiales a Esther A. y Rebe por saber escucharme y por tantos consejos; a Elisa por su inestimable ayuda observando el mundo microscópico; y a Nuria y Sergio por ayudarme a resolver tantas cuestiones. A ti, Igor, por involucrarte como lo hiciste en el mundo *hirsu*, y por ser un apoyo fundamental para lograr tantas cosas en un año particularmente complicado. Compi, ¡eres la pera limonera! No me olvido de mis estudiantes, Laura, José Luis, Miren y Silvia, por todo el tan valioso apoyo que me han brindado en la experimentación; y de los chicos de estuvieron de estancia, en particular de Luz, Milena y Carlos, con los que he tenido la oportunidad de compartir y seguir aprendiendo.

Mi reconocimiento a todos los técnicos, partes vitales de este trabajo y de todo el aprendizaje que me llevo. En especial, gracias a Enrique por velar por el buen funcionamiento de todo y sacarnos de tantos apuros, por tus bromas; a Jony por tu predisposición y el *trabajo fino* en la extracción de PHAs; a Araceli por todos los análisis de sólidos y por recordarnos lo verdaderamente importante, a Bea por la preparación de patrones y por tu inestimable ayuda; a Dani y Chema por poner todo a punto siempre.

A todos los compañeros de la asignatura “Tecnología Ambiental y de Procesos” por todo lo que he podido aprender de vosotros y por facilitar la difícil tarea de impartir clases, en especial a Isra por tu esfuerzo durante la pandemia y tu enorme ayuda en un curso tan complicado y atípico.

Thanks to Xueming and his old colleagues from the DTU. It was an enormous pleasure to work in collaboration with you.

A cada una de las personas que me han abierto una puerta en esta área hasta llegar hasta aquí, y a los que han dedicado parte de su tiempo a enseñarme. En especial, quisiera agradecer al Dr. Gonzalo Ruiz Filippi, siempre en mi memoria, todo el cariño y la confianza que depositó en mí durante mi estancia en Chile, haciéndome ver por primera vez que mi siguiente paso sería éste.

A Helena, por su generosidad y confianza, y por esos cafés exprés.

A la música, por esas bocanadas de aire fresco entre aquellas rutinas de *lab* de sábado y domingo, que de la mano de Jairo y familia Depedro, Xoel, Vetusta, Viva Suecia, Rufus, etc. fueron tan vitales para seguir mirando hacia delante.

A Isi y Rodolfo, los creadores de momentos en Pucela, gracias por vuestro cariño y por ser desconexión de la buena. Y a mis amigas de siempre, por seguir estando ahí de forma incondicional y hacerme sentir que no pasa el tiempo cuando nos reunimos. Gracias en particular a los que se animaron a visitarme: María, Álvaro y Lari.

A toda mi familia, mi cable a tierra en todos los sentidos. Siempre cerca acompañándome en cada meta a pesar de la distancia, por las escapadas y por darme toda la fuerza necesaria. A mis padres, mis pilares y mis mayores referentes, con cuyo apoyo incondicional cuento siempre. A mis hermanos Coral y Manuel, y cuñados Elena y Andoni, por estar al pie del cañón, haciendo que no me preocupase de nada. A mi abuelo (sé que allá donde estés, celebrarás esto como nadie) y a mi abuela, por serlo todo y más.

A mis queridísimos Duna y Lennon que tanto eché de menos, y a mis pequeños ayudantes Jacob y Bowie.

Por último, a Pablo, por ser el mejor compañero de viaje y estar a mi lado en esta aventura sin pensar en todo cuanto dejabas en el camino. Por cuidar(nos) y por esas grandes dosis de comprensión y paciencia, merecedoras casi de otro doctorado.

A todos los que pueda dejarme en el tintero, ¡mil gracias!

¡Gracias! Thank you! Obrigada! Dzięki! Teşekkürler!

The research developed in this PhD thesis was supported by the Ministry of Science and Innovation under the Grant No. BES-2016-077160 (Project CTM2015-70442-R).